THESIS APPROVAL

GRADUATE SCHOOL, KASETSART UNIVERSITY

Master of Engineering (Engineering Management)
DEGREE

Engineering Management
FIELD

Industrial Engineering
DEPARTMENT

TITLE: Determination of the Optimal Processing Conditions in Plastic Injection Molding Using Computer-aided Engineering, Artificial Neural Network Model, and Genetic Algorithm

NAME: Mr. Pitchakorn Chavanatnusorn

THIS THESIS HAS BEEN ACCEPTED BY

THESIS ADVISOR
(Mr. Chuckaphun Aramphongphun, Ph.D.)

THESIS CO-ADVISOR
(Mr. Pornthep Anussornnitisarn, Ph.D.)

DEPARTMENT HEAD
(Associate Professor Kongkiti Phusavat, Ph.D.)

APPROVED BY THE GRADUATE SCHOOL ON .....

DEAN
(Associate Professor Gunjana Theeragool, D.Agr.)

THESIS

DETERMINATION OF THE OPTIMAL PROCESSING CONDITIONS IN PLASTIC INJECTION MOLDING USING COMPUTER-AIDED ENGINEERING, ARTIFICIAL NEURAL NETWORK MODEL, AND GENETIC ALGORITHM

PITCHAKORN CHAVANATNUSORN

A Thesis Submitted in Partial Fulfillment of
the Requirements for the Degree of
Master of Engineering (Engineering Management)
Graduate School, Kasetsart University
2009

Pitchakorn Chavanatnusorn 2009: Determination of the Optimal Processing Conditions in Plastic Injection Molding Using Computer-aided Engineering, Artificial Neural Network Model, and Genetic Algorithm. Master of Engineering (Engineering Management), Major Field: Engineering Management, Department of Industrial Engineering. Thesis Advisor: Mr. Chuckaphun Aramphongphun, Ph.D. 232 pages.

This research work presents a systematic approach to determine the optimal processing conditions by optimizing the quality of plastic injection-molded parts and their process cycle time. Two plastic parts were used as study cases: (i) a rectangular lid and (ii) a roof tile. The part's qualities considered were the residual stress of the rectangular lid and the warpage of the roof tile. In addition, six process parameters in injection molding: (i) material type, (ii) melt temperature, (iii) injection speed, (iv) packing pressure, (v) packing time, and (vi) cooling time, were optimized by using Computer-aided Engineering (CAE) software, the Design of Experiments (DOE) technique, the Artificial Neural Network (ANN) model, and the Genetic Algorithm (GA) method. The well-known CAE software, Moldflow, was used to simulate the injection molding process, which significantly reduce the production time and cost. The 2^{k-p} Fractional Factorial design was employed to find the effects of the parameters on: (i) the residual stress and cycle time of the rectangular lid in Case 1 and (ii) the warpage and cycle time of the roof part in Case 2. A complex relationship among (i) the processing conditions, residual stress and cycle time in Case 1 and (ii) the processing conditions, warpage and cycle time in Case 2 was determined by using the ANN model. The GA method was then applied to optimize the processing conditions in terms of the minimum residual stress of the rectangular lid and the minimum warpage of the roof tile. According to the experimental results based on the optimized processing conditions, it was found that: (i) the residual stress of the rectangular lid in Case 1 was reduced by 26.43% with a 10.26% decrease of the cycle time and (ii) the warpage of the roof tile in Case 2 was reduced by 40.85% without an increase of the cycle time.

_____ _____ ___ / ___ / ___

Student's signature Thesis Advisor's signature

ACKNOWLEDGEMENTS

There are several people without whom this thesis would not have been possible. It is a pleasure to convey my gratitude to them all in my humble acknowledgements.

In my first place, I would sincerely like to record my gratitude to my thesis advisor, Dr. Chuckaphun Aramphongphun, for his supervision, encouragement, advice, and valuable suggestion from the very early stage of this thesis through out of the work.

I would like to thank Dr. Pornthep Anussornnitisarn, Assoc. Prof. Sompong Pitchetpinyo, and Dr. Rapee Kanchana for serving as members of the examination committee for their valuable suggestions and recommendations.

I am grateful to all others who helped me to perform experiments of this thesis: Mr. Watcharapong Chookaew, Mr. Somphong Inthong, Mr. Thanawat Sasimateepatch, Mr. Kumpanat Auamkul, and other staffs in Polymer Department, Instrumentation Department, and Product Development Department of Research and Development Institute of Production Technology (RDiPT), Kasetsart University.

Many thanks as well for the generous support of instructors, staffs, and friends of the International Graduate Program in Industrial Engineering, Kasetsart University for their sincere support.

I would also acknowledge my grandparents, my relative, and Ms. Chompunoot Duangjan for their continuing encouragements.

Finally, I would like to express my special thanks to my parents (Mr. Pichai and Mrs. Kingkoy Chavanatnusorn) and my sister (Ms. Pannika Chavanatnusorn) who always give me heartfelt love and inspiration support throughout my graduate study.

Pitchakorn Chavanatnusorn

March 2009

TABLE OF CONTENTS

Page

LIST OF TABLES

LIST OF TABLES (Continued)

LIST OF TABLES (Continued)

LIST OF TABLES (Continued)

LIST OF TABLES (Continued)

LIST OF TABLES (Continued)

LIST OF FIGURES

LIST OF FIGURES (Continued)

LIST OF FIGURES (Continued)

LIST OF FIGURES (Continued)

LIST OF ABBREVIATION

ADALINE	=	Adaptive Linear Neural Network
ANN	=	Artificial Neural Network
ANOVA	=	Analysis of Variance
b	=	bias
BPN	=	Back Propagation Network
CAD	=	Computer Aided Design
CAE	=	Computer Aided Engineering
CT	=	Cooling Time
DOE	=	Design of Experiment
f	=	Transfer Function
F_0	=	F-ratio
FE	=	Finite Element
FRP	=	Fiber Reinforced Plastic
GA	=	Genetic Algorithm
HDPE	=	High-density Polyethylene
IS	=	Injection Speed
LDPE	=	Low-density Polyethylene
logsig	=	Binary Sigmoid Function
lr	=	Learning rate
MLR	=	Multiple Linear Regression
MPa	=	Mega Pascal
MPI	=	Moldflow Plastics Insight
MS	=	Mean Square
MT	=	Melt Temperature
P_c	=	Crossover rate
PET	=	Polyethylene Terephthalate
P_m	=	Mutation rate
PP	=	Polypropylene
PP	=	Packing Pressure
PS	=	Polystyrene
PT	=	Packing Time

LIST OF ABBREVIATION (Continued)

purelin	=	Linear Transfer Function
PVC	=	Polyvinyl Chloride
RSM	=	Response Surface Methodology
SD	=	Standard Deviation
SS	=	Sum of Squares
tansig	=	Bipolar Sigmoid Function
T_k	=	Target for ANN output
W	=	Weight matrix
X	=	Input layer
$\bar{x}$	=	Mean
Y	=	Output layer
Z	=	Hidden layer
z-axis	=	Thickness direction
α	=	Alpha value of statistical hypothesis test
δ	=	Error information term of Back Propagation

DETERMINATION OF THE OPTIMAL PROCESSING CONDITIONS IN PLASTIC INJECTION MOLDING USING COMPUTER-AIDED ENGINEERING, ARTIFICIAL NEURAL NETWORK MODEL, AND GENETIC ALGORITHM

INTRODUCTION

Plastic industry is one of the major industries in Thailand. It makes great benefit and supports other industries in the country. The Ministry of Commerce (2008) stated that the export of plastic products stood at $1,097.69 million in January to May 2008, which increased 29.23% at the same period in 2007. Among plastic shaping processes, injection molding is a significant manufacturing process, which accounts for 47% of all plastic products manufactured (Kittisorn, 2004). To meet the global market standards, plastic manufacturers need to continuously improve their products' quality, process cycle time, and cost. It is therefore important to obtain the best products' quality and shortest cycle time. One simple way to achieve this goal is to optimize the processing conditions using engineering tools.

In this research work, two plastic parts were used as study cases: (i) a rectangular lid and (ii) a roof tile. The part's qualities considered were the residual stress of the rectangular lid and the warpage of the roof tile. Material grade, melt temperature, injection speed, packing pressure, packing time, and cooling time were considered to be process parameters that affect the plastic part's qualities. In order to determine the optimal processing conditions, CAE software – Moldflow – was used to simulate the injection molding process of the plastic parts instead of performing the experiments. Moreover, several efficient optimization tools including DOE, the ANN model, and the GA method, were applied to optimize the processing conditions to achieve the best quality of the products.

CAE software was used to simulate the manufacturing process and to study how the materials behave so that the design can be improved and the process can be optimized. CAE software named Moldflow is frequently used to support the simulation

of the plastic injection molding process. Kurtaran *et al.* (2005) exploited the advantages of Moldflow to simulate injection molding of a bus ceiling lamp base as a predictive model for warpage of the product. Imihezri *et al.* (2006) also used Moldflow to analyze polymer-based composite automotive clutch pedals for studying the difference between two types of profile in terms of stress and flow patterns. In this work, Moldflow was then applied to simulate the plastic injection molding process instead of the traditional build-and-test process.

DOE is a method that applies statistics to develop experiment planning. The primary build of DOE is to give a minimum experimental effort to determine a significance level of the variables (Jankrajang, 2003). DOE can apply in many applications. For example, Park and Ahn (2004) used DOE for both mold and process designs to improve the quality and productivity of electronic components. Dong (2006) used DOE to identify the significant process variables of the vacuum assisted resin transfer molding process. Davis (1999) also investigated the use of DOE to improve the management processes in the service sector. DOE involves in every step of this work including determining the significant parameters in the injection molding process and organizing structures of the ANN model.

The ANN model is an algorithm for cognitive tasks such as learning and optimizing, which are based on concepts derived from research into the nature of the brain (Muller and Reinhardt, 1990). Thus, ANN can be used to learn patterns and relationships of data even in a non-linear system. Chakraborty (2005) used the ANN model to predict fiber reinforced plastic (FRP) composite laminates in terms of size, shape, and location of lamination. Sadeghi (2000) built the neural network predictor model to predict the quality of injection-molded parts in terms of lack or existence of the short shot defect based on the melt flow rate of the materials and three key process parameters for CASIO backside body. In this work, the ANN model was used as a base model or fitness function for process optimization by using GA.

GA is an optimization approach based on the mechanics of natural selection. It is derived from the theory of natural evolution. GA simulates mechanisms of population genetics and natural rules of survival in pursuit of adaptation ideas (Goldberg, 1989).

Thus, GA is used in optimizing the processing conditions using the fitness function based on the ANN model. Therefore, using ANN model with GA is a promising natural computation technique for optimization because ANN has become a practical method for predictive capability to very complex non-linear systems. GA can be used to find the global optimum value of the process parameters (Kurtaran *et al.,* 2005 and Changyu *et al.,* 2007).

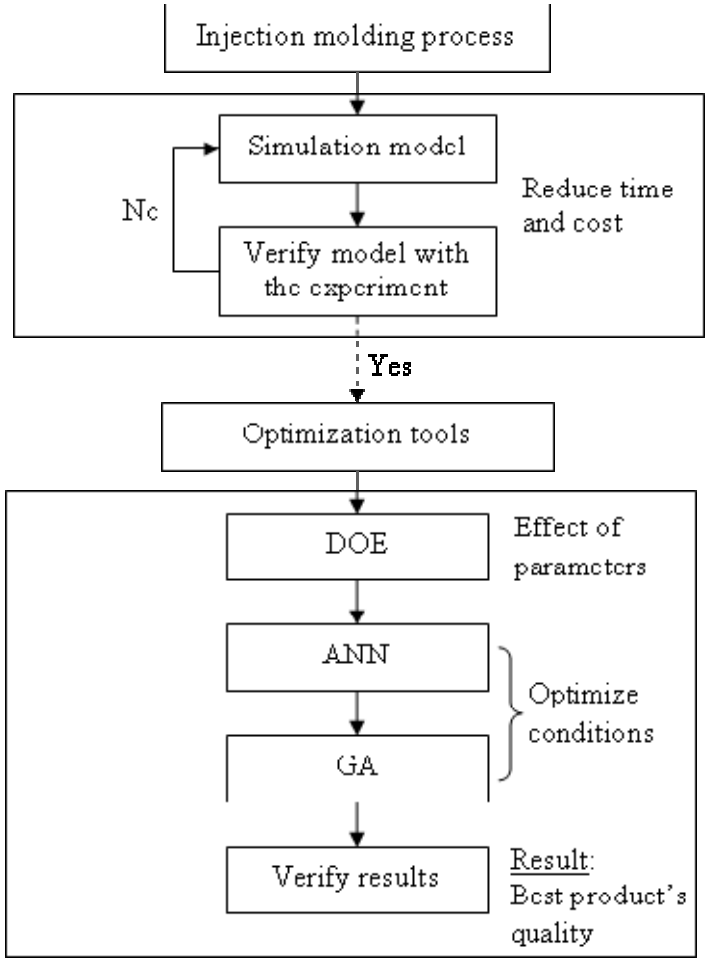

Figure 1 Overview of this research work

OBJECTIVES

The objectives of this research can be summarized as follows:

1. To verify the application of CAE software, Moldflow, in simulating the plastic injection molding process.
2. To determine what parameters significantly affect the plastic injection molding process.
3. To develop a systematic approach to determine the optimal processing conditions in plastic injection molding using CAE, DOE, ANN, and GA so as to achieve the best product's quality and cycle time.

LITERATURE REVIEW

Literature review consists of five parts: (i) Plastic injection molding process, (ii) MoldFlow Plastic Insight (MPI) software, (iii) Design of Experiment (DOE) techniques, (iv) Artificial Neural Network (ANN) model, and (v) Genetic Algorithm (GA) method.

1. Plastic injection molding process

In plastic industries, various products can be manufactured including plastic containers, pipes and joints, vehicle parts, electrical parts, floor and wall tiles. According to The Office of Small and Medium Enterprises Promotion (2004), there are about 30 plastic granule manufacturers in Thailand with 4,100 plastic product manufacturers and additional 300 machinery manufacturers. Both small and medium enterprises are facing two main problems including: (i) management and (ii) production and technology, respectively, as shown in Figures 2 and 3. The management-related problems include planning of their managers and supporting report data. For the production and technology-related problems, the planning and control and product quality are principal problems. To achieve the quality requirement, the focus of this study was mainly on determination of the optimal processing conditions and plastic parts quality.

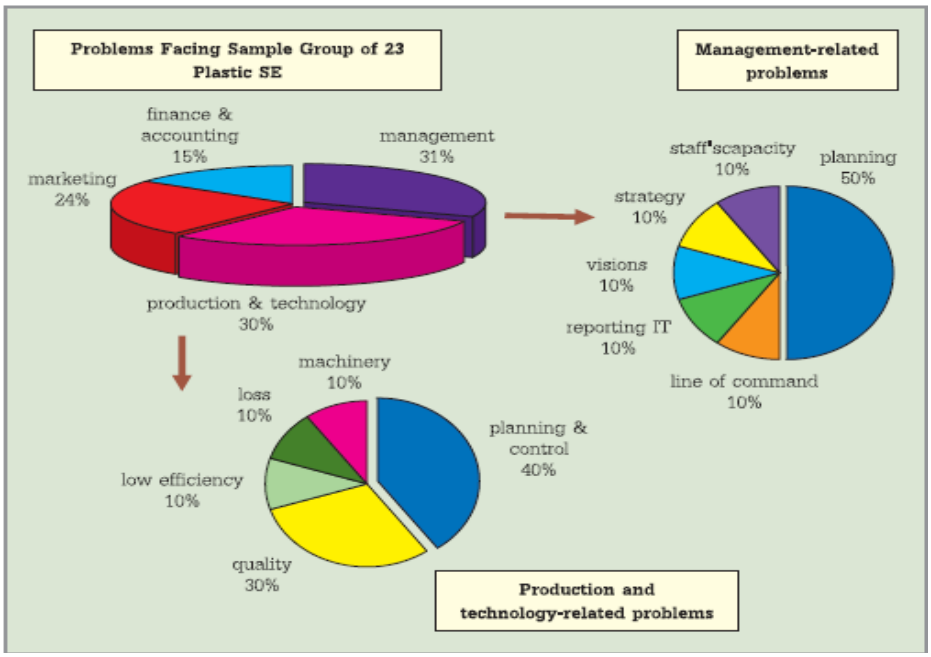

Figure 2 Problems that are facing the sample groups of 23 small enterprises

Source: The Office of Small and Medium Enterprises Promotion (2004)

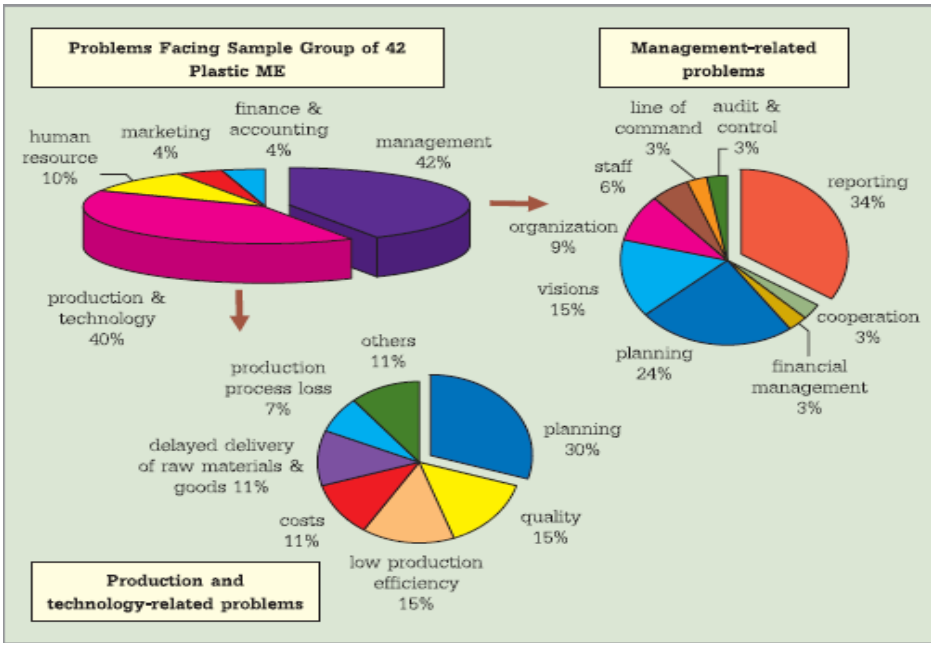

Figure 3 Problems that are facing the sample groups of 42 medium enterprises

Source: The Office of Small and Medium Enterprises Promotion (2004)

1.1 Types of plastic

There are various types of commonly used plastics such as Polyethylene terephthalate (PET), High Density Polyethylene (HDPE), Polyvinyl chloride (PVC), Low Density Polyethylene (LDPE), Polypropylene (PP), Polystyrene (PS), and others. All these types have different properties and common uses. For instance, PET is a hard, stiff, strong and dimensionally stable material that absorbs very little moisture. Thus, it can be used for bottles and electrical components (Goodfellow, 2007). PVC is often used for pipe and fitting because it gives excellent, maintenance-free performance over long periods of time and has outstanding chemical resistance (Scientific Glass & Plastic, 2002).

There are two types of plastic materials used in this research work: PS and HDPE, which are used to mold the rectangular lid in Case 1 and the roof tile in Case 2, respectively. In Case 1, PS is a clear, colorless polymer providing glassy surfaces, which is used extensively for low-cost applications. It is commonly used in protective packaging such as a lid. Nevertheless, PS is brittle and has poor weatherability and chemical resistance (RECOUP, 2008).

In Case 2, plastic roof tiles are growing in use because of their significant advantages over traditional roof tile materials such as ceramic, slate, or wood. They are light in weight, durable, low-cost, easy to install, and can be produced in a wide range of colors (Ciba, 2008). To meet these requirements, HDPE was therefore used in Case 2 as the roof tile. HDPE is particularly excellent in moisture barrier properties and chemical resistance, stiffness, and ease of forming and providing soft waxy surface (RECOUP, 2008).

1.2 Injection molding

Injection molding is a manufacturing process for making parts mostly from thermoplastic materials. Molten plastic is injected at high pressure into a mold, which forms the product's shape (Wikipedia, 2007). Marechal (2005) presented that injection molding was the most commonly used process in plastic processing due to its high

productivity and clean process (no waste formation). It was used in a great variety of applications ranging from tubes to finished products. It also maintained the flowability of the melt during its transportation to the cavities without major problems.

The process steps in injection molding include feeding, melting, injecting, cooling, and ejecting (Koch, 2005). In the feeding step, the screw rotates and pumps plastic melts from a hopper towards the front of the barrel, forming a reservoir of melted plastic as shown in Figure 4. During the screw rotation, electric heaters around a barrel and frictional heat melt the plastic pellets. Next, in the injection step, the screw moves forward and pushes the molten plastic into the mold. The cooling water in the mold draws away heat during the cooling step. After the plastic has solidified, the mold opens and ejects the newly formed plastic part from the mold cavity.

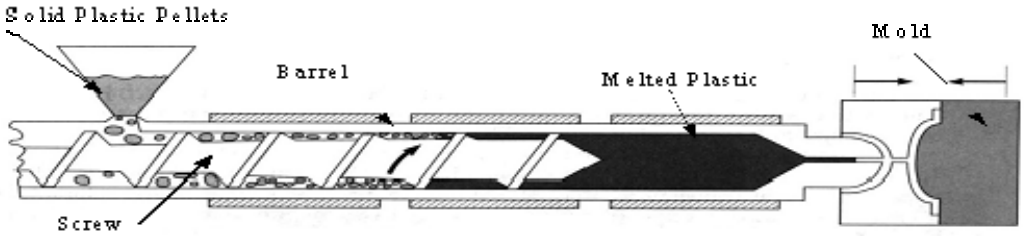

Figure 4 A model of the injection molding process

Source: Koch (2005)

1.3 Standard for setting injection unit

The principle of setting the injection molding process when the manufacturer launches new product consists of three steps: (i) setting of the parameters and standard (ii) set up the operation, and (iii) local optimization by manufacturer.

1.3.1 Setting of the parameters and standard with the change-over by position

a.) Set barrel temperature based on plastic's type.

b.) Set up the machine for change-over by position. Recommendation is on 15 to 20 mm.

c.) Determine the end-position for metering in a range of 80% of part's volume.

d.) Begin with one step injection if the part is not complicate.

e.) Set all injection pressure of 80%.

f.) Under consideration of plastic material and article configuration, set the injection speed in a range of 30 to 40%.

g.) Begin packing pressure with the halves of injection pressure (40%).

h.) Begin with 0.3 second of packing time. This is for determination of 90-95% injection sequence volume.

i.) Begin with 5% of back pressure.

j.) In order to get a high mixing effect, the maximum screw rotation should be set corresponding with the recommendation of the material supplier. The peripheral screw speed set to 0.2-0.3 m/s.

k.) The duration of cooling time is dependent on the material type, wall thickness, temperature of the coolant and cooling channel layout.

1.3.2 Set up operation

a.) Set the injection sequence as in 1.3.1.

b.) Set the packing pressure sequence with the parameter pressure and time as well as observing the screw movement in aim of uniform retardation to reach.

c.) Increase the injection speed on the possible maximum.

d.) Increase the metering part volume on 98%.

1.3.3 Local optimization by manufacturer

A basic idea of the optimization in the injection-molded product is to control the process parameters as follows:

a.) Reduction of tolerance for start and end position of dosage

b.) Change-over position of packing pressure and a screw retardation

c.) Stroke of packing pressure sequence

d.) Dimension of cushion

e.) Injection velocity

f.) Packing pressure

g.) Packing pressure time

h.) Back-pressure

1.4 Defects in the injection molding process

Common failure pattern normally occurs due to three main causes: (i) part and mold design, (ii) material selection, and (iii) processing. In many cases, the failures occur during the processing and these failures causes some defects that can be found in injection-molded parts such as warpage, shrinkage, sink mark, residual stress, air trap, weld line, and so on. These defects influence the quality and precision of the products. It is therefore important to effectively control the significant parameters during the molding process.

1.4.1 Residual stress problem

Residual stress is the stress that exists in structural sections in their unloaded state. Large residual stresses in injection molded parts can cause several problems such as early failure of the part or severe warpage and also undesirable birefringence in case of optical products. Therefore, it is often desirable to produce injection-molded parts with minimum residual stresses (Han et al., 2001). As these reasons, the rectangular lid in Case 1 was considered to minimize the residual stresses.

1.4.2 Warpage problem

Warpage is a plastic part's defect caused by a non-uniform change of internal stresses. Warpage in an injection-molded part is caused by variations in shrinkage including from region to region in the part through the thickness of the part as well as parallel and perpendicular to the direction of the material orientation (Moldflow Coporation, 2006). Therefore, warpage is a main indicator in uniform-quality of finished products. Moreover, since the product of this research in Case 2 is the roof tile, which has long and thin shape, the warpage is a major concern for this product's shape, especially at the end.

2. MoldFlow Plastic Insight 6.1 (MPI) software

According to Moldflow Corporation (2006), MPI is a complete suite of definitive tools for simulating, analyzing, optimizing and validating plastics part and mold designs in plastics injection molding. MPI products address the broadest range of manufacturing issues and design geometry types associated with plastics molding processes. Thus, MPI can work to reduce or eliminate time delays, improve part quality, and deliver projects within budget constraints.

With MPI analysis modules, filling, packing, and cooling stages of the plastic, the injection molding process can be simulated. MPI also predict post-molding phenomena such as shrinkage, sink mark, air trap, weld line, and warpage of the products. In addition, MPI offers an expanded material database, which includes over 7,800 unique materials for use in plastic process simulation software in order to ensure that users have access to the highest quality material data for plastic simulation.

There are three stages of the simulation in MPI software. The first stage of a Finite Element (FE) method based simulation is called “pre-process”. This can be performed by using either the simulation software itself or one of the Computer-Aided Design (CAD) computer programs such as Solid Works, AutoCAD, and Unigraphics. The geometric model is then meshed using triangular elements. Afterwards, the polymer is selected and the injection locations are set. To finish this first stage, it is required to set the process conditions into the simulation software. In the second stage of a simulation process, fluid mechanics and heat transfer calculations are performed and applied to a model analysis. The last stage of a simulation is called “post-process”, where the experience of the analyst is required to extract the reliable and most important information from multiples colored contour results offered by the simulation (Marcilla *et al.*, 2006).

Pre-process is very important for the efficiency of the simulation model. Hence, it must be thoroughly analyzed on the part geometry and its conditions as described in the following steps (Moldflow Corporation, 2001).

Step 1: Import a CAD model, which was previously created.

Step 2: Mesh the CAD model. MPI software is easy to mesh automatically using triangular elements to cover the model surface with least distortion. This is an important step. Thus, meshing is needed to rectify any errors, which are described in Mesh Statistics as displayed in Figure 5.

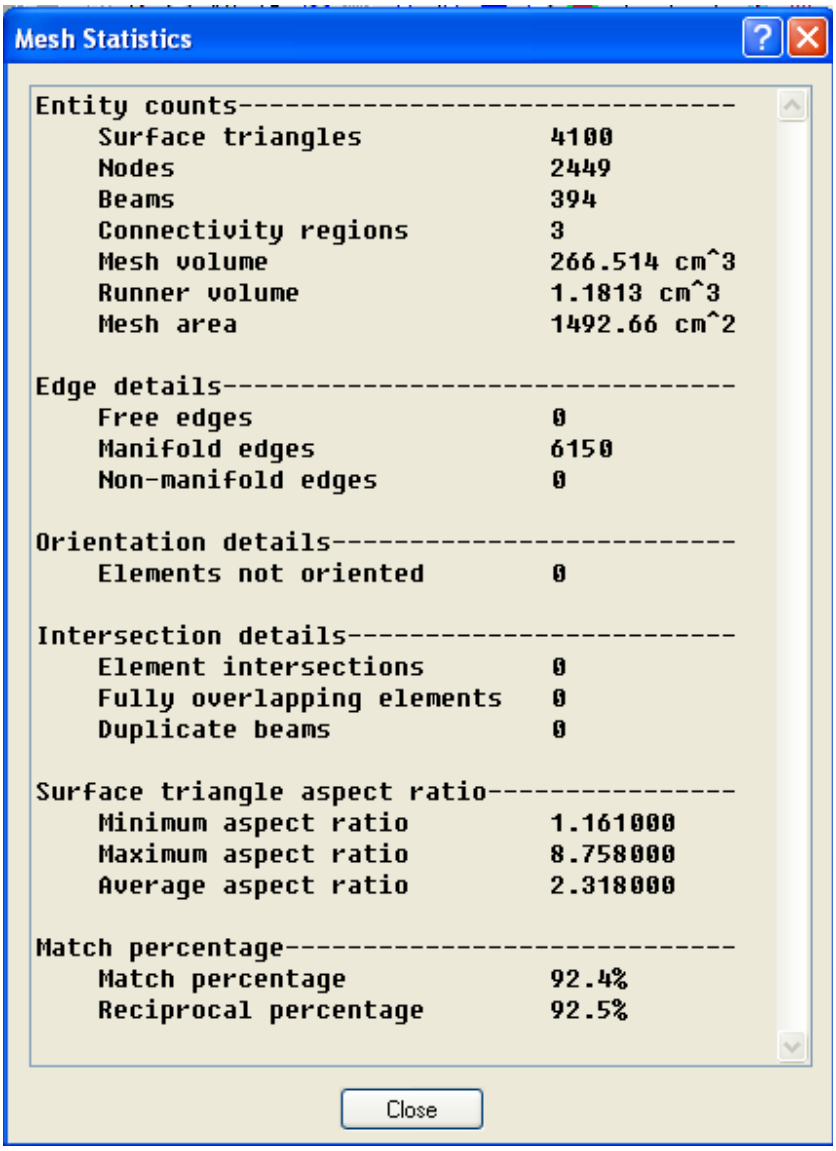

Figure 5 The Mesh Statistics pop-up window

In entity counts, the Connectivity regions, which describe the number of regions in the part, should be fixed to 1.

In edge details, there are three important values: (i) Free edges, (ii) Manifold edge, and (iii) Non-manifold. Free edges describe the outer edges of the model. For a fusion, model mesh cannot have any free edge, thus it must be edited to 0. Manifold edge is the two entities, which are connected into two nodes, so a fusion mesh model should contain only Manifold edge, excluding non-manifold edge, which has more than two entities in two nodes. Thus, the value of non-manifold edge must also be edited to 0.

In orientation details, the fusion mesh model elements cannot be oriented in the inward direction. Then, element not oriented value should be 0.

In intersection details, the two significant values that must equal to 0 are elements intersection and fully overlapping elements. Elements intersection occurs when two elements intersect each other and do not share common nodes. Fully overlapping elements appear when two elements overlap in the same plane.

For surface triangle aspect ratio, which is defined as the ratio of largest of the element to the height perpendicular to that side, it should be minimized as much as possible because they affect the accuracy of any analysis. Typically, the maximum aspect ratio is kept below the value of 10. In addition, match ratio and reciprocal ratio must be grater than 85%.

Step 3: Define the injection molding process. It consists of three steps: the analysis sequence, the injection molding material, and the process setting.

Step 4: Define the injection location and model a runner system.

As MPI is used to simulate the injection molding process, it is then used in many applications of plastic injection molding processes. Imihezri *et al.* (2006) used MPI and component design to analyze the polymeric-based composite automotive clutch pedals in terms of stress and flow patterns. Ozcelik and Erzurumlu (2006) used MPI and DOE as tools to analyze the plastic part model on the best conditions to meet the minimum warpage, which is shown in the post-process results of MPI.

3. Design of Experiment (DOE) techniques

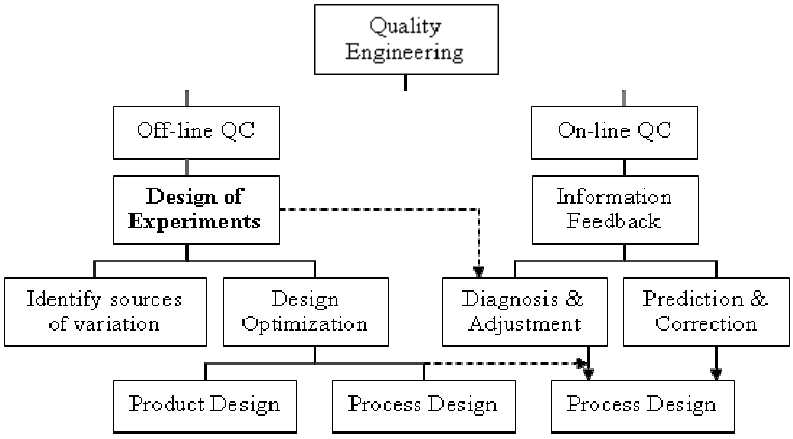

Figure 6 Quality engineering scheme

Source: Sudasna-na-Ayudthya (2006)

3.1 Off-line quality control

As shown in Figure 6, the purpose of off-line quality control is to optimize product and process design in support of on-line quality control (Sudasna-na-Ayudthya, 2006). Some of these efforts may be research and development activities. If it is process-related, they may be accomplished on prototype lines that simulate actual production, or they could be performed on the actual manufacturing process prior to production, on-off shifts, or during production shutdown. The aim of experimentation techniques are on two keys: (i) identifying sources of variation and (ii) determining design and process optimization.

3.2 Design of Experiment (DOE) concepts

Design of Experiment (DOE) is a technigue that applies statistics to develop a planning of experiments, which gives a minimum experimental effort to a determined significance level of the results. This is the way that experimenters perform experiments to discover something interesting for a particular process or system (Montgomery, 2005). In general, experiments are used to study the performance of processes and system. The process or system can be represented by the model as shown in Figure 7.

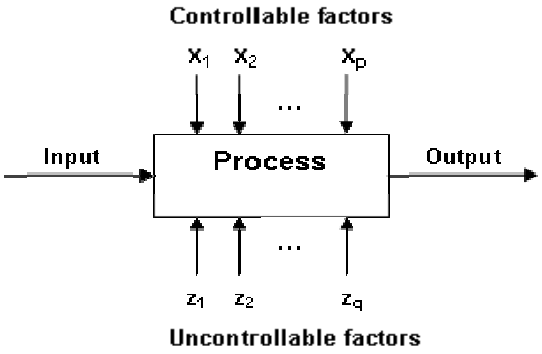

Figure 7 A general model of a process or a system.

Source: Montgomery (2005)

The DOE assumes that the system is composed of a set of principal variables (or parameters/factors) as inputs and as the output (or the response) for each input configuration. Some of the process variables and material properties (x_1, x_2, …, x_p) are controllable, whereas other variables (z_1, z_2, …, z_q) are uncontrollable. The objectives of the experiment may include the following (Montgomery, 2005):

1) Determining which variables are most influential on the response y.
2) Determining where to set the influential x's so that y is almost always near the desired nominal value.
3) Determining where to set the influential x's so that variable in y is small.
4) Determining where to set the influential x's so that the effects of the uncontrollable variables z_1, z_2, …, z_q are minimized.

DOE can be applied in many applications. Sanchez (2005) stated that there are three fundamental concepts in DOE: control, replication, and randomization. Control means that the experiment is conducted in a systematic way, rather than by using a trial-and-error approach. Replication is considered as a way to gain enough data to achieve narrow confidence intervals and powerful hypothesis tests. Randomization provides a probabilistic guard against the possibility of unknown, hidden sources of bias surfacing to create problems with data.

Recently, the DOE procedure has been used to systematically investigate process variables or product variables that influence the quality of products. It is possible to identify the process conditions and product components that influence product quality and costs, which in turn enhance the product manufacturability, quality, reliability, and productivity. The DOE procedure consists of the following four steps: planning, screening, optimization, and verification (Krottmaier, 1993). Planning defines the problem and objective, and development of an experimental plan. Screening reduces the number of variables by identifying the key variables that affect product quality. Optimization defines the optimal values for various experimental factors. Verification performs a follow-up experiment at the predicted best processing conditions to confirm the optimization results.

3.3 Factorial Designs

Many experiments involve the study of the effects of two or more factors. In general, Full Factorial designs are most efficient for this type of experiment. By using a Full Factorial design, in each complete trial or replication of the experiment, all possible combinations of the levels of the factors are investigated. When factors are arranged in a Full Factorial design, they are often said to be crossed. The effect of a factor is defined to be the change in response produced by a change in the level of the factor. This is frequently called a main effect because it refers to the primary factors of interest in the experiment. In this kind of experiments, there is also an interaction between the factors. This is because the difference between the levels of one factor is not the same at all levels of the other factors (Montgomery, 2005).

As the Full Factorial design is the most efficient design for all experiments, the experimenter reasonably assume that more than two interactions are negligible and can be thus ignored. Hence, it is often impractical to perform the experimental runs as Fractional Factorial design. Chankong (2006) stated that the motivation for Fractional Factorial designs was obvious as the factor screening experiment to identify the factors with large effects. Montgomery (2005) also stated that Fractional Factorial were usually performed for screening in the early stages of the work when many factors initially considered likely have little or no effect on the response.

In the Fractional Factorial designs, there are three types of resolution design including III, IV, and V designs. Park and Ahn (2004) explained the meaning of different resolutions as the degree of aliasing in the Fractional Factorial design matrix as follows: (Aliases mean that it is impossible to differentiate between two or more effects.)

1) Resolution III: a design does not alias main effects with one another, but does alias main effect with two-way interactions.

2) Resolution IV: a design does not alias main effects with two-way interactions, but it is generally recommended to analyze two-way interaction effectively. Thus, it is good analyze for main factors.

3) Resolution V: a design does not alias main effects with two-way interactions, and it also does not alias between two-way interactions. Thus, it is a good analyzer for both main factors and two-factor interaction.

In the 2^{k-p} Fractional Factorial design, it is important to select the p generator in such a way to obtain the best possible alias relationships with the highest possible resolution. For instance, consider the 2_{IV}^{6-2} design in Table 1, where the generators E = ABC and F = BCD, thereby producing a resolution IV design (Montgomery, 2005).

Montgomery (2005) also gave an example of injection part that had shrinkage problem within assembly operations downstream. In order to improve part's quality, six factors including mold temperature, screw speed, holding time, cycle time, gate size, and holding pressure were considered at each two level as 2_{IV}^{6-2} Fractional Factorial design. The objectives of this experiment were to learn how each factor affects shrinkage and how they interacted to each other.

Table 1 The 2^{6-2} Fractional Factorial design with resolution IV

Run	Basic Design				E=ABC	F=BCD
	A	B	C	D		
1	-	-	-	-	-	-
2	+	-	-	-	+	-
3	-	+	-	-	+	+
4	+	+	-	-	-	+
5	-	-	+	-	+	+

Table 1 (Continued)

Run	Basic Design				E=ABC	F=BCD
	A	B	C	D		
6	+	-	+	-	-	+
7	-	+	+	-	-	-
8	+	+	+	-	+	-
9	-	-	-	+	-	+
10	+	-	-	+	+	+
11	-	+	-	+	+	-
12	+	+	-	+	-	-
13	-	-	+	+	+	-
14	+	-	+	+	-	-
15	-	+	+	+	-	+
16	+	+	+	+	+	+

Luis et al. (2005) studied on the die-sinking electrical discharges machining (EDM) of silicon carbide. The five design factors including intensity supplied by the generator of the EDM machine (I), pulse time (t_i), duty cycle (η), open-circuit voltage (U) and dielectric flushing pressure (P). In this case, they use the technique of DOE in a 2^{5-1} Fractional Factorial design, whose resolution is V, to estimate all main effects, two-factor interactions and pure quadratic effects of the five design factors.

3.4 Prediction Performance Designs

In industrial engineering field, there are a various prediction methods including Multiple Linear Regression (MLR) Model, Response Surface Methodology (RSM), and Artificial Neural Network (ANN). MLR model is the relationship between response variable and independent variables in a linear term as an Equation (1).

$$y = \beta_0 + \beta_1 x_1 + \beta_2 x_2 + ... + \beta_k x_k + \in \qquad (1)$$

The parameters β_j, j = 0, 1, …, k are called the regression coefficients which represent the expected change in response y per unit change in x_j when all the remaining independent variables x_i ($i \neq j$) are held constant (Montgomery, 2005). Since the main weakness of MLR model is that transformations of the relation between these two parameters may not be met completely. Thus, the combination of DOE with Response Surface Methodology (RSM) gives a better efficient way for predictive response y.

RSM is also the form of the relationships between several independent variables and one or more response variables, and it's the model for both linear and nonlinear function model. Montgomery (2005) described that if the response is well modeled by a linear function of the independent variables, then the approximating function is the first-order model as Equation1. If there is curvature in the system, then a polynomial of higher degree must be used the second-order model which can solve nonlinear function problems as Equation (2).

$$y = \beta_0 + \sum_{i-1}^{k} \beta_i x_i + \sum_{i=1}^{k} \beta_{ii} x_i^2 + \sum_{i<j} \sum_{2}^{k} \beta_{ij} x_i x_j + \in \qquad (2)$$

RSM can be used experiment data to determine and simultaneously satisfy a set of desired specifications. Recently, a number of new prediction design models have been introduced, some involving the application of Artificial Neural Networks (ANN).

ANN is a massively interconnected network structure consisting of many simple processing elements (neurons) capable of performing parallel computation for data processing. ANN is designed to simulate data acquisition and processing of the human brain. ANN is able to learn and to generalize relations between input and output data from examples presented to the network. ANN can easily model nonlinear relationships between the response and the independent variables. In addition, ANN has elasticity so that they can be updated with new data (Bas and Boyaci, 2007).

The strength of ANN is pattern recognition and pattern classification, but these programs can also be used for predictive purposes (Dayhoff 1990). ANN is used in various fields such as in industrial process control, speech recognition, financial market forecasts and chemical compound identification (Nelson and Illingworth, 1991). In addition, the main advantage in using ANN for prediction is that there are the hidden learning relations in its neural architecture which cannot be in traditional mathematical term (Brey *et al.,* 1996).

Nowadays, there are many researches that compare the estimation capabilities between RSM and ANN. García-Gimeno *et al.* (2004) predicted growth rate, lag-time, and maximum population density of Leuconostoc mesenteroides under aerobic and

anaerobic conditions. This study used ANN to compare with RSM. The individual ANN model developed reliable estimates of these kinetic parameters studied, with SEP values ranged between 2.82% and 14.60%, betters than those of RSM model (17.62-27.63%). Lou and Nakai (2001), who studied of bacterial growth in a simulated medium of modified-atmosphere-packed cooked meat products, also supported that the accuracy of ANN model prediction was higher than that of RSM. Accordingly, in this research, the plastic injection molding process was optimized their process conditions by using the ANN model as well.

4. Artificial Neural Network (ANN) model

4.1 History of ANN

According to Hagan *et al.* (1996), the modern view of neural networks began in the 1940s with the work of Warren McCulloch (neurobiologist) and Walter Pitts (statistician), who showed that networks of artificial neurons could, in principle, compute any arithmetic or logical function. Their work is often acknowledged as the origin of the neural network field. In 1949, Donald Hebb (psychologist) proposed a mechanism for first learning law in biological neurons called *Hebbian Learning Rule*.

The first practical application of artificial neural networks came in the 1958, with the invention of the *perceptron network and associated learning rule* by Frank Rosenblatt. Rosenblatt and his colleagues built a perceptron network and demonstrated its ability to perform pattern recognition. This early success generated a great deal of interest in neural network research. Unfortunately, it was later shown that basic perceptron network could solve only a limited class of problems.

At about the same time, Bernard Widrow and Ted Hoff introduced a new learning algorithm and used it to train *adaptive linear neural networks (ADALINE)*, which is still in use today. Nevertheless, Marvin Minsky and Seymour Papert published a book in limitations of both Rosenblatt's and Widrow's networks. Although Rosenblatt and Widrow were aware of these limitations, they were not able to successfully modify their learning algorithms to train the more complex networks. Many people, influenced

by Minsky and Papert, believed that further research on neural networks was dead end and neural network research was largely suspended for a decade.

During the 1980s, new personal computers and workstations became widely available. Two new concepts were most responsible for the rebirth of neural networks. The first was the use of statistical mechanics to explain the operation of a certain class of *recurrent network*, which could be used as an associative memory. Second was the *backpropagation algorithm* for training multilayer perceptron networks, which was discovered independently by different researchers. The most influential publication of the backpropagation algorithm was by David Rumelhart and James McClelland because it was the answer to the criticisms Minsky and Papert had made in 1960s.

4.2 Basic concept of ANN

ANNs have emerged from studies of how human and animal brains perform operations. The human brain is made up of many millions of individual processing elements, called neurons, which are highly interconnected (Page et al., 1997). A schematic diagram of biological neurons is shown in Figure 8.

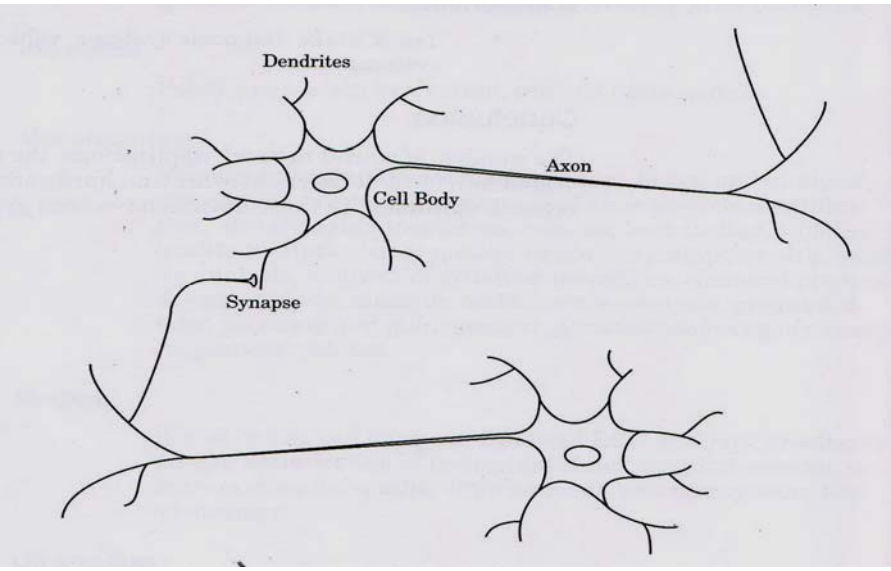

Figure 8 Schematic diagram of biological neurons

Source: Hagan *et al.* (1996)

It is a simple processing unit which receives and processes the signal from other neurons through its input paths called *dendrites*. An activity of a neuron is an 'all-or-none' process. If the combined signal is strong enough, it generates the output signal to its output path (called *axon*) which splits up and connects to other neurons' input paths through a junction referred to as a synapse. The amount of signals transferred depends on the synaptic strength of the junction which is chemical in nature. This synaptic strength is found to be modified during the learning process of the brain, therefore, it can be considered as a memory unit of each interconnection (Dagli, 1994).

4.3 Network Architecture

Visualize neuron is often arranged in layers. Typically, neurons have a same manner in the same layer. Key factors in determining the behavior of a neuron are its activation function and the pattern of weighted connections over which it sends and receives signals. Within each layer, neural usually have the same activation function and the same pattern of connections to other neurons. It means if any neuron in a layer is connected to a neuron in another layer, then each hidden unit is connected to every output neuron (Fausett, 1994).

Sivanandam *et al.* (2006) stated that there are various types of network architecture: Feed forward, feedback, fully interconnected net, competitive net, etc. In feed forward networks may have a single layer of weights where the inputs are directly connected to the outputs as Figure 9, or multiple layers with intervening sets of hidden units as Figure 10. Neural Networks use hidden unit in multiple layers net to create internal representations of the input patterns. So, it is possible to approximate arbitrarily any function with a simple feed forward network which can be used to solve more complicated problems.

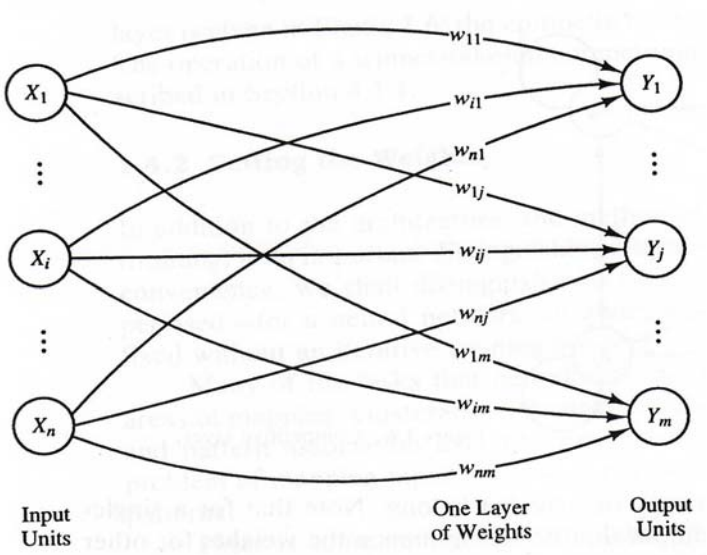

Figure 9 A single-layer neural network

Source: Fausett (1994)

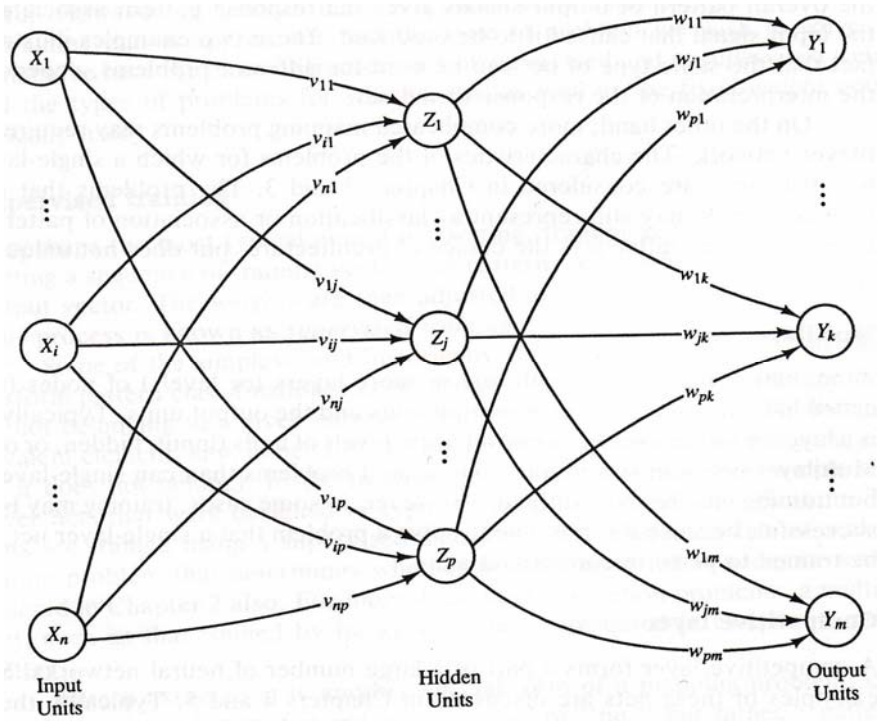

Figure 10 A multiple-layer neural network

Source: Fausett (1994)

4.4 Transfer Functions (Activation Functions)

The transfer function (*f*) may be a linear or a nonlinear function of n (or x). A particular transfer function is chosen to satisfy some specification of the problem that the neuron is attempting to solve. There are three functions that commonly use for transfer function as follow.

4.4.1 Hard Limit Transfer Function

The hard limit transfer function sets the output of the neuron to 0 if the function argument is less than 0, or 1 if its argument is greater than or equal to 0 as shown in Figure 11 and Equation (3). It is used extensively in Perceptron learning rule.

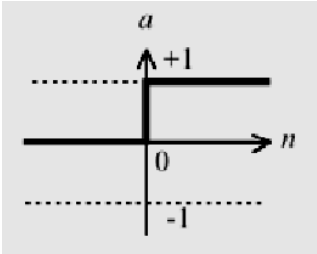

$$a = \text{hardlim}(n) \text{ or } f(x) = \begin{cases} 1 \text{ if } x \geq \theta \\ 0 \text{ if } x < \theta \end{cases} \qquad (3)$$

Figure 11 Hard limit transfer function

Source: Hagan *et al.* (1996)

4.4.2 Linear Transfer Function

Linear transfer function (purelin) is a function that the relationship between input and output is a linear. So, the output of a linear transfer function is equal to its input (f(x) = x). The output (a or f(x)) versus input characteristic of a single-input linear neuron is shown on Figure 12 and Equation (4). Neurons with this transfer function are used in the ADALINE networks.

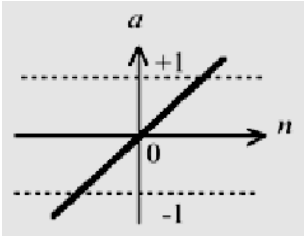

$$a = \text{purelin}(n) \text{ or } f(x) = x; \text{ for all } x \qquad (4)$$

Figure 12 Linear transfer function

Source: Hagan *et al.* (1996)

4.4.3 Sigmoid Transfer Function

Sigmoid functions are usually S-shaped curves. These are used in multiple layer nets like backpropagation network. There are two main types of sigmoid functions: binary sigmoid and bipolar sigmoid (Sivanandam et al., 2006).

4.4.3.1 Binary sigmoid

Binary sigmoid is also called logistic function (logsig). It ranges between 0 and 1 as Equation (5).

$$f(x) = \frac{1}{1 + \exp(-\sigma x)} \qquad (5)$$

where, σ is called the steepness parameter.

4.4.3.2 Bipolar sigmoid

Bipolar sigmoid is related to the hyperbolic tangent function (tansig), which is also often used as the transfer function when the desired range of output values is between -1 and 1. The bipolar sigmoid function is given as Equation (6).

$$f(x) = \frac{1 - \exp(-\sigma x)}{1 + \exp(-\sigma x)} \qquad (6)$$

Figure 13 shows the binary sigmoid function (logsig) and Figure 14 shows the bipolar sigmoid function (tansig).

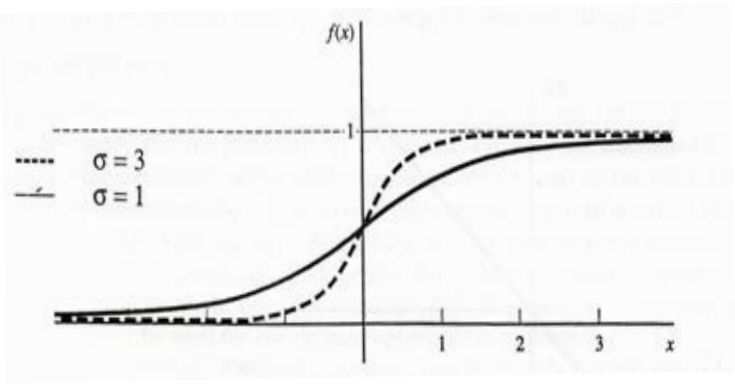

Figure 13 Binary sigmoid function

Source: Fausett (1994)

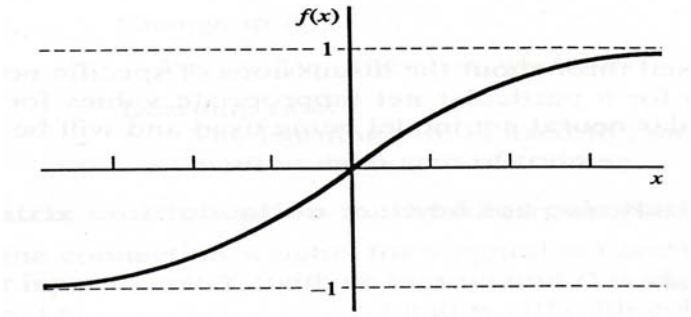

Figure 14 Bipolar sigmoid function

Source: Fausett (1994)

4.5 Bias

A bias acts exactly as a weight on a connection from a unit whose activation is always 1. Increasing the bias increases the net input to the unit ($b = w_0$). The bias improves the performance of the neural network. Similar to initialization of weights, bias should also be initialized either to 0, or to any specified value, based on the neural net. When bias is present as Figure 15, then net input is calculated as Net = $b + \sum x_i w_i$.

Where, "Net" is net input, "*b*" is bias, "x_i" is input from neuron i, and "w_i" is weight of neuron i to the output neuron. Hence, if bias is included, the transfer function is obtained as Equation (7).

$$f(Net) = \begin{cases} +1; if\ \_net \geq 0; \\ -1; if\ \_net < 0. \end{cases} \quad (7)$$

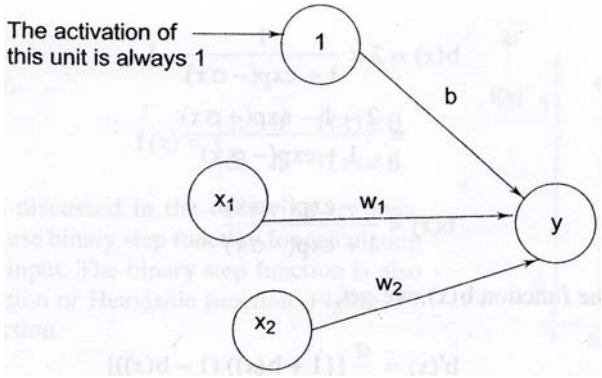

Figure 15 A simple net with bias

Source: Sivanandam *et al.* (2006)

4.6 Learning Rule

Learning rule is a procedure for modifying the weights and biases of a network. The purpose of the learning rule is to train the network to perform some task. There are three broad types of neural network learning rules: supervised learning, unsupervised learning, and reinforcement learning (Hagan et al., 1996).

4.6.1 Supervised Learning

In supervised learning, the learning rule is provided with a set of examples (the training set) of proper network behavior. As the inputs are applied to the network, the network outputs are compared to the targets. The learning rule is then used to adjust the weights and biases of the network in order to move the network outputs closer to the targets as shown in Figure 16.

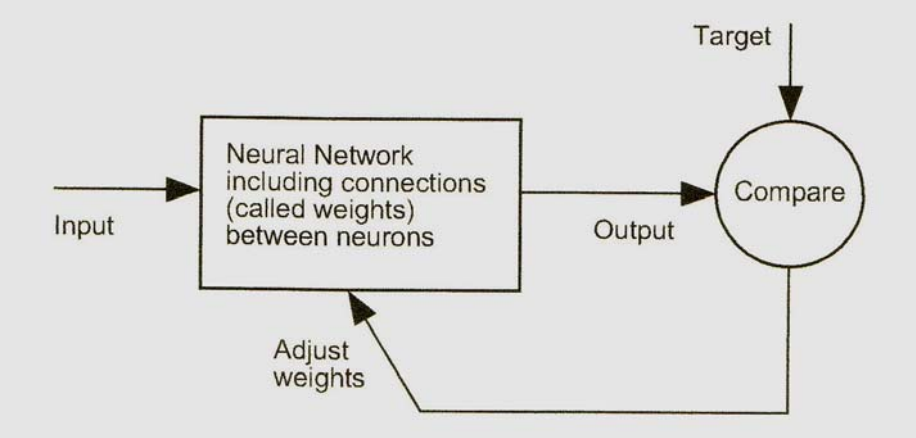

Figure 16 Supervised learning method.

Source: Demuth and Beale (2003)

Perceptron learning rule, Hebbian Learning Rule, Widrow-Hoff Learning Rule, and Backpropagation are all fall in this supervised learning type.

4.6.2 Reinforcement Learning

Reinforcement learning is similar to supervised learning, except that, in stead of being provided with the correct output for each network input, the algorithm is only given a grade. The grade is a measure of the network performance over some sequence of inputs. This type of learning is currently much less common than supervised learning. It appears to be most suited to control system applications.

4.6.3 Unsupervised Learning

In unsupervised learning, the weights and biases are modified in response to network inputs only. There are no target outputs available. The way to train a network is to categorize the input patterns into a finite number of classes. This is especially useful in such applications as vector quantization. Demuth and Beale (2003) explained that unsupervised networks can be used, for instance, to identify groups of data. Certain kinds of linear networks and Hopfield networks are designed directly.

For creating a network, first, recall that the number of inputs to the network and the number of outputs from the network are defined by external problem specifications. So if there are four external variables to be used as inputs, there are four inputs to the network. Similarly, if there are to be seven outputs from the network, there must be seven neurons in the output layer. Finally, the desired characteristics of the output signal also help to select the transfer function for the output layer. If we have more than two layers, here the external problem does not tell you directly the number of neurons required in the hidden layers. In fact, there are few problems for which one can predict the optimal number of neurons needed in a hidden layer. This problem is an active area of research which will be developed by using Backpropagation (Hagan *et al.*,1996).

4.7 Back propagation network (BPN)

Sivanandam *et al.* (2006) define that back propagation is a systematic method for training multilayer ANN. It is a multilayer forward network using gradient-descent base delta-learning rule, commonly known as back propagation of errors rule. BPN provides a computationally efficient method for changing the weights in a feed forward network, with differentiable transfer function units, to learn a training set of input-output examples.

4.7.1 Architecture of BPN

A multilayer neural network with one layer of hidden units (the Z units) is shown in Figure 17. The output units (the Y units) and the hidden units also may have biases. The bias on a typical output unit Y_k is denoted by w_{ok}; the bias on a typical hidden unit Z_j is denoted v_{oj}. These bias terms act like weights on connections from units whose output is always 1. From Figure 17, only the direction of information flow for the feedforward phase of operation. During the backpropagation phase of learning, signals are sent in the reverse direction (Fausett, 1994).

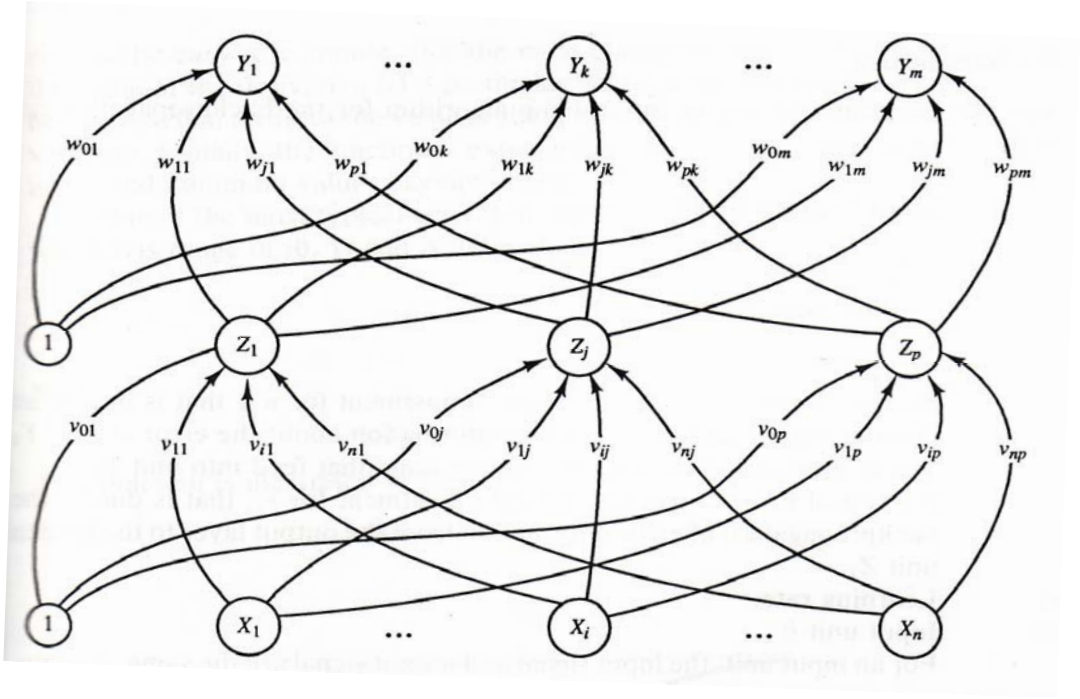

Figure 17 A multiple-layer neural network with one layer of hidden units

Source: Fausett (1994)

4.7.2 Training Algorithm

The training algorithm of back propagation involves four stages including initialization of weights, feed forward, back propagation of errors, and updating of the weights and biases (Sivanandam *et al.,* 2006).

1.) During the initialization of weight, some small random values are assigned.

2.) During feed forward stage each input unit (X_i) receives an input signal and transmits this signal to each of the hidden units Z_1 … Z_p. Each hidden unit then calculates the transfer function to form the response of the net for the given input pattern.

3.) During back propagation of errors, each output unit compares its computed activation Y_k with its target value T_k to determine the associated error for that pattern with that unit. Based on the error, the factor δ_k (k=1,…,m) is computed and is

used to distribute the error at output unit Y_k back to all units in the previous layer. Similarly, the factor δ_j (j=1,…,p) is computed for each hidden unit Z_j.

4.) During final stage, the weight and biases are updated using the δ factor and the activation.

The training algorithm used in the back propagation network is as follows (Sivanandam *et al.,* 2006).

Initialization of weight

Step 1: Initialization weight to small random values.

Step 2: While stopping condition is false, do step 3-10.

Step 3: For each training pair do step 4-9.

Feed forward

Step 4: Each input unit receives the input signal x_i and transmits this signals to all units in the layer above i.e. hidden units.

Step 5: Each hidden unit (z_j, j =1,…,p) sums its weighted input signals.

$$z_{inj} = v_{oj} + \sum_{j=1}^{p} z_j v_{ij}$$

applying transfer function $Z_j = f(z_{inj})$ and sends this signal to all units in the layer above i.e. output units.

Step 6: Each output unit (y_k, k=1,…,m) sums its weighted input signals

$$y_{ink} = w_{ok} + \sum_{k=1}^{m} y_k w_{jk}$$

and applying its transfer function to calculate the output signals.

$Y_k = f(y_{ink})$

Back propagation of errors

Step 7: Each output unit (y_k, k = 1,…,m) receives a target pattern corresponding to an input pattern, error information term is calculated as

$\delta_k = (t_k - y_k)\, f(y_{-ink})$

Step 8: Each hidden unit (z_j, j = 1,…,n) sums its delta inputs from units in the layer above

$$\delta_{-inj} = \sum_{k=1}^{m} \delta_j w_{jk}$$

The error information term is calculated as $\delta_j = \delta_{-inj}\, f(z_{-inj})$

Updating of weight and biases

Step 9: Each output unit (y_k, k = 1,…,m) updates its bias and weights (j = 0,…,p). The weight correction term is given by

$\Delta W_{jk} = \alpha \delta_k z_j$

and the bias correction term is given by

$\Delta W_{ok} = \alpha \delta_k$

Therefore, $W_{jk}(new) = W_{jk}(old) + \Delta W_{jk}$,

$W_{ok}(new) = W_{ok}(old) + \Delta W_{ok.}$

Each hidden unit (z_j, j = 1,…,p) updates its bias and weights (i = 0,…,n). The weight correction term is given by

$\Delta_{Vij} = \alpha \delta_j x_i$

and the bias correction term is given by

$\Delta V_{oj} = \alpha \delta_j$

Therefore, $V_{ij}(new) = V_{ij}(old) + \Delta V_{ij}$,

$V_{oj}(new) = V_{oj}(old) + \Delta V_{oj}.$

Step 10: Test the stopping condition. The stopping condition may be the minimization of the errors, number of epochs etc.

4.8 Literature Review of predictive process conditions by using ANN model

Chakraborty (2005) presented artificial neural network (ANN) model in term of prediction in fiber reinforced plastic (FRP) composite laminates. The work aimed at developing an ANN model for detection of size of delamination, its shape, and location

in FRP composite laminates by using natural frequencies as inputs and corresponding size, shape, and location of delamination as outputs of the network. In this case, there were 201 finite element models which 165 data sets choose for training with back propagation neural (BPN) network and 36 data sets keep for future testing. The network architecture had 10 input nodes, 9 hidden layers, and 3 output nodes (size, shape, and location). The results of prediction were the delaminated size and shape almost accurately with very little error, but the network couldn't provide for different location of delamination for training.

Shen *et al.* (2005) studied the effect of V-ribbed belt pulley system parameters on the contact mechanics, temperature and aging on belt material. They use a neural network based hyper-elastic material model to find the better performance of strain energy functions and used ABAQUS software to characterize belt rubber and its implement. At first, they collected the test data and train them by a feedforward neural network. Then the neural network could present the strain function of the belt material. After that, they used ABAQUS user subroutine to implement its model. From their study, there were many factors that contribute to the loss of drive transmission efficiency and increase of belt ware of V-ribbed belt. These factors included the influence of belt and pulley groove wedge angle, the affect of pulley diameter, the properties of belt materials, and the higher temperature that belts work under. They also represented that aging caused belt to lose some of their flexibility and accelerate belt fatigue.

Sadeghi (2000) builded a back-propagation 4-2-3 neural network predictor model for plastic injection molding process which was taken from simulation under the main CAE software to shorten the time in finding the optimum process conditions. The plastic injection part for simulations was backside body of CASIO scientific calculator fx-570s with a minimum thickness of 1 mm. This neural network model was able to predict the quality of injected parts in terms of lack or existence of short shot or weld line defect phenomenon based on melt flow rate (MFR) as in different injection material grades and three key process parameters (mold temperature, melt temperature, and injection pressure). Likewise, the model also gave the results on actual injection pressure and filling time which were higher in the material with lower MFR.

5. Genetic Algorithm (GA)

5.1 Basic concept of GA

Genetic Algorithm (GA) is a useful algorithm for optimizing solutions to problems; especially those that are analytically intractable. They are inspired by the biological theory of evolution through natural selection (Foran, 2002). Goldberg (1989) stated that GA starts with an initial set of random solutions called population. Each individual in the population is called chromosome. GA creates a set of artificial chromosomes representing the value of variable and reproduces a new generation by using bits and pieces of the fittest of the old and introducing new bits and pieces for better measure.

GA uses three main types of rules at each step to create the next generation from the current population (The MathWorks, 2007):

1.) Selection rules select the individuals, called parents that contribute to the population at the next generation.

2.) Crossover rules combine two parents to form children for the next generation.

3.) Mutation rules apply random changes to individual parents to form children.

5.2 General structure of GA

The general structure of GA presents on a population of problem solutions that is maintained in the form of chromosomes. These chromosomes are string encoding problems solutions. Gen and Cheng (1997) describe that chromosomes evolve through successive iterations, called generations. During each generation, the chromosome is evaluated, using some measure of fitness. To create the next generation, new chromosome, called offspring, are formed by either merging two chromosomes from current generation using a crossover operator or modifying a chromosome using a mutation operator. A new generation is formed by two terms: i) selecting, according to

the fitness values, some of the parents and offspring, and ii) rejecting others so as to keep the population size constant. Fitter chromosomes have higher probabilities of being selected. After several generations, the algorithms converge to the best chromosome, which hopefully represents the optimum or sub optimal to the problem. The general structure of GA is shown on Figure 18.

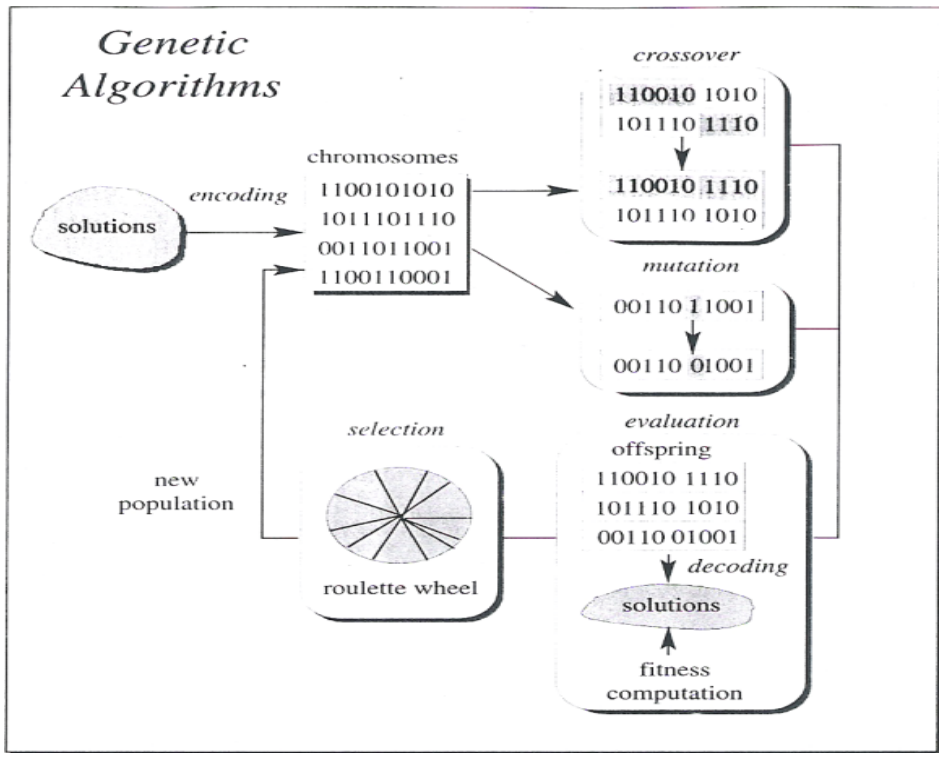

Figure 18 A general structure of GA

Source: Gen and Cheng (1997)

5.3 Example of GA for optimization problem

This section explains in detail about how a GA is applied to optimization problem (Mitsuo and Runwei, 1996). For example, the numerical of unconstrained optimization problem is given as follow:

$$\max f(x_1,x_2) = 21.5 + x_1 sin(4\pi x_1) + x_2 sin(20\pi x_2) \qquad (8)$$

$$-3.0 \le x_1 \le 12.1$$

$$-4.1 \le x_2 \le 5.8$$

5.3.1 Representation (Encoding)

Conventional GA, decision variables have to be encoded to binary strings. The length of the string depends on the required precision. For example, the domain of variable x_j is $[a_j, b_j]$ and required precision is five places after the decimal point. The precision requirement implies that the range of domain of each variable should be divided into at least $(b_j - a_j) \times 10^4$ size ranges. The required bits (denoted with m_j) for a variable is calculated as follow:

$$2^{m_j-1} < (b_j - a_j) \times 10^4 \leq 2^{m_j} - 1 \qquad (9)$$

The mapping from a binary string to a real number for variable x_i is straight forward and completed as follow:

$$x_j = a_j + decimal(substring_j) \times \frac{b_j - a_j}{2^{m_j} - 1} \qquad (10)$$

where *decimal (substring$_j$)* represents the decimal value of binary *substring$_j$* for decision variable x_j.

Suppose that the precision is set as five places after the decimal point. The required bits for variables x_1 and x_2 are calculated as follows:

$(12.1 - (-3.0)) \times 10^4 = 151{,}000$

$2^{17} < 151{,}000 < 2^{18}$, $\quad m_1 = 18$

$(5.8 - 4.1) \times 10^4 = 17{,}000$

$2^{14} < 17{,}000 \leq 2^{15}$, $\quad m_2 = 15$

m=m1+m2=18+15=33

The total length of a chromosome 33 is bits, which can be represented as follows:

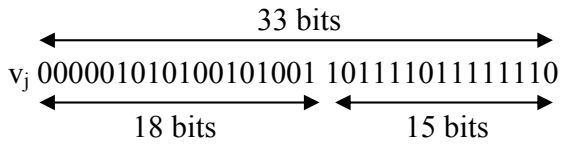

5.3.2 Decoding

The corresponding values for variables x_1 and x_2 are given as Table 2:

Table 2 The decimal number of the binary number

Binary Number	Decimal Number
x_1 000001010100101001	5417
x_2 101111011111110	24318

Source: Mitsuo and Runwei (1996)

$$x_1 = -3.0 + 5417 \times \frac{12.1-(-3.0)}{2^{18}-1} = -2.687969$$

$$x_2 = 4.1 + 24318 \times \frac{5.8-4.1}{2^{15}-1} = 5.361653$$

5.3.3 Initial population

Initial population is randomly generated as follows:

v_1 = [000001010100101001101111011111110]

v_2 = [001110101110011000000010101001000]

v_3 = [111000111000001000010101001000110]

v_4 = [100110110100101101000000010111001]

v_5 = [000010111101100010001110001101000]

v_6 = [111110101011011000000010110011001]

v_7 = [110100010011111000100110011101101]

v_8 = [001011010100001100010110011001100]

v_9 = [111110001011011000111010001111101]

v_{10} = [111101001110101010000010101101010]

The corresponding decimal values are:

$v_1 = [x_1, x_2]$ = [-2.687969, 5.361653]

$v_2 = [x_1, x_2] = [0.474101, 4.170144]$

$v_3 = [x_1, x_2] = [10.419457, 4.661461]$

$v_4 = [x_1, x_2] = [6.159951, 4.109598]$

$v_5 = [x_1, x_2] = [-2.301286, 4.477282]$

$v_6 = [x_1, x_2] = [11.788084, 4.174346]$

$v_7 = [x_1, x_2] = [9.342067, 5.121702]$

$v_8 = [x_1, x_2] = [-0.330256, 4.694977]$

$v_9 = [x_1, x_2] = [11.671267, 4.873501]$

$v_{10} = [x_1, x_2] = [11.446273, 4.171908]$

5.3.4 Evaluation

The process of evaluating the fitness of a chromosome consists of the following three steps:

Step 1: Convert the chromosome's genotype to its phenotype. Here, this means converting binary string into relative real values $x^k = \left(x_1^k, x_2^k\right)$, k = 1, 2, ..., *popsize*.

Step 2: Evaluate the objective function $f(x^k)$.

Step 3: Convert the value of objective function into fitness. For the maximization problem, the fitness is simply equal to the value of objective function $eval(v_k) = f(x^k), k=1, 2,\ldots, popsize.$

An evaluation function plays the role of the environment, and it rates chromosomes in terms of their fitness.

The fitness function values of above chromosomes are as follows:

$eval(v_1) = f$ (-2.687969, 5.361653) =19.805119

$eval(v_2) = f$ (0.474101, 4.170144) =17.370896

$eval(v_3) = f$ (10.419457, 4.661461) = 9.590546

$eval(v_4) = f$ (6.159951, 4.109598) = 29.406122

$eval(v_5) = f$ (-2.301286, 4.477282) = 15.686091

$\text{eval}(v_6) = f\,(11.788084, 4.174346) = 11.900541$

$\text{eval}(v_7) = f\,(9.342067, 5.121702) = 17.958717$

$\text{eval}(v_8) = f\,(-0.330256, 4.694977) = 19.763190$

$\text{eval}(v_9) = f\,(11.671267, 4.873501) = 26.401669$

$\text{eval}(v_{10}) = f\,(11.446273, 4.171908) = 10.252480$

Therefore, chromosome v_4 is the strongest one and that chromosome v_3 is the weakest one.

5.3.5 Selection

Selection process is used to select the some chromosome from parents and offspring to be the new population. There are many selection methods such as tournament selection, roulette wheel selection and ranking selection. These methods use the fitness value of each chromosome to decide whether it will survive or not. In most practices, a roulette wheel approach is adopted as the selection procedure; it belongs to the fitness-proportional selection and can select a new population with respect to the probability distribution based on the fitness values. The roulette wheel can be constructed as follows:

1.) Calculate the fitness value $eval(v_k)$ for each chromosome v_k:

$$eval(v_k) = f(x), \qquad k = 1, 2, \ldots, popsize \tag{11}$$

2.) Calculate the total fitness for the population

$$F = \sum_{k=1}^{popsize} eval(v_k) \tag{12}$$

3.) Calculate selection probability p_k for each chromosome v_k:

$$p_k = \frac{eval(v_k)}{F}, \qquad k = 1, 2, \ldots, popsize \tag{13}$$

4.) Calculate cumulative probability q_k for each chromosome v_k:

$$q_k = \sum_{j=1}^{k} p_j, \qquad k = 1, 2, \ldots, popsize \tag{14}$$

The selection process begins by spinning the roulette wheel equal to population size times; each time, a single chromosome is selected for a new population in the following way:

Procedure: Selection

Step 1: Generate a random number r form the range [0,1].

Step 2: If $r = q_1$, then select the first chromosome v_1; otherwise, select the k^{th} chromosome v_k ($2 \leq k \leq popsize$) such that $q_{k-1} < r \leq q_k$.

The total fitness Ftotal of the population is:

$$F = \sum_{k=1}^{10} eval(v_k) = 178.135372$$

The probability of a selection p_k for each chromosome v_k (j = 1,...,10) is as follows:

$p_1 = 0.111180$, $p_2 = 0.097515$, $p_3 = 0.053839$
$p_4 = 0.165077$, $p_5 = 0.088057$, $p_6 = 0.066806$
$p_7 = 0.100815$, $p_8 = 0.110945$, $p_9 = 0.148211$
$p_{10} = 0.057554$

The cumulative probabilities q_k for each chromosome v_k (k = 1,…,10) is as follows:

$q_1 = 0.111180$, $q_2 = 0.208695$, $q_3 = 0.262534$
$q_4 = 0.427611$, $q_5 = 0.515668$, $q_6 = 0.582475$
$q_7 = 0.683290$, $q_8 = 0.794234$, $q_9 = 0.942446$
$q_{10} = 1.000000$

Now we are ready to spin the roulette wheel 10 times, and each time we select a single chromosome for a new population. Let us assume that a random sequence of 10 numbers from the range [0,1] is as follows:

0.301431	0.322062	0.766503
0.881893	0.350871	0.583392
0.177618	0.343242	0.032685
0.197577		

The first number $r_1 = 0.301431$ is greater than q_3 and smaller than q_4, meaning that the chromosome v_4 is selected for the new population; the second number $r_2 = 0.322062$ is greater than q_3 and smaller than q_4, meaning that the chromosome v_4 is again selected for the new population; and so on. Finally, the new population consists of the following chromosomes:

$v'_1 = [10011011010010110100000010111001]$ (v_4)
$v'_2 = [10011011010010110100000010111001]$ (v_4)
$v'_3 = [00101101010000110001011001100]$ (v_8)
$v'_4 = [11111000101110110001110100011101]$ (v_9)
$v'_5 = [10011011010010110100000010111001]$ (v_4)
$v'_6 = [11010001001111100010011011101101]$ (v_7)
$v'_7 = [00111010111001100000001010100100]$ (v_2)
$v'_8 = [10011011010010110100000010111001]$ (v_4)
$v'_9 = [00000101010010100110111011111110]$ (v_1)
$v'_{10} = [00111010111001100000001010100100]$ (v_2)

5.3.6 Crossover

Crossover is the operator that randomly chooses a locus and exchanges the subsequences before and after that locus between two chromosomes to create two offspring. If the probability of crossover is set as $p_c = 0.25$, it can be expected that, on average, 25% of chromosomes undergo crossover. Crossover is performed in the following way:

Procedure: Crossover

begin
  k ← 0;
  while (k ≤10) *do*
    r_k ← random number from [0,1];
    if (r_k < 0.25) *then*
      select vk as one parent for crossover;
    end
    k ← k + 1;
  end
end

Assume that the sequence of random numbers is

0.625721	0.266823	0.288644
0.295114	0.163274	0.567461
0.085940	0.392865	0.770714
0.548656		

This means that the chromosomes v'_5 and v'_7 were selected for crossover. We generate random integer number *pos* from the range [1, 32] (because 33 is the total length of a chromosome) as cutting point or in other words, the position of the crossover point. Assume that the generated number *pos* equals to 1, the two chromosomes are cut after the first bit, and offspring are generated by exchanging the right parts of them as follows:

$v'_5 = [1 \mid 00110110100101101000000010111001]$
$v'_7 = [0 \mid 01110101110011000000010101001000]$

Then, the selected chromosome will be replaced with their resulting offspring as follows:

v'_5 = [1 01110101110011000000010101001000]

v'_7 = [0 00110110100101101000000010111001]

5.3.7 Mutation

Mutation operates on one individual (chromosome) at a time that makes the offspring very different from their parents by changing the value of some genes in chromosome randomly. For example in binary coding solutions, some genes are randomly selected and flipped from 1 to 0 and vise versa. From this operation, a population that is converging onto some optimum can jump into a different part of the solution space to get probability in detection the different optima that may be the global optimum.

The mutation rate (denoted by p_m) is defined as the percentage of the total number of genes in the population. The mutation rate controls the rate at which new genes are introduced into the population for trial. If it is too low, many genes that would have been useful are never tried out. But if it is too high, there will be much random perturbation. The offspring will start losing their resemblance to the parents, and the algorithm will lose the ability to learn from the history of the search.

Assume that the 18th gene of the chromosome v_1 is selected for a mutation. Since the gene is 1, it would be flipped into 0. Thus the chromosome after mutation would be

v_1 = [10011011010010110101000000010111001]

↓

v'_1 = [10011011010010110001000000010111001]

The probability of mutation is set as $p_m = 0.01$, so we expect that, on average, 1% of total bit of population would undergo mutation. There are $m \times popsize$ = 33 × 10 = 330 bits in the whole population; we expect 3.3 mutations per generation. Every bit has an equal chance to be mutated. Thus we need to generate a sequence of random numbers r_k (k = 1,…, 330) from the range [0, 1]. Suppose that the following genes in Table 3 will go through mutation:

Table 3 The position of mutated genes in mutated chromosomes

bit_pos	chrom_num	bit_no	random_num
105	4	6	0.009857
164	5	32	0.003113
199	7	1	0.000946
329	10	32	0.001282

Source: Mitsuo and Runwei (1996)

After replaced old chromosome with their mutated chromosome, we get the final population as follows:

v'_1 = [10011011010010110100000010111001]
v'_2 = [10011011010010110100000010111001]
v'_3 = [00101101010000110001011001100]
v'_4 = [11111100101110110001110100011101]
v'_5 = [10111010111001100000001010100101 0]
v'_6 = [11010001001111100010011001110 1101]
v'_7 = [10011011010010110100000010111001]
v'_8 = [10011011010010110100000010111001]
v'_9 = [00000101010010100110111011111110]
v'_{10} = [00111010111001100000001010100101 0]

The corresponding decimal values of variables [x_1, x_2] and fitness are as follows:

f(6.159951, 4.109598) = 29.406122
f(6.159951, 4.109598) = 29.406122
f(0.330256, 4.694977) = 19.763190
f(11.907206, 4.873501) = 5.702781
f(8.024130, 4.170248) = 19.91025
f(9.342067, 5.121702) = 17.958717

f(6.159951, 4.109598) = 29.406122
f(6.159951, 4.109598) = 29.406122
f(-2.687969, 5.361653) = 19.805119
f(0.474101, 4.170248) = 17.370896

This is completed one iteration of GA. The test run is terminated after 1000 generations. We have obtained the best chromosome, v*, in the 419th generation as follows:

v* = (11111000000011100011101001010110)
eval(v*) = f(11.631407, 5.724824) = 38.818208
x*1 = 11.631407
x*2 = 5.724824
f(x*1, x*2) = 38.818208

5.4 Example of GA for optimization problem based on Double Vector Population

Wongrat *et al.* (2005) presented on Wasanapradit's work on year 2000 that some methods in simple GA limit the performance of algorithm is poor. Thus, his thesis proposed new method for GA to improve performance described as follows:

5.4.1 Representation

The binary representation is easy to deal with genetic operators but it has some disadvantages when applied to multidimensional, high precision numerical problem. It requires long representation and is difficult to understand. Real number representation can deal with this problem and easy to understand. For example, the solution (chromosome) has 5 variables including x_1 = 4.5124, x_2 = 5.5819, x_3 = 1.9260, x_4 = 1.4560, and x_5 = 4.8545. The real number representation is [4.5124, 5.5819, 1.9260, 1.4560, 4.8545].

5.4.2 Crossover

Arithmetic crossover is used for crossover. This operator is defined as a linear combination of two vectors, which is modified to apply with real number representation. For example, if chromosome v_1 and v_2 are selected to be crossed, the resulting offspring are:

$$v'_1 = r \,.\, v_1 + (1 - r) \,.\, v_2 \quad (15)$$

$$v'_2 = r \,.\, v_2 + (1 - r) \,.\, v_1 \quad (16)$$

Where r is random number in interval [0,1]. For example, if v_1 = [4.5124, 5.5819, 1.9260, 1.4560, 4.8545], v_2 = [4.5279, 5.5727, 1.9239, 1.4627, 4.8514], and r = 0.6. The two new solutions (offspring) are as follows:

$$v'_1 = 0.6 \times [4.5124, 5.5819, 1.9260, 1.4560, 4.8545] +$$
$$(1 - 0.6) \times [4.5279, 5.5727, 1.9239, 1.4627, 4.8514]$$
$$v'_2 = 0.6 \times [4.5279, 5.5727, 1.9239, 1.4627, 4.8514] +$$
$$(1 - 0.6) \times [4.5124, 5.5819, 1.9260, 1.4560, 4.8545]$$
$$v'_1 = [4.5186, 5.5782, 1.9252, 1.4587, 4.8533]$$
$$v'_2 = [4.5217, 5.5764, 1.9247, 1.4600, 4.8526]$$

5.4.3 Mutation

This operator is also different from simple genetic algorithm. The multiposition mutation is used for mutation operator. Before explain this method, the uniform mutation will be introduced. The procedure of uniform mutation is the chromosome which is selected for undergoing mutated with the same strategy as simple GA. This operator requires a single parent v and produces a single offspring v′. The operator selects a random component $i \in (1, \ldots, n)$ of vector $v = [v_1,\ldots, v_i,\ldots, v_n]$ and produces $v' = [v_1, \ldots, v'_i, \ldots, v_n]$. Where v'_i is random value from the range $[v^L_i, v^U_i]$. Where v^L_i, v^U_i are lower and upper bound of variable v_i respectively. The mutated gene can be calculated as:

$$v_i^{'} = v_i^L + r(v_i^U - v_i^L) \quad (17)$$

r is random number from uniform probability distribution. For example, assume that the 3th gene of chromosome v = [4.5124, 5.5819, 1.9260, 1.4560, 4.8545] was selected for a mutation and r = 0.6. Lower and upper bound of the 3th gene of v is $[v^L_i, v^U_i]$ = [1.9160, 1.9360]. Thus, the mutated chromosome was calculated as follows:

$v'_3 = 1.9160 + 0.6 \times (1.9360 - 1.9160)$

$v'_3 = 1.928$

Then, $v' = [4.5124, 5.5819, 1.928, 1.4560, 4.8545]$

This paper we use multi-position mutation, the mutated chromosome will be set the amount and position of genes undergoing mutation by using mutation rate (P_m). After that, these genes were replaced with the new values by the same method as uniform mutation.

5.5 Steps combining GA method and ANN model

The combining GA method with ANN model for optimization algorithm is given in Figure 19. This hybrid GA and ANN system is started with the randomly generation of an initial population which contains a number of chromosomes. Each chromosome consists of a set of real coded on five process parameters of injection molding process. The fitness function based on the optimal ANN model is used to calculate the fitness for all initial population. Then, selection, crossover, and mutation are used to reproduce a new generation. This process is repeated until it reaches the maximum generation number or population convergence (Changyu *et al.,* 2007 and Mok *et al.,* 2001).

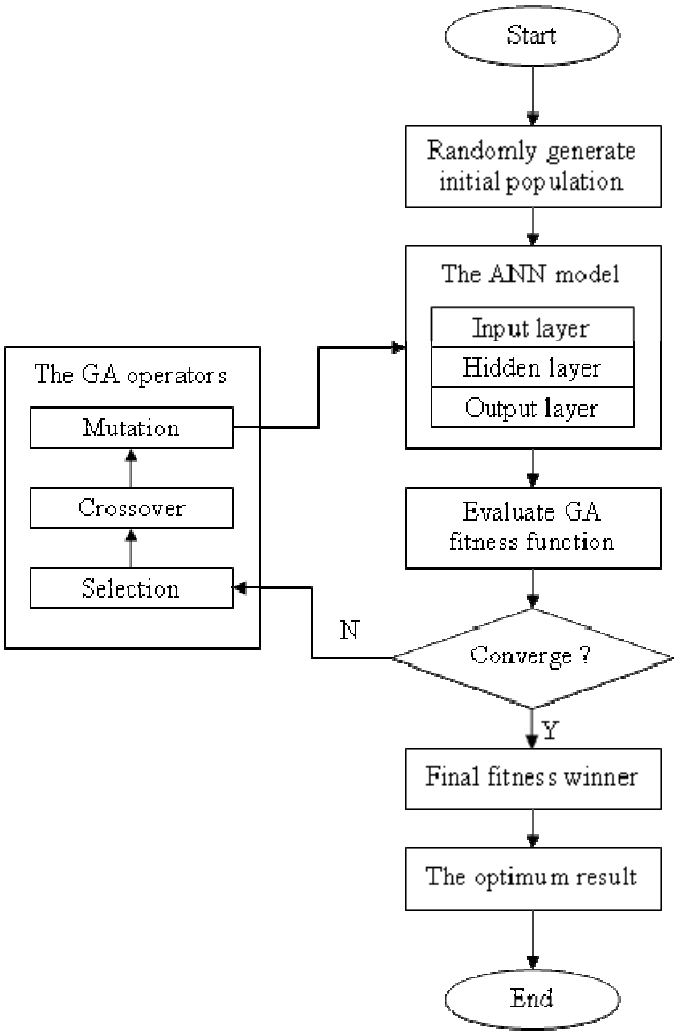

Figure 19 Steps of combining ANN and GA optimization

Source: Changyu *et al.* (2007) and Mok *et al.* (2001)

5.6 Literature Review of optimized process conditions by using ANN model with GA

Changyu *et al.* (2007) builded a back-propagation network (BPN) which was a typical artificial neural network (ANN) model to map the complex non-linear relationship between process conditions and quality index, and a genetic algorithm (GA) was used in the process conditions optimization with the fitness function based on an ANN model. They combined these tools together (ANN/GA) in order to improve quality index of the volumetric shrinkage variation in the plastic part. This plastic part was a top

cover of an industrial refrigerator. By using design of experiment (DOE) to select the significant process variables, there were five variables, which have significant influences on the volumetric shrinkage variation. These variables include melt temperature, mold temperature, injection time, packing time, and holding pressure. The optimization process condition results by GA were as follows: the melt temperature is 200°C, the mold temperature is 60°C, the injection time is 4.11 seconds, the packing time is 10.8 seconds, and the holding pressure is 34.42 MPa. The volumetric shrinkage variation under the optimized process condition was 0.487, the reciprocal of the maximum fitness.

Ozcelik and Erzurumlu (2006) investigated an efficient optimization methodology of plastic injection processes by using artificial neural network (ANN) and genetic algorithm (GA). The aim of their study was to minimize warpage of thin shell plastic parts. To achieve the minimum warpage, an appropriate process condition seven parameters were determined. These parameters included mold temperature, melt temperature, packing pressure, packing time, runner type, gate location, and cooling time. The effects of these process parameters were exploited using design of experiments (DOE), Taguchi orthogonal array and finite element software. From finite element analysis results based on analysis of variance (ANOVA), the most important process parameters were packing pressure, mold temperature, melt temperature, packing time, and cooling time, respectively. Later on, they used artificial neural network methodology to reduce the computational cost and to find the optimum of these five important process parameter values. After optimization, warpage was improved by 51%.

MATERIALS AND METHODS

Materials

Two types of materials were used in this research and they can be categorized into two groups as summarized in the following.

1. Hardware equipment

1.1. Computer (Intel Pentium M processor 740)

1.2. Injection molding machine

1.2.1 Battenfeld 1300/400 BK for the rectangular lid

1.2.2 Battenfeld 2000/630 BK for the roof tile

1.3. Molds: the rectangular lid and the roof tile

1.4. Stress viewer

1.5. Dial gauge

2. Software programs

2.1. Moldflow Plastics Insight (MPI, version 6.1): this software was used to simulate the plastic injection molding process.

2.2. Minitab version 14: this software was used for supporting DOE technique to identify significant parameters that affect the products' quality.

2.3. MATLAB version 7.1: this software was used for building a neural network model and a genetic algorithm to train and test data for optimizing processing conditions.

Methods

In order to achieve the optimization of the plastic injection molding process of the rectangular lid and the roof tile with minimum residual stress and minimum warpage, respectively, there were many tasks that have to be undertaken in these two cases. First, the simulation models of the rectangular lid and the roof tile were both created with mesh geometry by MPI 6.1 and run for the results. Then, verifying the accuracy of these

simulation models by comparing their results with the actual testing results. A Fractional Factorial design was then used to find the significant parameters in the injection molding process according to the simulation results. Next, the processing conditions relationships in both cases were determined by using the Artificial Neural Network (ANN) model. Genetic Algorithm (GA) was then used to optimize the processing condition in terms of minimum residual stress in Case 1 and minimum warpage in Case 2. Finally, the optimized processing conditions were applied to mold the actual parts. The optimized molded part was then compared in terms of the quality and cycle time to the original molded part. These five steps are shown in Figure 20.

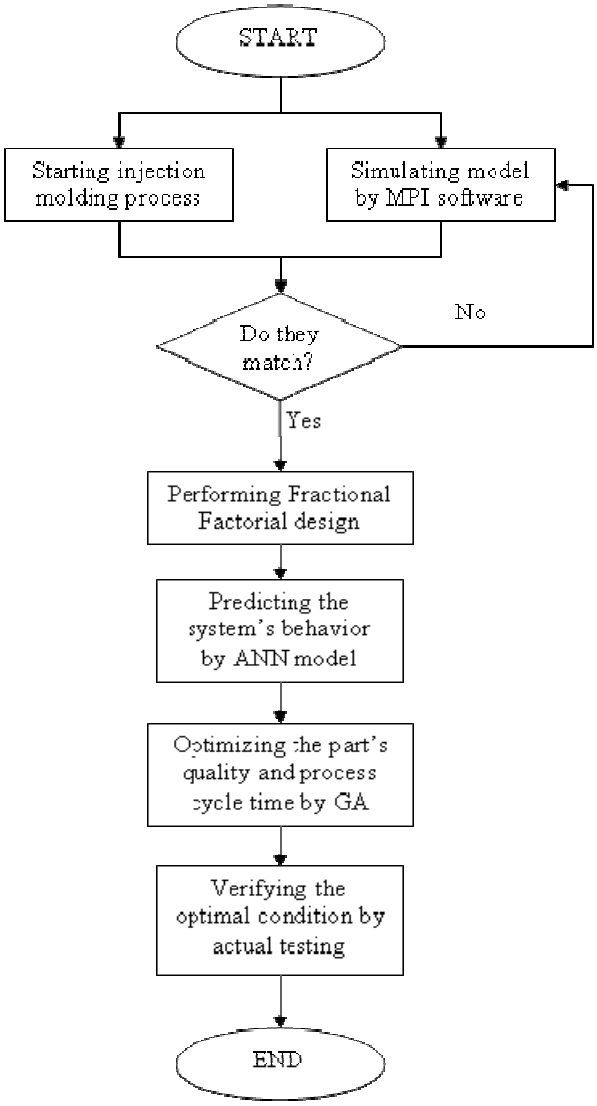

Figure 20 Steps of methodology

1. Starting the injection molding process

There were many variables to be considered before starting the injection molding process. These include the injection molding machine, the mold, the plastic part, the material used, and the process parameters.

1.1 Starting the injection molding process of the rectangular lid (Case 1)

1.1.1 Descriptions of the injection molding process of the rectangular lid

For the rectangular lid production (Case 1), a horizontal plastic injection machine manufactured by Battenfeld, Model 1300/400BK was used. An injection mold made of NAK80 steel was used. Descriptions of the molded part are shown in Table 4.

Table 4 Properties of the injection molding machine, the mold material, and the molded part in Case 1

Specification of the injection molding machine (Battenfeld Model 1300/400 BK)	
Maximum machine injection stroke (mm)	160
Maximum machine injection rate (cm^3/s)	107
Machine screw diameter (mm)	40
Maximum machine hydraulic pressure (MPa)	17.5
Maximum machine clamp force (tonne)	132.5
Properties of the mold material	
Material type	Steel NAK80
Mold thermal conductivity (W/m-°C)	41.3
Mold coefficient of thermal expansion (1/°C)	1.13×10^{-5}
Elastic modulus (MPa)	207,000
Descriptions of the molded part	
Product name	Rectangular lid
Material type	PS
Material trade name	Styron 656D

1.1.2 Determine the sample treatments of the rectangular lid

Numerical experiments had been conducted based on the two sample treatment conditions as shown in Table 5.

Table 5 Two treatment conditions of the rectangular lid

Process parameters	Condition 1	Condition 2
Mold temperature (°C)	35	35
Melt temperature (°C)	228	228
Injection speed (%)	40	45
Injection stroke (mm.)	60	60
Packing pressure (MPa)	4	4.5
Packing time (sec.)	2	1.8
Cooling time (mm.)	15	15

From Table 5, Condition 1 was the first processing condition used to injection mold the plastic product. Condition 2 was the processing condition in production by using the trial and error method from the manufacturer. In this study, these two conditions were used for the pattern comparison between the residual stress of the actual plastic part and the simulation model.

1.1.3 Residual stresses analysis of the rectangular lid

Residual stresses are the stresses that exist in structural sections in their unloaded state. These residual stresses can be the cause of premature part failure in service or of part warpage and distortion. In this research, the analysis of the residual stresses of the plastic parts was performed qualitatively using an instrument named "Stress Viewer". The result of the residual stress of the rectangular lid is displayed in Figure 21.

Figure 21 Residual stress analysis by using Stress Viewer

The residual stresses displayed by Stress Viewer indicate by different colors. It was found that the residual stresses mostly occur in the central area of the part, which can be seen by the different colors. This is due to the effect of the high injection pressure and molecular orientation in this area. Therefore, the comparison method between product from actual plastic product and from the simulation model was point out on their pattern and their size of the circle in the central area.

1.2 Starting the injection molding process of the roof tile (Case 2)

1.2.1 Compositions of injection molding process of the roof tile

For the roof tile production (Case 2), a horizontal plastic injection machine manufactured by Battenfeld model 2000/630BK was used. A injection mold made of S50C steel was used. Descriptions of the molded part are shown in Table 6.

Table 6 Properties of the injection molding machine, the mold material, and the molded part in Case 2

Specififcation of the injection molding machine (Battenfeld 2000/630 BK)	
Maximum machine injection stroke (mm)	180
Maximum machine injection rate (cm^3/s)	169.9
Machine screw diameter (mm)	40
Maximum machine hydraulic pressure (MPa)	17.5
Maximum machine clamp force (tonne)	203.88
Properties of the mold material	
Material type	Steel S50C
Mold thermal conductivity (W/m-°C)	24.3
Mold coefficient of thermal expansion (1/°C)	1.24×10^{-5}
Elastic modulus (MPa)	200000
Descriptions of the molded part	
Product name	Roof tile
Material type	HDPE
Material trade name	Thai-Zex 1600J

1.2.2 Determine the sample treatment of the roof tile

The conditions tested for model validation were (i) processing condition in production by manufacturer and (ii) other two sample conditions. The numerical conditions of these three samples are shown in Table 7.

Table 7 Three treatment conditions of the roof tile

Process parameters	Processing Condition in Production	Sample 1	Sample 2
Mold temperature (°C)	35	35	35
Melt temperature (°C)	160	140	180
Injection speed (%)	58	30	30
Injection stroke (mm)	170	170	170
Packing pressure (MPa)	5.5	4.0	8.0
Packing time (sec)	1.5	2.0	1.0
Cooling time (mm)	50	40	60

1.2.3 Warpage analysis of the roof tile

Warpage is a part defect caused by a non-uniform change of internal stresses. This warpage can be the cause of the poor product's quality. In this research, the analysis of warpage in plastic product, which focused on z-axis, was performed by measuring the z-axis deflection using a dial guage. The roof tile with warpage in z-axis is displayed in Figure 22.

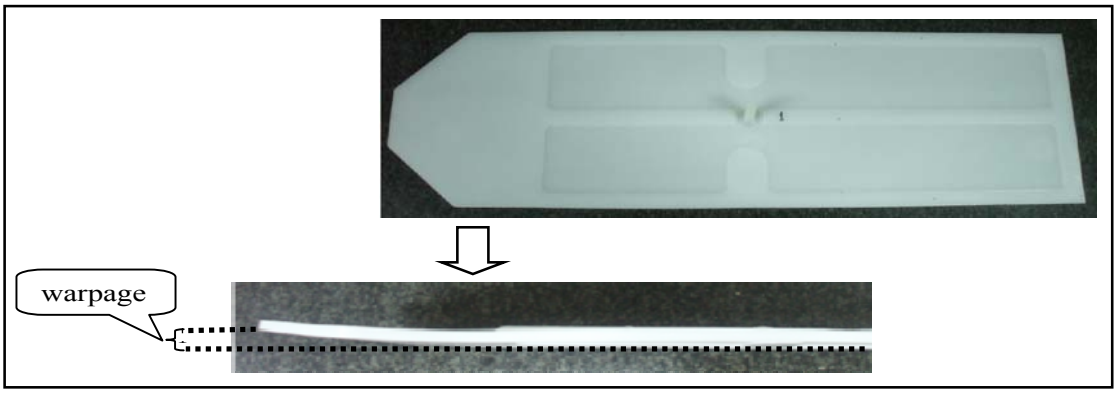

Figure 22 Warpage of the roof tile

2. Simulation model by Moldflow Plastic Insight 6.1 (MPI 6.1)

In the rectangular lid (Case 1) and the roof tile (Case 2), although application of the simulation model can reduce the setup time, production time and cost, it is imperative to verify the results by comparing to those measured by the actual injection molding testing provided by the manufacturer. Thus, the rectangular lid was taken to compare the residual stress results between the FE model and actual testing regarding on their patterns. The roof tile was taken to compare the warpage results between the FE model and actual testing.

2.1 Simulation model of the rectangular lid (Case1)

2.1.1 Finite element model of the rectangular lid

In this study, the finite element (FE) analysis of the rectangular lid was performed to validate the model using MPI 6.1. Geometry of the rectangular lid utilized in the research is shown in Figure 23. The part has the width, length, height, and thickness of 101 mm, 235 mm, 25.5 mm, and 2.5 mm, respectively. For the rectangular lid, the FE model consists of 8,798 elements with the maximum aspect ratio of 10, the match ratio of 90%, and the reciprocal ratio of 84%.

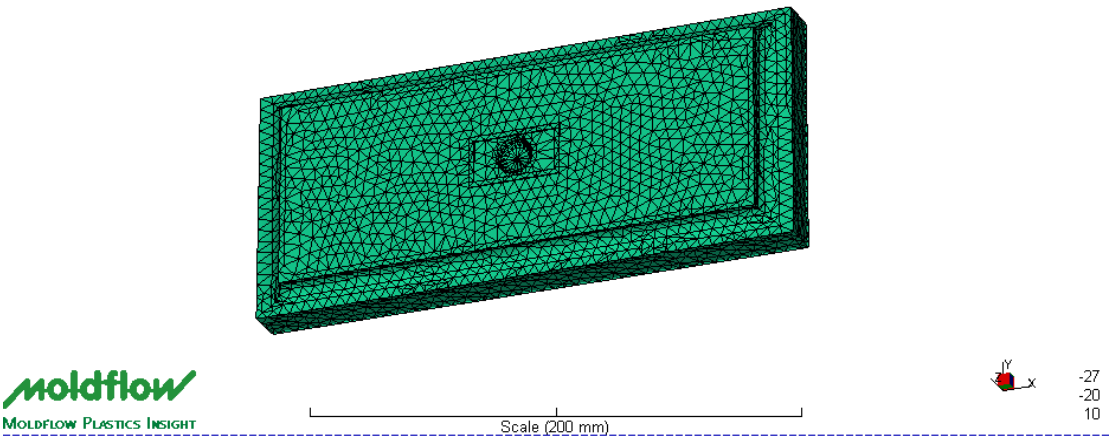

Figure 23 The mesh geometry of the rectangular lid

2.1.2 Material selection of the rectangular lid

In the experimental stage, the rectangular lid was made of RS from Dow Chemical (Styron 656D). However, it was not available on the materials database of MPI software. Thus, similar material types, Styron 666D and 678D, were used. These two materials were tested for the substitution of Styron 656D by using the Fractional Factorial design in the next section.

2.1.3 Identify the potential parameters

There were many parameters used in the experiments related to the residual stress analysis of the rectangular lid. Previous studies indicated that mold temperature, melt temperature, injection time, packing pressure, packing time, and cooling time showed the significant effects on the plastic injection molding processes. In this study, an injection molding machine could not control the injection time directly. Therefore, the injection speed was controlled instead. Moreover, the machine did not have a mold-temperature control device. In order to keep the mold temperature constant at 35°C, the cooling water was used at a room temperature. Therefore, melt temperature, injection speed, packing pressure, packing time, and cooling time were selected as the significant process parameters affecting the residual stress and process cycle time of the rectangular lid.

2.1.4 Residual stress analysis of the rectangular lid using MPI

As patterns of the residual stress from the simulation and actual part are the same, the value of the residual stress were measured from the results of MPI software at four different reference points as shown in Figure 24.

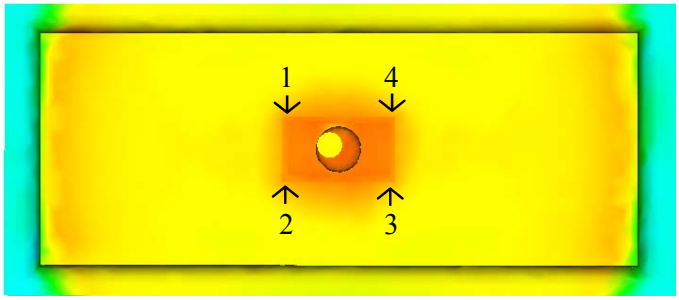

Figure 24 Four reference points that were used to measure the residual stress of the rectangular lid

The value of residual stresses of each condition was obtained from the average residual stresses values of these four points. This average residual stress value would be used on all the experiments in the later sections.

2.2 Simulation model of the roof tile (Case2)

2.2.1 Finite element model of the roof tile

Geometry of the roof tile utilized in the research is shown in Figure 25. It has the width, length, and thickness of 152 mm, 485 mm, and 4.5 mm, respectively. In this research, the FE model was created by MPI 6.1. It consists of 4,494 elements with the maximum aspect ratio of 8.8, the match ratio of 92.4%, and the reciprocal ratio of 92.5%.

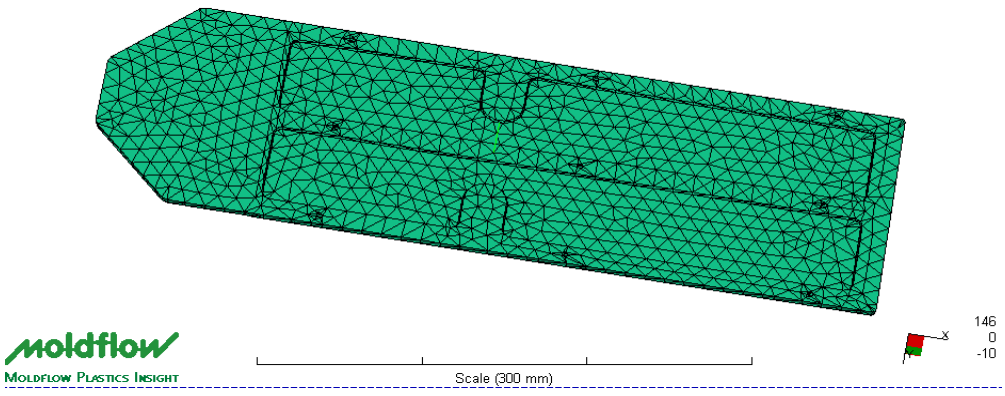

Figure 25 The mesh geometry of the roof tile

2.2.2 Material selection of the roof tile

In the experimental stage, the plastic roof tile was made of HDPE (Thai-Zex 1600J) manufactured by Bangkok Polyethylene Public Company Limited (BPE). Because this material is not available in MPI materials database, a similar material, Hi-Zex 2200J, was used for this research work.

2.2.3 Identify the potential parameters of the roof tile

There were many parameters used in the experiments related to the warpage analysis of the roof tile. In this research work, mold temperature, injection speed, packing pressure, packing time, and cooling time were considered as the process parameters that significantly affect the warpage and process cycle time of the roof tile.

2.2.4 The warpage analysis of the roof tile using MPI software

After injection molding, the maximum deflection occurred at the end of the part. Therefore, the warpage was measured based on the deflection in the thickness direction (z-axis) as shown in Figure 26.

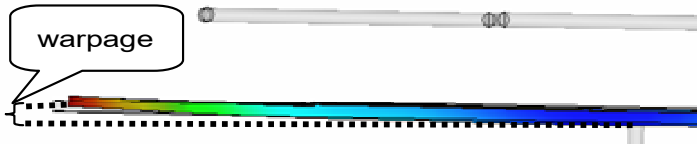

Figure 26 Deflection in z-axis of the roof tile

3. The Fractional Factorial design

In this research work, the Fractional Factorial design was used to identify the significant processing parameters. This was a screening method to determine the processing parameters that significantly affected the product's quality in terms of the residual stress and process cycle time of the rectangular lid in Case 1, and the warpage and process cycle time of the roof tile in Case 2. The steps of the Fractional Factorial design can be presented in Figure 27.

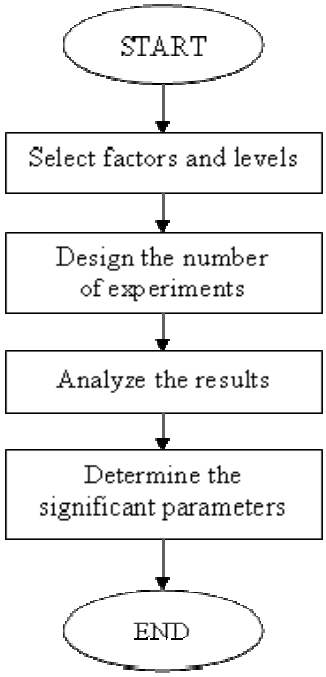

Figure 27 Steps of the Fractional Factorial design

3.1 The Fractional Factorial design of the rectangular lid (Case 1)

3.1.1 Select parameters and levels of Case 1

In the present work, there were six design parameters considered to be the experimental factors including material grade, melt temperature, injection speed, packing pressure, packing time, and cooling time. These six parameters were considered in the Fractional Factorial design with two levels as shown in Table 8.

Table 8 Design parameters in Case 1

Design Parameters	Low Level	High Level
Material grade (Styron^{TM})	666D	678D
Melt temperature (°C)	200	260
Injection speed (%)	30	50
Packing pressure (MPa)	3	5
Packing time (sec.)	1.5	3.5
Cooling time (sec.)	10	25

According to the design parameters in Table 8, two PS grades –Styron 666D and 678D- available in the moldflow database were selected to use instead of Styron 656D. Ranges of melt temperature and packing pressure were selected according to the recommended values in MPI software. Range of injection speed is converted from the relationship between recommended injection time obtained from MPI software and the constant injection stroke of 65 mm at 95% part's volume. The packing time and cooling time were chosen based on the experience of the manufacturer.

3.1.2 Design the number of experiments of the rectangular lid

The implement of the Full Factorial with two levels design on six parameters takes totally 64 runs. For screening significant parameters, there is no need to do the experiments completely. Therefore, the 2^{6-2} Fractional Factorial design with resolution IV was employed. Regarding to the Fractional Factorial design, the number of the experiments could be reduced to 16 runs as shown in Table 9.

Table 9 The 2^{6-2} Fractional Factorial design with 16 runs in Case 1 (Experiment 1)

StdOrder	Material Grade	Melt Temp. (°C)	Injection Speed (%)	Packing Pressure (MPa)	Packing Time (sec)	Cooling Time (sec)
1	Styron 666D	200	30	3	1.5	10
2	Styron 678D	200	30	3	3.5	10
3	Styron 666D	260	30	3	3.5	25
4	Styron 678D	260	30	3	1.5	25
5	Styron 666D	200	50	3	3.5	25
6	Styron 678D	200	50	3	1.5	25
7	Styron 666D	260	50	3	1.5	10
8	Styron 678D	260	50	3	3.5	10
9	Styron 666D	200	30	5	1.5	25
10	Styron 678D	200	30	5	3.5	25
11	Styron 666D	260	30	5	3.5	10
12	Styron 678D	260	30	5	1.5	10
13	Styron 666D	200	50	5	3.5	10
14	Styron 678D	200	50	5	1.5	10

Table 9 (Continued)

StdOrder	Material Grade	Melt Temp. (°C)	Injection Speed (%)	Packing Pressure (MPa)	Packing Time (sec)	Cooling Time (sec)
15	Styron 666D	260	50	5	1.5	25
16	Styron 678D	260	50	5	3.5	25

3.1.3 Analyze the statistical results of Case 1

3.1.3.1 Analysis of Variance (ANOVA)

After the data was collected, the statistical tool used for finding the significant parameters on this experiment was ANOVA. The fundamental technique of ANOVA is a partitioning of the total sum of squares into components related to the effects used in the model. F-test is the statistic that uses to compare the components of the total deviation. The example of a simplified ANOVA for the two-parameter Factorial design is shown in Table 10.

Table 10 The ANOVA table for the two-parameter Factorial design

Source of Variance	sum of squares	degree of freedom	mean square	F-ratio
A treatment	SS_A	a-1	$MS_A=\frac{SS_A}{a-1}$	$F_0=\frac{MS_A}{MS_E}$
B treatment	SS_B	b-1	$MS_B=\frac{SS_B}{b-1}$	$F_0=\frac{MS_B}{MS_E}$
Interaction	SS_{AB}	(a-1)(b-1)	$MS_{AB}=\frac{SS_{AB}}{(a-1)(b-1)}$	$F_0=\frac{MS_{AB}}{MS_E}$
Error	SS_E	ab(n-1)	$MS_E=\frac{SS_E}{ab(n-1)}$	
total	SS_T	abn-1		

$$SS_T = \sum_{i=1}^{a}\sum_{j=1}^{b}\sum_{k=1}^{n} y_{ijk}^2 - \frac{y_{...}^2}{abn}$$

$$SS_A = \frac{1}{bn}\sum_{i=1}^{a} y_{i..}^2 - \frac{y_{...}^2}{abn}$$

$$SS_B = \frac{1}{an}\sum_{j=1}^{b} y_{.j.}^2 - \frac{y_{...}^2}{abn}$$

$$SS_{Subtotals} = \frac{1}{an}\sum_{i=1}^{a}\sum_{j=1}^{b} y_{.j.}^2 - \frac{y_{...}^2}{abn}$$

$$SS_{AB} = SS_{Subtotals} - SS_A - SS_B$$

$$SS_E = SS_T - SS_{Subtotals}$$

From the above equations, let y_{ijk} be the observed response when parameter A is at the i^{th} level (i = 1, 2, …, a) and parameter B is at the j^{th} level (j = 1, 2, …, b) for the k^{th} replicate (k = 1, 2, …, n).

In order to find out the significant parameters of the residual stresses on the rectangular lid, experimenters usually consider F-ratio value from ANOVA table of each treatment by comparing with the value of F-critical at 95% confidence interval ($\alpha = 0.05$). If F-ratio is more than F-critical, this treatment has the effect on the residual stresses of the part. Moreover, in the MINITAB analysis, p-value is also a popular indicator for this experiment. P-value is the probability of obtaining a test statistic by comparing with α value. If p-value is less than α value, it means that these parameters have an effect on the residual stresses of the part. In this research, the α value used is equal to 0.05.

3.1.3.2 Model adequacy checking

Model adequacy checking is the confirmation method to make sure that data collected is not abnormality and can be used for the statistical analysis. There are mainly two plots for checking the adequate model, which are (i) normal probability plot and (ii) residual versus the fitted value.

a.) Normal probability plot

The normal probability plot is a robust statistical test that can be applied to the residuals to see whether they do indeed follow a normal distribution. It is the plot between % normal probability and residual. The points in this plot should generally form a straight line if the residuals are normally distributed. If the points on the plot depart from a straight line, the normality assumption may be invalid.

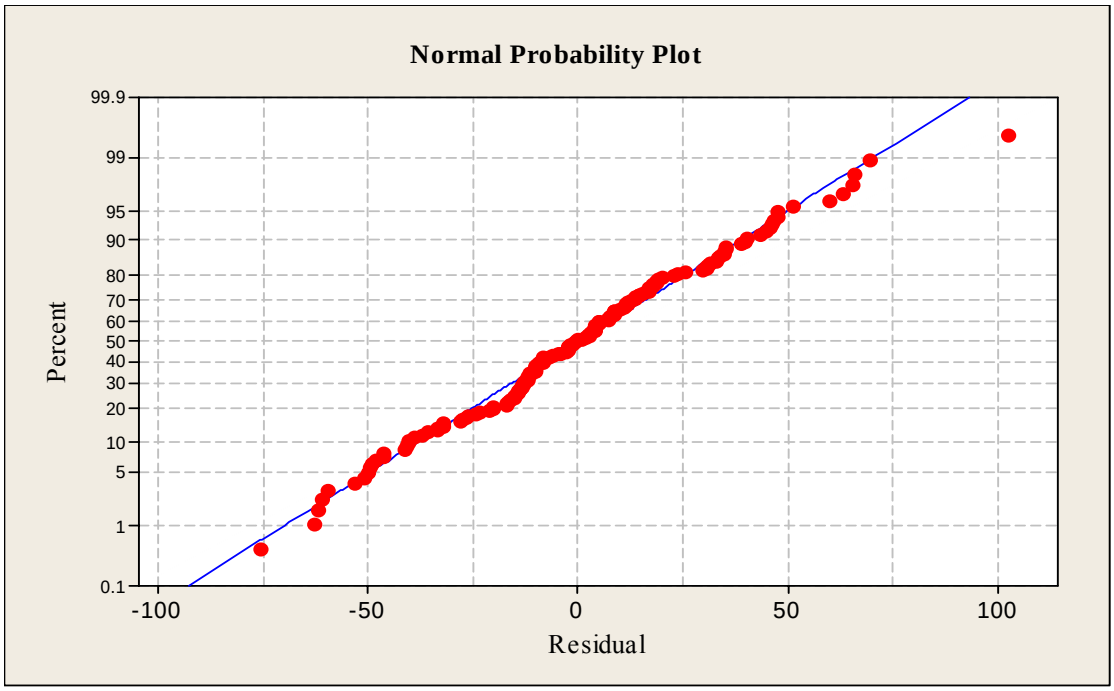

Figure 28 Example of the normal probability plot

b.) Residual versus the fitted value

The plot of residual versus fitted value is used to check constant variance of the residual. This plot should show a random pattern of the residuals on both sides of 0. Also, there should not be any recognizable patterns in the residual plot.

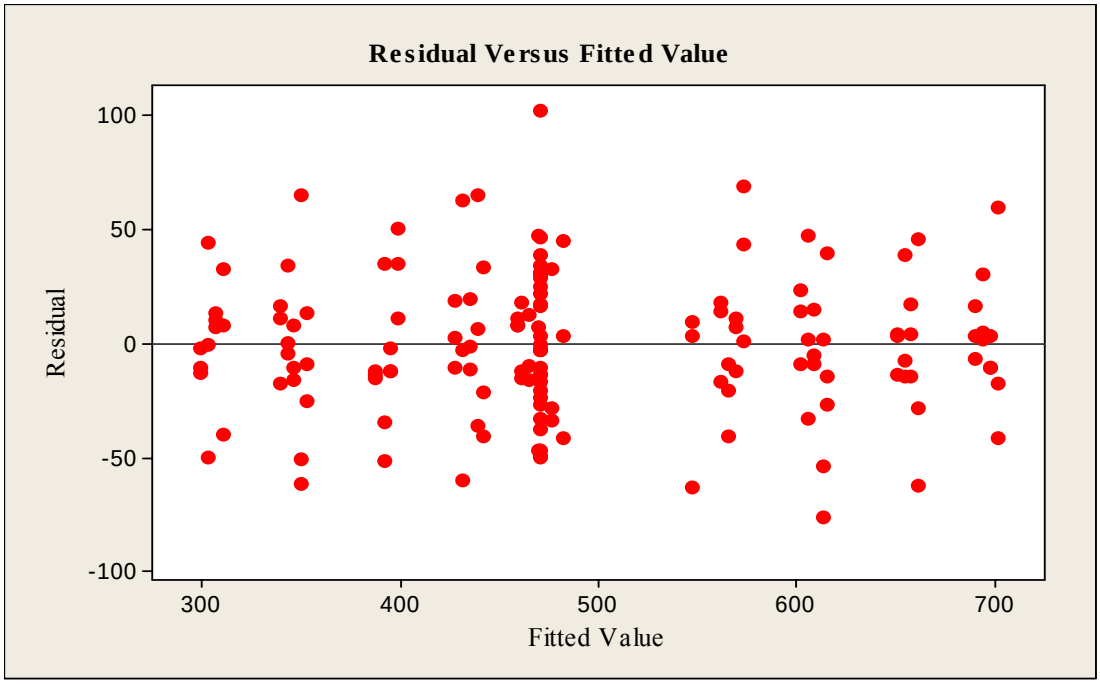

Figure 29 Example of the plot of residual versus fitted value

3.2 The Fractional Factorial design of the roof tile (Case2)

3.2.1 Select processing parameters and levels of Case 2

In this case, the Fractional Factorial design was also used to identify the significant processing parameters. The five processing parameters considered as important parameters to the roof tile's warpage and its process cycle time including melt temperature ranged from 140 to 180°C, injection speed ranged from 30 to 90%, packing pressure ranged from 4 to 8 MPa, packing time ranged from 1 to 2 second, and cooling time ranged from 40 to 60 second. All of these five parameters with each of two levels are displayed as shown in Table 11.

Table 11 Design parameters in Case 2

Design Parameters	Low Level	High Level
Melt temperature (°C)	140	180
Injection speed (%)	30	90

Table 11 Design parameters in Case 2

Design Parameters	Low Level	High Level
Packing pressure (MPa)	4	8
Packing time (sec.)	1	2
Cooling time (sec.)	40	60

3.2.2 Design the number of experiment of Case 2

The implement of the Full Factorial with two levels design on five parameters takes totally 32 runs. For screening significant parameters, there is no need to do the experiments completely. Therefore, the 2^{5-1} Fractional Factorial design with resolution IV was employed. Regarding to the Fractional Factorial design, the number of the experiments could be reduced to 16 runs as shown in Table 9.

Table 12 The 2^{5-1} Fractional Factorial design with 16 runs in Case 2 (Experiment 2)

StdOrder	Melt Temp. (°C)	Injection Speed (%)	Packing Pressure (MPa)	Packing Time (sec)	Cooling Time (sec)
1	140	30	4	1	60
2	180	30	4	1	40
3	140	90	4	1	40
4	180	90	4	1	60
5	140	30	8	1	40
6	180	30	8	1	60
7	140	90	8	1	60
8	180	90	8	1	40
9	140	30	4	2	40
10	180	30	4	2	60
11	140	90	4	2	60
12	180	90	4	2	40
13	140	30	8	2	60
14	180	30	8	2	40
15	140	90	8	2	40
16	180	90	8	2	60

3.2.3 Analyze the statistical results of Case 2

After the data was collected, the ANOVA was used for finding the significant parameters on this experiment. After the significant parameters of Case 2 are obtained, the two model adequacy checking, which are (i) normal probability plot and (ii) residual versus fitted value, were employed to confirm the appropriate of the experiment result as the same way of Case 1.

4. Artificial Neural Network (ANN) for prediction model

The ANN model is a simpler and more efficient predictive tool for the complex relationship among part quality index, process cycle time, and process parameters. The characteristic of the ANN technique is then suitable for modeling the quality prediction of the injection molded part in terms of the residual stress and the warpage. Figure 30 demonstrates the steps of the ANN model.

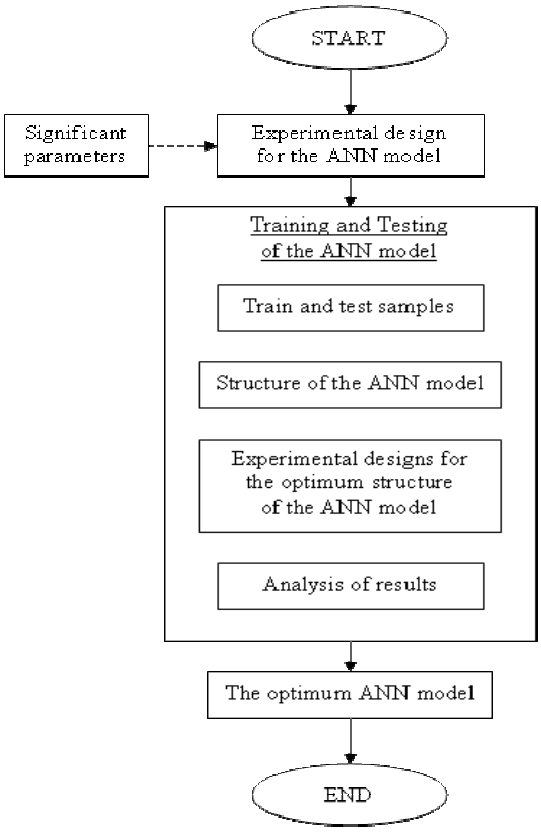

Figure 30 Steps of the Artificial Neural Network (ANN) model

4.1 The ANN model of the rectangular lid (Case 1)

4.1.1 Experimental design for the ANN model of Case 1

In this section, the simulation model based on MPI analysis was used to determine the target or desired outputs of the ANN model in term of the residual stress. Desired output values were referred to as training data set. The training data set in this work was created with the assistance of the experimental design method. In a common experimental design named a Full Factorial design, the variable space was divided into three levels: low, middle, and high levels. The three-level Full Factorial design creates 3^n training data, where n is the number of variables. From the results of the residual stress analysis in this study, there were five process parameters: (i) melt temperature, (ii) injection speed, (iii) packing pressure, (iv) packing time, and (v) cooling time, which significantly affect on the residual stress and process cycle time of the rectangular lid. Therefore, it took totally 243 (3^5) runs. The three-level values of these five process parameters are shown in Table 13.

Table 13 The three-level values of five processing parameters in the 3^5 Full Factorial design of Case 1

Level	Melt Temp (°C)	Injection Speed (%)	Packing Pressure (MPa)	Packing Time (sec)	Cooling Time (sec)
low	200	30	3	1.5	10
middle	230	40	4	2.5	17.5
high	260	50	5	3.5	25

4.1.2 Training and testing of the ANN model of Case 1

4.1.2.1 Train and test samples of Case 1

According to the experimental design, the three-level Full Factorial design was used (3^5 = 243 data). In this work, the samples were randomly divided into two groups. The first 200 data were used as training data while the remaining 43 data were used as testing data.

4.1.2.2 Structure of the ANN model in Case 1

The structure of the ANN model typically consists of five components including (i) input layer, (ii) hidden layer, (iii) output layer, (iv) transfer function, and (v) training parameters. Each component can be defined as follows:

a.) Number of neuron in the input and output layers of the ANN model

The selection of process variables was used to determine the neuron number of the input layer of the ANN model. The neuron number of the output layer is determined by the number of the objective indices, residual stress and process cycle time of the rectangular lid. The structure of the ANN model used in this study is shown in Figure 31, in which the input layers corresponding to melt temperature (MT), injection speed (IS), packing pressure (PP), packing time (PT), and cooling time (CT). The output layers correspond to the residual stress and process cycle time.

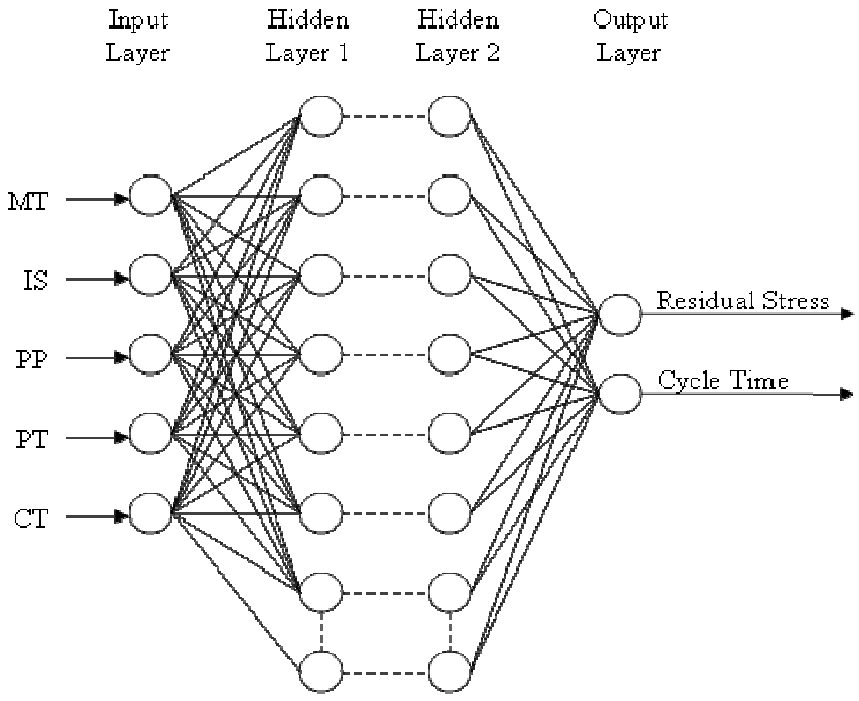

Figure 31 Structure of the ANN model that has two outputs: residual stress and cycle time.

b.) Number of neuron in the hidden layer of the ANN model

The ANN model is multilayered architecture made up of one or more hidden layers placed between the input and output layers. Although a multilayer neural network with a single hidden layer is sufficient to solve any function approximation problem, some problems may be easier to solve using two hidden layer. Thus, the number of the hidden layer and neuron number in each hidden layer were determined by the trial method. In this study, in order to find the optimum structure of the ANN model, the experiment was trialed of both single and two hidden layer. For the number of neuron in each hidden layer, there are two formulae used to limit their range as shown in Equation (18) and (19).

$$\text{Minimum Neuron} = \frac{(Output + Input)}{2} \qquad (18)$$

$$\text{Maximum Neuron} = 2\ (\text{Input}) + 1 \qquad (19)$$

c.) Transfer function

In this research, three transfer functions are used between each layer. The transfer function between the input layer and the hidden layer 1 is 'logsig'(Equation 5) or 'tansig' (Equation 6), the transfer function between the hidden layer 1 and the hidden layer 2 is also 'logsig' or 'tansig', while the transfer function between the hidden layer 2 and the output layer is 'purelin' (Equation 4).

d.) Training parameters

The simplest implementation of backpropagation learning updates the network weights and biases in the direction of the negative gradient of the performance function. In this research, the Levenberg-Marquardt training algorithm (*trainlm*) was used to update the weights and biases. There are three important training parameters associated with *trainlm* including *epochs, goal,* and *lr*. The learning rate (*lr*) is multiplied by the negative of the gradient to determine the changes to the weights and biases. The high learning rate leads to rapid learning but the weights may unstable, while

low learning rate takes a long time to converge. *Epochs* and *goal* are the parameters that determine when the training should be stopped. The training stops if the number of iterations exceeds *epochs*, or the performance function drops below *goal*. This work analyzed the three values of *lr* and *epochs* to 0.01, 0.05, 0.09 and 1,000, 3,000, 5,000, respectively. Moreover, the goal was set to 10^{-5}.

4.1.2.3 Experimental designs for optimum structure of the ANN model in Case 1

According to the experimental design, there are five sets of parameters associated with the structure of the ANN model: (i) characteristic of the input data and transfer function in the hidden layer, (ii) *epochs* and *lr*, (iii) initial *bias* value, (iv) number of neuron in the 1st hidden layer, and (v) number of neuron in the 2nd hidden layer.

a.) Experimental design of characteristic of the input data and transfer function in the hidden layer where the residual stress and process cycle time were outputs (Experiment 3).

The first experiment was the design for determining an appropriate input value by with or without normalization for training the ANN model where the residual stress and cycle time were outputs. The two transfer functions: (i) binary sigmoid function (logsig) and (ii) bipolar sigmoid function (tansig) of the hidden layer were mostly used for this kind of problems. Hence, this experiment was designed for both characteristics of the input data and transfer function, whereas the other parameters were fixed as shown in Table 14.

Table 14 Experiment 3

1. Output	Indicator	
average accuracy	%	
2. Design factors	Level	
characteristic of the input data and	unnormalization	normalization
transfer function in the hidden layer	logsig	tansig

Table 14 (Continued)

3. Controllable factors	Controllable value
number of neuron in theinput layer	5
number of neuron in thehidden layer	11
learning rate (*lr*)	0.01
epochs	1000
initial *bias* value	0.5
transfer function in the output layer	purelin
goal	10^{-5}
4. Number of experimental runs	4 runs ×5 times = 20 runs

b.) Experimental design of *epochs* and *lr* where the residual stress and process cycle time were outputs (Experiment 4).

Experiment 4 was the design for determining an appropriate value of *epochs* and *lr* for training the ANN model where the residual stress and cycle time were outputs. In this experiment, *epochs* was divided into three levels: 0.01, 0.05, and 0.09 while *lr* was also divided into three levels: 1,000, 3,000, and 5,000. Moreover, the other parameters must be fixed to stable values as displayed in Table 15.

Table 15 Experiment 4

1. Output		Indicator	
average accuracy		%	
2. Design factors		Level	
learning rate (*lr*)	0.01	0.05	0.09
epochs	1,000	3,000	5,000
3. Controllable factors		Controllable value	
characteristic of input		from Experiment 3 (=normalization)	
number of neuron in the input layer		5	
number of neuron in the hidden layer		11	
initial *bias* value		0.5	
transfer function in the hidden layer		from Experiment 3 (= logsig)	
transfer function in the output layer		purelin	
goal		10^{-5}	
4. Number of experimental runs		9 runs ×5 times = 45 runs	

c.) Experimental design of the initial *bias* value where the residual stress and process cycle time were outputs (Experiment 5).

Experimental design of the initial *bias* value was used for determining the appropriate value of bias in the structural ANN model where the residual stress and the process cycle time were outputs. In this experiment, *bias* was divided into three levels: 0, 0.5, and 1. The other parameters were fixed as displayed in Table 16.

Table 16 Experiment 5

1. Output	Indicator		
average accuracy	%		
2. Design factors	Level		
initial *bias* value	0	0.5	1.0
3. Controllable factors	Controllable value		
characteristic of input	normalization		
number of neuron in input layer	5		
number of neuron in hidden layer	11		
learning rate (*lr*)	from Experiment 4 (=0.01)		
epochs	from Experiment 4 (=1000)		
transfer function in hidden layer	logsig		
transfer function in output layer	purelin		
goal	10^{-5}		
4. Number of experimental runs	3 runs ×5 times = 15 runs		

d.) Experimental design of number of neuron in 1st hidden layer where the residual stress and process cycle time were outputs (Experiment 6).

In order to find the optimum number of neuron in the 1st hidden layer, two formulae in equation (18) and (19) were used to define the range of neuron. As this ANN model had five input parameters and two output parameters, the range of the number of neuron would be within 3 to 11 neurons while other parameters are fixed. The experimental design of the neuron's number in the 1st hidden layer is displayed in Table 17.

Table 17 Experiment 6

1. Output	Indicator
average accuracy	%
2. Design factors	Level
	3, 4, 5, …, 11
3. Controllable factors	Controllable value
characteristic of input	normalization
number of neuron in the input layer	5
learning rate (*lr*)	0.01
epochs	1,000
initial *bias* value	from Experiment 5 (= 1.0)
transfer function in the hidden layer	logsig
transfer function in the output layer	purelin
goal	10^{-5}
4. Number of experimental runs	9 runs ×5 times = 45 runs

e.) Experimental design of number of neuron in 2nd hidden layer where the residual stress and process cycle time were outputs (Experiment 7).

The number of neuron in the 2nd hidden layer can be determined by two formulae on equation (18) and (19). In this case, the number of neuron in the 1st hidden layer of the ANN model was obtained from the previous experiment as input for the 2nd hidden layer. In this case, seven input parameters and two output parameters were used to determine the neuron's number in the 2nd hidden layer of the ANN model. Hence, the range of the number of neuron in the 2nd hidden layer is between 5 and 15 neurons whereas the other parameters were fixed. The experimental design of the neuron's number in the 2nd hidden layer is shown in Table 18.

Table 18 Experiment 7

1. Output	Indicator
average accuracy	%
2. Design factors	Level
	5, 6, 7, …, 15

Table 18 (Continued)

3. Controllable factors	Controllable value
characteristic of input	normalization
number of neuron in input layer	5
number of neuron in 1st hidden layer	from Experiment 5 (= 7)
learning rate (*lr*)	0.01
epochs	1,000
initial *bias* value	1.0
transfer function in hidden layer	logsig
transfer function in output layer	purelin
goal	10^{-5}
4. Number of experimental runs	11 runs ×5 times = 55 runs

4.1.2.4 Analysis of results

In this study, there were three statistical tools: (i) the box-plot, (ii) analysis of variance (ANOVA), and (iii) the mean and standard deviation analysis, which were used to analyze the results by comparing among experimental data for finding the optimum structure of the ANN model.

a.) Box-plot analysis

The box-plot is a graphical display that describes important features of the data including median, minimum, and maximum of the data on a rectangular box. Therefore, the box-plot is very useful in graphical comparisons among data sets because it has high visual impact and is easy to understand. Figure 32 displays the example feature of comparative box-plots for a quality index, average accuracy (%) on nine different numbers of neuron in the hidden layer that would be used on the test for optimum structure of the ANN model.

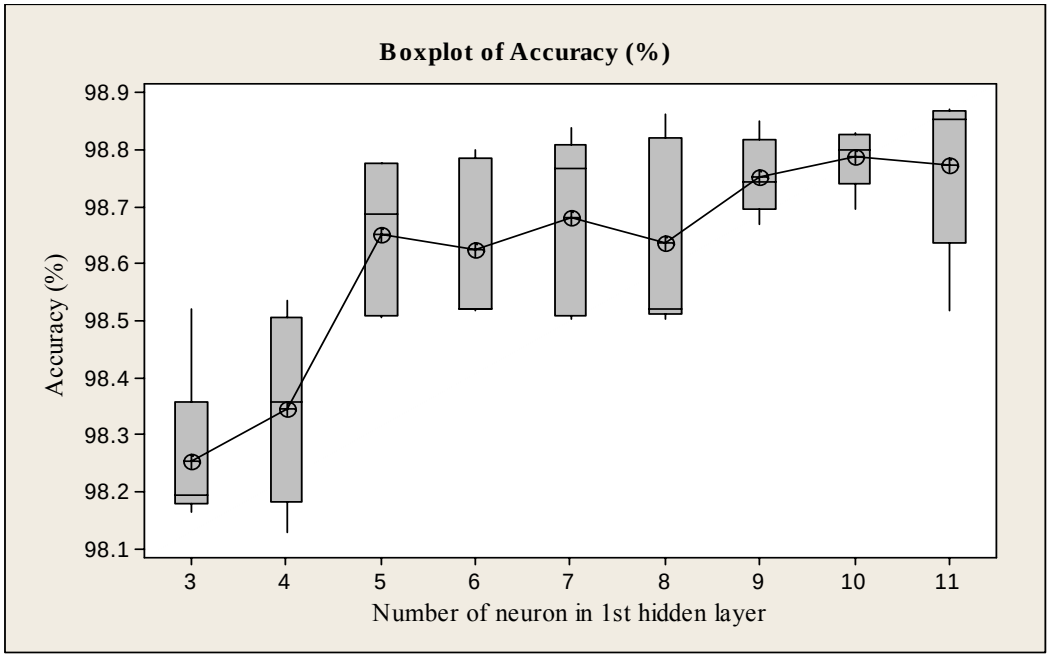

Figure 32 Example feature of the box-plots

b.) ANOVA analysis

ANOVA is another statistical tool used for finding an appropriate ANN model by using the formal comparative method among treatments.

c.) The mean and standard deviation (SD) analysis

The mean ($\bar{x}$) and standard deviation (SD) are often used to summarize a probability distribution for random variable x. The mean is a measure of the average value of the distribution. Standard deviation is a measure of dispersion in the distribution. These two numbers can be calculated as written in Equations (20) and (21).

$$\bar{x} = \frac{\sum_{i=1}^{n} x_i}{n} \tag{20}$$

$$SD = \sqrt{\frac{\sum_{i=1}^{n} \left(x_i - \bar{x}\right)^2}{n-1}} \tag{21}$$

4.2 The ANN model of the roof tile (Case 2)

4.2.1 Experimental design for the ANN model in Case 2

The training data set in this research was created with the help of experimental design method. From the result of the previous section, there are totally four parameters: (i) injection speed (IS), (ii) packing pressure (PP), (iii) packing time (PT), and (iv) cooling time (CT) which significantly affect the warpage and process cycle time of the roof tile. Therefore, in order to obtain enough training data, these four parameter space was divided into four levels. A Full Factorial design created 4^4 training data or 256 runs. The four levels of these four process parameters are shown in Table 19.

Table 19 The four-level values of four processing parameters in the 4^4 Full Factorial design in Case 2

Level	Injection Speed (%)	Packing Pressure (MPa)	Packing Time (sec.)	Cooling Time (sec.)
1	30	4	1	40
2	50	5.33	1.33	46.67
3	70	6.67	1.67	53.33
4	90	8	2	60

4.2.2 Training and testing of the ANN model in Case 2

4.2.2.1 Train and test samples in Case 2

According to the experimental design, the four-level Full Factorial design was used (4^4 = 256 data). In this work, the samples were randomly divided into two groups. The first 200 data were used as training data while the remaining 56 data were used as testing data.

4.2.2.2 Structure of the ANN model in Case 2

The structure of the ANN model typically consists of five components including (i) input layer, (ii) hidden layer, (iii) output layer, (iv) transfer function, and (v) training parameters. Each component can be defined as follows.

a.) Number of neuron in the input and output layer of the ANN model

The selection of process variables was used to determine the neuron number of the input layer of the ANN model. The neuron number of the output layer was determined by the number of the objective indice: warpage and process cycle time of the roof tile. The structure of the ANN model used in this study is shown in Figure 33 in which the input layers correspond to injection speed (IS), packing pressure (PP), packing time (PT), and cooling time (CT). The output layers correspond to the warpage and process cycle time.

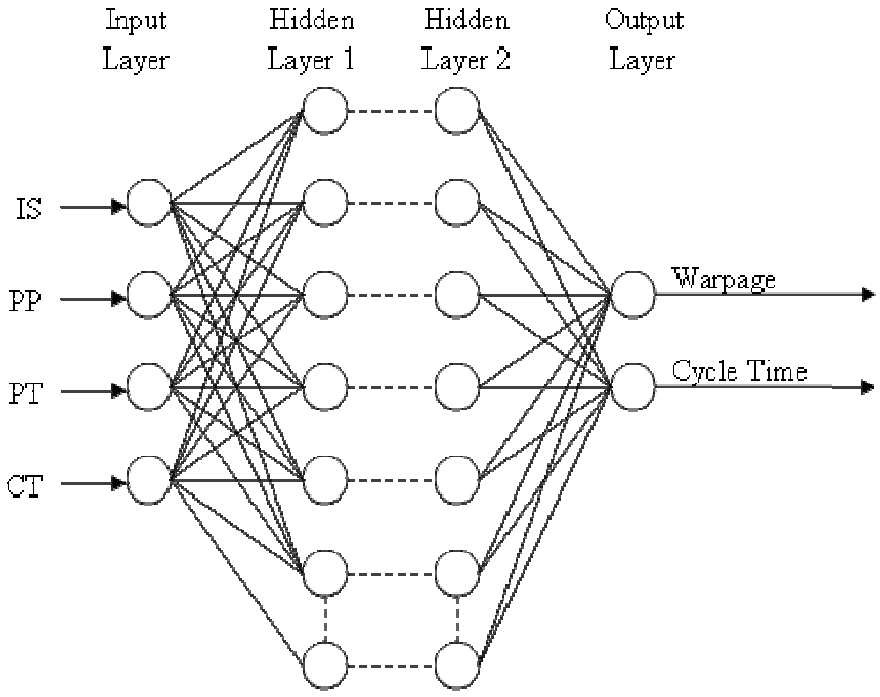

Figure 33 Structure of the ANN model that has two outputs, warpage and cycle time.

b.) Number of neuron in the hidden layer of the ANN model

In this study, the optimum structure of the ANN model was performed on both single and two hidden layers. In each hidden layer, the number of neuron is within the range of equation (18) and (19) similar to Case 1.

c.) Transfer function

In this research, there were three positions of the transfer functions. First was the transfer function between the input layer and the hidden layer 1 which was 'logsig'or 'tansig' function. Second was the transfer function between the hidden layer 1 and the hidden layer 2 which was also 'logsig' or 'tansig' function. Last was the transfer function between the hidden layer 2 and the output layer which was 'purelin' function.

d.) Training parameters

In this case, there were the same training parameters as in Case 1. The Levenberg-Marquardt training algorithm (*trainlm*) was used to update the weights and biases. There were 3 important training parameters associated with *trainlm* including *epochs, goal,* and *lr*. The learning rate (*lr*) is multiplied times the negative of the gradient to determine the changes to the weights and biases. The high learning rate leads to rapid learning but the weights may unstable, while low learning leads the algorithm to take a long time to converge. *Epochs* and *goal* are the parameters that determine when the training should be stopped. The training stop if the number of iterations exceeds *epochs*, or the performance function drops below *goal*. This research analyzed the three values of *lr* and *epochs* to 0.01, 0.05, 0.09 and 1,000, 3,000, 5,000, respectively. Moreover, the *goal* value was determined to 10^{-5}.

4.2.2.3 Experimental designs for optimum structure of ANN model of Case 2

According to the experimental design, there were 5 set of parameters associated with the structure of ANN model: (i) characteristic of input data and transfer function in hidden layer, (ii) *epochs* and *lr*, (iii) initial *bias* value, (iv) number of neuron in first hidden layer, and (v) number of neuron in second hidden layer.

a.) Experimental design of characteristic of input data and transfer function in hidden layer that warpage and process cycle time were outputs (Experiment 8).

The first experiment was the design for determining an appropriate input value by with or without normalization for training ANN model that the warpage and cycle time were outputs. The two transfer functions, binary sigmoid function (logsig) and bipolar sigmoid function (tansig), of hidden layer were mostly used for this kind of problems. Hence, this experiment was designed for both characteristic of input data and transfer function, whereas the other parameters were fixed as shown in Table 20.

Table 20 Experiment 8

1. Output	Indicator	
average accuracy	%	
2. Design factors	Level	
characteristic of input	unnormalization	normalization
transfer function in hidden layer	logsig	tansig
3. Controllable factors	Controllable value	
number of neuron in the input layer	4	
number of neuron in the hidden layer	9	
learning rate (*lr*)	0.01	
epochs	1000	
initial *bias* value	0.5	
transfer function in the output layer	purelin	
goal	10^{-5}	
4. Number of experimental runs	4 runs ×5 times = 20 runs	

b.) Experimental design of *epochs* and *lr* where the warpage and process cycle time were outputs (Experiment 9).

Experiment 9 was the design for determining an appropriate value of epochs and lr for training the ANN model that the warpage and cycle time were outputs. This experiment was divided epochs into 3 levels: 0.01, 0.05, and 0.09. It was also divided lr into 3 levels: 1,000, 3,000, and 5,000. Moreover, the other parameters must be fixed as shown in Table 21.

Table 21 Experiment 9

1. Output		Indicator	
average accuracy		%	
2. Design factors		Level	
learning rate (*lr*)	0.01	0.05	0.09
epochs	1,000	3,000	5,000
3. Controllable factors		Controllable value	
characteristic of input		from Experiment 8 (=normalization)	
number of neuron in the input layer		4	
number of neuron in the hidden layer		9	
initial *bias* value		0.5	
transfer function in the hidden layer		from Experiment 8 (=logsig)	
transfer function in the output layer		purelin	
goal		10^{-5}	
4. Number of experimental runs		9 runs ×5 times = 45 runs	

c.) Experimental design of the initial *bias* value where the warpage and process cycle time were outputs (Experiment 10).

Experimental design of initial *bias* value was used for determining the appropriate *bias* value in structural ANN model that warpage and process cycle time were outputs. In this experiment, *bias* was divided into 3 levels: 0, 0.5, and 1. The other parameters were fixed as displayed in Table 22.

Table 22 Experiment 10

1. Output		Indicator	
average accuracy		%	
2. Design factors		Level	
initial *bias* value	0	0.5	1.0
3. Controllable factors		Controllable value	
characteristic of input		normalization	
number of neuron in the input layer		4	
number of neuron in the hidden layer		9	

Table 22 (Continued)

3. Controllable factors (Continued)	Controllable value
learning rate (*lr*)	from Experiment 9 (=0.09)
epochs	from Experiment 9 (=3000)
transfer function in the hidden layer	logsig
transfer function in the output layer	purelin
goal	10^{-5}
4. Number of experimental runs	3 runs ×5 times = 15 runs

d.) Experimental design of number of neuron in 1st hidden layer where warpage and process cycle time were outputs (Experiment 11).

In order to find the optimum number of neuron in the 1st hidden layer, two formulae on equation (18) and (19) were used to define the range of neuron. As this ANN model had four input parameters and two output parameters, so the range of the number of neuron would be within 3 to 9 neurons while other parameters were fixed. The experimental design of the neuron's number in the 1st hidden layer is displayed in Table 23.

Table 23 Experiment 11

1. Output	Indicator
average accuracy	%
2. Design factors	Level
	3, 4, 5, …, 9
3. Controllable factors	Controllable value
characteristic of input	normalization
number of neuron in the input layer	4
learning rate (*lr*)	0.09
epochs	3,000
initial *bias* value	from Experiment 10 (=1.0)
transfer function in the hidden layer	logsig
transfer function in the output layer	purelin
goal	10^{-5}
4. Number of experimental runs	7 runs ×5 times = 35 runs

e.) Experimental design of number of neuron in 2nd hidden layer where warpage and process cycle time were outputs (Experiment 12).

The number of neuron in the 2nd hidden layer can be determined by two formulae in equation (18) and (19). In this case, the number of neuron in the 1st hidden layer of the ANN model was obtained from the previous experiment as input for the 2nd hidden layer. In this case, nine input parameters and two output parameters were used to determine the neuron's number in the 2nd hidden layer of the ANN model. Hence, the range of the number of neuron in the 2nd hidden layer was between 6 and 19 neurons whereas the other parameters were fixed. The experimental design of the neuron's number in the 2nd hidden layer was shown in Table 24.

Table 24 Experiment 12

1. Output	Indicator
average accuracy	%
2. Design factors	Level
	6, 7, 8, …, 19
3. Controllable factors	Controllable value
characteristic of input	normalization
number of neuron in the input layer	4
number of neuron in the 1st hidden layer	from Experiment 11 (= 9)
learning rate (*lr*)	0.09
epochs	3,000
Initial *bias* value	1.0
transfer function in the hidden layer	logsig
transfer function in the output layer	purelin
goal	10^{-5}
4. Number of experimental runs	14 runs ×5 times = 70 runs

4.2.2.4 Analysis of results

Three statistical tools: (i) the box-plot, (ii) analysis of variance (ANOVA), and (iii) the mean and standard deviation analysis were used to analyze the results by comparing among experimental data for finding the optimum structure of the ANN model. All these three statistical tools are already explained in Case 1.

5. Genetic Algorithm (GA) for quality indices optimization

The main objective of the present research was to optimize the injection molding process conditions in order to improve the part quality indices. There are 2 types of part quality indices: (i) minimum residual stress and process cycle time of the rectangular lid (Case 1) and (ii) minimum warpage and process cycle time of the roof tile (Case2).

In Case 1, the optimum value of 5 parameters, melt temperature (MT), injection speed (IS), packing pressure (PP), packing time (PT), and cooling time (CT) could be efficiently obtained by formulating residual stress as the standard mathematical format shown below:

Find: MT, IS, PP, PT, CT
Minimize: Residual Stress (MT, IS, PP, PT, CT)
Within variable ranges:
$200\ °C \leq MT \leq 260\ °C$
$30\% \leq IS \leq 50\%$
$3\ MPa \leq PP \leq 5\ MPa$
$1.5\ second \leq PT \leq 3.5\ second$
$10\ second \leq CT \leq 25\ second$

In Case 2, the optimum value of 4 parameters, injection speed (IS), packing pressure (PP), packing time (PT), and cooling time (CT) could be efficiently obtained by formulating warpage as the standard mathematical format shown below:

Find: IS, PP, PT, CT
Minimize: Warpage (IS, PP, PT, CT)
Within variable ranges:
$30\% \leq IS \leq 90\%$
$4\ MPa \leq PP \leq 8\ MPa$
$1\ second \leq PT \leq 2\ second$
$40\ second \leq CT \leq 60\ second$

The GA is used to converge a global optimum among several possible local optimums. In this research, an effective GA was coupled with the ANN model for quality indices minimization. The steps of combining ANN and GA optimization on Figure 34 are applied to solve the optimization problem.

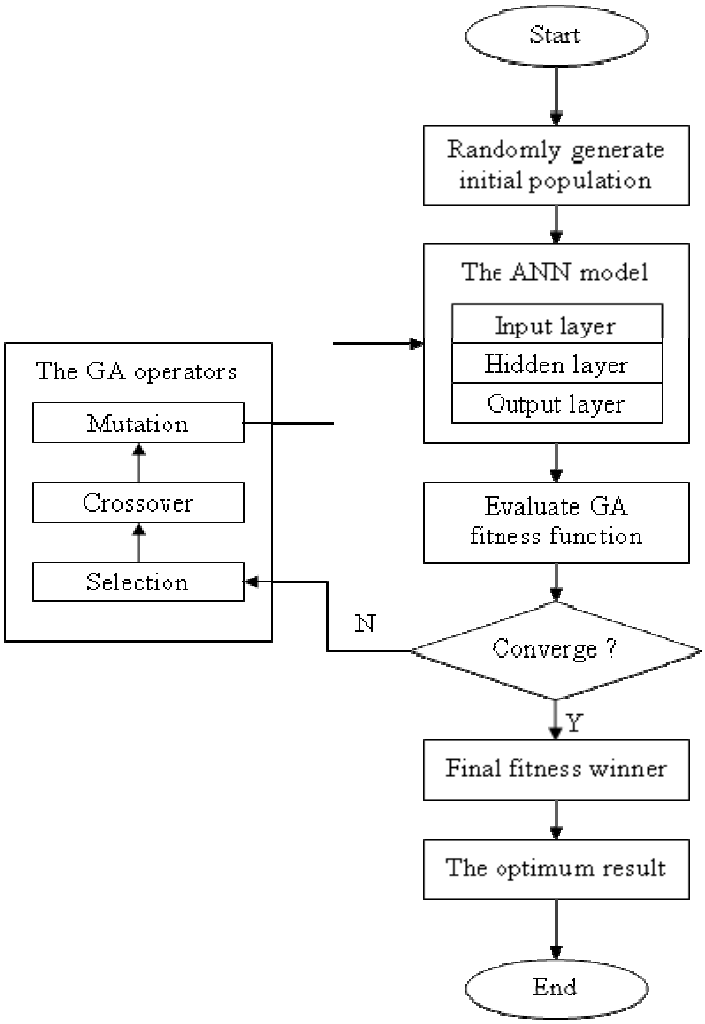

Figure 34 Steps of combining ANN and GA optimization

In order to appropriate GA parameters for estimation of residual stress problem (Case 1) and of warpage problem (Case 2), the 4 critical parameter in Case 1 and the 4 critical parameters in Case 2 were used to study the performance of the processing system by GA including (i) the size of the population, (ii) crossover rate, (iii) mutation rate, and (iv) the number of generations.

5.1 The population size of GA

The GA must be provided an initial population. The appropriate population size can maintain the appropriate diversity of population for global or near global optimum solution. There were 3 level of population size including 10, 30, and 50 tested in this experiment. The other GA parameters are shown were fixed to stable values as shown in Table 25.

Table 25 An experimental design of the population size

1. Output	Indicator		
The best solution	Residual stress value (Case 1) Warpage value (Case 2)		
2. Design factors	Level		
Population size	10	30	50
3. Controllable factors	Controllable value		
Population type	Double vector		
Selection	Roulette wheel		
Fitness scaling	Rank		
Crossover rate (P_c)	0.3		
Mutation rate (P_m)	0.1		
Maximum generation	500		
4. Number of experimental runs	3 runs ×3 times = 9 runs		

5.2 Crossover rate (P_c)

The objective of this section was to find the appropriate crossover rate (P_C). The chosen crossover rates for study were equal to 0.3, 0.5, and 0.7. However, result from 5.1 indicated the optimal population size for GA. The other GA parameters are shown in Table 26.

Table 26 An experimental design of crossover rate (P_c)

1. Output	Indicator
The best solution	Residual stress value (Case 1) Warpage value (Case 2)

Table 26 (Continued)

2. Design factors		Level	
Crossover rate (P_c)	0.3	0.5	0.7
3. Controllable factors		Controllable value	
Population type		Double vector	
Selection		Roulette wheel	
Fitness scaling		Rank	
Population size		from 5.1 result	
Mutation rate (P_m)		0.1	
Maximum generation		500	
4. Number of experimental runs		3 runs ×3 times = 9 runs	

5.3 Mutation rate (P_m)

In this experiment, the appropriate mutation rate (Pm) were investigated. The chosen mutation rate for study was equal to 0.1, 0.2, and 0.3. However, results from 5.2 and 5.3 indicated the optimal population size and P_c value for GA. The other GA parameters are displayed on Table 27.

Table 27 An experimental design of mutation rate (P_m)

1. Output		Indicator	
The best solution		Residual stress value (Case 1) Warpage value (Case 2)	
2. Design factors		Level	
Mutation rate (P_m)	0.1	0.2	0.3
3. Controllable factors		Controllable value	
Population type		Double vector	
Selection		Roulette wheel	
Fitness scaling		Rank	
Population size		from 5.2 result	
Crossover rate (P_c)		from 5.3 result	
Maximum generation		500	
4. Number of experimental runs		3 runs ×3 times = 9 runs	

5.4 The number of generations

'Generations' is a stopping criterion algorithm. The GA moves from generation to generation selecting and reproducing parents until a termination criterion met. Mostly, the number of generations is specified on the maximum value that is enough for finding global optimum solution. If GA converges to an optimum before 500 generations as in Figure 35, there is no need to increase the number of generations. Otherwise, the number of generations must be increased until the GA converges to an optimum line.

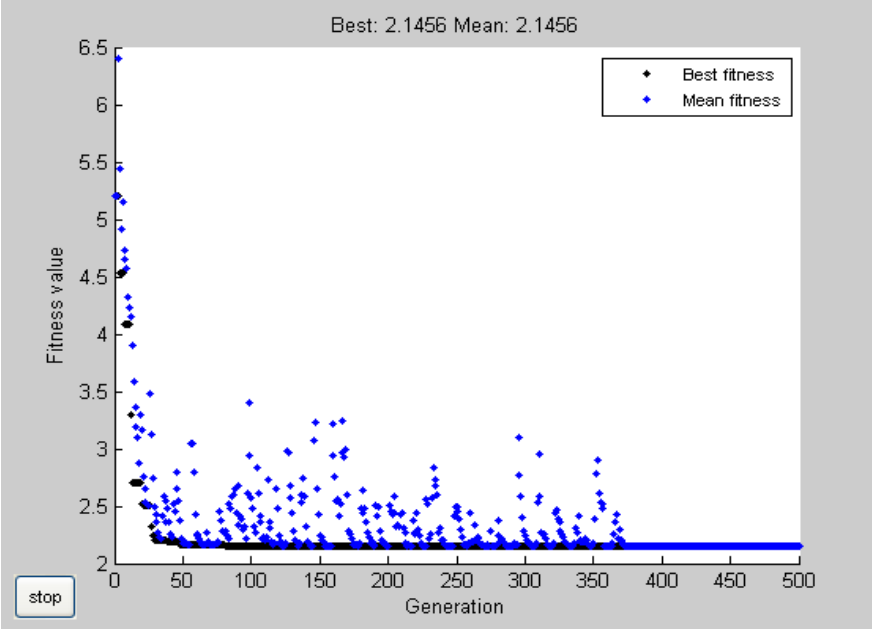

Figure 35 Example of GA that converges to an optimum before 500 generations

RESULTS AND DISCUSSION

Results

In this study, the experiment results were divided into four parts, which consisted of the study on (i) simulation model verification, (ii) the results of the Fractional Factorial design, (iii) the results of the optimal structural ANN model, and (iv) the results of the optimal processing condition using GA.

1. Simulation model verification

1.1 Simulation model verification of the rectangular lid's residual stress

The conditions tested for the model validation were in two conditions including (i) the initial processing condition and (ii) the processing condition in production by manufacturer. The verification of these molding conditions was performed by comparing the residual stress of the part between the simulation model and actual testing as follows:

1.1.1 The verification of the rectangular lid's residual stress based on condition 1

Condition 1 of the rectangular lid was the inital processing condition. Verification of condition 1 was to compare the residual stress results of the part between the actual testing and simulation model as shown in Figures 36 and 37.

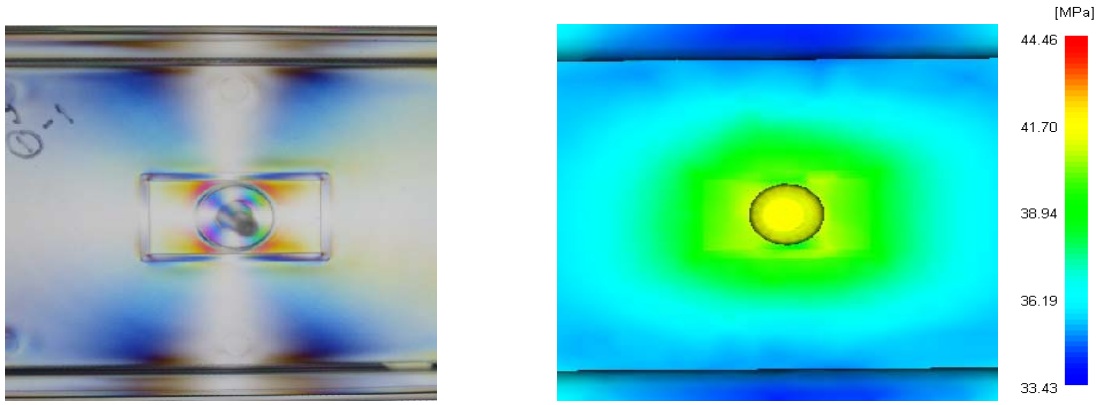

(a) The actual testing (b) The simulation model

Figure 36 The results of the residual stress in a front side of the rectangular lid based on condition 1.

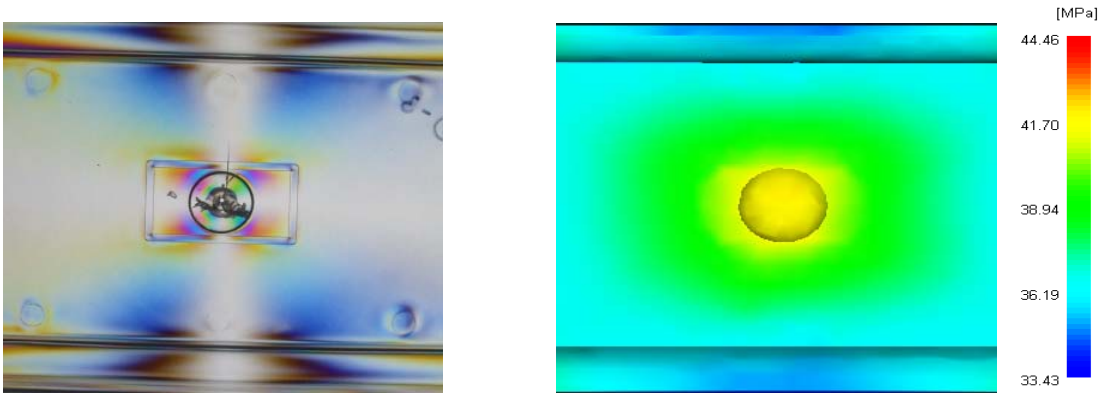

(a) The actual testing (b) The simulation model

Figure 37 The results of the residual stress in a back side of the rectangular lid based on condition 1.

A comparison of the residual stress of the rectangular lid between the actual testing and simulation model was mainly focused on their pattern and color contour in the middle area. According to Figures 36 and 37, the middle area of both results showed similar pattern and color contour. The product's residual stress of the simulation model, therefore, was used to approximate the value of the residual stress in the actual part.

1.1.2 The verification of the rectangular lid's residual stress based on condition 2

Condition 2 was the processing condition in production of the rectangular lid by manufacturer. Verification of condition 2 was to compare the residual stress results of the part between the actual testing and simulation model as shown in Figures 38 and 39.

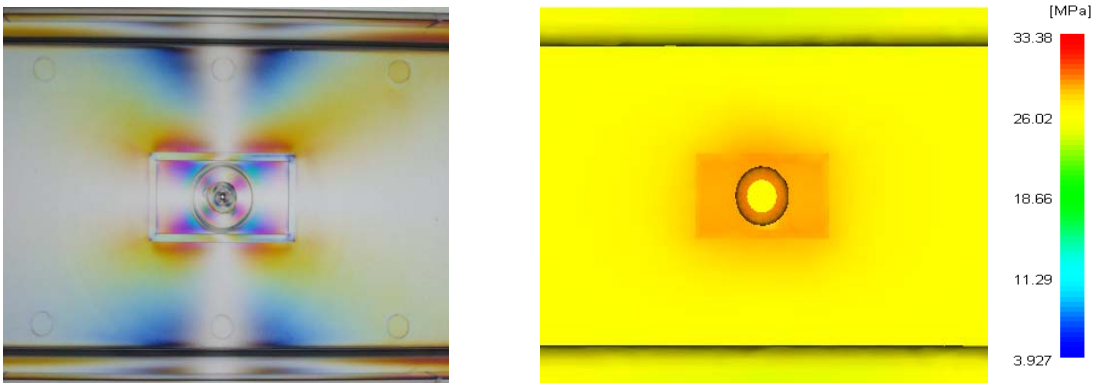

(a) The actual testing (b) The simulation model

Figure 38 The results of the residual stress in a front side of the rectangular lid based on condition 2.

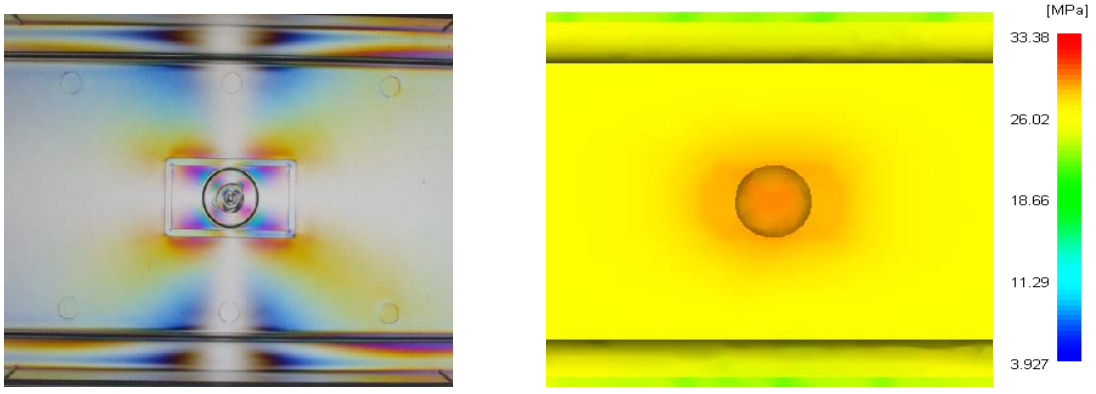

(a) The actual testing (b) The simulation model

Figure 39 The results of the residual stress in a back side of the rectangular lid based on condition 2.

A comparison of the residual stress of the rectangular lid between the actual testing and simulation model was mainly focused on their pattern and color contour in the middle area. According to Figures 38 and 39, the middle area of both results showed similar pattern and color contour, especially on the back side. The product's residual stress of the simulation model, therefore, was used to approximate the value of the residual stress in the actual part. In addition, the rectangular lid's residual stress was calculated by averaging the residual stress at four referent points as shown in Figure 24. The values of the processing condition used and residual stress at four reference points were summarized in Table 28.

Table 28 The processing condition in production and the residual stress values of the rectangular lid

Process conditions				
Melt Temp	Injection Speed	Packing Pressure	Packing time	Cooling time
228°C	45%	4.5 MPa	1.8 s	15 s
Residual Stress (MPa)				
Point 1	Point 2	Point 3	Point 4	Average
28.97	28.98	28.99	28.97	28.98

1.2 Simulation model verification of the roof tile's warpage

The processing conditions tested for the model validation of the roof tile were in three conditions including (i) the processing condition in production by manufacturer and (ii) other two processing conditions. The verification of these molding conditions was performed by comparing the warpage of the part between the simulation model and actual testing as follows:

1.2.1 The verification of the roof tile's warpage based on condition 1

Condition 1 was the processing condition in production of the roof tile by manufacturer. Verification of condition 1 was to compare the warpage results of the part between the actual testing and simulation model as shown in Figure 40.

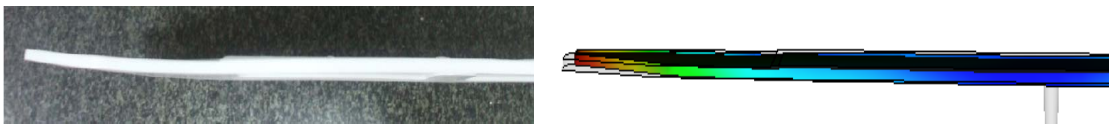

(a) The actual testing (b) The simulation model

Figure 40 The results of the roof tile's warpage based on condition 1.

1.2.2 The verification of the roof tile's warpage based on conditions 2 and 3

Conditions 2 and 3 were other two processing conditions of the roof tile used to confirm the simulation model validation. Verification of conditions 2 and 3 were to compare the warpage pf the part between the actual testing and simulation model as shown in Figures 41 and 42, respectively.

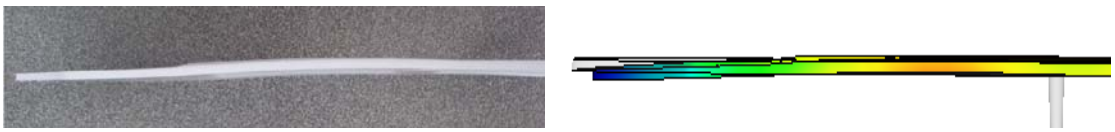

(a) The actual testing (b) The simulation model

Figure 41 The results of the roof tile's warpage based on condition 2.

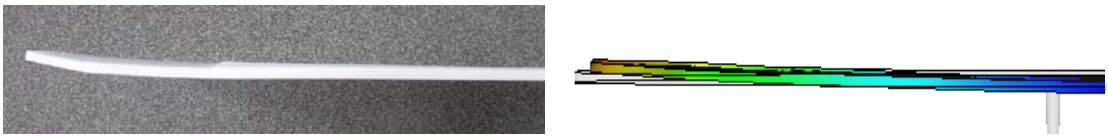

(a) The actual testing (b) The simulation model

Figure 42 The results of the roof tile's warpage based on condition 3.

According to Figures 40, 41, and 42, the roof tile's warpage between the actual testing and simulation model based on conditions 1, 2, and 3, respectively, was focused on the maximum z-axis deflection at the end of the part. The values of the processing condition used and the deflection were summarized in Table 29.

Table 29 The processing conditions and deflection values of the roof tile from the actual testing and simulation model based on conditions 1, 2, and 3.

Type	Process conditions					Warpage (mm)		
	Melt Temp	Injection Speed	Packing Pressure	Packing time	Cooling time	MPI results	Actual testing	Accuracy (%)
In production	160°C	58%	5.5 MPa	1.5 s	50 s	3.19	3.28	97.26
Sample 1	140°C	30%	4 MPa	2 s	40 s	-3.64	-3.75	97.07
Sample 2	180°C	30%	8 MPa	1 s	60 s	4.37	4.48	97.54

According to the results in Table 29, the warpage values of the simulation results closely match the actual testing results. Therefore, Moldflow can be applied to analyze the part's warpage instead of the actual testing.

2. The results of the Fractional Factorial design

2.1 The results of the Fractional Factorial design that the residual stress and process cycle time of the rectangular lid were outputs (Experiment 1)

Based on the 2^{6-2} Fractional Factorial design with six input process parameters and two outputs, the results of the residual stress and process cycle time of the rectangular lid are shown in Table 30.

Table 30 The results of Experiment 1

StdOrder	Material grade	Melt temperature (°C)	Injection speed (%)	Packing pressure (MPa)	Packing time (sec.)	Cooling time (sec.)	Residual stress (MPa)	Cycle time (sec.)
1	Styron 666D	200	30	3	1.5	10	28.69	19.35
2	Styron 678D	200	30	3	3.5	10	23.22	21.23
3	Styron 666D	260	30	3	3.5	25	24.89	36.16
4	Styron 678D	260	30	3	1.5	25	31.56	34.15
5	Styron 666D	200	50	3	3.5	25	23.71	35.22
6	Styron 678D	200	50	3	1.5	25	29.69	33.17
7	Styron 666D	260	50	3	1.5	10	32.74	18.12
8	Styron 678D	260	50	3	3.5	10	26.36	20.11
9	Styron 666D	200	30	5	1.5	25	26.80	34.19

Table 30 (Continued)

StdOrder	Material grade	Melt temperature (°C)	Injection speed (%)	Packing pressure (MPa)	Packing time (sec.)	Cooling time (sec.)	Residual stress (MPa)	Cycle time (sec.)
10	Styron 678D	200	30	5	3.5	25	21.66	36.15
11	Styron 666D	260	30	5	3.5	10	24.40	21.12
12	Styron 678D	260	30	5	1.5	10	31.49	19.12
13	Styron 666D	200	50	5	3.5	10	22.29	20.13
14	Styron 678D	200	50	5	1.5	10	29.72	18.12
15	Styron 666D	260	50	5	1.5	25	31.90	33.09
16	Styron 678D	260	50	5	3.5	25	25.44	35.09

According to Table 30, there were two steps of analysis to find the significant parameters that affect the residual stress and process cycle time of the rectangular lid: (i) ANOVA table and (ii) model adequacy checking.

2.1.1 The ANOVA table of Experiment 1

2.1.1.1 The ANOVA table that the residual stress of the rectangular lid was a response.

The ANOVA results of the 2^{6-2} Fractional Factorial design for finding the significant process parameters that affect the residual stress of the rectangular lid are shown in Table 31.

Table 31 The ANOVA results in which the residual stress of the rectangular lid was a response in Experiment 1

Source	DF	Seq SS	Adj SS	Adj MS	F	P
Material grade	1	0.858	0.858	0.858	2.36	0.159
Melt temperature	1	39.094	39.094	39.094	107.64	0.000
Injection speed	1	5.216	5.216	5.216	14.36	0.004
Packing pressure	1	5.244	5.244	5.244	14.44	0.004
Packing time	1	173.054	173.054	173.054	476.49	0.000
Cooling time	1	0.666	0.666	0.666	1.83	0.209
Error	9	3.269	3.269	0.363		
Total	15	227.4				

From the results of Table 31, the *F*-value of melt temperature, injection speed, packing pressure, and packing time are more than F-critical value ($F_{0.05,1,9}$ = 5.12). Moreover, corresponding p-value of these four parameters, which are 0.000, 0.004, 0.004, and 0.000, are less than α value (0.05). It means these four parameters have a significant affect on the residual stress of the rectangular lid. However, another two parameters (material grade and cooling time), which have more p-value than α value, do not affect on the residual stresses of the part at 95% confident interval.

2.1.1.2 The ANOVA table that process cycle time of the rectangular lid was a response.

The ANOVA results of the 2^{6-2} Fractional Factorial design for finding the significant process parameters that affect the process cycle time of the rectangular lid are shown in Table 32.

Table 32 The ANOVA results in which the process cycle time of the rectangular lid was a response in Experiment 1

Source	DF	Seq SS	Adj SS	Adj MS	F	P
Material grade	1	0.000	0.000	0.000	2.810	0.128
Melt temperature	1	0.020	0.020	0.020	17.570	0.002
Injection speed	1	4.430	4.430	4.430	3460.240	0.000
Packing pressure	1	0.020	0.020	0.020	12.200	0.007
Packing time	1	15.800	15.800	15.800	12338.880	0.000
Cooling time	1	898.800	898.800	898.800	701883.180	0.000
Error	9	0.010	0.010	0.000		
Total	15	919.090				

From the results of Table 32, the p-value of melt temperature, injection speed, packing pressure, packing time, and cooling time, which are 0.002, 0.000, 0.007, 0.000 and 0.000, are less than α value (0.05). It means these five parameters have a significant affect on the process cycle time of the rectangular lid. However, the material

grade, which has more p-value than α value, still do not affect on the process cycle time at 95% confident interval.

2.1.2 Model adequacy checking of Experiment 1

Model adequacy checking is used to verify that the results of ANOVA table are reliable. There are mainly two graphs for checking the adequate model which are normal probability plot and residual versus the fitted value plot.

2.1.2.1 Model adequate checking that residual stress of the rectangular lid was a response.

The model adequacy checking, which residual stresses of the rectangular lid was a response, had two mainly plots which are normal probability plot on Figure 43 and residual versus the fitted value plot on Figure 44.

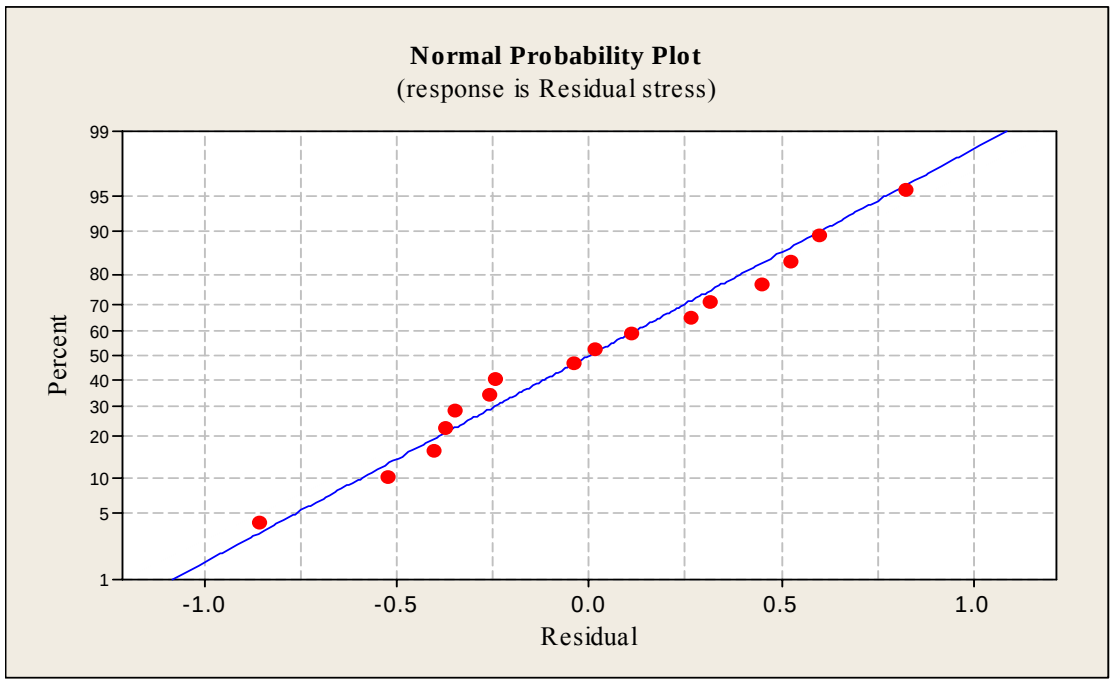

Figure 43 Normal probability plot that residual stress of the rectangular lid was a response in Experiment 1

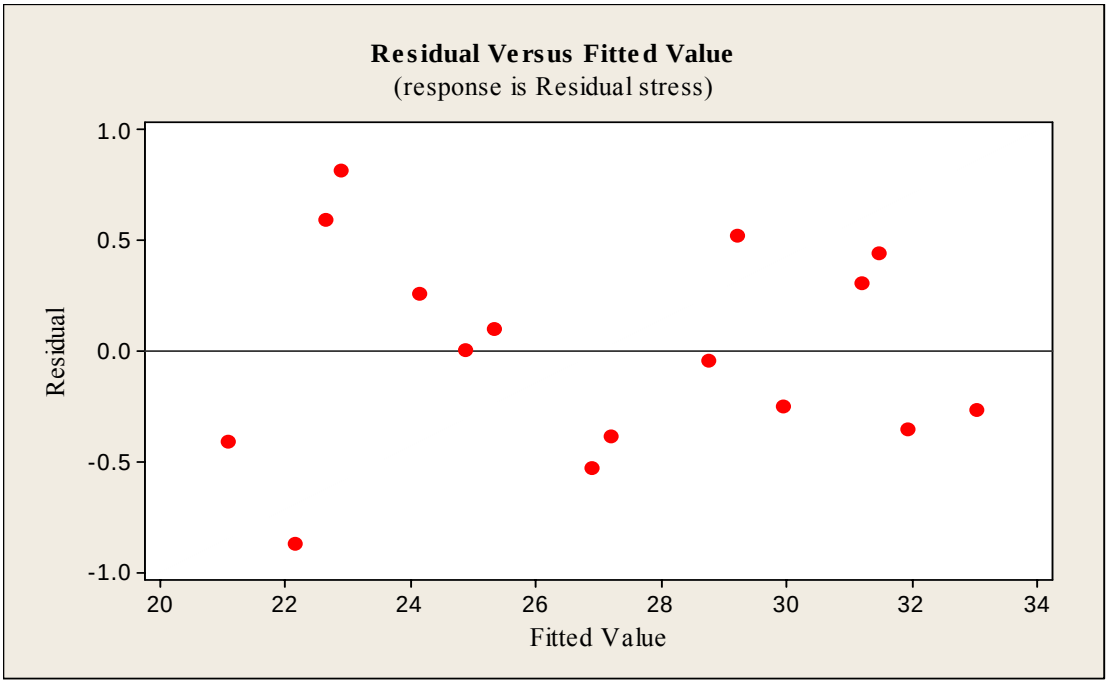

Figure 44 Residual versus the fitted value plot that residual stress of the rectangular lid was a response in Experiment 1

According to Figures 43 and 44, there is nothing unusual about the residual plots. The graph of normal probability plot of the residual is close to straight line. It implies that the data is the normal distribution. For the plot of residual versus fitted value, its characteristic has no pattern and no balanced, so it can be assumed that the variance is constant and independent.

2.1.2.2 Model adequacy checking that process cycle time of the rectangular lid was a response.

The model adequacy checking, which process cycle time of the rectangular lid was a response, had two plots for checking the adequate model which are normal probability plot on Figure 45 and residual versus fitted value plot on Figure 46.

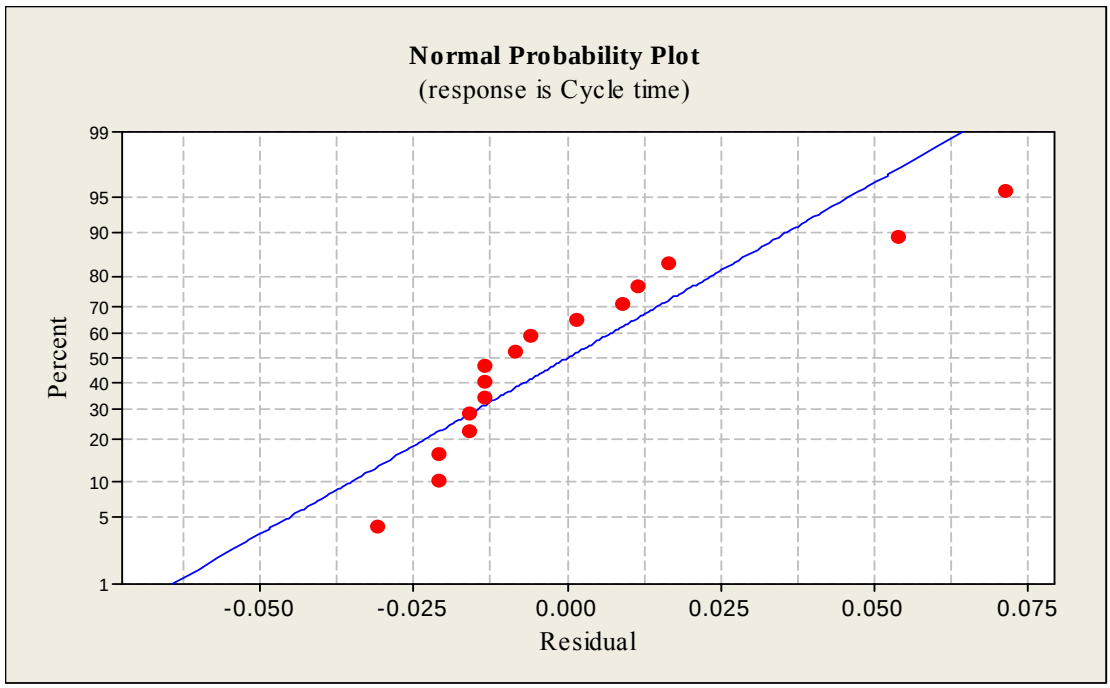

Figure 45 Normal probability plot that process cycle time of the rectangular lid was a response in Experiment 1

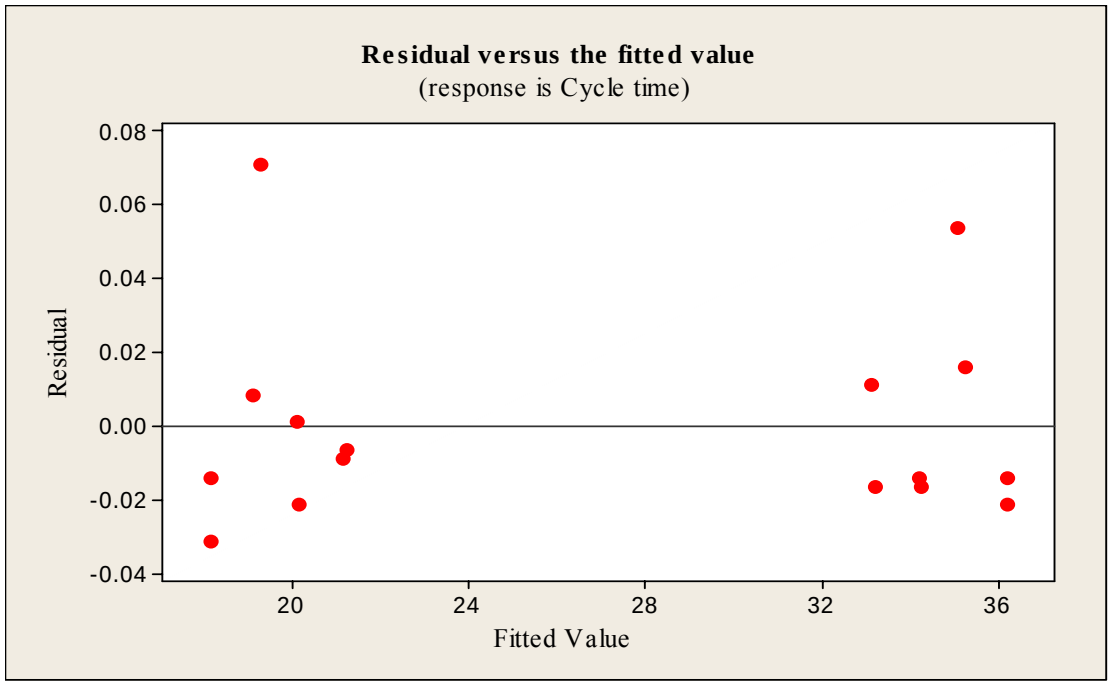

Figure 46 Residual versus fitted value plot that process cycle time of the rectangular lid was a response in Experiment 1

From Figure 45, the graph of normal probability plot of the residual is close to straight line. It implies the normal distribution data. However, the plot of the residual versus the fitted value plot as Figure 46 is very unusual shape indicating non-constant variance. Therefore, the solution is to add other input data from the obtained results to help the model to be more fitted. In this case, the added inputs were the interaction parameters of material grade with other parameters as on Table 33.

Table 33 The new ANOVA results in which the process cycle time of the rectangular lid was a response in Experiment 1

Source	DF	Seq SS	Adj SS	Adj MS	F	P
Material grade	1	0.004	0.004	0.004	2.46	0.192
Melt temperature	1	0.022	0.022	0.022	15.38	0.017
Injection speed	1	4.431	4.431	4.431	3029.76	0.000
Packing pressure	1	0.016	0.016	0.016	10.68	0.031
Packing time	1	15.801	15.801	15.801	10803.85	0.000
Cooling time	1	898.8	898.8	898.8	614564.38	0.000
Material grade*Melt temperature	1	0.003	0.003	0.003	1.71	0.261
Material grade*Injection speed	1	0.001	0.001	0.001	0.43	0.549
Material grade*Packing pressure	1	0.001	0.001	0.001	0.84	0.412
Material grade*Packing time	1	0.001	0.001	0.001	0.84	0.412
Material grade*Cooling time	1	0	0	0	0.07	0.807
Error	4	0.006	0.006	0.001		
Total	15	919.085				

From Table 33, the results are on the same direction as the results of Table 31. The p-value of melt temperature, injection speed, packing pressure, packing time, and cooling time, which are 0.017, 0.000, 0.031, 0.000 and 0.000, are less than α value (0.05). It means these five parameters still have a significant affect on the cycle time of the rectangular lid. However, the material grade do not affect on the process cycle time yet at 95% confident interval.

From the new ANOVA table, the normal probability plot and residual versus fitted value have to be checked for the results reliable. The new normal probability plot and new residual versus fitted value plot are shown in Figure 47 and 48.

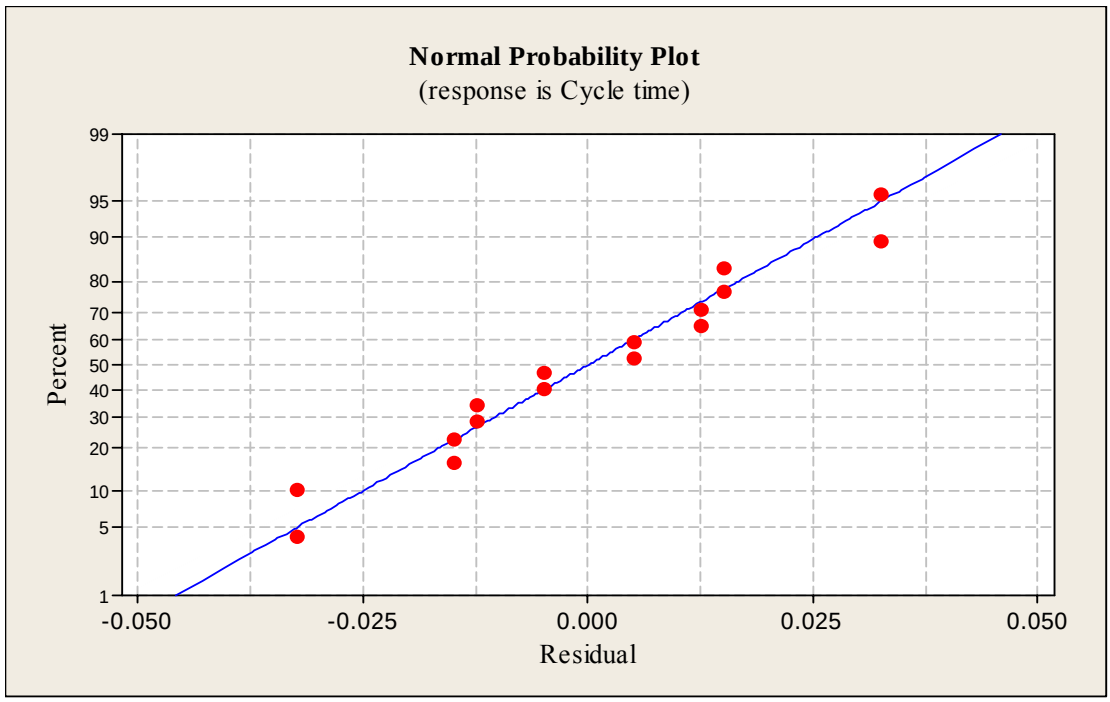

Figure 47 New normal probability plot that process cycle time of the rectangular lid was a response of Experiment 1

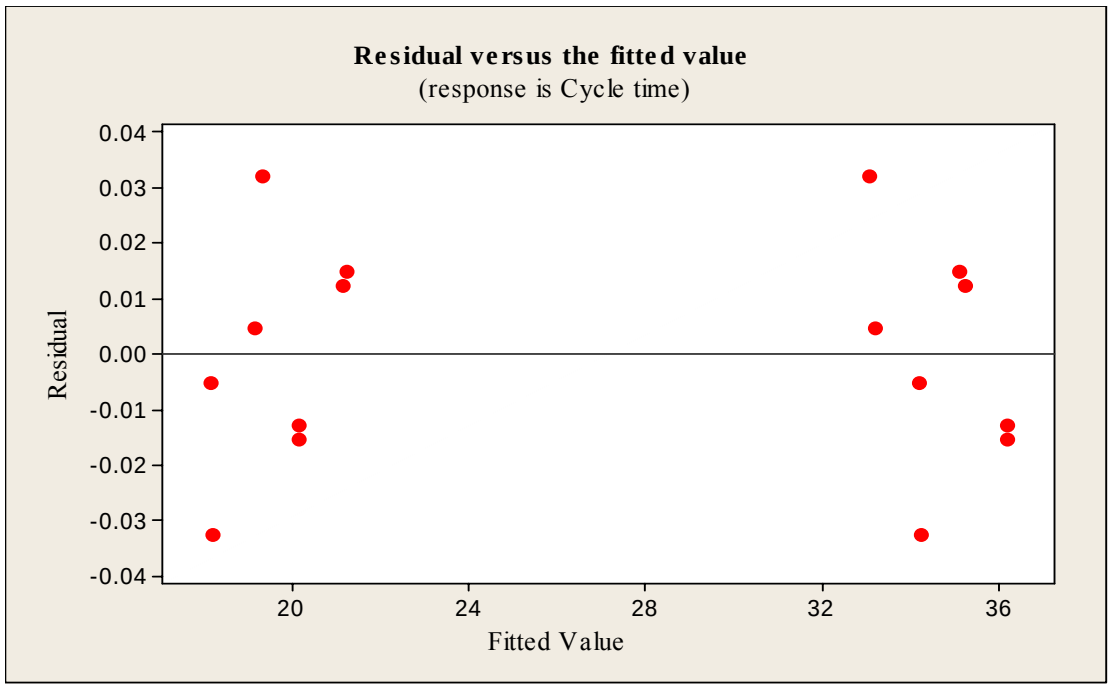

Figure 48 New residual versus the fitted value plot that the process cycle time of the rectangular lid was a response in Experiment 1.

According to Figure 47 and 48, the residual plots are much improved. The graph of normal probability plot of the residual is close to straight line. It implies that the data is the normal distribution. For the residual versus the fitted value, the plot characteristic shows a random pattern of residuals on both sides of 0. Thus, it can be assumed that the variance is constant and independent.

Finally, from the results of Fractional Factorial design that the residual stress and process cycle time of the rectangular lid were outputs (Experiment 1), there were totally five processing parameters including (i) melt temperature, (ii) injection speed, (iii) packing pressure, (iv) packing time, and (v) cooling time, significantly affected on the residual stress and the process cycle time of the rectangular lid. Therefore, the selection of these five processing parameters was used to determine the five input neuron number of ANN model on the next section.

2.2 The results of the Fractional Factorial design that the warpage and process cycle time of the roof tile were outputs (Experiment 2)

Based on the 2^{5-1} Fractional Factorial design with five input process parameters and two outputs, the results of the warpage and process cycle time of the roof tile are shown in Table 34.

Table 34 The results of Experiment 2

StdOrder	Melt temperature (°C)	Injection speed (%)	Packing pressure (MPa)	Packing time (second)	Cooling time (second)	Warpage (mm.)	Cycle time (second)
1	140	30	4	1	60	13.21	70.53
2	180	30	4	1	40	5.32	50.44
3	140	90	4	1	40	8.09	47.63
4	180	90	4	1	60	16.71	67.60
5	140	30	8	1	40	1.75	50.34
6	180	30	8	1	60	4.37	70.32
7	140	90	8	1	60	6.78	67.52
8	180	90	8	1	40	12.01	47.51
9	140	30	4	2	40	3.64	51.53
10	180	30	4	2	60	3.96	71.44

Table 34 (Continued)

StdOrder	Melt temperature (°C)	Injection speed (%)	Packing pressure (MPa)	Packing time (second)	Cooling time (second)	Warpage (mm.)	Cycle time (second)
11	140	90	4	2	60	9.84	68.63
12	180	90	4	2	40	4.58	48.60
13	140	30	4	2	60	3.08	71.34
14	180	30	8	2	40	4.51	51.32
15	140	90	8	2	40	2.36	48.52
16	180	90	8	2	60	3.62	68.51

According to Table 34, there were two steps of analysis to find the significant parameters that affect the warpage and process cycle time of the roof tile: (i) ANOVA table and (ii) model adequacy checking.

2.2.1 ANOVA table of Experiment 2

2.2.1.1 The ANOVA table that the warpage of the roof tile was a response.

The ANOVA results of 2^{5-1} Fractional Factorial design for finding the significant process parameters that affect the warpage of the roof tile are shown in Table 35.

Table 35 The ANOVA results in which the warpage of the roof tile was a response in Experiment 2

Source	DF	Seq SS	Adj SS	Adj MS	F	P
Melt temperature	1	2.50	5.88	5.88	0.54	0.478
Injection speed	1	36.45	46.85	46.85	4.33	0.064
Packing pressure	1	37.33	44.18	44.18	4.09	0.071
Packing time	1	81.41	80.21	80.21	7.42	0.021
Cooling time	1	15.44	15.44	15.44	1.43	0.260
Error	10	108.12	108.12	10.81		
Total	15	281.24				

According to the results of Table 36, p-value of the five processing parameters: (i) melt temperature, (ii) injection speed, (iii) packing pressure, (iv) packing time, and (v) cooling time are 0.478, 0.064, 0.071, 0.021,0.260, respectively. In the first place, p-value of packing time is 0.021 which is less than α value (0.05) is a significant parameter. Another, p-value of injection speed and packing pressure (0.064 and 0.071) is more than α value, but is less than $\alpha = 0.1$. Thus, they are also attractive enough to consider these two parameters as significant parameters. Therefore, there were three parameters significantly affected the warpage of the roof tile at 95% confident interval, which are injection speed, packing pressure, and packing time.

2.2.1.2 The ANOVA table that the process cycle time of the roof tile was a response.

The ANOVA results of the 2^{5-1} Fractional Factorial design for finding the significant process parameters that affect the process cycle time of the roof tile are shown in Table 36.

Table 36 The ANOVA results in which the process cycle time of the roof tile was a response in Experiment 2

Source	DF	Seq SS	Adj SS	Adj MS	F	P
Melt temperature	1	0.01	0.00	0.00	2.83	0.124
Injection speed	1	32.49	31.62	31.62	24828.73	0.000
Packing pressure	1	31.41	0.05	0.05	40.30	0.000
Packing time	1	1.71	3.88	3.88	3044.07	0.000
Cooling time	1	1572.19	1572.19	1572.19	1234570.03	0.000
Error	9	0.01	0.010	0.00		
Total	15	1637.82				

From the results of Table 36, the p-value of injection speed, packing pressure, packing time, and cooling time, which are 0.000, 0.000, 0.000 and 0.000, are less than α value (0.05). Nevertheless, the p-value of melt temperature is 0.124 that more than α value. It means that injection speed, packing pressure, packing time, and cooling time have a significant affect on the cycle time of the roof tile process. However, the melt temperature still do not affect the process cycle time at 95% confident interval.

2.2.2 Model adequacy checking of Experiment 2

Model adequacy checking is used to verify that the results of ANOVA table were reliable. There were mainly two graphs for checking the adequate model which are normal probability plot and residual versus the fitted value plot.

2.2.2.1 Model adequacy checking that the warpage of the roof tile was a response.

The model adequacy checking, which warpage of the roof tile was a response, had two plots for checking the adequate model which were normal probability plot in Figure 49 and residual versus the fitted value plot in Figure 50.

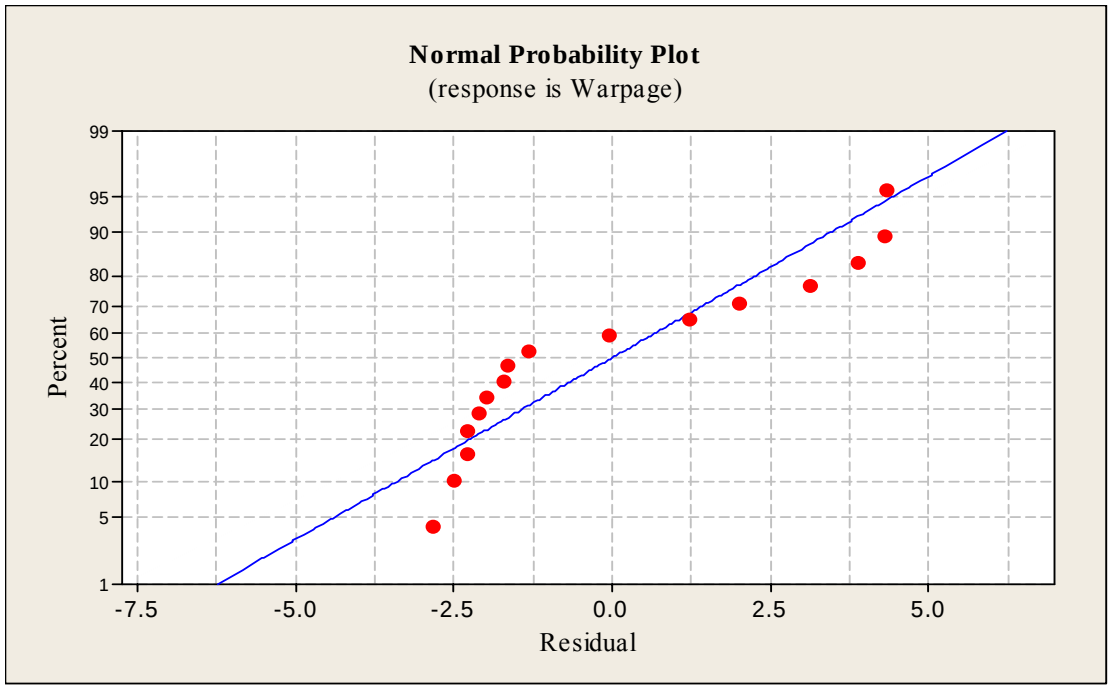

Figure 49 Normal probability plot that warpage of the roof tile was a response in Experiment 2

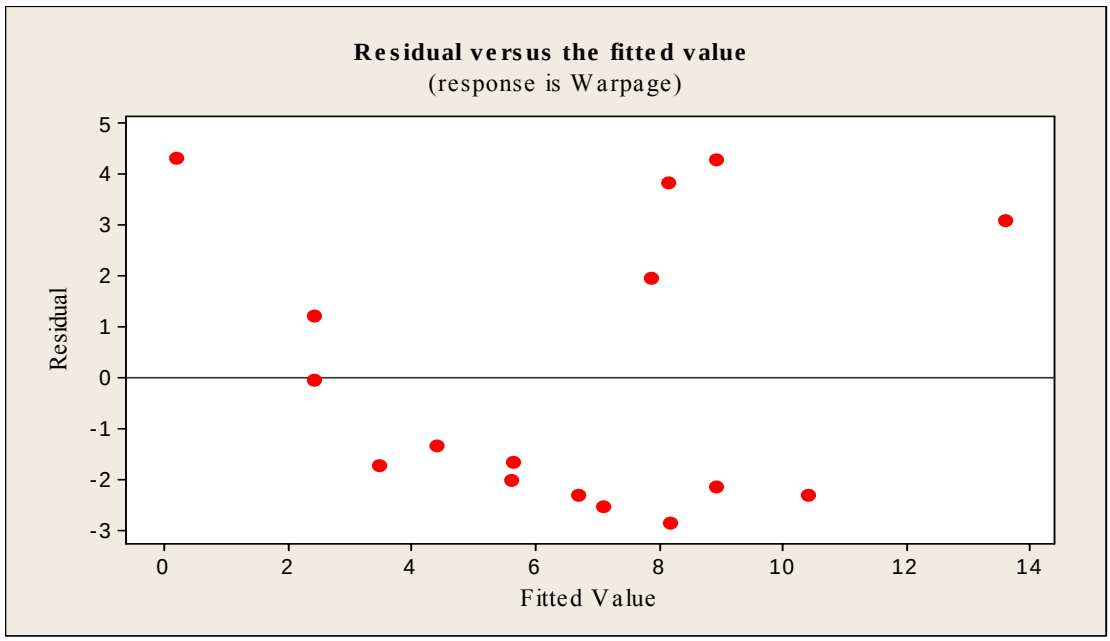

Figure 50 Residual versus the fitted value plot that warpage of the roof tile was a response in Experiment 2

From Figure 49, the graph of normal probability plot of the residual has unusual shape implied the data is not the normal distribution. In the same manner, the plot of the residual versus the fitted value as Figure 50 is also very unusual shape indicating non-constant variance. Therefore, the solution of them is to add other input data from the obtained results to help the model to be more fitted. In this case, the added three more inputs were the interaction parameters of packing pressure with packing time, packing pressure with cooling time, and packing time with cooling time as shown in Table 37.

Table 37 The new ANOVA results in which the warpage of the roof tile was a response in Experiment 2

Source	DF	Seq SS	Adj SS	Adj MS	F	P
Melt temperature	1	2.496	10.597	10.597	1.63	0.243
Injection speed	1	36.445	57.362	57.362	8.80	0.021
Packing pressure	1	37.329	56.363	56.363	8.65	0.022
Packing time	1	81.407	92.864	92.864	14.24	0.007
Cooling time	1	15.445	8.725	8.725	1.34	0.285
Packing pressure*Packing time	1	5.695	1.325	1.325	0.20	0.666

Table 37 (Continued)

Source	DF	Seq SS	Adj SS	Adj MS	F	P
Packing pressure*Cooling time	1	42.500	49.503	49.503	7.59	0.028
Packing time*Cooling time	1	14.289	14.289	14.289	2.19	0.182
Error	7	45.637	45.637	6.520		
Total	15	281.242				

From Table 37, the results are on the same direction as the results of Table 35. The p-value of injection speed, packing pressure, and packing time, which are 0.021, 0.022 and 0.007, are less than α value (0.05). Nevertheless, the p-value of melt temperature and cooling time are still more than α value (0.05). It means the first three parameters still have a significant affect on the warpage of the roof tile. However, the last two parameters do not affect on the roof tile's warpage at 95% confident interval.

After obtain the new ANOVA table, the normal probability plot and residual versus the fitted value have to be checked for the result's reliable. The new normal probability plot and new residual versus the fitted value are shown in Figures 51 and 52.

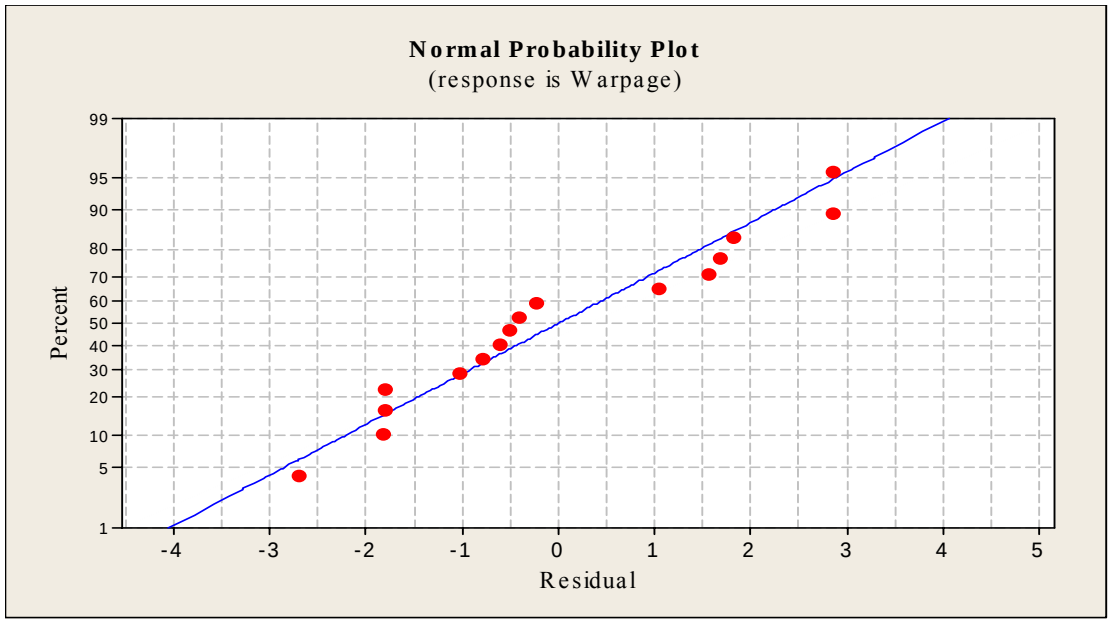

Figure 51 New normal probability plot that the warpage of the roof tile was a response in Experiment 2

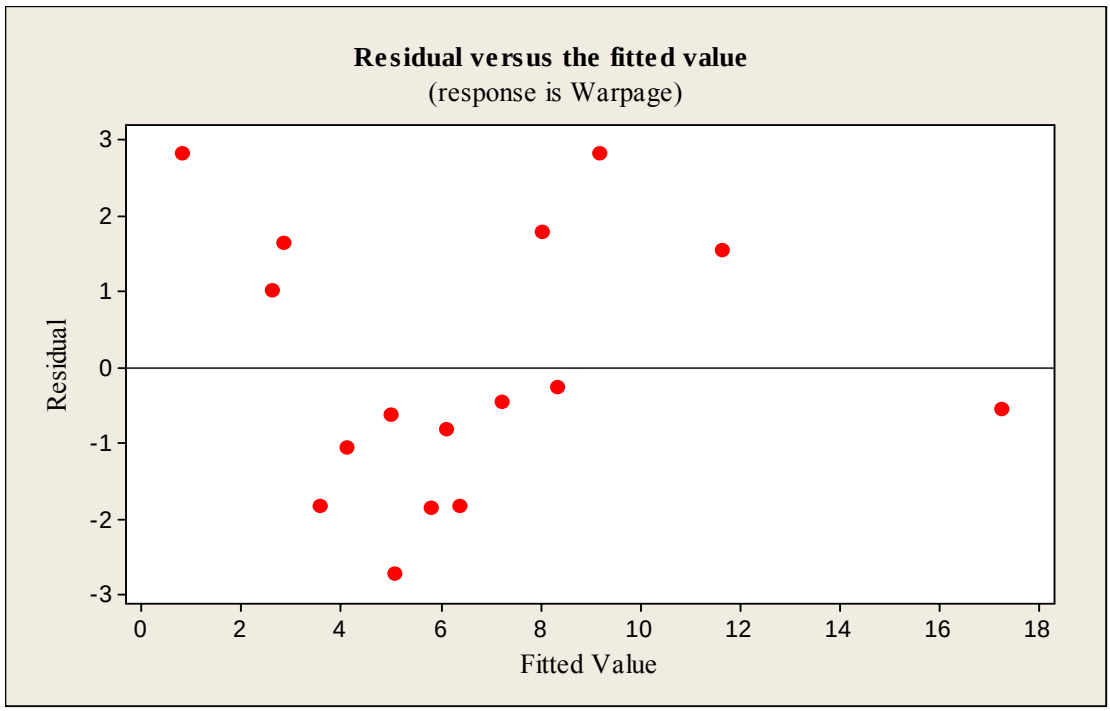

Figure 52 New residual versus the fitted value plot that the warpage of the roof tile was a response in Experiment 2

According to Figure 51 and 52, the residual plots are much improved. The graph of normal probability plot of the residual is close to straight line. It implies that the data is the normal distribution. For the residual versus the fitted value, the plot characteristic shows a random pattern of residuals on both equal sides of 0. Thus, it can be assumed that the variance is constant and independent.

2.2.2.2 Model adequacy checking that process cycle time of the roof tile was a response.

The model adequacy checking, which process cycle time of the roof tile was a response, had two graphs for checking the adequate model which were the normal probability plot on Figure 53 and the residual versus the fitted value plot on Figure 54.

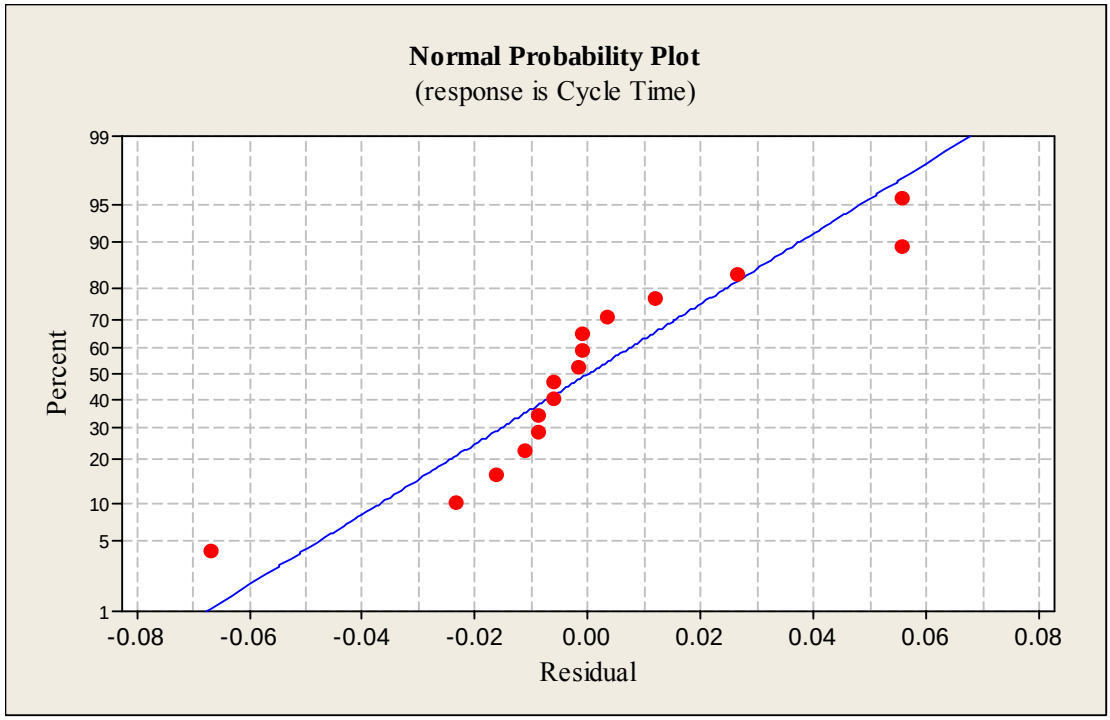

Figure 53 Normal probability plot that the process cycle time of the roof tile was a response in Experiment 2.

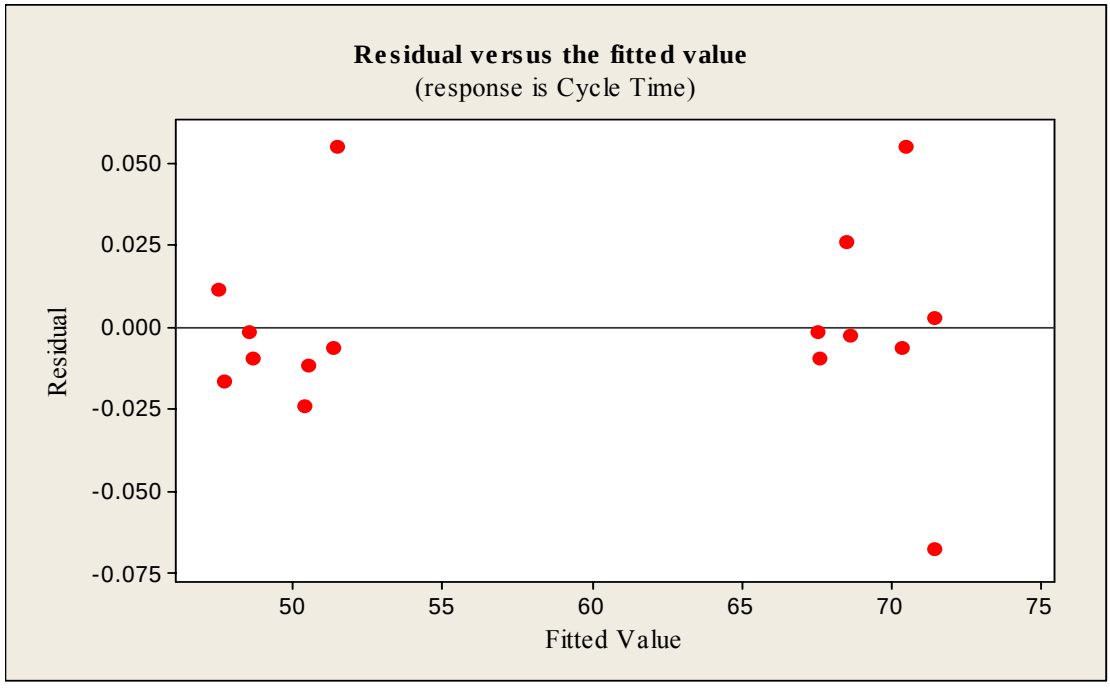

Figure 54 Residual versus fitted value plot that the process cycle time of the roof tile was a response in Experiment 2

According to Figures 53 and 54, there is nothing unusual about the residual plots. The graph of normal probability plot of the residual is quite close to straight line. It implies that the data is the normal distribution. For the residual versus the fitted value, the plot characteristic has no pattern and its both sides is quite balanced, so it can be assumed that the variance is constant and independent.

Finally, from the results of the Fractional Factorial design that the warpage and the process cycle time of the roof tile were outputs (Experiment 2), there were totally four parameters including (i) injection speed, (ii) packing pressure, (iii) packing time, and (iv) cooling time, significantly affected the warpage and process cycle time of the roof tile. Therefore, the selection of these four processing parameters was used to determine as the four input neuron number of the ANN model in the next section.

3. The results of the optimal structural ANN model

3.1 The results of the optimal structural ANN model that the residual stress and process cycle time of the rectangular lid were outputs

3.1.1 The result of Experiment 3

Experiment 3 is the design to determine the appropriate characteristic of input value and transfer function of hidden layer for training the ANN model that the residual stress and process cycle time were outputs. Hence, this experiment was divided into four types: (i) unnormalization with logsig, (ii) unnormalization with tansig, (iii) normalization with logsig, and (iv) normalization with tansig. The total average accuracy results of these four types are as shown in Table 38.

Table 38 The total results of Experiment 3

Type	Characteristic of input	Transfer function	Total Accuracy (%) Residual Stress	Total Accuracy (%) Cycle Time	Total Average Accuracy (%)
1	Unnormalization	logsig	96.75748	99.0459	97.90169
2	Unnormalization	tansig	96.40004	99.13408	97.76706
3	Normalization	logsig	99.15950	99.70260	99.43105
4	Normalization	tansig	99.05996	99.60192	99.33094

From Table 38, there were three steps of analysis to find the appropriate characteristic of input value and transfer function of hidden layer for training the ANN model that the residual stress and process cycle time were outputs: (i) ANOVA table, (ii) the box-plot, and (iii) standard deviation analysis.

3.1.1.1 The ANOVA table of Experiment 3

The ANOVA result of Experiment 3 was used for analyzing whether the means of average accuracy on these four types for training the ANN model were different. The result of ANOVA table of Experiment 3 is shown in Table 39.

Table 39 The result of ANOVA table in Experiment 3

Source	DF	SS	MS	F	P
Characteristic of input	1	11.9602	11.9602	13.50	0.002
transfer function	1	0.0689	0.0689	0.08	0.784
Interaction	1	0.0015	0.0015	0.00	0.968
Error	16	14.1732	0.8858		
Total	19	26.2037			

From the results on Table 39, the p-value of characteristic of input (0.002) is less than α value (0.05), unless transfer function (0.784) and interaction (0.968) are more than α value (0.05). It means that the characteristic of input, which is unnormalization and noralization, is different. However, the transfer function of logsig and tansig has no difference at 95% confident interval.

3.1.1.2 Box-plot of Experiment 3

Box-plot is a simple tool to determine what type of input's characteristic and transfer function of hidden layer on ANN model should be used for predicting the pattern of the system. Figure 55 shows the different mean and the range of % accuracy of residual stress among four types of Experiment 3.

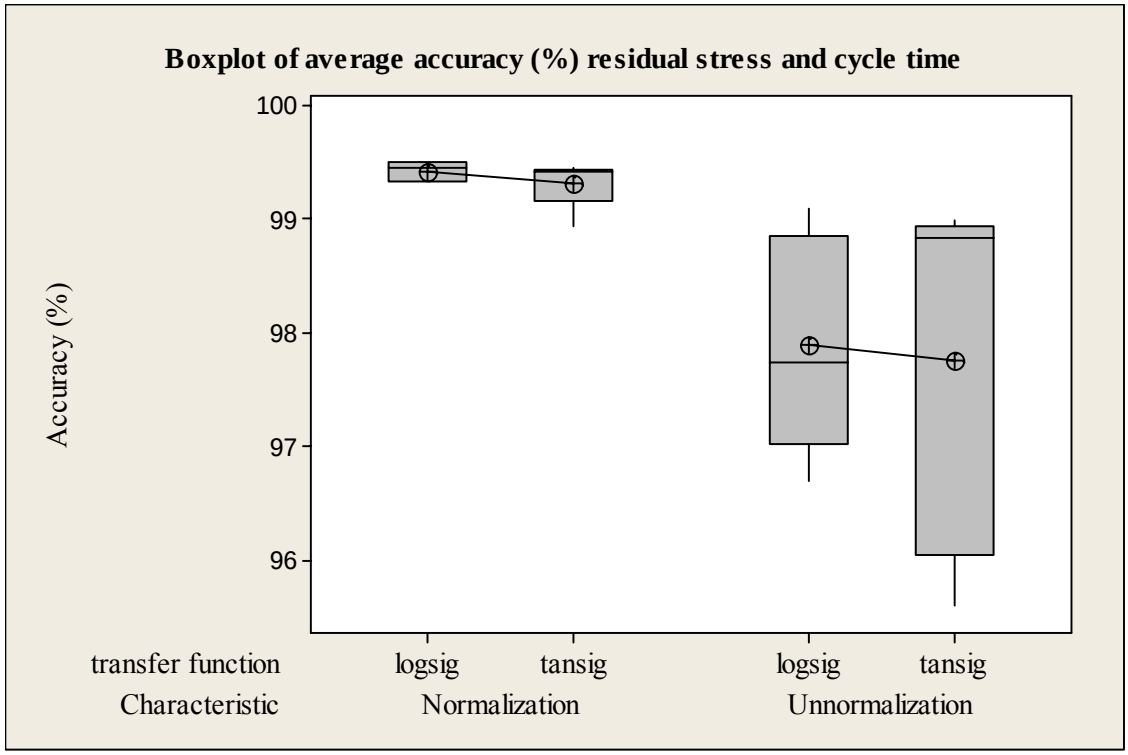

Figure 55 Box-plot of Experiment 3

3.1.1.3 Standard deviation analysis of Experiment 3

Standard deviation (SD) is the common measure of dispersion data from the mean. It can be used as preliminary benchmark for estimating the overall variation of among groups of data. In this case, SD was applied to benchmark among four types of Experiment 3. Table 41 displays the mean and SD of all four types for analyzing what type was the most appropriate for training the ANN model.

Table 40 The result of mean and standard deviation analysis of Experiment 3

Type	Characteristic of input	Transfer function	Total Accuracy (%) Residual Stress	Total Accuracy (%) Cycle Time	Total Average Accuracy (%)	SD
1	Unnormalization	logsig	96.75748	99.0459	97.90169	0.9616
2	Unnormalization	tansig	96.40004	99.13408	97.76706	1.6014
3	Normalization	logsig	99.1595	99.7026	99.43105	0.0836
4	Normalization	tansig	99.05996	99.60192	99.33094	0.2175

According to Figure 55 and Table 40, the normalization input and 'logsig' transfer function has the best result for the total average accuracy (%) of residual stress and process cycle time because of its maximum mean (99.43105) and minimum SD (0.0836). Therefore, the normalization input value and 'logsig' transfer function were appropriate for the optimal structure of ANN model that had one hidden layer and two outputs, residual stress and process cycle time.

3.1.2 The result of Experiment 4

Experiment 4 was the experiment used for determining an appropriate *epochs* and *lr* for training the ANN model that had one hidden layer and two outputs, the rectangular lid's residual stress and its process cycle time. The total average accuracy of residual stress and process cycle time results of Experiment 4 are shown in Table 41.

Table 41 The total results of Experiment 4

Type	Learning Rate	Epoch	Total Accuracy (%) Residual Stress	Total Accuracy (%) Cycle Time	Total Average Accuracy (%)
1	0.01	1000	99.1309	99.6865	99.4087
2	0.01	3000	99.0826	99.6264	99.3545
3	0.01	5000	99.1816	99.6543	99.4179
4	0.05	1000	99.0837	99.6278	99.3558
5	0.05	3000	99.1284	99.1271	99.1278
6	0.05	5000	99.1475	99.5776	99.3626
7	0.09	1000	99.0177	99.4077	99.2127
8	0.09	3000	99.0561	99.7030	99.3796
9	0.09	5000	99.0708	99.6405	99.3556

From Table 41, there were three steps to find the appropriate *epochs* and *lr* for training the ANN model that had one hidden layer and two outputs, the rectangular lid's residual stress and its process cycle time: (i) ANOVA table, (ii) the box-plot, and (iii) standard deviation analysis.

3.1.2.1 ANOVA table of Experiment 4

The ANOVA result of Experiment 4 was used for analyzing whether the means of average accuracy on residual stress and process cycle time among nine types for the training ANN model, two training parameters with three levels, were different. The result of ANOVA table of Experiment 4 is shown in Table 42.

Table 42 The result of ANOVA table in Experiment 4

Source	DF	SS	MS	F	P
Learning Rate	2	0.09836	0.04918	0.85	0.437
Epoch	2	0.06321	0.03161	0.54	0.585
Interaction	4	0.20855	0.05214	0.90	0.475
Error	36	2.09084	0.05808		
Total	44	2.46096			

From the results on Table 42, the p-value of learning rate (*lr*), *epoch*, and their interaction, which are 0.437, 0.585, and 0.475, are more than α value (0.05). It means that learning rate (*lr*) and *epoch* have no difference at 95% confident interval. Hence, box-plot and standard deviation analysis can be ignored. Therefore, any levels of learning rate and epoch can be used to train the ANN model.

In this study, the minimum learning rate (0.01) and epoch (1,000) were selected for saving a training time of the ANN model that had one hidden layer and two outputs, residual stress and process cycle time.

3.1.3 The result of Experiment 5

Experiment 5 was the experiment used for determining an appropriate initial *bias* value in structural ANN model that had one hidden layer and two outputs, the rectangular lid's residual stress and its process cycle time. The total average accuracy of residual stress and process cycle time results of Experiment 5 are shown in Table 43.

Table 43 The total results of Experiment 5

Type	Bias	Total Accuracy (%) Residual Stress	Total Accuracy (%) Cycle Time	Total Average Accuracy (%)
1	without bias	99.1122	99.6261	99.3691
2	bias = 0.5	99.1410	99.3979	99.2695
3	bias = 1	99.1364	99.6459	99.3911

From Table 43, there were three steps of analysis to find the appropriate initial *bias* value in structural ANN model that had one hidden layer and two outputs, the rectangular lid's residual stress and its process cycle time: (i) ANOVA table, (ii) the box-plot, and (iii) standard deviation analysis.

3.1.3.1 ANOVA table of Experiment 5

The ANOVA result of Experiment 5 was used for analyzing whether the means of average accuracy on residual stress and process cycle time among three types of initial *bias* value in structural ANN model were different. The result of ANOVA table of Experiment 5 is shown in Table 44.

Table 44 The result of ANOVA table in Experiment 5

Source	DF	SS	MS	F	P
Bias	2	0.0420	0.0210	0.68	0.524
Error	12	0.3695	0.0308		
Total	14	0.4116			

From the results on Table 44, the p-value of bias (0.524) is more than α value (0.05). It means that bias value has no difference at 95% confident interval. Hence, box-plot and standard deviation analysis can be ignored. Hence, any value of bias can be used to train the ANN model. In this research, bias of 1 had maximum mean (99.3911). Therefore, bias of 1 was appropriate for the optimal structure of the ANN model that had one hidden layer and two outputs, the rectangular lid's residual stress and its process cycle time.

3.1.4 The result of Experiment 6

Experiment 6 was the experiment used for determining an appropriate number of neuron in the 1st hidden layer in structural ANN model that had one hidden layer and two outputs, the rectangular lid's residual stress and its process cycle time. The total average accuracy of residual stress and process cycle time results of Experiment 6 are shown in Table 45.

Table 45 The total results of Experiment 6

Type	Number of neuron in 1st hidden layer	Total Accuracy (%) Residual Stress	Total Accuracy (%) Cycle Time	Total Average Accuracy (%)
1	3	98.7104	99.0725	98.8915
2	4	98.8746	99.6137	99.2441
3	5	98.8972	99.4772	99.1872
4	6	99.1457	99.6425	99.3941
5	7	99.3952	99.7384	99.5668
6	8	99.3669	99.7203	99.5436
7	9	99.2240	99.6708	99.4474
8	10	99.1569	99.7283	99.4426
9	11	99.1815	99.7040	99.4428

From Table 45, there were three steps of analysis to find the appropriate number of neuron in 1st hidden layer in structural ANN model that had 1 hidden layer and two outputs, the rectangular lid's residual stress and its process cycle time: (i) ANOVA table, (ii) box-plot, and (iii) standard deviation analysis.

3.1.4.1 ANOVA table of Experiment 6

The ANOVA result of Experiment 6 was used for analyzing whether the means of accuracy on the ANN models that have 3 to 11 neurons in the 1st hidden layer and two outputs, the rectangular lid's residual stress and its process cycle time, were different. The result of ANOVA table of Experiment 6 is shown in Table 46.

Table 46 The result of ANOVA table in Experiment 6

Source	DF	SS	MS	F	P
Number of neuron in 1st hidden layer	8	1.8052	0.2257	3.04	0.010
Error	36	2.6753	0.0743		
Total	44	4.4805			

From the results on Table 46, the p-value of neuron's number in the 1st hidden layer (0.010) is less than α value (0.05). It means the neuron's numbers in the 1st hidden layer are different from each other at 95% confident interval.

3.1.4.2 Box-plot of Experiment 6

On Figure 56, box-plot displays how many neurons' number in the 1st hidden layer should be used in the structural ANN model that has one hidden layer and two outputs: the rectangular lid's residual stress and its process cycle time.

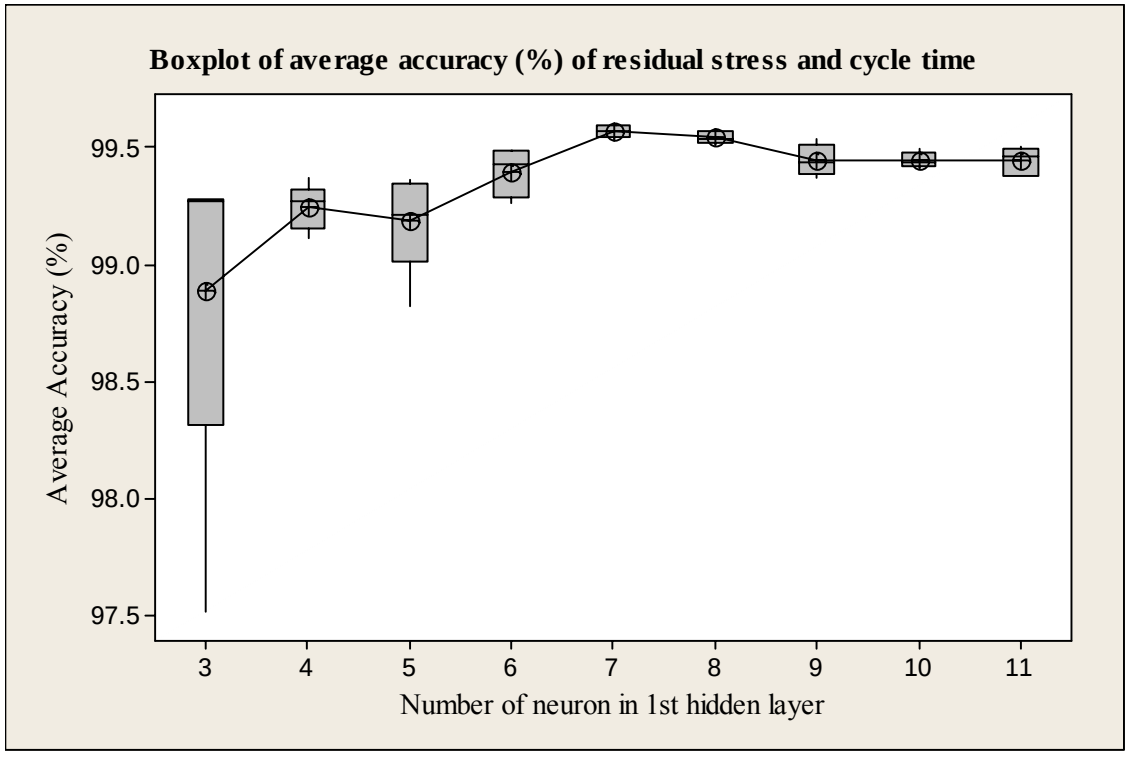

Figure 56 Box-plot of Experiment 6

3.1.4.3 Standard deviation analysis of Experiment 6

In this case, standard deviation (SD) is applied to benchmark among nine types of Experiment 6. Table 47 displays the mean and SD of these nine types for analyzing what type is the most appropriate for structural ANN model that has one hidden layer and two outputs, the rectangular lid's residual stress and its process cycle time.

Table 47 The result of mean and standard deviation analysis of Experiment 6

Type	Number of neuron in 1st hidden layer	Total Accuracy (%) Residual Stress	Total Accuracy (%) Cycle Time	Total Average Accuracy (%)	SD
1	3	98.7104	99.0725	98.8915	0.7705
2	4	98.8746	99.6137	99.2441	0.0937
3	5	98.8972	99.4772	99.1872	0.2134
4	6	99.1457	99.6425	99.3941	0.1004
5	7	99.3952	99.7384	99.5668	0.0270
6	8	99.3669	99.7203	99.5436	0.0288
7	9	99.2240	99.6708	99.4474	0.0668
8	10	99.1569	99.7283	99.4426	0.0340
9	11	99.1815	99.7040	99.4428	0.0603

As shown in Figure 56 and Table 47, the 7 neurons in the 1st hidden layer of the experiment (type 5) has the best result for the average accuracy (%) of the rectangular lid's residual stress and its cycle time because of maximum mean (99.5668) and also minimum SD (0.0270). Therefore, the 7 neurons in the 1st hidden layer was an appropriate component for the structure of ANN model that had one hidden layer and two outputs, the rectangular lid's residual stress and its process cycle time.

3.1.5 The result of Experiment 7

Experiment 7 was the experiment used for determining an appropriate number of neuron in the 2nd hidden layer in structural ANN model that had two hidden layers and two outputs, the rectangular lid's residual stress and its process cycle time. The total average accuracy (%) of residual stress and process cycle time results of Experiment 7 are shown in Table 48.

Table 48 The total results of Experiment 7

Type	Number of neuron in 2nd hidden layer	Total Accuracy (%) Residual Stress	Total Accuracy (%) Cycle Time	Total Average Accuracy (%)
1	5	99.1074	99.6608	99.3841
2	6	99.3642	99.7264	99.5453
3	7	98.8764	99.6213	99.2488
4	8	99.1034	99.6668	99.3851
5	9	99.1125	99.6619	99.3872
6	10	99.2239	99.6354	99.4297
7	11	98.9616	99.6130	99.2873
8	12	98.8794	99.6523	99.2658
9	13	98.5179	99.6896	99.1038
10	14	99.1645	99.6187	99.3916
11	15	98.3334	99.5286	98.9310

From Table 48, there were three steps of analysis to find the appropriate number of neuron in the 2nd hidden layer in structural ANN model that had two hidden layers and two outputs, the rectangular lid's residual stress and its process cycle time: (i) ANOVA table, (ii) the box-plot, and (iii) standard deviation analysis.

3.1.5.1 ANOVA table of Experiment 7

The ANOVA result of Experiment 7 was used for analyzing whether the means of average accuracy on the ANN models that had 5 to 15 neurons in the 2nd hidden layer and two outputs, the rectangular lid's residual stress and its process cycle time, were different. The result of ANOVA table of Experiment 7 is shown in Table 49.

Table 49 The result of ANOVA table in Experiment 7

Source	DF	SS	MS	F	P
Number of neuron in 2nd hidden layer	10	1.4279	0.1428	8.68	0.000
Error	44	0.7235	0.0164		
Total	54	2.1514			

From the results on Table 49, the p-value of neuron's number in the 2nd hidden layer (0.002) is less than α value (0.05). It means the neuron's numbers in the 2nd hidden layer are different from each other at 95% confident interval.

3.1.5.2 Box-plot of Experiment 7

On Figure 57, the box-plot displays what neuron's number in the 2nd hidden layer should be used in structural ANN model that has two hidden layers and two outputs, the rectangular lid's residual stress and its process cycle time.

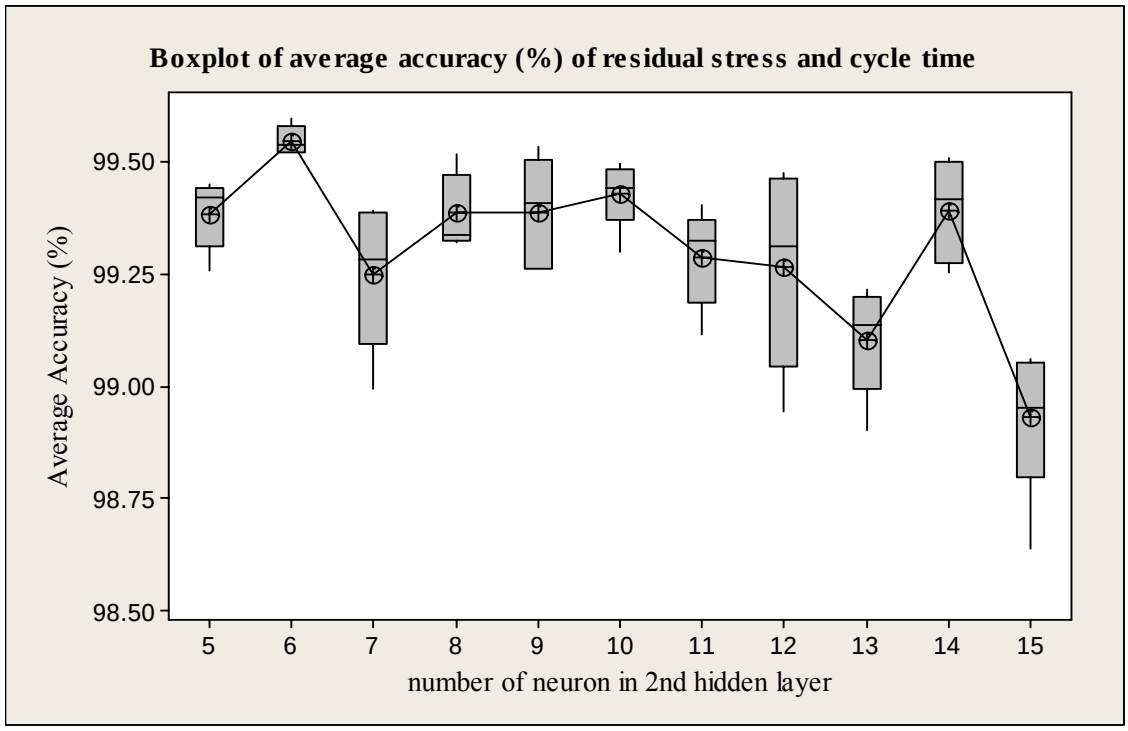

Figure 57 Box-plot of Experiment 7

3.1.5.3 Standard deviation analysis of Experiment 7

In this case, standard deviation (SD) was applied to benchmark among eleven types of Experiment 7. Table 50 displays the mean and SD of these eleven types for analyzing what type was the most appropriate for structural ANN model that had two hidden layer and two outputs, the rectangular lid's residual stress and its process cycle time.

Table 50 The result of mean and standard deviation analysis of Experiment 7

Type	Number of neuron in 2nd hidden layer	Total Accuracy (%) Residual Stress	Total Accuracy (%) Cycle Time	Total Average Accuracy (%)	SD
1	5	99.1074	99.6608	99.3841	0.0779
2	6	99.3642	99.7264	99.5453	0.0325
3	7	98.8764	99.6213	99.2488	0.1636
4	8	99.1034	99.6668	99.3851	0.0847
5	9	99.1125	99.6619	99.3872	0.1244
6	10	99.2239	99.6354	99.4297	0.0766
7	11	98.9616	99.6130	99.2873	0.1092
8	12	98.8794	99.6523	99.2658	0.2225
9	13	98.5179	99.6896	99.1038	0.1233
10	14	99.1645	99.6187	99.3916	0.1138
11	15	98.3334	99.5286	98.9310	0.1700

As shown in Figure 57 and Table 50, the 6 neurons in the 2nd hidden layer of the experiment (type 2) has the best result for the total average accuracy (%) of the rectangular lid's residual stress and its process cycle time. This is because it has maximum mean (99.5453) and also minimum SD (0.0325). Therefore, the 6 neurons in the 2nd hidden layer was an appropriate component for the optimal structure of the ANN model that had two hidden layers and two outputs: the rectangular lid's residual stress and its process cycle time.

3.1.6 The comparison between 1 and 2 hidden layers of the structural ANN model that the rectangular lid's residual stress and its cycle time are outputs.

A structural ANN model mostly has one or two hidden layers placed between the input and output layer. Finding the optimal structure of the ANN model, which the rectangular lid's residual stress and its process cycle time were outputs, the best result of both one and two hidden layers needed to compare to each other as in Table 51. Later on, Table 52 displays the comparison data of the optimal structure of one and two hidden layers that the rectangular lid's residual stress and its process cycle time were outputs.

Table 51 The data of the optimal ANN models of the rectangular lid that had 1 and 2 hidden layers

No	Type	Average Accuracy (%)
1	1 hidden layer	99.6015
2	1 hidden layer	99.5526
3	1 hidden layer	99.5706
4	1 hidden layer	99.5302
5	1 hidden layer	99.5795
	average of 1 hidden layer	99.5668
6	2 hidden layers	99.5963
7	2 hidden layers	99.5369
8	2 hidden layers	99.5186
9	2 hidden layers	99.5183
10	2 hidden layers	99.5566
	average of 2 hidden layers	99.5453

Table 52 The total results of the optimal structure of 1 and 2 hidden layers on the ANN model that residual stress and process cycle of the rectangular lid were outputs

Type	ANN structure (input-hidden-output)	Accuracy (%) Residual Stress
1 hidden layer	5 - 7 - 2	99.5668
2 hidden layers	5 - 7 - 6 - 2	99.5453

The ANOVA analysis used to find the appropriate type of hidden layer in structural ANN model that the rectangular lid's residual stress and its process cycle time were outputs. It was used for analyzing whether the means of average accuracy on each five data of the optimal ANN models that had one and two hidden layers were different. The result of ANOVA table is shown in Table 53.

Table 53 The results of ANOVA table for finding the optimal structure of ANN model that the rectangular lid's residual stress and its process cycle time were outputs.

Source	DF	SS	MS	F	P
Type of the hidden layer	1	0.00116	0.00116	1.29	0.288
Error	8	0.00716	0.00090		
Total	9	0.00832			

From the results in Table 53, the p-value of the type of the hidden layer (0.288) is more than α value (0.05). It means that single and two hidden layers have no difference at 95% confident interval. Therefore, both type of hidden layer can be used as a structural ANN model. In this study, 1 hidden layer type was selected for the ANN model that the rectangular lid's residual stress and its process cycle time were outputs so as to minimize training time. Therefore, the optimal structure of the ANN model that had two outputs, the rectangular lid's residual stress and its process cycle time, is displayed in Table 54. In addition, the fitted predicted of this ANN model is obviously shown in Figure 58.

Table 54 The optimal structure of the ANN model that residual stress and process cycle time were outputs

ANN parameters	Optimal values
1. characteristic of input	normalization
2. number of neuron in the input layer	5
3. number of neurons in the 1st hidden layer	7
4. learning rate (*lr*)	0.01
5. *epochs*	1,000
6. initial *bias* value	1.0
7. transfer function of the 1st hidden layer	logsig
8. transfer function of the 2nd hidden layer	purelin
9. average accuracy (%) of the residual stress	99.3952
10. average accuracy (%) of the process cycle time	99.7384
11. total average accuracy (%)	99.5668

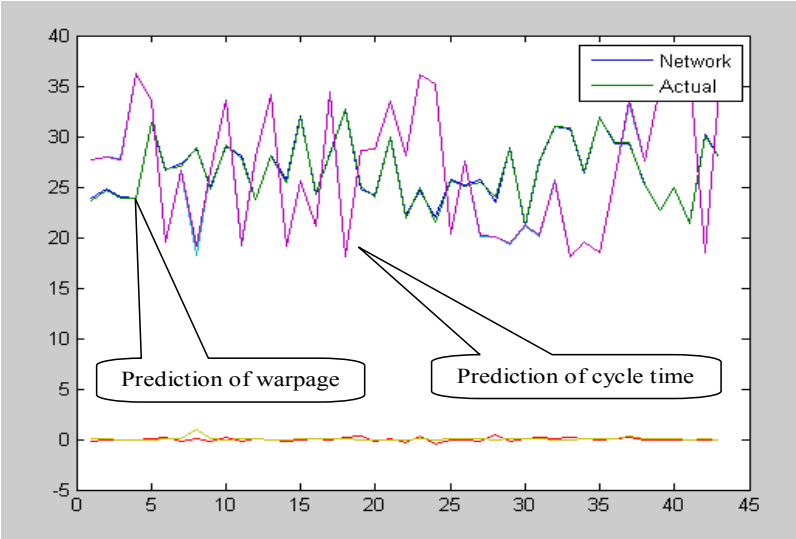

Figure 58 The fitted ANN model prediction of 5-7-2 configuration of the rectangular lid

3.2 The results of optimal structural ANN model that the warpage and process cycle time of the roof tile were outputs

3.2.1 The result of Experiment 8

Experiment 8 was the design to determine the appropriate characteristic of input value and transfer function of hidden layer for training the ANN model that the roof tile's warpage and its process cycle time were outputs. Hence, this experiment was divided into four types: (i) unnormalization with logsig, (ii) unnormalization with tansig, (iii) normalization with logsig, and (iv) normalization with tansig. The total average accuracy results of these four types are as shown in Table 55.

Table 55 The total results of Experiment 8

Type	Characteristic of input	Transfer function	Total Accuracy (%) Warpage	Total Accuracy (%) Cycle Time	Total Average Accuracy (%)
1	Unnormalization	logsig	58.7306	93.9893	76.3600
2	Unnormalization	tansig	58.4662	93.2076	75.8369
3	Normalization	logsig	90.1453	99.6482	94.8968
4	Normalization	tansig	88.9977	99.6805	94.3391

From Table 55, there were three steps of analysis to find the appropriate characteristic of input value and transfer function of hidden layer for training the ANN model that the roof tile's warpage and its process cycle time were outputs: (i) ANOVA table, (ii) the box-plot, and (iii) standard deviation analysis.

3.2.1.1 The ANOVA table of Experiment 8

The ANOVA result of Experiment 8 was used for analyzing whether the means of average accuracy on these four types for training the ANN model were different. The result of ANOVA table of Experiment 8 is shown in Table 56.

Table 56 The result of ANOVA table of Experiment 8

Source	DF	SS	MS	F	P
Characteristic of input	1	1714.86	1714.86	377.93	0.000
transfer function	1	1.46	1.46	0.32	0.578
Interaction	1	0.00	0.00	0.00	0.986
Error	16	72.60	4.54		
Total	19	1788.92			

From the results on Table 56, the p-value of characteristic of input (0.000) is less than α value (0.05), unless transfer function (0.578) and interaction (0.986) are more than α value (0.05). It means that the characteristic of input, which is unnormalization and noralization, is different from each other. However, the transfer function of logsig and tansig has no difference at 95% confident interval.

3.2.1.2 Box-plot of Experiment 8

In this case, box-plot was a simple tool to determine what type of input's characteristic and transfer function of hidden layer on ANN model should be used for predicting the pattern of the system. Figure 59 shows the different mean and the range of % accuracy of the roof tile's warpage and its process cycle time among 4 types of Experiment 8.

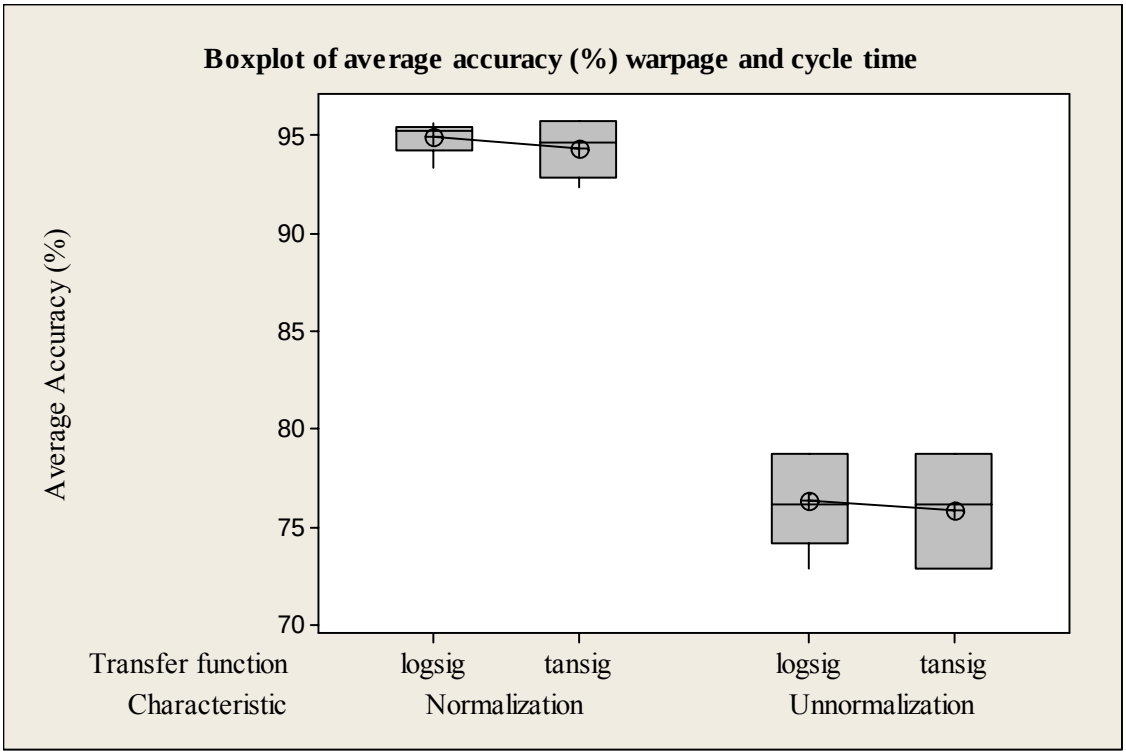

Figure 59 Box-plot of Experiment 8

3.2.1.3 Standard deviation analysis of Experiment 8

Standard deviation (SD) is the common measure of dispersion data from the mean. It can be used as preliminary benchmark for estimating the overall variation of among groups of data. In this case, SD was applied to benchmark among four types of Experiment 8. Table 57 displays the mean and SD of all four types for analyzing what type is the most appropriate for training the ANN model.

Table 57 The result of mean and standard deviation analysis of Experiment 8

Type	Characteristic of input	Transfer function	Total Accuracy (%) Warpage	Total Accuracy (%) Cycle Time	Total Average Accuracy (%)	SD
1	Unnormalization	logsig	58.7306	93.9893	76.3600	2.4979
2	Unnormalization	tansig	58.4662	93.2076	75.8369	2.9728
3	Normalization	logsig	90.1453	99.6482	94.8968	0.9141
4	Normalization	tansig	88.9977	99.6805	94.3391	1.4958

According to Figure 58 and Table 57, the normalization input and ‘logsig’ transfer function has the best result for the total average accuracy (%) of the roof tile’s warpage and its process cycle time, maximum mean (94.8968) and minimum SD (0.9141). Therefore, the normalization input value and ‘logsig’ transfer function were appropriate for the optimal structure of ANN model that had one hidden layer and two outputs, the roof tile’s warpage and its process cycle time.

3.2.2 The result of Experiment 9

Experiment 9 was the experiment used for determining an appropriate epochs and lr for training the ANN model that had one hidden layer and two outputs: the roof tile’s warpage and its process cycle time. The total average accuracy of warpage and process cycle time results of Experiment 9 is shown in Table 58.

Table 58 The total results of Experiment 9

Type	Learning Rate	Epoch	Total Accuracy (%) Warpage	Total Accuracy (%) Cycle Time	Total Average Accuracy (%)
1	0.01	1000	89.5241	99.7972	94.6607
2	0.01	3000	93.2577	99.7957	96.5267
3	0.01	5000	92.5296	99.7303	96.1299
4	0.05	1000	92.0447	99.8236	95.9342
5	0.05	3000	93.6669	99.8373	96.7521
6	0.05	5000	93.3483	99.8722	96.6102
7	0.09	1000	93.8035	99.9102	96.8568
8	0.09	3000	94.3445	99.9106	97.1276
9	0.09	5000	93.3074	99.8496	96.5785

From Table 58, there were three steps to find the appropriate *epochs* and *lr* for training the ANN model that had one hidden layer and two outputs, the roof tile’s warpage and its process cycle time: (i) ANOVA table, (ii) the box-plot, and (iii) standard deviation analysis.

3.2.2.1 ANOVA table of Experiment 9

The ANOVA result of Experiment 9 was used for analyzing whether the means of average accuracy on the roof tile's warpage and its process cycle time among nine types for training the ANN model, two training parameters with each three levels, were different. The result of ANOVA table of Experiment 9 is shown in Table 59.

Table 59 The result of ANOVA table of Experiment 9

Source	DF	SS	MS	F	P
Learning Rate	2	8.9192	4.4596	4.25	0.022
Epoch	2	7.4441	3.7221	3.55	0.039
Interaction	4	4.8839	1.2210	1.16	0.343
Error	36	37.7862	1.0496		
Total	44	59.0335			

From the results on Table 59, the p-value of learning rate and epoch, which are 0.022 and 0.039, are less than α value (0.05). It means that learning rate and epoch on each level were difference at 95% confident interval. Hence, the box-plot and standard deviation analysis were later used to obtain the appropriate learning rate and epoch for this problem.

3.2.2.2 Box-plot of Experiment 9

In this case, the box-plot was a simple tool to determine what type of learning rate and epoch on ANN model should be used for predicting the pattern of the system. Figure 60 displays the different mean and the range of % accuracy of the roof tile's warpage and its process cycle time among nine types of Experiment 9.

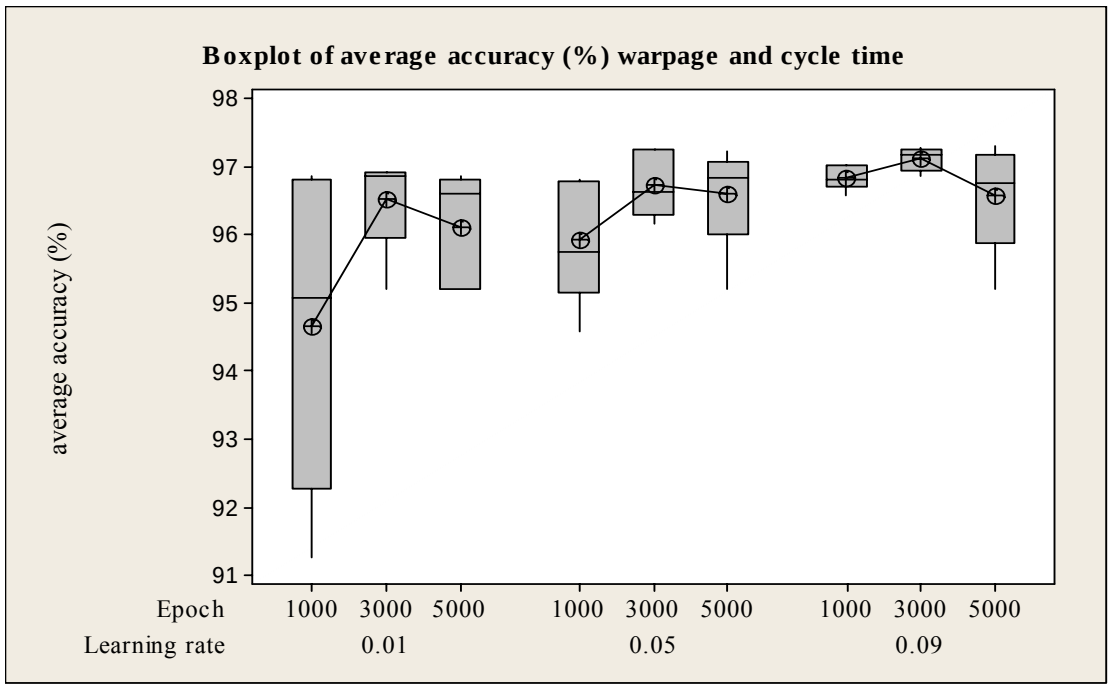

Figure 60 Box-plot of Experiment 9

3.2.2.3 Standard deviation analysis of Experiment 9

In this case, standard deviation (SD) was applied to benchmark among nine types of Experiment 9. Table 60 displays the mean and SD of the nine types for analyzing what type was the most appropriate for training the ANN model.

Table 60 The result of mean and standard deviation analysis of Experiment 9

Type	Learning Rate	Epoch	Total Accuracy (%) Warpage	Total Accuracy (%) Cycle Time	Total Average Accuracy (%)	SD
1	0.01	1000	89.5241	99.7972	94.6607	2.3939
2	0.01	3000	93.2577	99.7957	96.5267	0.7415
3	0.01	5000	92.5296	99.7303	96.1299	0.8457
4	0.05	1000	92.0447	99.8236	95.9342	0.9195
5	0.05	3000	93.6669	99.8373	96.7521	0.4874
6	0.05	5000	93.3483	99.8722	96.6102	0.8003
7	0.09	1000	93.8035	99.9102	96.8568	0.1767
8	0.09	3000	94.3445	99.9106	97.1276	0.1675
9	0.09	5000	93.3074	99.8496	96.5785	0.8174

According to Figure 59 and Table 60, learning rate of 0.09 and epoch of 3,000 had the best results for the total average accuracy (%) of the roof tile's warpage and its process cycle time, maximum mean (97.1276) and also minimum SD (0.1675). Therefore, learning rate of 0.09 and epoch of 3,000 were appropriate for the optimal structure of ANN model that had one hidden layer and two outputs: the roof tile's warpage and its process cycle time.

3.2.3 The result of Experiment 10

Experiment 10 was the experiment used for determining an appropriate *bias* value in structural ANN model that had one hidden layer and two outputs, the roof tile's warpage and its process cycle time. The total average accuracy of warpage and process cycle time results of Experiment 10 is shown in Table 61.

Table 61 The total results of Experiment 10

Type	Bias	Total Accuracy (%) Warpage	Total Accuracy (%) Cycle Time	Total Average Accuracy (%)
1	without bias	94.3087	99.9277	97.1182
2	bias = 0.5	93.9439	99.9442	96.9441
3	bias = 1	94.7147	99.9412	97.3280

From Table 61, there were three steps of analysis to find the appropriate *bias* value in the structural ANN model that had one hidden layer and two outputs: the roof tile's warpage and its process cycle time: (i) ANOVA table, (ii) the box-plot, and (iii) standard deviation analysis.

3.2.3.1 ANOVA table of Experiment 10

The ANOVA result of Experiment 10 was used for analyzing whether the means of average accuracy on the roof tile's warpage and its process cycle time among three types of bias value in structural ANN model were different. The result of ANOVA table of Experiment 10 is shown in Table 62.

Table 62 The result of ANOVA table of Experiment 10

Source	DF	SS	MS	F	P
Bias	2	0.3695	0.1848	17.27	0.000
Error	12	0.1284	0.0107		
Total	14	0.4979			

From the results on Table 62, the p-value of *bias* (0.000) is less than α value (0.05). It means these three initial *bias* values were difference at 95% confident interval. Therefore, box-plot and standard deviation analysis were later used to select the appropriate initial *bias* value for this problem.

3.2.3.2 Box-plot of Experiment 10

In this case, box-plot was a simple tool to determine what initial bias value should be used on training ANN model so as to predict the pattern of the system. Figure 61 displays the different mean and the range of % accuracy of the roof tile's warpage and its process cycle time among 3 types of Experiment 10.

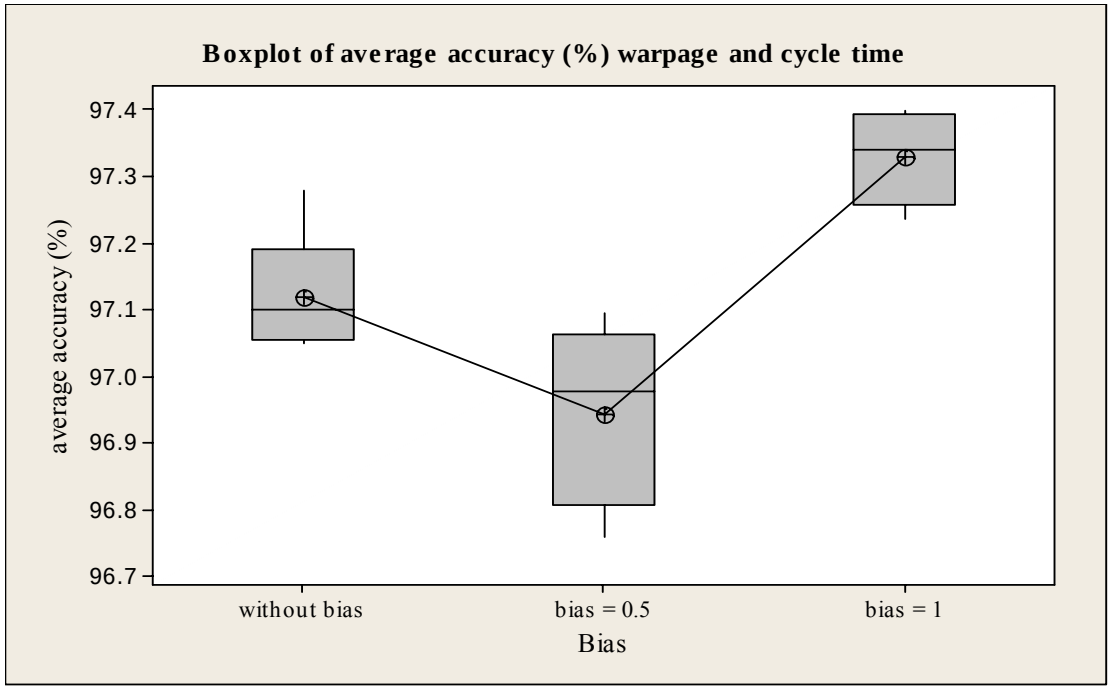

Figure 61 Box-plot of Experiment 10

3.2.3.3 Standard deviation analysis of Experiment 10

In this case, standard deviation (SD) was applied to benchmark among three types of Experiment 10. Table 63 displays the mean and SD of these three types for analyzing what type was the most appropriate for training the ANN model.

Table 63 The result of mean and standard deviation analysis of Experiment 10

Type	Learning Rate	Total Accuracy (%) Warpage	Total Accuracy (%) Cycle Time	Total Average Accuracy (%)	SD
1	without bias	94.3087	99.9277	97.1182	0.0936
2	bias = 0.5	93.9439	99.9442	96.9441	0.1356
3	bias = 1	94.7147	99.9412	97.3280	0.0704

According to Figure 61 and Table 63, bias of 1 had the best results for the total average accuracy (%) of the roof tile's warpage and its process cycle time, maximum mean (97.3280) and minimum SD (0.0704). Therefore, initial bias of 1 was appropriate for the optimal structure of ANN model that had one hidden layer and two outputs, the roof tile's warpage and its process cycle time.

3.2.4 The result of Experiment 11

Experiment 11 was the experiment used for determining an appropriate number of neuron in the 1st hidden layer in structural ANN model that had one hidden layer and two outputs, the roof tile's warpage and its process cycle time. The total average accuracy of warpage and process cycle time results of Experiment 11 is shown in Table 64.

Table 64 The total results of Experiment 11

Type	Number of neuron in 1st hidden layer	Total Accuracy (%) Warpage	Total Accuracy (%) Cycle Time	Total Average Accuracy (%)
1	3	80.0484	99.5843	89.8164
2	4	89.0732	99.5933	94.3333
3	5	91.6662	99.7437	95.7050
4	6	94.0002	99.8860	96.9431
5	7	94.1605	99.9152	97.0378
6	8	94.7383	99.9363	97.3373
7	9	94.7470	99.9479	97.3474

From Table 64, there were three steps of analysis to find the appropriate number of neuron in the 1st hidden layer in structural ANN model that had one hidden layer and two outputs, the roof tile's warpage and its process cycle time: (i) ANOVA table, (ii) the box-plot, and (iii) standard deviation analysis.

3.2.4.1 ANOVA table of Experiment 11

The ANOVA result of Experiment 11 was used for analyzing whether the means of accuracy on the ANN models that had 3 to 9 neurons in the 1st hidden layer and two outputs: the roof tile's warpage and its process cycle time, were different. The result of ANOVA table of Experiment 11 is shown in Table 65.

Table 65 The result of ANOVA table of Experiment 11

Source	DF	SS	MS	F	P
Number of neuron in 1st hidden layer	6	224.716	37.453	52.26	0.000
Error	28	20.065	0.717		
Total	34	244.781			

From the results on Table 65, the p-value of neuron's number in 1st hidden layer (0.000) is less than α value (0.05). It means the seven neuron numbers in the 1st hidden layer were different at 95% confident interval.

3.2.4.2 Box-plot of Experiment 11

As shown in Figure 62, box-plot displays how many neurons' number in the 1st hidden layer should be used in the structural ANN model that had 1 hidden layer and two outputs: the roof tile's warpage and its process cycle time.

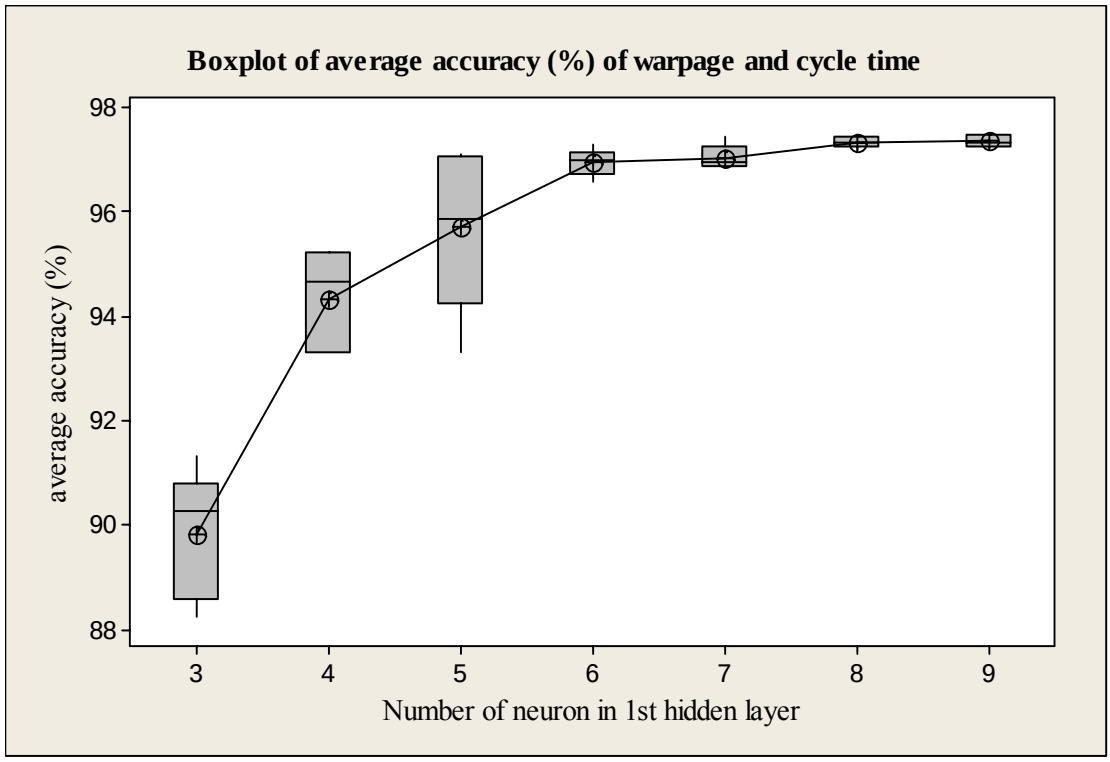

Figure 62 Box-plot of Experiment 11

3.2.4.3 Standard deviation analysis of Experiment 11

In this case, standard deviation (SD) was applied to benchmark among seven types of Experiment 11. Table 66 displays mean and SD of these seven types for analyzing what type was the most appropriate for the structural ANN model that had one hidden layer and two outputs: the roof tile's warpage and its process cycle time.

Table 66 The result of mean and standard deviation analysis of Experiment 11

Type	Number of neuron in 1st hidden layer	Total Accuracy (%) Warpage	Total Accuracy (%) Cycle Time	Total Average Accuracy (%)	SD
1	3	80.0484	99.5843	89.8164	1.2218
2	4	89.0732	99.5933	94.3333	0.9687
3	5	91.6662	99.7437	95.7050	1.5588
4	6	94.0002	99.8860	96.9431	0.2629
5	7	94.1605	99.9152	97.0378	0.2447
6	8	94.7383	99.9363	97.3373	0.1103
7	9	94.7470	99.9479	97.3474	0.1178

As shown in Figure 62 and Table 66, the 9 neurons in the 1st hidden layer of the experiment (type 7) had the best result for the average accuracy (%) of the roof tile's warpage and its process cycle time because of maximum mean (97.3474) and second minimum SD (0.1178). Therefore, the 9 neurons in the 1st hidden layer was an appropriate component for the optimal structure of the ANN model that had one hidden layer and two outputs: the roof tile's warpage and its process cycle time.

3.2.5 The result of Experiment 12

Experiment 12 was the experiment used for determining an appropriate number of neuron in the 2nd hidden layer in structural ANN model that had two hidden layers and two outputs, the roof tile's warpage and its process cycle time. The total average accuracy (%) of warpage and cycle time results of Experiment 12 is shown in Table 67.

Table 67 The total results of Experiment 12

Type	Number of neuron in 2nd hidden layer	Total Accuracy (%) Warpage	Total Accuracy (%) Cycle Time	Total Average Accuracy (%)
1	6	93.7650	99.9384	96.8517
2	7	93.4838	99.9488	96.7163
3	8	94.3731	99.9464	97.1598
4	9	89.1532	99.8638	94.5085

Table 67 (Continued)

Type	Number of neuron in 2nd hidden layer	Total Accuracy (%) Warpage	Total Accuracy (%) Cycle Time	Total Average Accuracy (%)
5	10	90.6739	99.9217	95.2978
6	11	87.5509	99.9433	93.7471
7	12	92.9982	99.9376	96.4679
8	13	88.2828	99.8272	94.0550
9	14	90.8965	99.9551	95.4258
10	15	90.9374	99.9483	95.4428
11	16	95.0384	99.9424	97.4904
12	17	94.1726	99.9314	97.0520
13	18	93.3648	99.9318	96.6483
14	19	86.8304	99.9509	93.3906

From Table 67, there were three steps of analysis to find the appropriate number of neuron in the 2nd hidden layer in structural ANN model that had two hidden layers and two outputs, the roof tile's warpage and its process cycle time: (i) ANOVA table, (ii) the box-plot, and (iii) standard deviation analysis.

3.2.5.1 ANOVA table of Experiment 12

The ANOVA result of Experiment 12 was used for analyzing whether the means of average accuracy on the ANN models that had 6 to 19 neurons in the 2nd hidden layer and two outputs, the roof tile's warpage and its process cycle time, were different. The result of ANOVA table of Experiment 12 is shown in Table 68.

Table 68 The result of ANOVA table of Experiment 12

Source	DF	SS	MS	F	P
Number of neuron in 2nd hidden layer	13	122.87	9.45	2.90	0.003
Error	56	182.65	3.26		
Total	69	305.52			

From the results in Table 68, the p-value of neuron's number in the 2nd hidden layer (0.003) is less than α value (0.05). It means the fourteen neuron numbers in the 2nd hidden layer were different at 95% confident interval.

3.2.5.2 Box-plot of Experiment 12

In Figure 63, the box-plot displays what neuron's number in the 2nd hidden layer should be used in structural ANN model that had two hidden layers and two outputs: the roof tile's warpage and its process cycle time.

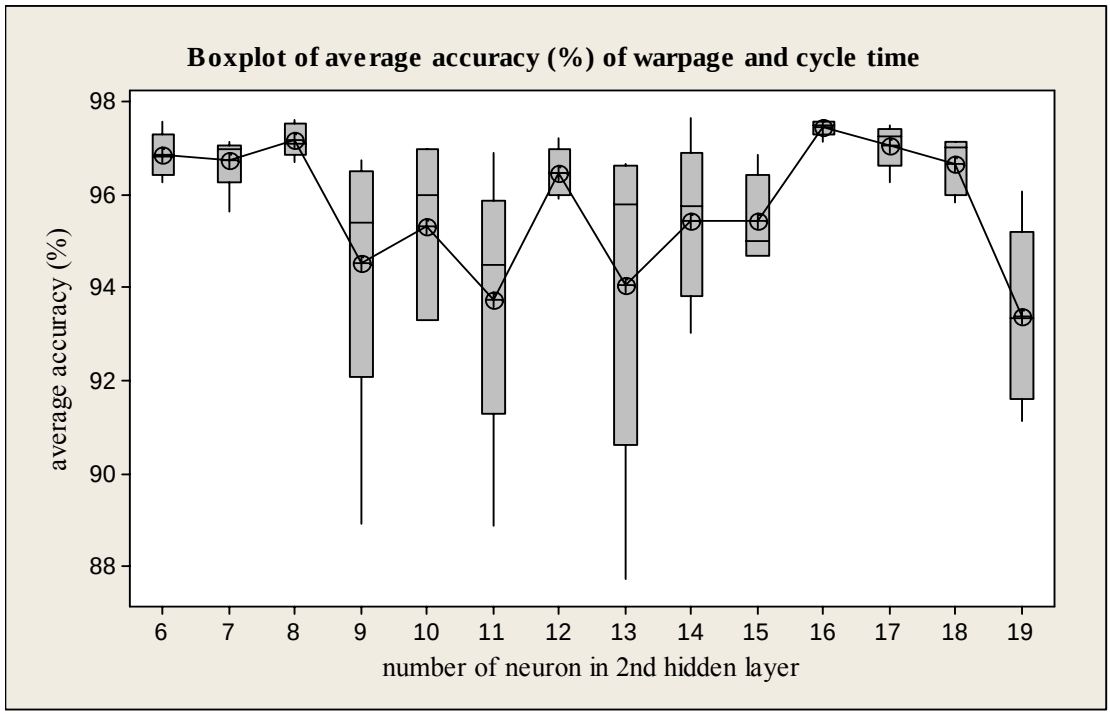

Figure 63 Box-plot of Experiment 12

3.2.5.3 Standard deviation analysis of Experiment 12

In this case, standard deviation (SD) was applied to benchmark among fourteen types of Experiment 12. Table 69 displays the mean and SD of these fourteen types for analyzing what type was the most appropriate for structural ANN model that had two hidden layer and two outputs: the roof tile's warpage and its process cycle time.

Table 69 The result of mean and standard deviation analysis of Experiment 12

Type	Number of neuron in 2nd hidden layer	Total Accuracy (%) Warpage	Total Accuracy (%) Cycle Time	Total Average Accuracy (%)	SD
1	6	93.7650	99.9384	96.8517	0.4866
2	7	93.4838	99.9488	96.7163	0.6108
3	8	94.3731	99.9464	97.1598	0.3615
4	9	89.1532	99.8638	94.5085	3.1780
5	10	90.6739	99.9217	95.2978	1.8769
6	11	87.5509	99.9433	93.7471	2.9654
7	12	92.9982	99.9376	96.4679	0.5190
8	13	88.2828	99.8272	94.0550	3.7503
9	14	90.8965	99.9551	95.4258	1.7184
10	15	90.9374	99.9483	95.4428	0.9498
11	16	95.0384	99.9424	97.4904	0.0657
12	17	94.1726	99.9314	97.0520	0.4761
13	18	93.3648	99.9318	96.6483	0.6165
14	19	86.8304	99.9509	93.3906	1.9249

As Figure 63 and Table 69, the 16 neurons in 2nd hidden layer of the experiment (type 11) has the best result for the total average accuracy (%) of the roof tile's warpage and its process cycle time. This was because it had maximum mean (97.4904) and minimum SD (0.0657). Therefore, the 16 neurons in the 2nd hidden layer was an appropriate component for the optimal structure of the ANN model that had two hidden layers and two outputs: the roof tile's warpage and its process cycle time.

3.2.6 The comparison between 1 and 2 hidden layers of the structural ANN model that the roof tile's warpage and its process cycle time were outputs.

A structural ANN model mostly has one or two hidden layers placed between the input and output layer. To find the optimal structure of the ANN model in which the roof tile's warpage and its process cycle time were outputs, the best result of both 1 and 2 hidden layers need to compare to each other as shown in Table 70. In addition, Table 71 displays the comparison data of the optimal structure of one and two hidden layers in which the warpage and process cycle time are outputs.

Table 70 The data of the optimal ANN models of the roof tile that had 1 and 2 hidden layers

No	Type	Average Accuracy (%)
1	1 hidden layer	97.21325
2	1 hidden layer	97.31745
3	1 hidden layer	97.38905
4	1 hidden layer	97.52575
5	1 hidden layer	97.29170
	average of 1 hidden layer	97.34744
6	2 hidden layers	97.50330
7	2 hidden layers	97.43440
8	2 hidden layers	97.41940
9	2 hidden layers	97.58210
10	2 hidden layers	97.51265
	average of 2 hidden layers	97.49037

Table 71 The total results of the optimal structure of 1 and 2 hidden layers on the ANN model in which the warpage and process cycle time of the roof tile were outputs

Type	ANN structure (input-hidden-output)	Total Average Accuracy (%)
1 hidden layer	4 - 9 - 2	97.3474
2 hidden layers	4 - 9 - 16- 2	97.4904

The ANOVA analysis used to find the appropriate type of the hidden layer in the structural ANN model in which the roof tile's warpage and its process cycle time were outputs. It was used for analyzing whether the means of average accuracy on the ANN models that had one and two hidden layers were different. The result of ANOVA table is shown in Table 72.

Table 72 The results of ANOVA table for finding the optimal structure of the ANN model in which the warpage and process cycle time of the roof tile were outputs.

Source	DF	SS	MS	F	P
Type of the hidden layer	1	0.05107	0.05107	5.61	0.045
Error	8	0.07279	0.00910		
Total	9	0.12386			

From the results on Table 72, the p-value of the type of the hidden layer (0.045) is less than α value (0.05). It means that single and two hidden layers were difference at 95% confident interval. Moreover, as the box-plot result in Figure 64 and standard deviation analysis in Table 73, the structural ANN model with two hidden layers was the most appropriate for this problem.

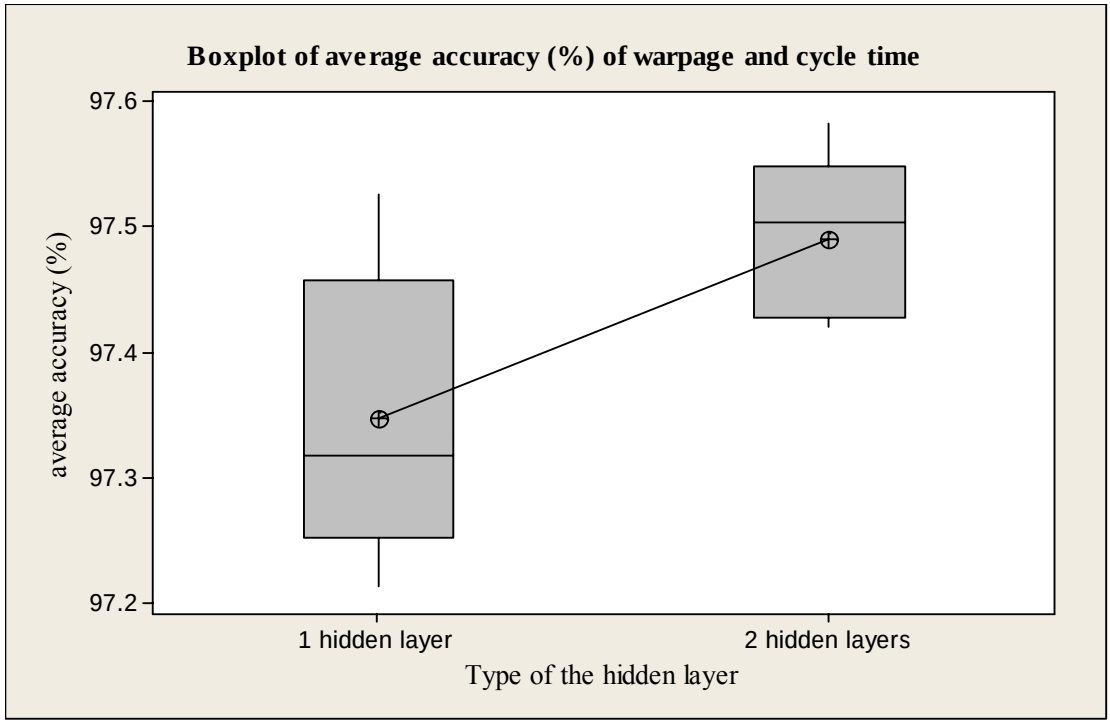

Figure 64 Box-plot for an appropriate type of the hidden layer of the roof tile problem

Table 73 The result of mean and standard deviation for an appropriate structural ANN model of the roof tile problem

Type	ANN structure (input-hidden-output)	Total Average Accuracy (%)	SD
1 hidden layer	4 - 9 - 2	97.3474	0.1178
2 hidden layers	4 - 9 - 16- 2	97.4904	0.0657

Finally, the optimal structure of the ANN model that had two outputs: the roof tile's warpage and its process cycle time, is displayed in Table 74. In addition, the fitted prediction of this ANN model is obviously shown in Figure 65 as well.

Table 74 The optimal structure of ANN models in which the warpage and process cycle time of the roof tile were outputs

The ANN parameters	The optimal values
1. number of input	4
2. characteristic of input	normalization
3. learning rate (*lr*)	0.09
4. *epoch*	3,000
5. initial *bias* value	1.0
6. number of neurons in 1st hidden layer	9
7. number of neurons in 2nd hidden layer	16
8. transfer function of 1st hidden layer	logsig
9. transfer function of 2nd hidden layer	logsig
10. transfer function of output layer	purelin
11. average accuracy (%) of warpage	95.0384
12. average accuracy (%) of process cycle time	99.9424
13. total average accuracy (%)	97.4904

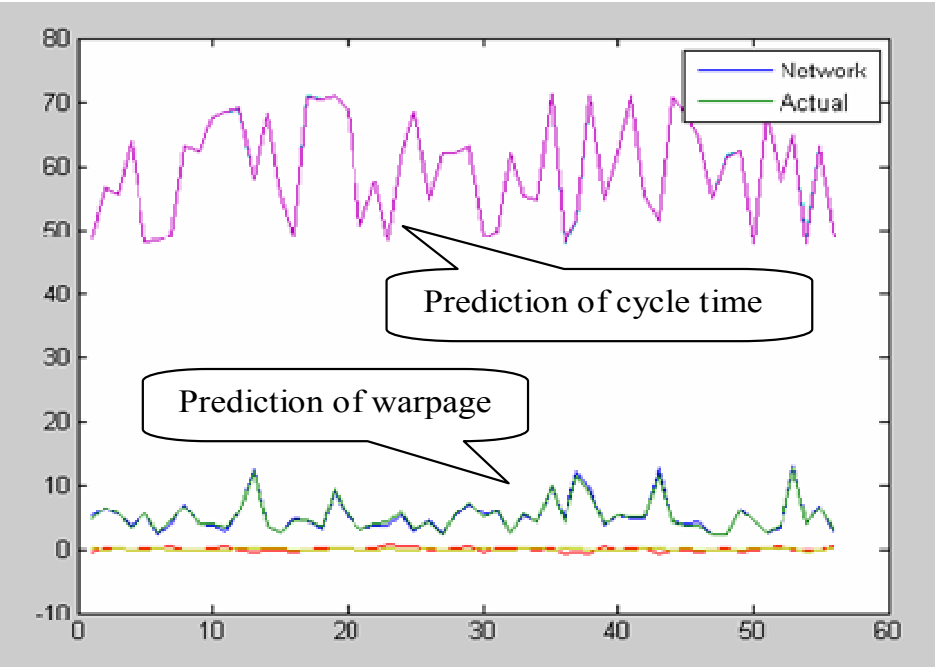

Figure 65 The fitted ANN model prediction of 4-9-16-2 configuration of the roof tile

4. The results of the optimal processing conditions for quality indices by GA

In this section, an effective GA was coupled with the ANN model for quality indices minimization of the rectangular lid's residual stress (Case 1) and the roof tile's warpage (Case 2). At first, the optimal structures of ANN models are transformed into term of equations by using final weights and final biases within ANN model. These all weights and biases combined with transfer function in each layer are used to build an objective function for GA method. Then, the appropriate GA parameters are investigated and tested with the objective functions under variations limit of Case 1 and Case 2. Finally, the optimal processing conditions by GA are verified with the actual testing to confirm the optimum results.

4.1 The results of the optimal processing conditions by GA for the minimum residual stress and process cycle time of the rectangular lid (Case 1).

4.1.1 Transformation of the ANN model's configuration to GA objective function of the rectangular lid.

For cap- block part problem, the optimal structure of ANN model in previous section is 5-7-2 with 99.6% of accuracy as shown in Figure 66.

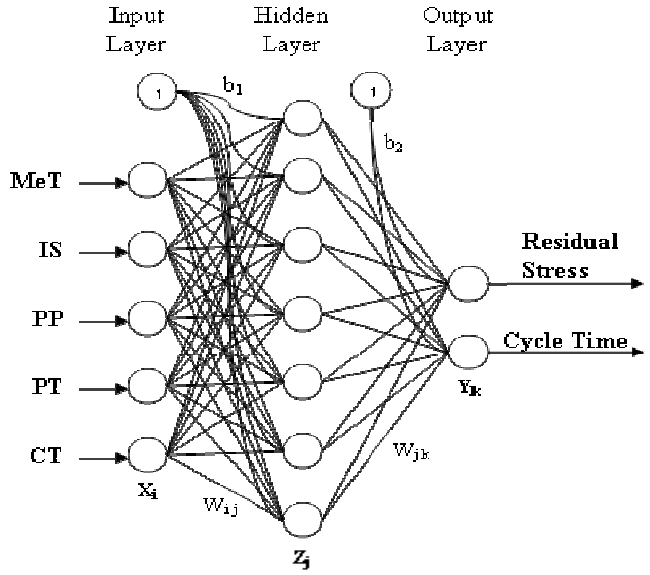

Figure 66 The optimal 5-7-2 configuration of the ANN model for the rectangular lid

Weights and biases of all layers of neurons in Figure 66 were combined with transfer functions of ANN model to achieve an ANN equation pattern as the following steps.

1.) The 5 input layer nodes with the 1st bias node connected to 7 nodes of hidden layer. Thus, there were 35 values of weights and 7 values of biases on the layers between input and hidden layer. On the hidden layer, the 'logsig' transfer function was used to calculate the sum of the 35 weighted inputs ($W_{i\,j}$) and the 7 biases (b_j^1). The sum of weights and biases in hidden layer is displayed on Equation (22).

$$Z_j = f^1\left(W_{i,j}X_i + b_j^1\right), \text{ i} = 1,2,3,4,5 \qquad \text{j} = 1,2,3,\ldots,7 \tag{22}$$

where, Z_j is the 7 outputs of hidden layer

f^1 is the 'logsig' transfer function of hidden layer

$W_{i,j}$ is the weights from input layer i to hidden layer j

X_i is the 5 inputs of input layer

b_j^1 is the 7 biases of hidden layer

2.) The 7 nodes of hidden layer connected to 2 nodes of output layer. It means the layers between hidden layer and output layer had 14 values of weights by 7 columns and 2 rows and 2 values of biases. On the output layer, the 'purelin' transfer function was used to calculate the sum of the 14 weighted inputs ($W_{j\,k}$) and the 2 biases (b_k^2). The sum of weights and biases in output layer is displayed on Equation (23).

$$Y_k = f^2\left(W_{j,k}Z_j + b_k^2\right), \text{ j} = 1,2,3,\ldots,7 \quad \text{k} = 1,2 \tag{23}$$

where, Y_k is the 2 outputs, warpage and cycle time

f^2 is the 'purelin' transfer function of output layer

W_{jk} is the weights from hidden layer j to output layer k

Z_j is the 7 inputs of hidden layer

b_k^2 is the 2 biases of output layer

From the MATLAB result, 35 weights with 7 biases of hidden layer and 14 weights with 2 biases of output layer are displayed on Table 75 and Table 76, respectively.

Table 75 The 35 weights and 7 biases of hidden layer

Last weights 1 (w1_out)					Last biases 1 (b1_out)
13.7096	2.1782	-1.9389	-1.2917	-0.3189	-5.2266
-57.9492	-9.1160	38.1069	-41.8994	6.4926	27.4737
58.4151	9.2167	-38.2465	41.8264	-6.5737	-27.631
-35.9639	-6.9557	-11.2393	8.4858	0.5568	16.8824
-0.0108	-0.0498	-0.0027	0.0813	0.6454	-0.2396
1.1789	0.1687	1.0771	92.1578	-0.1518	-33.6696
2.2022	111.3461	0.4024	1.2613	-0.1756	-29.4613

Table 76 The 7 weights and 2 biases of output layer

Last weights 2 (w2_out)							Last biases 2 (b2_out)
11.6537	68.2686	67.8477	3.2519	-6.7003	-5.7610	71.6124	-113.029
0.2308	-5.5690	-5.5552	0.1764	310.4970	0.1916	-61.3591	-60.774

The weights and biases from Table 75 and 76 were substituted on the Equation (22) and (23), respectively. These steps of equations are shown as follows.

1.) From Equation (22): There are 7 equations (Z_1 to Z_7) on this step.

$$Z_1 = \frac{1}{1+e^{-\{13.7096(X_1)+2.1782(X_2)-1.9389(X_3)-1.2917(X_4)-0.3189(X_5)-5.2266\}}};$$

$$Z_2 = \frac{1}{1+e^{-\{-57.9492(X_1)-9.1160(X_2)+38.1069(X_3)-41.8994(X_4)+6.4926(X_5)+27.4737\}}};$$

$$\vdots$$

$$Z_7 = \frac{1}{1+e^{-\{2.2022(X_1)+111.3461(X_2)+0.4024(X_3)+1.2613(X_4)-0.1756(X_5)-29.4613\}}}.$$

2.) From Equation (23): There are two equations: Y_1 and Y_2, on this step. Y_1 is the rectangular lid's residual stress equation. Y_2 is the rectangular lid's process cycle time equation.

$$Y_1 = 11.6537(Z_1) + 68.2686(Z_2) + 67.8477(Z_3) + 3.2519(Z_4) - 6.7003(Z_5) - 5.7610(Z_6) + 71.6124(Z_7) - 113.029 \quad (24)$$

$$Y_2 = 0.2308(Z_1) - 5.5690(Z_2) - 5.5552(Z_3) + 0.1764(Z_4) + 310.4970(Z_5) + 0.1916(Z_6) - 61.3591(Z_7) - 60.774 \quad (25)$$

In order to give the objective function to GA, the 7 equations of Z_j were substituted on Y_1 for minimum the rectangular lid's residual stress objective function and Y_2 for minimum the rectangular lid's process cycle time objective function. As this research was emphasized on minimum residual stress, the Y_1 was the GA objective function as shown in Equation (26).

```
Function Y = min_residual_stress(x)
Y = (11.6537*(1/(1 + exp(-13.7096*x(1) - 2.1782*x(2) + 1.9389*x(3) + 1.2917*x(4) +
0.3189*x(5) + 5.2266)))) +
(68.2686*(1/(1 + exp(57.9492*x(1) + 9.116*x(2) - 38.1069*x(3) + 41.8994*x(4) -
6.4926*x(5) - 27.4737)))) +
(67.8477*(1/(1 + exp(-58.4151*x(1) - 9.2167*x(2) + 38.2465*x(3) - 41.8264*x(4) +
6.5737*x(5) + 27.631)))) +
(3.2519*(1/(1 + exp(35.9639*x(1) + 6.9557*x(2) + 11.2393*x(3) - 8.4858*x(4) -
0.5568*x(5) - 16.8824)))) +
(-6.7003*(1/(1 + exp(0.0108*x(1) + 0.0498*x(2) + 0.0027*x(3) - 0.0813*x(4) -
0.6454*x(5) + 0.2396)))) +
(-5.761*(1/(1 + exp(-1.1789*x(1) - 0.1687*x(2) - 1.0771*x(3) - 92.1578*x(4) +
0.1518*x(5) + 33.6696)))) +
(71.6124*(1/(1 + exp(-2.2022*x(1) - 111.3461*x(2) - 0.4024*x(3) - 1.2613*x(4) +
0.1756*x(5) + 29.4613)))) - 113.029;                                    (26)
```

4.1.2 Appropriate GA parameters for the rectangular lid

In this section, the appropriate GA parameters were investigated and tested with the rectangular lid's residual stress problem. The results of the appropriate GA parameters are displayed as follows.

4.1.2.1 The result of appropriate the population size of GA

The result of appropriate the population size of GA is displayed in Table 77. According to the best minimum solution of each population size in Table 77, the population size of 50 is on the best result. Therefore, an appropriate population size of this problem is equal to 50.

Table 77 The results of the population size for the residual stress of the rectangular lid problem

GA parameters	Changeable value = Population size		
	Pop = 10	Pop = 30	Pop = 50
Crossover rate (Pc)	0.3	0.3	0.3
Mutation rate (Pm)	0.1	0.1	0.1
Number of generation	500	500	500
The best solution	21.4075	21.3039	21.2313

4.1.2.2 The result of the appropriate crossover rate (P_c) of GA

The result of the appropriate crossover rate (P_c) of GA is displayed in Table 79. According to the best minimum solution of each crossover rate in Table 78, the crossover rate of 0.7 shows the best result. Therefore, the appropriate crossover rate of this problem is equal to 0.7.

Table 78 The results of the crossover rate for the residual stress of the rectangular lid problem

GA parameters	Changeable value = Crossover rate (Pc)		
	Pc = 0.3	Pc = 0.5	Pc = 0.7
Population size	50	50	50
Mutation rate (Pm)	0.1	0.1	0.1
Number of generation	500	500	500
The best solution	21.3032	21.2615	21.1588

4.1.2.3 The result of appropriate mutation rate (P_m) of GA

The result of appropriate mutation rate (P_m) of GA is displayed in Table 79. The solution of Table 79 shows that there is no difference among three types

of mutation rate. Therefore, these three values of the mutation rate can be used for this problem. In this case, the mutation rate of 0.1 was chosen as an appropriate value for minimum the rectangular lid's residual stress.

Table 79 The results of the mutation rate for the residual stress ot the rectangular lid problem

GA parameters	Changeable value = Mutation rate (Pm)		
	Pm = 0.1	Pm = 0.2	Pm = 0.3
Population size	50	50	50
Crossover rate (Pc)	0.7	0.7	0.7
Number of generation	500	500	500
The best solution	21.1588	21.1588	21.1588

4.1.2.4 The result of the appropriate number of generations

The number of generations is specified on the maximum value that is enough for finding global optimum solution. In this case, using population size of 50, crossover rate of 0.7, and mutation rate of 0.1, the GA converges to an optimum before 500 generations as shown in Figure 67. Finally, the optimal process conditions and residual stress result of the rectangular lid by GA are shown in Table 81.

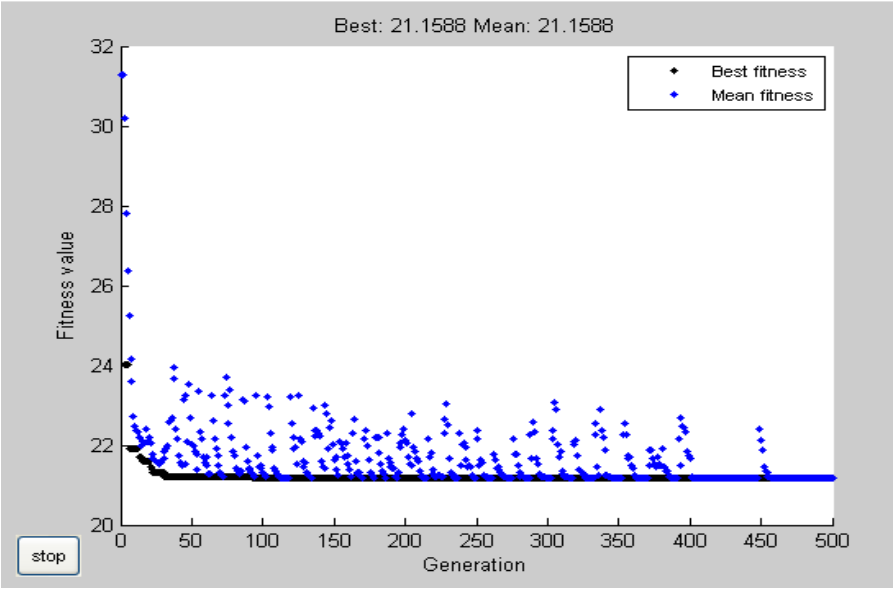

Figure 67 Optimizating the residual stress of the rectangular lid by GA

Table 80 The optimal processing conditions and residual stress result of the rectangular lid by GA

Optimal processing condition (Normalization)	
1. Melt temperature	0.41939
2. Injection speed	0.3
3. Packing pressure	0.46503
4. Packing time	0.5
5. Cooling time	0.5
Optimal processing condition (Real values)	
1. Melt temperature (°C)	218
2. Injection speed (%)	30
3. Packing pressure (MPa)	4.65
4. Packing time (second)	3.5
5. Cooling time (second)	25
The minimum residual stress (MPa)	21.1588
The process cycle time (second)	36.17

From Table 80, although the optimal processing condition produced the rectangular lid with minimum residual stress, the process cycle time increased. To solve this problem, the cooling time of the process must be decreased. As this demand, the same objective function was again solved by GA with fixed cooling time of 10 second.

In this case, it used the same GA parameters as the previous ones, which were population size of 50, crossover rate of 0.7, and mutation rate of 0.1, the GA also converges to the optimum value of 21.296 MPa before 500 generations as shown in Figure 68. Finally, the new optimal process conditions and new residual stress result of the rectangular lid by GA are shown in Table 81.

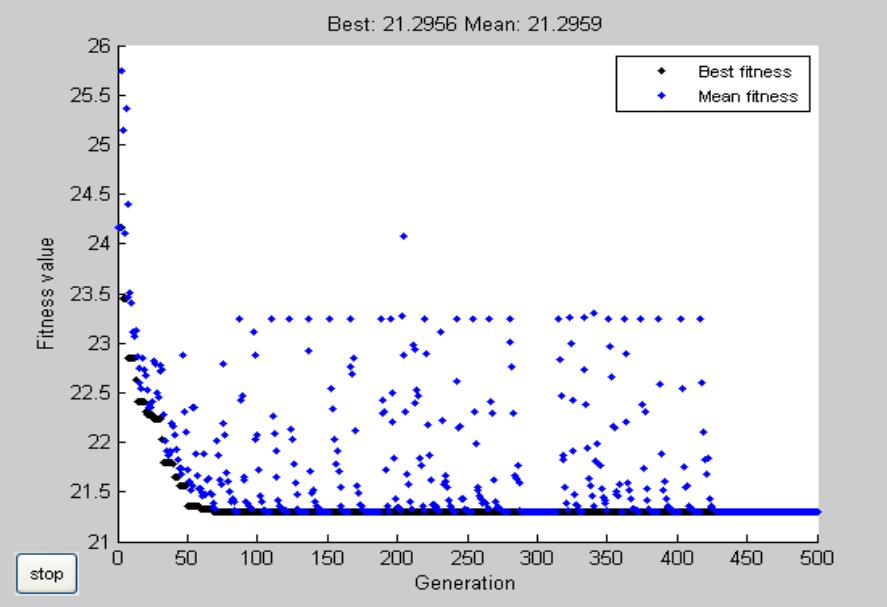

Figure 68 New optimizing the residual stress of the rectangular lid by GA

Table 81 The new optimal processing conditions and residual stress result of the rectangular lid by GA

Optimal processing condition (Normalization)	
1. Melt temperature	0.40642
2. Injection speed	0.3
3. Packing pressure	0.49936
4. Packing time	0.5
5. Cooling time	0.2
Optimal processing condition (Real values)	
1. Melt temperature (°C)	211
2. Injection speed (%)	30
3. Packing pressure (MPa)	4.99
4. Packing time (second)	3.5
5. Cooling time (second)	10
The minimum residual stress (MPa)	21.2956
The process cycle time (second)	21.17

From Table 81, the new optimal process conditions produced the rectangular lid with the residual stress of 21.2956 MPa, which was slightly greater than the former optimal process condition (21.1588 MPa). However, the process cycle time was reduced from 36.17 to 21.17 second.

4.1.3 Confirmation of optimum process condition of the rectangular lid

The comparison between the rectangular lid's residual stress of before (local optimization) and after optimization by GA was focused on the residual stresses on average of four reference points of the part. The residual stresses of the rectangular lid before and after optimization are display in Figures 69.

In addition, the comparison between the rectangular lid's residual stress before and after optimization is displayed in Table 82. After optimization, the rectangular lid's residual stress between GA result (=21.2956) and simulation model, MPI, result (=21.32) had 99.89% accuracy. Moreover, not only the rectangular lid's residual stress was reduced from 28.98 to 21.32 MPa (-26.43%) but also the process cycle time was reduced from 23.59 to 21.17 second (-10.26%).

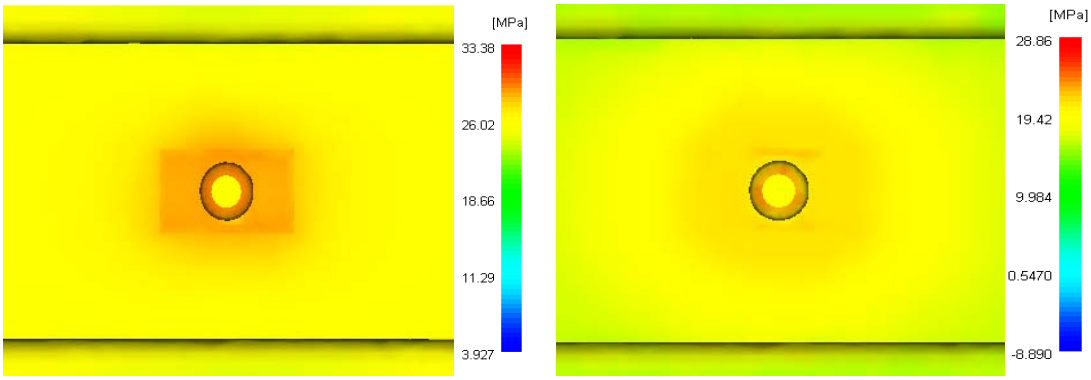

(a) Before optimization (b) After optimization

Figure 69 The rectangular lid's residual stress before (a) and after (b) optimization

Table 82 Comparison of the process parameters, residual stress, and process cycle time of the rectangular lid before and after optimization.

Types	Processing conditions					Residual stress values			Cycle time (sec.)
	MeT (°C)	IS (%)	PP (MPa)	PT (sec.)	CT (sec.)	GA results	MPI results	Accuracy (%)	
1. Before optimization	228	45	4.5	1.8	15	-	28.98	-	23.59
2. After optimization	211	30	4.99	3.5	10	21.2956	21.32	99.89	21.17

4.2 The results of the optimal process conditions optimized by GA for minimum warpage and process cycle time of the roof tile (Case 2).

4.2.1 Transformation of the ANN model's configuration to GA objective function of the roof tile.

For the roof tile problem, the optimal structure of the ANN model in previous section was 4-9-16-2 with accuracy of 97.431% as shown in Figure 70.

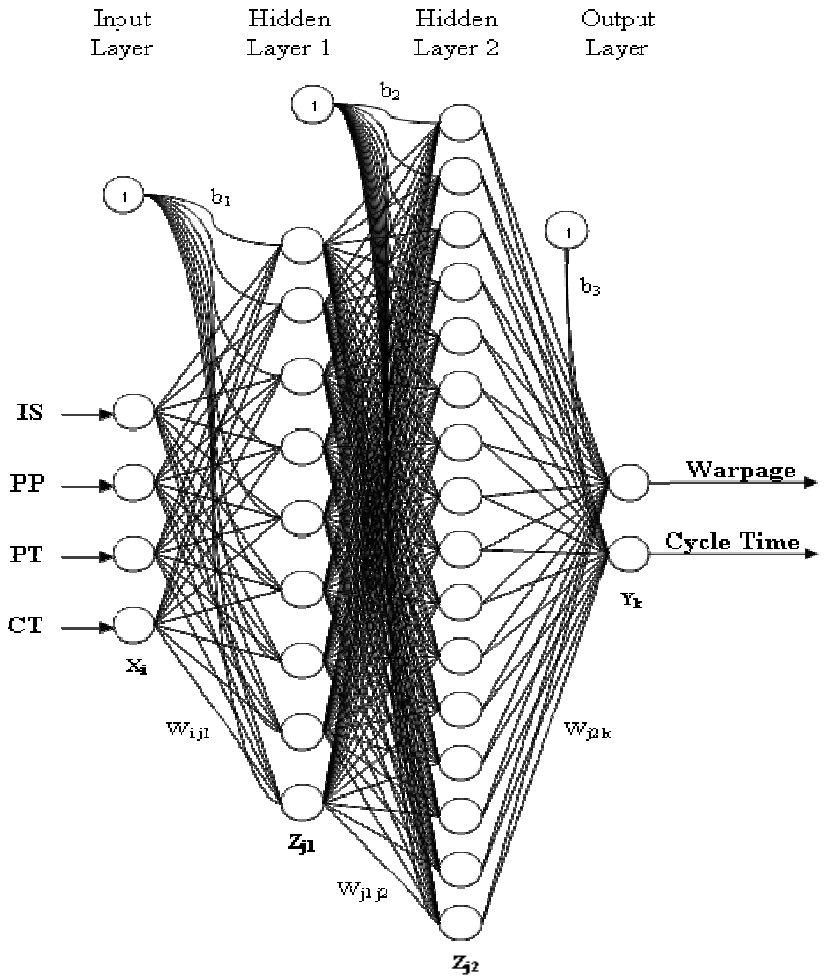

Figure 70 The optimal 4-9-16-2 configuration of the ANN model for the roof tile

As shown in Figure 70, weights and biases of all layers of neurons were combined with transform functions of ANN model to achieve the ANN equation pattern as the following steps.

1.) The 4 input layer nodes with 1st bias node connected to 9 nodes of 1st hidden layer. Thus, there were 36 values of weights and 9 values of biases on the layers between input and 1st hidden layer. On the 1st hidden layer, the 'logsig' transfer function was used to calculate the sum of the 36 weighted inputs ($W_{i\,j1}$) and the 9 biases (b_{j1}^{1}). The sum of weights and biases in 1st hidden layer is displayed on Equation (27).

$$Z_{j1}^{1} = f^{1}\left(W_{i,j1}X_{i} + b_{j1}^{1}\right),\ \mathrm{i} = 1,2,3,4 \qquad \mathrm{j}_1 = 1,2,3,\ldots,9 \qquad (27)$$

where, Z_{j1}^{1} is the 9 outputs of 1st hidden layer

f^{1} is the 'logsig' transfer function of 1st hidden layer

$W_{\mathrm{i,j1}}$ is the weights from input layer i to 1st hidden layer j_1

X_{i} is the 4 inputs of input layer

b_{j1}^{1} is the 9 biases of 1st hidden layer

2.) The 9 nodes of 1st hidden layer and 2nd bias node connected to 16 nodes of 2nd hidden layer. It means the layers between 1st hidden layer and 2nd hidden layer had 144 values of weights by 9 columns and 16 rows and 16 values of biases. On the 2nd hidden layer, the 'logsig' transfer function was used to calculate the sum of the 144 weighted inputs ($W_{\mathrm{j1\,j2}}$) and the 16 biases (b_{j2}^{2}). The sum of weights and biases in 2nd hidden layer is displayed in Equation (28).

$$Z_{j2}^{2} = f^{2}\left(W_{j1,j2}Z_{j1}^{1} + b_{j2}^{2}\right),\ \mathrm{j}_1 = 1,2,3,\ldots,9 \qquad \mathrm{j}_2 = 1,2,3,\ldots,16 \qquad (28)$$

where, Z_{j2}^{2} is the 16 outputs of 2nd hidden layer

f^{2} is the 'logsig' transfer function of 2nd hidden layer

$W_{\mathrm{j1,j2}}$ is the weights from 1st hidden layer j_1 to 2nd hidden layer j_2

Z_{j1}^{1} is the 9 inputs of 1st hidden layer

b_{j2}^{2} is the 16 biases of 2nd hidden layer

3.) The 16 nodes of 2nd hidden layer connected to 2 nodes of output layer. It means the layers between 2nd hidden layer and output layer had 32 values of weights by 16 columns and 2 rows and 2 values of biases. On the output layer, the

'purelin' transfer function was used to calculate the sum of the 32 weighted inputs ($W_{j2\,k}$) and the 2 biases (b_k^3). The sum of weights and biases in output layer is displayed in Equation (29).

$$Y_k = f^3\left(W_{j2,k} Z_{j2}^2 + b_k^3\right), \mathrm{j_2} = 1,2,3,\ldots,16 \quad \mathrm{k} = 1,2 \tag{29}$$

where, Y_k is the 2 outputs, warpage and cycle time

f^3 is the 'purelin' transfer function of output layer

$W_{j2,k}$ is the weights from 2nd hidden layer j_2 to output layer k

Z_{j2}^2 is the 16 inputs of 2nd hidden layer

b_k^3 is the 2 biases of output layer

From the MATLAB result, 36 weights and 9 biases of 1st hidden layer, 144 weights and 16 biases of 2nd hidden layer, and 16 weights and 2 biases of output layer are displayed in Tables 83, 84, and 85, respectively.

Table 83 The 36 weights and 9 biases of the 1st hidden layer

Last weights 1 (w_out)				Last biases 1 (b1_out)
-54.0455	-38.9409	-24.3803	-20.6501	-100.4514
-150.5630	-3.6771	20.7800	179.1086	-63.4062
-0.0784	-0.0103	0.0827	2.2089	-0.6891
8.5726	6.9785	4.8842	12.9788	16.4334
-24.5693	0.1307	-3.5480	1.9571	5.9975
31.0470	35.2221	31.1944	43.2806	88.4763
-0.0215	-0.0095	-1.0064	2.8766	-0.0044
-6.9054	-1.8834	154.0428	4.4988	-64.4938
9.1921	7.0994	-18.0335	-4.7049	-3.0521

Table 84 The 144 weights and 16 biases of the 2nd hidden layer

Last weights 2 (w2_out)									Last biases 2 (b2_out)
-2.2018	-1.6510	-1.9150	-2.8862	-0.2230	-5.9451	-3.1217	-2.2425	-1.4911	-5.5929
-1.0715	-1.4724	-4.4911	-7.6497	-0.4375	-8.6399	1.2229	-3.3062	-0.2651	-8.3978
-0.9443	14.8610	-45.888	-68.763	-0.1703	-69.964	-46.719	-35.459	-0.3726	-68.670
1.2010	18.1112	9.8372	17.2983	9.7161	8.5843	4.7557	4.7252	-0.7873	1.5093

Table 84 (Continued)

Last weights 2 (w2_out)									Last biases 2 (b2_out)
8.8940	-0.0458	17.5962	5.3578	-2.0473	-0.4931	-17.080	-0.9355	-0.8280	0.7466
-1.3615	-1.6009	-2.9649	-2.1558	-0.3639	-7.9410	-3.6214	-2.3785	-2.0536	-7.2818
-0.4215	-0.1237	-2.5759	-2.6143	-1.1850	-10.771	-4.6265	-2.1886	-2.4735	-11.848
-2.3267	-1.4249	-25.380	69.9513	-245.74	67.4741	-277.01	-100.43	-283.23	67.2318
-5.2964	-15.890	-7.9828	-1.4364	5.8093	-9.1127	-8.6263	2.9404	-0.7853	-11.692
-1.5457	-1.2444	-2.3194	-4.4451	-0.1955	-7.1923	-2.7546	-2.3485	-1.1234	-6.5713
8.7746	9.7976	-3.8679	11.3138	469.451	2.4878	1.4803	-19.169	377.524	8.4877
44.8029	0.1841	-69.706	7.8896	7.2133	-10.560	64.9478	1.9141	0.7583	-7.6056
9.8736	0.0027	4.5539	1.3829	0.0638	-5.5498	-0.0284	-0.0033	0.0049	1.4534
15.1018	15.2225	12.0479	10.1567	0.0810	2.2409	12.8857	12.6332	-1.1262	5.7534
3.0629	2.5259	0.7573	-2.4548	-0.6298	-13.152	-1.0632	0.8713	-3.1800	-10.936
-2.7810	-2.6883	-3.5072	-2.8128	-0.6563	-11.028	-6.5175	-4.3236	-2.4483	-12.578

Table 85 The 16 weights and 2 biases of the output layer

Last weights 3 (w3_out)								Last biases 3 (b3_out)
column 1-8								
0.6868	1.6571	-0.3383	73.6557	-285.9972	-0.3816	-0.9582	0.8289	92.5797
3.3631	1.9444	-11.593	-12.0137	-11.1067	1.6838	0.0039	-0.0027	-3.8561
column 9-16								
-0.6548	1.0407	19.6449	-31.1077	-6.8008	98.5479	-3.3713	-0.0491	
3.9998	5.0716	1.2649	-1.5623	197.8374	-5.2434	0.1264	-0.4305	

The weights and biases from Table 83, 84, and 85 were substituted in Equations (27), (28), and (29), respectively. These three steps of equations are shown as follows.

1.) From Equation (27): There were 9 equations (Z_1^1 to Z_9^1) in this step.

$$Z_1^1 = \frac{1}{1+e^{-\{-54.0455(X_1)-38.9409(X_2)-24.3803(X_3)-20.6501(X_4)-100.451\}}};$$

$$Z_2^1 = \frac{1}{1+e^{-\{-150.564(X_1)-3.6771(X_2)+20.78(X_3)+179.1086(X_4)-63.4062\}}};$$

$$\vdots$$

$$Z_9^1 = \frac{1}{1+e^{-\{9.1921(X_1)+7.0994(X_2)-18.0335(X_3)-4.7049(X_4)-3.0521\}}}.$$

2.) From Equation (28): there were 16 equations (Z_1^2 to Z_{16}^2) in this step.

$$Z_1^2 = \frac{1}{1+e^{-\{-2.2018(Z_1^1)-1.651(Z_2^1)-1.915(Z_3^1)-2.8862(Z_4^1)-0.223(Z_5^1)-5.9451(Z_6^1)-3.1217(Z_7^1)-2.2425(Z_8^1)-1.4911(Z_9^1)-5.5929\}}};$$

$$Z_2^2 = \frac{1}{1+e^{-\{-1.0715(Z_1^1)-1.4724(Z_2^1)-4.4911(Z_3^1)-7.6497(Z_4^1)-0.4375(Z_5^1)-8.6399(Z_6^1)+1.2229(Z_7^1)-3.3062(Z_8^1)-0.2651(Z_9^1)-8.3978\}}};$$

$$\vdots$$

$$Z_9^2 = \frac{1}{1+e^{-\{-2.781(Z_1^1)-2.6883(Z_2^1)-3.5072(Z_3^1)-2.8128(Z_4^1)-0.6563(Z_5^1)-11.028(Z_6^1)-6.5175(Z_7^1)-4.3236(Z_8^1)-2.4483(Z_9^1)-12.578\}}}.$$

3.) From Equation (29): there were 2 equations, Y_1 and Y_2, on this step. Y_1 is the roof tile's warpage equation. Y_2 is the roof tile's process cycle time equation.

$$\begin{aligned} Y_1 = {} & 0.6868(Z_1^2) + 1.6571(Z_2^2) - 0.3383(Z_3^2) + 73.6557(Z_4^2) - 285.9972(Z_5^2) - \\ & 0.3816(Z_6^2) - 0.9582(Z_7^2) + 0.8289(Z_8^2) - 0.6548(Z_9^2) + 1.0407(Z_{10}^2) + \\ & 19.6449(Z_{11}^2) - 31.1077(Z_{12}^2) - 6.8008(Z_{13}^2) + 98.5479(Z_{14}^2) - 3.3713(Z_{15}^2) - \\ & 0.0491(Z_{16}^2) + 92.5797 \end{aligned} \quad (30)$$

$$\begin{aligned} Y_2 = {} & 3.3631(Z_1^2) + 1.9444(Z_2^2) - 11.593(Z_3^2) - 12.0137(Z_4^2) - 11.1067(Z_5^2) + \\ & 1.6838(Z_6^2) + 0.0039(Z_7^2) - 0.0027(Z_8^2) + 3.9998(Z_9^2) + 5.0716(Z_{10}^2) + \\ & 1.2649(Z_{11}^2) - 1.5623(Z_{12}^2) + 197.8374(Z_{13}^2) - 5.2434(Z_{14}^2) + 0.1264(Z_{15}^2) - \\ & 0.4305(Z_{16}^2) - 3.8561 \end{aligned} \quad (31)$$

In order to give the objective function to GA, the 9 equations of Z_{j1}^1 were substituted in 16 equations of Z_{j2}^2. Then, the 16 equations of Z_{j2}^2 were substituted in Y_1 for the objective function of the minimum warpage and Y_2 for the objective function of the minimum process cycle time. As this research was emphasized on minimum warpage, the Y_1 was the objective function as shown in Equation (32).

```
Function Y = min_warpage(x)
Y =(0.6868*(1/(1 + exp(2.2018*(1/(1 + exp(54.0455*x(1) + 38.9409*x(2) + 4.3803*x(3) +
20.6501*x(4) + 100.451))) + 1.651*(1/(1 + exp(150.564*x(1) + 3.6771*x(2) - 0.78*x(3) -
```

179.1086*x(4) + 63.4062))) + 1.915*(1/(1 + exp(0.0784*x(1) + 0.0103*x(2) - 0.0827*x(3) - 2.2089*x(4) + 0.6891))) + 2.8862*(1/(1 + exp(-8.5726*x(1) - .9785*x(2) - 4.8842*x(3) - 12.9788*x(4) - 16.4334))) + 0.223*(1/(1 + exp(24.5693*x(1) - 0.1307*x(2) + 3.548*x(3) + 1.9571*x(4) - 5.9975))) + 5.9451*(1/(1 + exp(-31.047*x(1) - 35.2221*x(2) - 31.1944*x(3) - 43.2806*x(4) - 88.4763))) + 3.1217*(1/(1 + exp(0.0215*x(1) + 0.0095*x(2) + 1.0064*x(3) - 2.8766*x(4) + 0.0044))) + 2.2425*(1/(1 + exp(6.9054*x(1) + 1.8834*x(2) - 154.0428*x(3) - 4.4988*x(4) + 64.4938))) + 1.4911*(1/(1 + exp(-9.1921*x(1) - 7.0994*x(2) + 18.0335*x(3) + 4.7049*x(4) + 3.0521))) + 5.5929)))) +
(1.6571*(1/(1 + exp(1.0715*(1/(1 + exp(54.0455*x(1) + 38.9409*x(2) + 24.3803*x(3) + 20.6501*x(4) + 100.451))) + 1.4724*(1/(1 + exp(150.564*x(1) + 3.6771*x(2) - 20.78*x(3) - 179.1086*x(4) + 63.4062))) + 4.4911*(1/(1 + exp(0.0784*x(1) + 0.0103*x(2) - 0.0827*x(3) - 2.2089*x(4) + 0.6891))) + 7.6497*(1/(1 + exp(-8.5726*x(1) - 6.9785*x(2) - 4.8842*x(3) - 12.9788*x(4) - 16.4334))) + 0.4375*(1/(1 + exp(24.5693*x(1) - 0.1307*x(2) + 3.548*x(3) + 1.9571*x(4) - 5.9975))) + 8.6399*(1/(1 + exp(-31.047*x(1) - 35.2221*x(2) - 31.1944*x(3) - 43.2806*x(4) - 88.4763))) - 1.2229*(1/(1 + exp(0.0215*x(1) + 0.0095*x(2) + 1.0064*x(3) - 2.8766*x(4) + 0.0044))) + 3.3062*(1/(1 + exp(6.9054*x(1) + 1.8834*x(2) - 154.0428*x(3) - 4.4988*x(4) + 64.4938))) + 0.2651*(1/(1 + exp(-9.1921*x(1) - 7.0994*x(2) + 18.0335*x(3) + 4.7049*x(4) + 3.0521))) + 8.3978)))) + … +
(-0.0491*(1/(1 + exp(2.781*(1/(1 + exp(54.0455*x(1) + 38.9409*x(2) + 24.3803*x(3) + 20.6501*x(4) + 100.451))) + 2.6883*(1/(1 + exp(150.564*x(1) + 3.6771*x(2) - 20.78*x(3) - 179.1086*x(4) + 63.4062))) + 3.5072*(1/(1 + exp(0.0784*x(1) + 0.0103*x(2) - 0.0827*x(3) - 2.2089*x(4) + 0.6891))) + 2.8128*(1/(1 + exp(-8.5726*x(1) - 6.9785*x(2) - 4.8842*x(3) - 12.9788*x(4) - 16.4334))) + 0.6563*(1/(1 + exp(24.5693*x(1) - 0.1307*x(2) + 3.548*x(3) + 1.9571*x(4) - 5.9975))) + 11.0279*(1/(1 + exp(-31.047*x(1) - 35.2221*x(2) - 31.1944*x(3) - 43.2806*x(4) - 88.4763))) + 6.5175*(1/(1 + exp(0.0215*x(1) + 0.0095*x(2) + 1.0064*x(3) - 2.8766*x(4) + 0.0044))) + 4.3236*(1/(1 + exp(6.9054*x(1) + 1.8834*x(2) - 154.0428*x(3) - 4.4988*x(4) + 64.4938))) + 2.4483*(1/(1 + exp(-9.1921*x(1) - 7.0994*x(2) + 18.0335*x(3) + 4.7049*x(4) + 3.0521))) + 12.5776)))) + 92.5797; (32)

4.2.2 Appropriate GA parameters for the roof tile

In this section, the appropriate GA parameters were investigated and tested with the roof tile's warpage problem. The results of the appropriate GA parameters are displayed as follows.

4.2.2.1 The result of the appropriate population size of GA

The result of the appropriate population size of GA is displayed in Table 86. According to the best minimum solution of each population size in Table 86, the population size of 50 showed the best result. Therefore, an appropriate population size of this problem was equal to 50.

Table 86 The results of the population size for the roof tile's warpage problem

GA parameters	Changeable value = Population size		
	Pop = 10	Pop = 30	Pop = 50
Crossover rate (Pc)	0.3	0.3	0.3
Mutation rate (Pm)	0.1	0.1	0.1
Number of generation	500	500	500
The best solution	2.1992	2.1148	2.0170

4.2.2.2 The result of appropriate crossover rate (P_c) of GA

The result of the appropriate crossover rate (P_c) of GA is displayed in Table 87. According to the best minimum solution of each crossover rate in Table 87, the crossover rate of 0.5 and 0.7 shower the best result. Therefore, these two numbers could be used as the appropriate crossover rate of this problem.

Table 87 The results of the crossover rate for the roof tile's warpage problem

GA parameters	Changeable value = Crossover rate (Pc)		
	Pc = 0.3	Pc = 0.5	Pc = 0.7
Population size	50	50	50
Mutation rate (Pm)	0.1	0.1	0.1
Number of generation	500	500	500
The best solution	2.0303	2.0036	2.0036

4.2.2.3 The result of the appropriate mutation rate (P_m) of GA

The result of the appropriate mutation rate (P_m) of GA is displayed in Table 88. The solution of Table 89 showed that there was no difference among the three types of the mutation rate. Therefore, these three values of the mutation

rate could be used in this problem. In this case, the mutation rate of 0.1 was chosen as an appropriate value for minimizing the roof tile's warpage.

Table 88 The results of the mutation rate for the roof tile's warpage problem

GA parameters	Changeable value = Mutation rate (Pm)		
	Pm = 0.1	Pm = 0.2	Pm = 0.3
Population size	50	50	50
Crossover rate (Pc)	0.5	0.5	0.5
Number of generation	500	500	500
The best solution	1.9903	1.9903	1.9903

4.2.2.4 The result of the appropriate number of generations

The number of generations is specified on the maximum value that is enough for finding the global optimum solution. In this case, using population size of 50, crossover rate of 0.5, and mutation rate of 0.1, the GA converged to an optimum before 500 generations as shown in Figure 71. Finally, the optimal process conditions and warpage result of the roof tile optimized by GA are shown in Table 89.

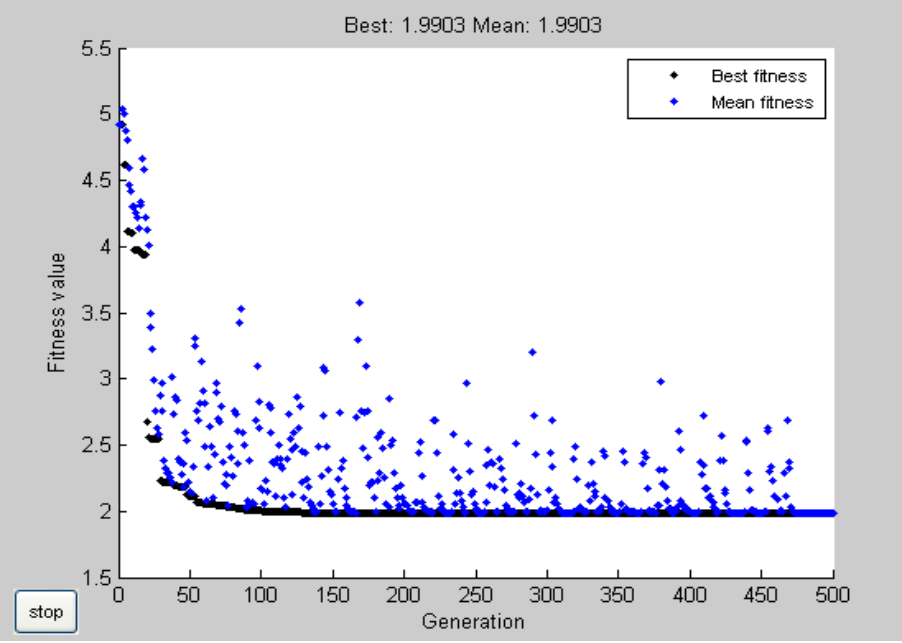

Figure 71 Optimization of the roof tile's warpage by GA.

Table 89 The optimal process conditions and warpage result of the roof tile optimized by GA

Optimal processing condition (Normalization)	
1. Injection speed	0.3847
2. Packing pressure	0.5
3. Packing time	0.4075
4. Cooling time	0.4122
Optimal processing condition (Real values)	
1. Injection speed (%)	69.25
2. Packing pressure (MPa)	8
3. Packing time (second)	1.63
4. Cooling time (second)	49.47
The minimum warpage (mm.)	1.9903
The process cycle time (second)	58.03

4.2.3 Confirmation of the optimum process condition of the roof tile

The comparison between the roof tile's warpage before and after optimization by GA was focused on the maximum warpage. In this case, the maximum the roof tile's warpage was calculated by the z-aixs deflection, distance in the thickness direction between the reference plane and the end of the part as previously shown in Figure 26. The warpage of the roof tile before and after optimization are displayed in Figures 72.

In addition, the comparison between the roof tile's warpage before and after optimization is displayed in Table 90. After optimization, the roof tile's warpage between the GA result (=1.99) and actual testing (=1.94) had 97.42% accuracy. Moreover, although the warpage of the roof tile was reduced from 3.28 to 1.94 mm (-40.85%), it did not take longer process cycle time.

(a) Before optimization (b) After optimization

Figure 72 The roof tile's warpage before (a) and after (b) optimization

Table 90 Comparison of the process parameters, warpage, and process cycle time of the roof tile before and after optimization.

Types	Processing conditions				Warpage values				Cycle time (sec)
	IS (%)	PP (MPa)	PT (sec)	CT (sec)	GA results	MPI results	Actual testing	Accuracy (%)	
1. Before optimization	58	5.5	1.5	50	-	3.19	3.28	97.26	58.84
2. After optimization	69.25	8	1.63	49.47	1.99	-	1.94	97.42	58.03

Discussion

1. The results of simulation model verification displayed that the CAE software, Moldflow, could be conducted instead of actual processing. For the rectangular lid (Case 1), the residual stresses of the actual testing and the simulation model were on the same pattern of the residual stresses at the middle area of the part as shown in Figure 73 and Figure 74. For the roof tile (Case 2), the warpage of the actual testing and of simulation model showed a similar level especially for the maximum warpage in the thickness direction (z-axis deflection) at the end of the part as displayed in Figures 75, 76, and 77.

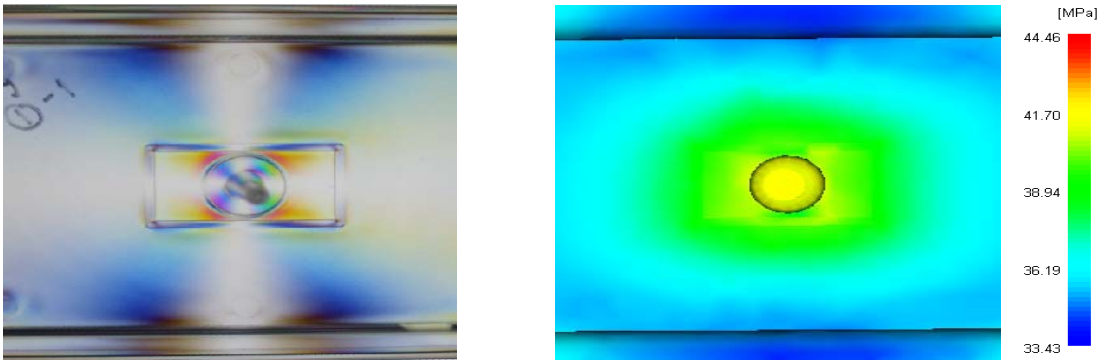

(a) The actual testing (b) The simulation model

Figure 73 The residual stress of the rectangular lid from (a) the actual testing and (b) the simulation model based on condition 1 (Case 1)

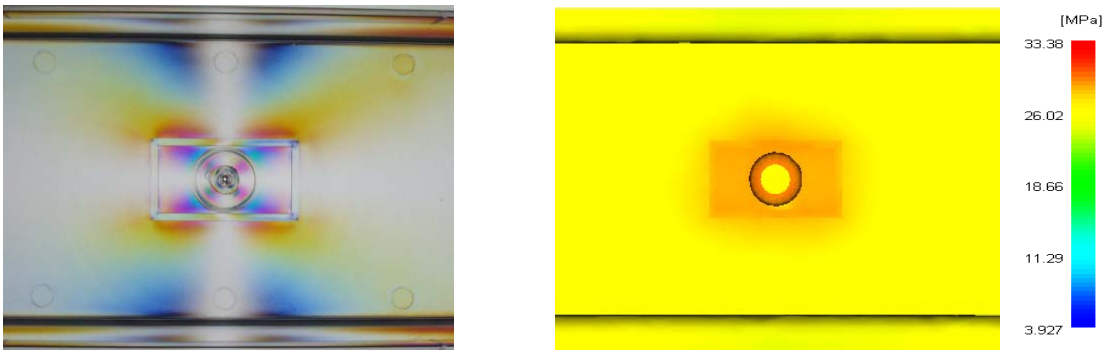

(a) The actual testing (b) The simulation model

Figure 74 The residual stress of the rectangular lid from (a) the actual testing and (b) the simulation model based on condition 2 (Case 1)

(a) The actual testing (3.28 mm) (b) The simulation model (3.19 mm)

Figure 75 The 97.26% warpage accuracy of the roof tile between (a) the actual testing and (b) the simulation model based on condition 1 (Case 2).

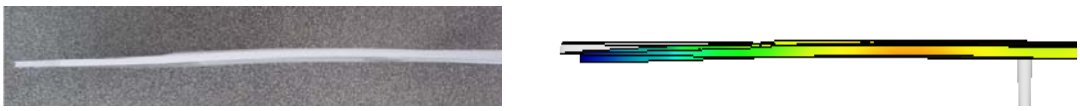

(a) The actual testing (-3.75 mm) (b) The simulation model (-3.64 mm)

Figure 76 The 97.07% warpage accuracy of the roof tile between (a) the actual testing and (b) the simulation model based on condition 2 (Case 2).

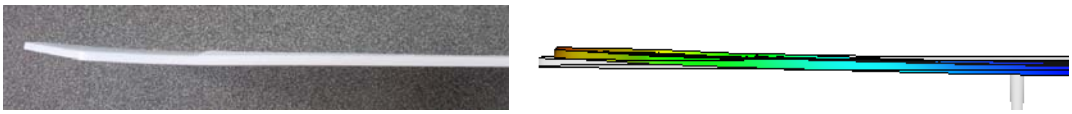

(a) Warpage of actual testing (4.48 mm.) (b) Warpage of simulation model (4.37 mm.)

Figure 77 The 97.54% warpage accuracy of the roof tile between (a) the actual testing and (b) the simulation model based on condition 3 (Case 2).

2. The results of Fractional Factorial design displayed that it could be used to reduce the number of parameters by identifying the key parameters affecting on the products' quality. For the rectangular lid (Case 1), there were totally five processing parameters affecting on the residual stress and process cycle time, which include (i) melt temperature, (ii) injection speed, (iii) packing pressure, (iv) packing time, and (v) cooling time. However, material grade parameter was removed because it had a small effect on these two response variables.

For the roof tile (Case 2), the melt temperature had a small effect to the warpage and process cycle time, so it was screened out. Therefore, there were totally four processing parameters that affected these two response variables of the roof tile including (i) injection speed, (ii) packing pressure, (iii) packing time, and (iv) cooling time.

3. The results of the optimal structure of the ANN model consisted of five set of parameters including (i) characteristic of input data and transfer function in hidden layer, (ii) *epochs* and *lr*, (iii) initial *bias* value, (iv) number of neuron in the 1st hidden layer,

and (v) number of neuron in the 2nd hidden layer. The comparison of these five ANN parameters resulted on two product cases: the rectangular lid and the roof tile, as shown in Table 91.

Table 91 The comparison of the ANN parameters results of Case 1: the rectangular lid and Case 2: the roof tile.

The ANN Parameters	The Optimal ANN values	
	Rectangular lid	Roof tile
1. Number of input	5	4
2. Characteristic of input	normalization	normalization
3. Learning rate (*lr*)	0.01	0.09
4. *Epoch*	1,000	3,000
5. Initial *bias* value	1.0	1.0
6. Number of neurons in the 1st hidden layer	7	9
7. Number of neurons in the 2nd hidden layer	-	16
8. Transfer function of the 1st hidden layer	logsig	logsig
9. Transfer function of the 2nd hidden layer	-	logsig
10. Transfer function of output layer	purelin	purelin
11. ANN configeration	5-7-2	4-9-16-2
12. Number of output	2	2
12.1 Average accuracy (%) of residual stress	99.3952	-
12.2 Average accuracy (%) of warpage	-	95.0384
12.3 Average accuracy (%) of cycle time	99.7384	99.9424
12.4 Total average accuracy (%)	99.5668	97.4904

From Table 91, the normalization input, binary sigmoid function (logsig), and initial bias value of 1 were appropriate types for both cases. However, the appropriate values of *epochs* and *lr* between both cases were different. The *epochs* and *lr* for the rectangular lid (Case 1) were 1,000 and 0.01 while the *epochs* and *lr* for the roof tile (Case 2) were 3,000 and 0.09.

In addition, the ANN configuration of the rectangular lid (Case 1) was 5-7-1, while the ANN configuration of the roof tile (Case 2) was 4-9-16-2. It means that a multilayer neural network model with a single hidden layer was a sufficient structure for

the rectangular lid's problem. For the roof tile's problem, double hidden layers type was an appropriate ANN configuration. Moreover, these two ANN models could effectively predict system's behavior among the relationship of the process parameters, quality index, and process cycle time because the predicted average accuracy of all response variables of these two cases were more than 95%.

4. The results of the optimal processing condition using the GA method consisted of four important GA parameters including (i) population size, (ii) crossover rate, (iii) mutation rate, and (iv) number of generations. The comparison of these four GA parameters of the rectangular lid (Case 1) and the roof tile (Case 2) are summarized in Table 92.

Table 92 Comparison of the GA parameters of the rectangular lid (Case 1) and the roof tile (Case 2)

GA Parameters	Optimal GA values	
	Rectangular lid	Roof tile
1. population size	50	50
2. crossover rate (P_c)	0.7	0.5 or 0.7
3. mutation rate (P_m)	0.1	0.1
4. number of generations	500	500
5. optimal solution	21.2956 MPa	1.9903 mm

From Table 92, the optimal values of four GA parameters of the rectangular lid (Case 1) and the roof tile (Case 2) were on the same levels. It means that the population size of 50, crossover rate of 0.7, mutation rate of 0.1 caused by GA for both cases converged to a fitness value before 500 generations and displayed the optimal solutions. Therefore, using high value of the population size and crossover rate often found the optimal solution of the problems.

CONCLUSION AND RECOMMENDATION

Conclusion

In this research work, there were two cases of the injection-molded parts: (i) the optimization of the rectangular lid's residual stress and its process cycle time (Case1) and (ii) the optimization of the roof tile's warpage and its process cycle time (Case 2). These two cases were achieved by applications of CAE software (MPI), DOE technigue, ANN model, and GA method. The details of these applications were summarized as follows:

1. Based on Case 1, using of the simulation model by CAE software (MPI) was conducted instead of the actual processing. The effect of the process parameters on the residual stress and process cycle time of the rectangular lid were determined by the 2^{6-2} Fractional Factorial design and statistical analysis. According to the results of the DOE technique, the significant parameters were (i) melt temperature, (ii) injection speed, (iii) packing pressure, (iv) packing time, and (v) cooling time. In order to achieve the minimum residual stress and process cycle time, the combination of ANN and GA techniques was then applied to provide satisfactory results. The optimal structure of the ANN model for the relationship among the residual stress, process cycle time, and processing parameters was 5-7-2 ANN configuration. By using this optimal structure of the ANN model as an objective function for the GA method, the values of the optimal process parameters were summarized as follows: melt temperature of 210°C, injection speed of 30%, packing pressure of 4.99 MPa, packing time of 3.5 second, and cooling time of 10 second. According to these optimal processing conditions, the residual stress of the rectangular lid was reduced from 28.98 to 21.32 mm (-26.43%) and the process cycle time was also reduced from 23.59 to 21.17 second (-10.26%).

2. Based on Case 2, the CAE software (MPI) was also able to conduct instead of the actual processing. The effects of the processing parameters on the warpage and process cycle time of the roof tile were determined by the 2^{5-1} Fractional Factorial design and statistical analysis. By the results of this DOE technique, the significant parameters were (i) injection speed, (ii) packing pressure, (iii) packing time, and (iv) cooling time.

To achieve the minimum warpage and process cycle time, the ANN and GA techniques were then applied to provide satisfactory results. The optimal structure of the ANN model for the relationship among the process parameters, warpage, and process cycle time was 4-9-16-2 ANN configuration. The optimal process parameters obtained by the GA method were summarized as follows: injection speed of 69.25%, packing pressure of 8 MPa, packing time of 1.63 second, and cooling time of 49.47 second. According to these optimal processing conditions, the warpage of the roof tile was reduced from 3.28 to 1.94 mm (-40.85%) without an increase of the process cycle time.

Recommendation

1. In this study work, the process parameters were determined within constraints of machine tools and mold steel. Thus, some parameters could not be considered as the parameters for optimizing the parts' quality. For example, the mold temperature could not be changed its level because the machine did not have the mold temperature changing device. Because of the fixed mold constraint, the gate location and coolant point could not be changed their locations. For future study, the researcher should perform the experiments using this study based on methodology before producing new products and its mold.

2. In Case 2 (the roof tile), the injection molding machine, Battenfeld model 2000/630BK, has maximum injection stroke of 180 mm while the required injection stroke needed to fill the roof tile was 170 mm. Thus, the machine had only 10 mm for packing the part which was not enough to produce a good quality of the roof tile. Therefore, in order to produce better quality of the roof tile, the injection molding machine with higher capacity would be recommended.

LITERATURE CITED

Bas, D., and I.H. Boyaci. 2007. Modeling and optimization II: Comparison of estimation capabilities of response surface methodology with artificial neural networks in a biochemical reaction. **Journal of Food Engineering.** 78: 846-854.

Brey, T., A. Jarre-Teichmann, and O. Borlich. 1996. Artificial neural network versus multiple linear regression: predicting P/B ratios from empirical data. **Marine Ecology Progress Series.** 140: 251-256.

Chakraborty, D. 2005. Artificial neural network based delamination prediction in laminated composites. **Materials and Design.** 26: 1-7.

Chankong, V. 2006. **Handout of Engineering Experiment Designs.**

Changyu, S., W. Lixia, and L. Qian. 2007. Optimization of injection molding process parameters using combination of artificial neural network and genetic algorithm method. **Journal of Materials Processing Technology.** 183: 412-418.

Chookaew, W. 2006. **A Prediction of Rubber Product Shrinkage in Compression Moulding Process Using the Neural Network Model.** M.S. Thesis, Kasetsart University.

Dagli, C.H. 1994. **Artificial neural networks for intelligent manufacturing.** Chapman & Hall, London.

Dayhoff, J.E. 1999. **Neural Network Architectures.** Van Nostrand Reinhold, New York.

Davis, B.JR. 1999. A system for design of experiments, response surface modeling and optimization using process and device simulation. **IIE Transaction.** 14(2): 90-98.

Demuth, H., and M. Beale. 2003. **Neural Networks Toolbox User Guide.** Mathworks, Inc., Natick, MA.

Dong, C. 2006. Development of a process model for the vacuum assisted resin transfer molding simulation by the response surface method. **Composites: Part A.** 37: 1316–1324.

Ezrin, M., G. Lavigne and J. Helwig. 1999. **Plastic Product Failure due to Design, Material or Processing Problems.** National Manufacturing Week**,** Design for Manufacturability of Plastic Parts, Chicago.

Fausett, L.V. 1994. **Fundamentals of Neural Networks: Architectures, Algorithms, and Applications.** Prentice-Hall, Inc. Upper Saddle River, New Jersey.

Foran, J. 2002. **Optimization of a Fuzzy Logic Controller Using Genetic Algorithms.** M.Eng Project Report. 2002.

Garcia-Gimeno, R.M., C. Hervas-Martinez, R. Rodriguez-Perez, and G. Zurera-Cosano. 2004. Modelling the growth of Leuconostoc mesenteroides by Artificial Neural Networks. **International Journal of Food Microbiology.** 105: 317-332.

Gen, M. and R. Cheng. 1997. **Genetic algorithms and engineering design.** A Wiley-Interscience Publishing, John Wiley & Sons, Inc. New York, USA.

GLS Corporation. 2006. **The first annual TPE product design and development innovation awards program TPEs making a difference.** TPE Product Design and Development Innovation Awards. Available Source: http://www.glscorporation.com/pdf/GLSaward.pdf, July 28, 2007.

Goldberg, D.E. 1989. **Genetic Algorithms in Search, Optimization and Machine Learning.** Addison-Wesley Publishing Company, Inc. Boston MA, USA.

Goodfellow. 2007. **Polyethylene terephthalate (Polyester, PET, PETP) - Material Information.** Goodfellow, online source. Available Source: http://www.goodfellow.com/csp/active/static/a/polyethylene_terephthalate.html, July 31, 2007.

Hagan, M.T., H.B. Demuth, and M. Beale. 1996. **Neural Network Design.** PWS Publishing Company, Boston.

Huang, M.C., and C.C. Tai. 2001. The effective factors in the warpage problem of an injection-molded part with a thin shell feature. **Journal of Materials Processing Technology.** 110: 1-9.

Imihezri, S.S.S., S.M. Sapuan, S. Sulaiman, M.M. Hamdan, E.S. Zainuddin, M.R. Osman and M.Z.A Rahman. 2006. Mould flow and component design analysis of polymeric based composite automotive clutch pedals. **Journal of Materials Processing Technology.** 171: 358-365.

Jankrajang, W. 2003. **Design of Experiment Approach for Improving Rice Milling Quality.** M.S. Thesis, Kasetsart University.

Kittisorn, S. 2004. **A. Market highlights and best prospects**. Plastics Manufacturing Machinery. Available Source: http://strategis.ic.gc.ca/epic/site/imr-ri.nsf/en/gr127451e.html, July 15, 2007.

Koch, P.E. 2005. **Injection molding of thermoplastics**. Injection Molding of Thermoplastics. Available Source: http://ehgr.bd.psu.edu/pkoch/plasticdesign/IM_Thermoplastic.htm.

Krottmaier, J. 1993. **Optimizing Engineering Designs.** McGraw-Hill, New York.

Kurtaran, H., B. Ozcelik and T. Erzurumlu. 2005. Warpage optimization of a bus ceiling lamp base using neural network model and genetic algorithm. **Journal of Materials Processing Technology.** 169: 314-319.

Law, A.M., and W.D. Kelton. 2000. **Simulation modeling and analysis.** 4th ed. The McGraw-Hill Book, Co., Singapore.

Lou, W., and S. Nakai. 2001. Artificial Neural Network-Based Predictive Model for Bacterial Growth in a Simulated Medium of Modified-Atmosphere-Packed Cooked Meat Products. **J. Agric. Food Chem.** 49: 1799-1804.

Luis, C.J., I. Puertas, and G. Villa. 2005. Material removal rate and electrode wear study on the EDM of silicon carbide. **Journal of Materials Processing Technology.** 164-165: 889-896.

Marcilla, A., A. Odjo-Omoniyi, R. Ruiz-Femenia, and J.C. Garcia-Quesada. 2006. Simulation of the gas-assisted injection molding process using a mid-plane model of a contained-channel part. **Journal of Materials Processing Technology.** 178: 350-357.

Marechal, E. 2005. Creation and Development of Thermoplastic Elastomers, and Their Position Among Organic Materials, pp. 3-20. *In* S. Fakirov, eds. **Handbook of Condensation Thermoplastic Elastomers.** Wiley-vch, Deutsch.

Ministry of Commerce. 2008. **Export Situation of Plastic Resins & Plastic Products 2005 – 2008 (Jan – May).** Business Development. Available Source: http://ftiweb.off.fti.or.th/demo/6101/sitedata/site39/articles/ATC20_Export_resins_&_Products_,July_08.ppt, November 20, 2008.

Mok, S. L., C. K. Kwong, and W. S. Lau. 2001. A Hybrid Neural Network and Genetic Algorithm Approach to the Determination of Initial Process Parameters for Injection Moulding. **The international Journal of Advanced Manufacturing Technology.** 18: 404-409.

Moldflow Corporation. 2006. **MPI information.** Moldflow Plastics Insight. Available Source: http://www.moldflow.com/stp/english/products/mpi.htm, June 10, 2008.

Montgomery, D.C. 2005. **Design and analysis of experiments.** 6th ed. John Wiley & Sons, Inc., United States of America.

Muller, B., and J. Reinhardt. 1990. **Neural network : an introduction.** Springer-Verlag, Inc., Berlin.

Nelson, M.M., and W.T. Illingworth. 1991. **A practical guide to neural nets.** Addison-Wesley, Reading.

Ozcelik, B., and T. Erzurumlu. 2006. Comparison of the warpage optimization in the plastic injection molding using ANOVA, neural network model and genetic algorithm. **Journal of Materials Processing Technology.** 171: 437-445.

Page, G.F., J.B. Gomm, and D. Williams. 1993. **Application of neural networks to modelling and control.** Chapman & Hall, London.

Park, K. and J.H. Ahn. 2004. Design of experiment considering two-way interactions and its application to injection molding processes with numerical analysis. **Journal of Materials Processing Technology.** 146: 221-227.

Sadeghi, B.H.M. 2000. A BP-neural network predictor model for plastic injection molding process. **Journal of Materials Processing Technology.** 103: 411-416.

Shah, V. 2007. **Handbook of Plastics Testing and Failure Analysis.** 3rd ed**.** John Wiley & Sons, Inc., Hoboken.

Sanchez, S.M. 2005. Work smarter, not harder: Guidelines for designing simulation experiments, pp. 69-82. *In* M.E. Kuhl, N.M. Steiger, F.B. Armstrong, and J.A. Joines, eds. **The Proceedings of the 2005 Winter Simulation Conference.** Institute of Electrical and Electronics Engineers, Piscataway, New Jersey.

Scientific Glass & Plastic, Inc. 2002. **Material Selection: Polyvinyl Chloride.** Custom Fabrication of Thermoplastics & Scientific Glassware. Available Source: http://www.sg-p.com/material_selection.htm#pvc, July 31, 2007.

Shen, Y., K. Chandrashekhara, W.F. Breig, and L.R. Oliver. 2005. Finite element analysis of V-ribbed belts using neural network based hyperelastic material model. **International Journal of Non-Linear Mechanics.** 40: 875-890.

Sivanandam, S.N., S. Sumathi, and S.N. Deepa. 2006. **Introduction to Neural Networks Using MATLAB 6.0.** Tata McGraw-Hill, New Delhi.

Sudasna-na-Ayudthya, P. 2006. **Handout of Design and Analysis of Experiment II.**

The Office of Small and Medium Enterprises Promotion. 2004. **The White Paper on Small and Medium Enterprises of Thailand in 2004 and Trends 2005.** pp. 6-49 – 6-58.

Tonsura, J. 2005. **Natural Rubber and Polypropylene Blend for Gasket Production**. M.S. Thesis, Rajamangala University of Technology Thanyaburi.

VTC Franceschetti Elastomeri. 2006. **A general introduction to Thermoplastic Elastomers world**. VTC Franceschetti Elastomeri. Available Source: http:// www.vtcfranceschetti.it/prodotti/about-tpe.htm, July 28, 2007.

Versteegen, R.M. 2003. **Well-defined thermoplastic elastomers : reversible networks based on hydrogen.** Technische Universiteit Eindhoven, Eindhoven.

Wikipedia. 2007. Injection molding. **Wikipedia The Free Encyclopedia.**

Wongrat, W., T. Srinophakun, and P. Srinophakun. 2005. Modified genetic algorithm for nonlinear data reconciliation. **Computers and Chemical Engineering.** 29: 1059-1067.

APPENDICES

Appendix A

Results of the 2^{6-2} Fractional Factorial design

Apendix Table A1 Results of the 2^{6-2} Fractional Factorial design that residual stress and process cycle time of the rectangular lid were outputs (Experiment 1)

Std Order	Material grade	Melt temperature (°C)	Injection speed (%)	Packing pressure (MPa)	Packing time (sec.)	Cooling time (sec.)	Point 1	Point 2	Point 3	Point 4	Residual stress	Cycle time
1	Styron 666D	200	30	3	1.5	10	28.62	28.74	28.72	28.69	28.69	19.35
2	Styron 678D	200	30	3	3.5	10	23.12	23.28	23.23	23.23	23.22	21.23
3	Styron 666D	260	30	3	3.5	25	24.84	24.94	24.92	24.84	24.89	36.16
4	Styron 678D	260	30	3	1.5	25	31.54	31.59	31.56	31.56	31.56	34.15
5	Styron 666D	200	50	3	3.5	25	23.66	23.73	23.76	23.7	23.71	35.22
6	Styron 678D	200	50	3	1.5	25	29.64	29.69	29.69	29.72	29.69	33.17
7	Styron 666D	260	50	3	1.5	10	32.71	32.77	32.75	32.73	32.74	18.12
8	Styron 678D	260	50	3	3.5	10	26.33	26.38	26.38	26.36	26.36	20.11
9	Styron 666D	200	30	5	1.5	25	26.74	26.83	26.84	26.8	26.80	34.19
10	Styron 678D	200	30	5	3.5	25	21.72	21.72	21.62	21.57	21.66	36.15
11	Styron 666D	260	30	5	3.5	10	24.34	24.45	24.42	24.4	24.40	21.12
12	Styron 678D	260	30	5	1.5	10	31.49	31.5	31.49	31.48	31.49	19.12
13	Styron 666D	200	50	5	3.5	10	22.25	22.31	22.32	22.28	22.29	20.13
14	Styron 678D	200	50	5	1.5	10	29.72	29.73	29.7	29.71	29.72	18.12
15	Styron 666D	260	50	5	1.5	25	31.87	31.94	31.91	31.87	31.90	33.09
16	Styron 678D	260	50	5	3.5	25	25.41	25.46	25.46	25.43	25.44	35.09

Apendix Table A2 Results of the 2^{5-1} Fractional Factorial design that warpage and process cycle time of the roof tile were outputs (Experiment 2)

Std Order	Melt temperature (°C)	Injection speed (%)	Packing pressure (MPa)	Packing time (sec.)	Cooling time (sec.)	End point	Middle point	Warpage	Cycle time
1	140	30	4	1	60	9.05	4.16 (-)	13.21	70.53
2	180	30	4	1	40	2.25	3.07	5.32	50.44
3	140	90	4	1	40	5.57	2.52 (-)	8.09	47.63
4	180	90	4	1	60	10.63	6.08	16.71	67.60
5	140	30	8	1	40	0.36	1.39	1.75	50.34
6	180	30	8	1	60	1.71	2.66	4.37	70.32
7	140	90	8	1	60	4.41	2.37 (-)	6.78	67.52
8	180	90	8	1	40	7.62	4.39	12.01	47.51
9	140	30	4	2	40	1.83	1.81 (-)	3.64	51.53
10	180	30	4	2	60	1.29	2.67	3.96	71.44
11	140	90	4	2	60	6.27	3.57 (-)	9.84	68.63
12	180	90	4	2	40	2.00	2.58	4.58	48.60
13	140	30	8	2	60	1.87	1.21 (-)	3.08	71.40
14	180	30	8	2	40	1.64	2.87	4.51	51.32
15	140	90	8	2	40	1.10	1.26	2.36	48.52
16	180	90	8	2	60	1.39	2.23	3.62	68.51

Appendix B

Data for train and test ANN model

Apendix Table B1 Data for train ANN model that residual stress and process cycle time of the rectangular lid were outputs

Run Order	Std. Order	Input train					Output train					
		Melt temperature (°C)	Injection speed (%)	Packing pressure (MPa)	Packing time (sec.)	Cooling time (sec.)	Point 1	Point 2	Point 3	Point 4	Residual stress	Cycle time
1	92	230	30	4	1.5	17.5	29.38	29.47	29.46	29.45	29.44	26.66
2	198	260	40	3	3.5	25	24.95	25.03	25.09	25.09	25.04	35.51
3	107	230	30	5	3.5	17.5	21.83	21.85	21.88	21.93	21.87	28.64
4	83	230	30	3	1.5	17.5	29.61	29.89	29.90	29.84	29.81	26.70
5	204	260	40	4	2.5	25	27.60	27.72	27.69	27.62	27.66	34.49
6	11	200	30	4	1.5	17.5	27.39	27.52	27.58	27.49	27.50	26.73
7	45	200	40	4	3.5	25	21.81	21.88	21.84	21.75	21.82	35.56
8	111	230	40	3	1.5	25	30.32	30.33	30.27	30.40	30.33	33.54
9	108	230	30	5	3.5	25	21.35	21.35	21.36	21.34	21.35	36.14
10	129	230	40	5	1.5	25	29.69	29.81	29.78	29.71	29.75	33.50
11	203	260	40	4	2.5	17.5	27.82	27.93	27.92	27.86	27.88	26.99
12	180	260	30	4	3.5	25	24.18	24.21	24.26	24.17	24.21	36.14
13	126	230	40	4	3.5	25	23.17	23.26	23.27	23.22	23.23	35.51
14	14	200	30	4	2.5	17.5	24.29	24.28	34.31	24.35	26.81	27.73
15	119	230	40	4	1.5	17.5	30.21	30.32	30.27	30.24	30.26	26.01
16	235	260	50	5	1.5	10	32.31	32.38	32.36	32.32	32.34	18.09
17	46	200	40	5	1.5	10	28.31	28.38	28.36	28.30	28.34	18.53
18	218	260	50	3	1.5	17.5	32.25	32.25	32.22	32.12	32.21	25.62
19	100	230	30	5	1.5	10	29.46	29.44	29.51	29.51	29.48	19.14
20	113	230	40	3	2.5	17.5	26.63	26.90	26.64	26.60	26.69	27.04

Apendix Table B1 (Continued)

Run Order	Std. Order	Input train					Output train					
		Melt temperature (°C)	Injection speed (%)	Packing pressure (MPa)	Packing time (sec.)	Cooling time (sec.)	Point 1	Point 2	Point 3	Point 4	Residual stress	Cycle time
21	191	260	40	3	1.5	17.5	31.55	31.78	31.80	31.63	31.69	26.01
22	51	200	40	5	2.5	25	24.27	24.42	24.42	24.31	24.36	34.53
23	156	230	50	5	1.5	25	30.21	30.41	30.37	30.33	30.33	33.11
24	19	200	30	5	1.5	10	27.29	27.40	27.38	27.37	27.36	19.19
25	124	230	40	4	3.5	10	23.93	23.95	23.99	23.97	23.96	20.51
26	209	260	40	5	1.5	17.5	31.55	31.66	31.62	31.59	31.61	25.98
27	47	200	40	5	1.5	17.5	28.00	28.07	28.08	28.00	28.04	26.03
28	135	230	40	5	3.5	25	21.76	21.77	21.83	21.74	21.78	35.50
29	144	230	50	3	3.5	25	24.23	24.44	24.38	24.22	24.32	35.15
30	237	260	50	5	1.5	25	31.59	31.80	31.79	31.62	31.70	33.09
31	153	230	50	4	3.5	25	23.87	23.97	23.95	23.91	23.93	35.12
32	227	260	50	4	1.5	17.5	32.24	32.32	32.30	32.27	32.28	25.60
33	168	260	30	3	2.5	25	27.29	27.47	27.41	27.37	27.39	35.16
34	155	230	50	5	1.5	17.5	30.53	30.61	30.58	30.53	30.56	25.61
35	222	260	50	3	2.5	25	28.15	28.23	28.23	28.20	28.20	34.12
36	53	200	40	5	3.5	17.5	21.69	21.68	21.69	21.68	21.69	28.03
37	106	230	30	5	3.5	10	22.30	22.51	22.30	22.25	22.34	21.14
38	159	230	50	5	2.5	25	26.47	26.55	26.53	26.48	26.51	34.11
39	219	260	50	3	1.5	25	32.24	32.30	32.29	32.27	32.28	33.12
40	112	230	40	3	2.5	10	27.07	27.08	27.12	27.12	27.10	19.54

Apendix Table B1 (Continued)

Run Order	Std. Order	Input train					Output train					
		Melt temperature (°C)	Injection speed (%)	Packing pressure (MPa)	Packing time (sec.)	Cooling time (sec.)	Point 1	Point 2	Point 3	Point 4	Residual stress	Cycle time
41	234	260	50	4	3.5	25	24.95	25.03	25.08	25.05	25.03	35.10
42	240	260	50	5	2.5	25	27.87	27.95	27.93	27.88	27.91	34.09
43	150	230	50	4	2.5	25	26.62	26.69	26.67	26.64	26.66	34.12
44	80	200	50	5	3.5	17.5	21.65	21.65	21.68	21.66	21.66	27.63
45	123	230	40	4	2.5	25	26.16	26.18	26.21	26.20	26.19	34.51
46	140	230	50	3	2.5	17.5	27.13	27.19	27.17	27.16	27.16	26.65
47	8	200	30	3	3.5	17.5	23.06	23.09	23.13	22.66	22.99	28.85
48	24	200	30	5	2.5	25	23.35	23.37	23.28	23.48	23.37	35.19
49	163	260	30	3	1.5	10	31.78	31.85	31.86	31.81	31.83	19.16
50	39	200	40	4	1.5	25	28.17	28.30	28.34	28.17	28.25	33.56
51	116	230	40	3	3.5	17.5	24.37	24.62	24.46	24.24	24.42	28.04
52	68	200	50	4	2.5	17.5	25.42	25.4	25.38	25.4	25.40	26.66
53	179	260	30	4	3.5	17.5	24.25	24.37	24.37	24.3	24.32	28.64
54	199	260	40	4	1.5	10	32.03	32.07	32.08	32.08	32.07	18.49
55	201	260	40	4	1.5	25	31.57	31.68	31.67	31.62	31.64	33.49
56	152	230	50	4	3.5	17.5	24.03	24.11	24.08	24.05	24.07	27.62
57	43	200	40	4	3.5	10	23.31	23.38	23.32	22.53	23.14	20.56
58	58	200	50	3	2.5	10	26.6	26.58	26.58	26.32	26.52	19.22
59	147	230	50	4	1.5	25	30.53	30.55	30.55	30.54	30.54	33.12
60	178	260	30	4	3.5	10	24.52	24.64	24.62	24.58	24.59	21.14

Apendix Table B1 (Continued)

Run Order	Std. Order	Input train					Output train					
		Melt temperature (°C)	Injection speed (%)	Packing pressure (MPa)	Packing time (sec.)	Cooling time (sec.)	Point 1	Point 2	Point 3	Point 4	Residual stress	Cycle time
61	15	200	30	4	2.5	25	24.15	24.29	24.33	24.3	24.27	35.23
62	200	260	40	4	1.5	17.5	31.79	31.92	31.87	31.82	31.85	25.99
63	66	200	50	4	1.5	25	28.77	28.78	28.76	28.8	28.78	33.16
64	33	200	40	3	2.5	25	25.92	26.06	26.06	25.98	26.01	34.64
65	122	230	40	4	2.5	17.5	26.4	26.5	26.46	26.42	26.45	27.01
66	16	200	30	4	3.5	10	22.09	21.99	22.06	21.72	21.97	21.23
67	63	200	50	3	3.5	25	23.4	23.5	23.54	23.22	23.42	35.22
68	37	200	40	4	1.5	10	28.7	28.67	28.74	28.68	28.70	18.56
69	229	260	50	4	2.5	10	27.99	28.07	28.05	28.04	28.04	19.1
70	157	230	50	5	2.5	10	26.94	26,97	26.93	26.94	26.94	19.11
71	70	200	50	4	3.5	10	22.2	22.24	22.34	22.35	22.28	20.16
72	21	200	30	5	1.5	25	26.77	26.84	26.8	26.78	26.80	34.19
73	128	230	40	5	1.5	17.5	29.92	30.05	30.01	29.95	29.98	26
74	176	260	30	4	2.5	17.5	27.19	27.28	27.27	27.22	27.24	27.64
75	98	230	30	4	3.5	17.5	22.79	22.99	22.94	22.68	22.85	28.66
76	56	200	50	3	1.5	17.5	29.69	29.75	29.77	29.64	29.71	25.72
77	101	230	30	5	1.5	17.5	29.12	29.14	29.18	29.17	29.15	26.64
78	71	200	50	4	3.5	17.5	23.10	23.00	22.93	22.68	22.93	27.66
79	93	230	30	4	1.5	25	29.01	29.26	29.24	29.21	29.18	34.16
80	186	260	30	5	2.5	25	26.70	26.79	26.80	26.49	26.70	35.12

Apendix Table B1 (Continued)

Run Order	Std. Order	Input train					Output train					
		Melt temperature (°C)	Injection speed (%)	Packing pressure (MPa)	Packing time (sec.)	Cooling time (sec.)	Point 1	Point 2	Point 3	Point 4	Residual stress	Cycle time
81	114	230	40	3	2.5	25	26.50	26.62	26.64	26.61	26.59	34.54
82	115	230	40	3	3.5	10	24.55	24.63	24.67	24.45	24.58	20.54
83	213	260	40	5	2.5	25	27.42	27.51	27.51	27.46	27.48	34.48
84	28	200	40	3	1.5	10	29.41	29.65	29.66	29.55	29.57	18.64
85	99	230	30	4	3.5	25	22.85	22.89	22.82	22.73	22.82	36.16
86	105	230	30	5	2.5	25	24.93	24.99	25.00	25.04	24.99	35.14
87	64	200	50	4	1.5	10	28.99	29.13	29.07	29.09	29.07	18.16
88	172	260	30	4	1.5	10	31.46	31.53	31.51	31.51	31.50	19.14
89	238	260	50	5	2.5	10	28.36	28.43	28.42	28.37	28.40	19.09
90	182	260	30	5	1.5	17.5	30.94	31.01	31.01	30.99	30.99	26.62
91	48	200	40	5	1.5	25	27.76	27.85	27.82	27.79	27.81	33.53
92	69	200	50	4	2.5	25	25.04	25.18	25.15	25.09	25.12	34.16
93	31	200	40	3	2.5	10	26.19	26.29	26.16	26.25	26.22	19.64
94	194	260	40	3	2.5	17.5	28.09	28.20	28.15	28.14	28.15	27.01
95	27	200	30	5	3.5	25	21.43	21.44	21.45	21.45	21.44	36.19
96	166	260	30	3	2.5	10	27.57	27.69	27.98	27.96	27.80	20.16
97	50	200	40	5	2.5	17.5	24.44	24.56	24.57	24.49	24.52	27.03
98	65	200	50	4	1.5	17.5	28.90	28.95	28.94	28.85	28.91	25.66
99	189	260	30	5	3.5	25	23.71	23.97	23.96	23.93	23.89	36.12
100	41	200	40	4	2.5	17.5	25.07	25.15	25.24	25.09	25.14	27.06

Apendix Table B1 (Continued)

Run Order	Std. Order	Input train					Output train					
		Melt temperature (°C)	Injection speed (%)	Packing pressure (MPa)	Packing time (sec.)	Cooling time (sec.)	Point 1	Point 2	Point 3	Point 4	Residual stress	Cycle time
101	32	200	40	3	2.5	17.5	25.93	26.12	26.10	26.09	26.06	27.14
102	7	200	30	3	3.5	10	23.23	23.41	23.48	23.22	23.34	21.35
103	134	230	40	5	3.5	17.5	22.61	22.86	22.96	22.43	22.72	28.00
104	138	230	50	3	1.5	25	30.73	30.88	30.88	30.68	30.79	33.15
105	183	260	30	5	1.5	25	30.32	30.51	30.75	30.74	30.58	34.12
106	202	260	40	4	2.5	10	28.14	28.24	28.22	28.17	28.19	19.49
107	196	260	40	3	3.5	10	25.68	25.81	25.80	25.72	25.75	20.51
108	141	230	50	3	2.5	25	26.98	27.03	27.04	27.01	27.02	34.15
109	148	230	50	4	2.5	10	27.11	27.16	27.14	27.13	27.14	19.12
110	241	260	50	5	3.5	10	25.19	25.37	25.36	25.32	25.31	20.09
111	151	230	50	4	3.5	10	24.25	24.32	24.30	24.27	24.29	20.12
112	223	260	50	3	3.5	10	25.84	26.01	25.99	25.92	25.94	20.12
113	205	260	40	4	3.5	10	25.10	25.20	25.19	25.15	25.16	20.49
114	96	230	30	4	2.5	25	25.49	25.58	25.58	25.56	25.55	35.16
115	158	230	50	5	2.5	17.5	26.53	26.61	26.71	26.67	26.63	26.61
116	143	230	50	3	3.5	17.5	24.60	24.79	24.63	24.58	24.65	27.65
117	22	200	30	5	2.5	10	23.85	23.84	23.93	23.90	23.88	20.19
118	133	230	40	5	3.5	10	23.26	23.35	23.36	23.53	23.38	20.50
119	81	200	50	5	3.5	25	21.66	21.64	21.66	21.64	21.65	35.13
120	9	200	30	3	3.5	25	23.11	23.18	23.12	22.51	22.98	36.35

Apendix Table B1 (Continued)

Run Order	Std. Order	Input train					Output train					
		Melt temperature (°C)	Injection speed (%)	Packing pressure (MPa)	Packing time (sec.)	Cooling time (sec.)	Point 1	Point 2	Point 3	Point 4	Residual stress	Cycle time
121	54	200	40	5	3.5	25	21.65	21.66	21.69	21.66	21.67	35.53
122	197	260	40	3	3.5	17.5	25.13	25.26	25.24	25.17	25.20	28.01
123	226	260	50	4	1.5	10	32.50	32.55	32.51	32.52	32.52	18.10
124	207	260	40	4	3.5	25	24.65	24.74	24.78	24.66	24.71	35.49
125	61	200	50	3	3.5	10	24.22	24.21	24.20	24.09	24.18	20.22
126	117	230	40	3	3.5	25	23.99	24.20	24.23	24.22	24.16	35.54
127	169	260	30	3	3.5	10	24.97	25.14	25.10	24.97	25.05	21.16
128	76	200	50	5	2.5	10	25.12	25.16	25.20	25.11	25.15	19.13
129	102	230	30	5	1.5	25	28.85	28.96	28.94	28.91	28.92	34.14
130	95	230	30	4	2.5	17.5	25.72	25.73	25.80	25.77	25.76	27.66
131	85	230	30	3	2.5	10	26.50	26.59	26,57	26.54	26.54	20.20
132	91	230	30	4	1.5	10	29.72	29.81	29.80	29.78	29.78	19.16
133	36	200	40	3	3.5	25	23.25	23.76	23.67	23.34	23.51	35.64
134	42	200	40	4	2.5	25	24.87	25.05	25.00	24.97	24.97	34.56
135	174	260	30	4	1.5	25	30.84	30.98	30.96	30.91	30.92	34.14
136	88	230	30	3	3.5	10	24.19	24.35	24.28	24.26	24.27	21.20
137	131	230	40	5	2.5	17.5	26.12	26.26	26.21	26.15	26.19	27.00
138	40	200	40	4	2.5	10	25.26	25.35	25.31	25.32	25.31	19.56
139	109	230	40	3	1.5	10	30.89	30.98	30.93	30.92	30.93	18.54
140	52	200	40	5	3.5	10	21.69	21.71	21.72	21.70	21.71	20.53

Apendix Table B1 (Continued)

Run Order	Std. Order	Input train					Output train					
		Melt temperature (°C)	Injection speed (%)	Packing pressure (MPa)	Packing time (sec.)	Cooling time (sec.)	Point 1	Point 2	Point 3	Point 4	Residual stress	Cycle time
141	214	260	40	5	3.5	10	24.93	25.05	25.04	24.97	25.00	20.48
142	167	260	30	3	2.5	17.5	27.55	27.69	27.65	27.62	27.63	27.66
143	224	260	50	3	3.5	17.5	25.58	25.69	25.71	25.63	25.65	27.62
144	49	200	40	5	2.5	10	24.67	24.76	24.74	24.70	24.72	19.53
145	212	260	40	5	2.5	17.5	27.66	27.76	27.74	27.67	27.71	26.98
146	84	230	30	3	1.5	25	29.54	29.67	29.62	29.62	29.61	34.20
147	149	230	50	4	2.5	17.5	26.81	26.87	26.86	26.84	26.85	26.62
148	188	260	30	5	3.5	17.5	24.07	24.17	24.19	24.12	24.14	28.62
149	165	260	30	3	1.5	25	30.85	31.05	30.97	30.72	30.90	34.16
150	94	230	30	4	2.5	10	25.96	26.13	26.10	26.09	26.07	20.16
151	211	260	40	5	2.5	10	27.95	28.06	28.03	27.97	28.00	19.48
152	232	260	50	4	3.5	10	25.42	25.47	25.46	25.47	25.46	20.10
153	97	230	30	4	3.5	10	23.44	23.51	23.51	23.52	23.50	21.16
154	206	260	40	4	3.5	17.5	24.79	24.91	24.89	24.85	24.86	27.99
155	145	230	50	4	1.5	10	31.03	31.06	31.03	31.04	31.04	18.12
156	26	200	30	5	3.5	17.5	21.68	21.68	21.69	21.68	21.68	28.69
157	35	200	40	3	3.5	17.5	23.54	23.71	23.79	23.70	23.69	28.14
158	55	200	50	3	1.5	10	29.96	29.99	30.00	29.76	29.93	18.22
159	82	230	30	3	1.5	10	30.06	30.15	30.11	30.12	30.11	19.20
160	221	260	50	3	2.5	17.5	28.38	28.47	28.42	28.38	28.41	26.62

Apendix Table B1 (Continued)

Run Order	Std. Order	Input train					Output train					
		Melt temperature (°C)	Injection speed (%)	Packing pressure (MPa)	Packing time (sec.)	Cooling time (sec.)	Point 1	Point 2	Point 3	Point 4	Residual stress	Cycle time
161	181	260	30	5	1.5	10	31.28	31.35	31.31	31.31	31.31	19.12
162	87	230	30	3	2.5	25	25.81	26.06	26.08	26.00	25.99	35.20
163	230	260	50	4	2.5	17.5	28.19	28.26	28.26	28.22	28.23	26.60
164	78	200	50	5	2.5	25	24.72	24.78	24.83	24.72	24.76	34.13
165	86	230	30	3	2.5	17.5	26.19	26.29	26.26	26.20	26.24	27.70
166	192	260	40	3	1.5	25	31.73	31.96	31.96	31.90	31.89	33.51
167	13	200	30	4	2.5	10	24.59	24.68	24.60	24.63	24.63	20.23
168	173	260	30	4	1.5	17.5	31.10	31.19	31.19	31.09	31.14	26.64
169	185	260	30	5	2.5	17.5	26.95	27.05	27.04	26.99	27.01	27.62
170	228	260	50	4	1.5	25	32.03	32.10	32.09	32.05	32.07	33.10
171	38	200	40	4	1.5	17.5	28.37	28.53	28.55	28.40	28.46	26.06
172	104	230	30	5	2.5	17.5	25.12	25.21	25.23	25.26	25.21	27.64
173	17	200	30	4	3.5	17.5	21.72	21.76	21.74	21.77	21.75	28.73
174	132	230	40	5	2.5	25	25.90	26.05	26.03	25.96	25.99	34.50
175	136	230	50	3	1.5	10	31.31	31.35	31.34	31.32	31.33	18.15
176	177	260	30	4	2.5	25	26.91	27.02	27.03	26.98	26.99	35.14
177	2	200	30	3	1.5	17.5	28.33	28.44	28.44	28.38	28.40	26.85
178	12	200	30	4	1.5	25	27.22	27.34	27.38	27.27	27.30	34.23
179	220	260	50	3	2.5	10	28.70	28.78	28.74	28.73	28.74	19.12
180	110	230	40	3	1.5	17.5	30.59	30.70	30.65	30.64	30.65	26.04

Apendix Table B1 (Continued)

Run Order	Std. Order	Input train					Output train					
		Melt temperature (°C)	Injection speed (%)	Packing pressure (MPa)	Packing time (sec.)	Cooling time (sec.)	Point 1	Point 2	Point 3	Point 4	Residual stress	Cycle time
181	5	200	30	3	2.5	17.5	25.39	25.54	25.49	25.50	25.48	27.85
182	60	200	50	3	2.5	25	26.02	26.10	26.06	26.06	26.06	35.35
183	75	200	50	5	1.5	25	28.36	28.43	28.46	28.38	28.41	33.13
184	239	260	50	5	2.5	17.5	28.08	28.15	28.13	28.09	28.11	26.59
185	193	260	40	3	2.5	10	28.44	28.52	28.48	28.48	28.48	19.51
186	184	260	30	5	2.5	10	27.28	27.35	27.35	27.32	27.33	20.12
187	146	230	50	4	1.5	17.5	30.63	30.78	30.75	30.75	30.73	25.62
188	118	230	40	4	1.5	10	30.54	30.62	30.58	30.56	30.58	18.12
189	6	200	30	3	2.5	25	25.21	25.38	25.36	25.30	25.31	35.35
190	34	200	40	3	3.5	10	23.77	24.03	23.90	23.83	23.88	20.64
191	59	200	50	3	2.5	17.5	26.07	26.09	26.05	26.10	26.08	26.72
192	164	260	30	3	1.5	17.5	31.45	31.58	31.53	31.51	31.52	26.66
193	79	200	50	5	3.5	10	21.71	21.66	21.64	21.66	21.67	20.13
194	190	260	40	3	1.5	10	32.33	32.42	32.36	32.38	32.37	18.51
195	139	230	50	3	2.5	10	27.28	27.44	27.42	27.26	27.35	19.15
196	225	260	50	3	3.5	25	25.41	24.56	25.48	25.44	25.22	35.12
197	74	200	50	5	1.5	17.5	28.40	28.60	28.54	28.56	28.53	25.63
198	161	230	50	5	3.5	17.5	23.29	23.50	23.55	23.17	23.38	27.61
199	216	260	40	5	3.5	25	24.47	24.59	24.60	24.52	24.55	35.48
200	142	230	50	3	3.5	10	24.79	24.91	24.89	24.89	24.87	20.15

Apendix Table B2 Data for test ANN model that residual stress and process cycle time of the rectangular lid were outputs

Run Order	Std. Order	Input train					Output train					
		Melt temperature (°C)	Injection speed (%)	Packing pressure (MPa)	Packing time (sec.)	Cooling time (sec.)	Point 1	Point 2	Point 3	Point 4	Residual stress	Cycle time
201	23	200	30	5	2.5	17.5	23.61	23.70	23.67	23.67	23.66	27.69
202	215	260	40	5	3.5	17.5	24.64	24.78	24.77	24.71	24.73	27.98
203	62	200	50	3	3.5	17.5	23.86	23.87	23.92	23.77	23.86	27.72
204	90	230	30	3	3.5	25	23.79	23.88	23.90	23.89	23.87	36.20
205	210	260	40	5	1.5	25	31.35	31.47	31.44	31.39	31.41	33.48
206	121	230	40	4	2.5	10	26.69	26.78	26.75	26.73	26.74	19.51
207	20	200	30	5	1.5	17.5	27.01	27.07	27.08	27.05	27.05	26.69
208	73	200	50	5	1.5	10	28.81	28.85	28.88	28.79	28.83	19.19
209	77	200	50	5	2.5	17.5	24.84	24.86	24.85	24.89	24.86	26.63
210	30	200	40	3	1.5	25	29.09	29.25	29.22	29.12	29.17	33.64
211	10	200	30	4	1.5	10	27.78	27.86	27.81	27.81	27.82	19.23
212	125	230	40	4	3.5	17.5	23.68	23.80	23.79	23.75	23.76	28.01
213	231	260	50	4	2.5	25	27.99	28.05	28.04	28.02	28.03	34.10
214	67	200	50	4	2.5	10	25.41	25.62	25.59	25.44	25.52	19.16
215	236	260	50	5	1.5	17.5	31.73	31.90	32.13	32.08	31.96	25.59
216	187	260	30	5	3.5	10	24.34	24.43	24.44	24.39	24.40	21.12
217	3	200	30	3	1.5	25	28.18	28.27	28.23	28.21	28.22	34.35
218	217	260	50	3	1.5	10	32.70	32.77	32.75	32.72	32.74	18.12
219	170	260	30	3	3.5	17.5	25.07	25.11	25.09	25.04	25.08	28.66
220	89	230	30	3	3.5	17.5	23.97	24.03	24.05	24.04	24.02	28.70

Apendix Table B2 (Continued)

Run Order	Std. Order	Input train					Output train					
		Melt temperature (°C)	Injection speed (%)	Packing pressure (MPa)	Packing time (sec.)	Cooling time (sec.)	Point 1	Point 2	Point 3	Point 4	Residual stress	Cycle time
221	120	230	40	4	1.5	25	29.99	23.10	23.05	23.02	24.79	33.51
222	44	200	40	4	3.5	17.5	22.05	21.72	21.80	22.05	21.91	28.06
223	171	260	30	3	3.5	25	24.83	24.99	24.92	24.86	24.90	36.16
224	72	200	50	4	3.5	25	22.02	21.64	21.62	22.02	21.83	35.16
225	4	200	30	3	2.5	10	25.63	25.67	25.53	25.59	25.61	20.35
226	242	260	50	5	3.5	17.5	25.04	25.12	25.11	25.07	25.09	27.59
227	103	230	30	5	2.5	10	25.47	25.54	25.50	25.54	25.51	20.14
228	160	230	50	5	3.5	10	23.92	23.97	23.97	23.96	23.96	20.11
229	1	200	30	3	1.5	10	28.64	28.74	28.68	28.69	28.69	19.35
230	25	200	30	5	3.5	10	21.59	21.59	21.61	21.58	21.59	21.19
231	175	260	30	4	2.5	10	27.49	27.59	27.60	27.58	27.57	20.14
232	137	230	50	3	1.5	17.5	30.96	31.07	31.04	31.08	31.04	25.65
233	154	230	50	5	1.5	10	30.82	30.89	30.85	30.82	30.85	18.11
234	130	230	40	5	2.5	10	26.43	26.56	26.52	26.49	26.50	19.50
235	208	260	40	5	1.5	10	31.78	31.84	31.81	31.81	31.81	18.48
236	29	200	40	3	1.5	17.5	29.25	29.43	29.47	29.31	29.37	26.14
237	57	200	50	3	1.5	25	29.45	29.46	29.44	29.45	29.45	33.64
238	233	260	50	4	3.5	17.5	25.16	25.23	25.21	25.22	25.21	27.60
239	162	230	50	5	3.5	25	22.74	23.03	22.24	22.66	22.67	35.11
240	243	260	50	5	3.5	25	24.86	24.92	24.90	24.90	24.90	35.09

Apendix Table B2 (Continued)

Run Order	Std. Order	Input train					Output train					
		Melt temperature (°C)	Injection speed (%)	Packing pressure (MPa)	Packing time (sec.)	Cooling time (sec.)	Point 1	Point 2	Point 3	Point 4	Residual stress	Cycle time
241	18	200	30	4	3.5	25	21.59	21.64	21.63	21.62	21.62	36.23
242	127	230	40	5	1.5	10	29.82	29.97	30.31	30.26	30.09	18.50
243	195	260	40	3	2.5	25	27.86	27.98	27.96	27.92	27.93	34.51

Apendix Table B3 Data for train ANN model that warpage and process cycle time of the roof tile were outputs

RunOrder	StdOrder	Input train				Output train			
		Injection speed (%)	Packing pressure (MPa)	Packing time (sec.)	Cooling time (sec.)	End point	Middle point	Warpage	Cycle time
1	149	70	5.33	1.33	40	1.61	2.67	4.27	48.30
2	236	90	6.67	1.67	60	1.18	0.83 (-)	2.11	68.20
3	46	30	6.67	2	46.67	8.75	3.92 (-)	12.67	58.02
4	210	90	5.33	1	46.67	2.39	2.92	5.31	54.23
5	207	90	4	2	53.33	3.04	1.44 (-)	4.48	61.94
6	53	30	8	1.33	40	2.10	1.02 (-)	3.12	50.65
7	215	90	5.33	1.33	53.33	1.40	2.37	3.77	61.22
8	2	30	4	1	46.67	1.00	2.41	3.42	57.13
9	120	50	8	1.33	60	1.16	2.55	3.71	68.97
10	153	70	5.33	1.67	40	1.72	1.11 (-)	2.85	48.64

Apendix Table B3 (Continued)

RunOrder	StdOrder	Input train				Output train			
		Injection speed (%)	Packing pressure (MPa)	Packing time (sec.)	Cooling time (sec.)	End point	Middle point	Warpage	Cycle time
11	162	70	6.67	1	46.67	2.10	2.78	4.88	54.61
12	88	50	5.33	1.33	60	1.16	2.67	3.83	69.03
13	237	90	6.67	2	40	2.99	1.57 (-)	4.57	48.53
14	80	50	4	2	60	5.13	2.35 (-)	7.48	69.76
15	1	30	4	1	40	0.92	2.22	3.13	50.46
16	245	90	8	1.33	40	1.41	2.31	3.72	47.84
17	110	50	6.67	2	46.67	4.33	2.01 (-)	6.35	56.33
18	42	30	6.67	1.67	46.67	5.93	2.47 (-)	8.40	57.69
19	251	90	8	1.67	53.33	1.49	0.83 (-)	2.31	61.51
20	195	90	4	1	53.33	2.28	2.95	5.22	60.94
21	230	90	6.67	1.33	46.67	1.54	2.36	3.90	54.53
22	133	70	4	1.33	40	1.41	2.58	3.99	48.35
23	28	30	5.33	1.67	60	6.93	2.95 (-)	9.87	71.05
24	92	50	5.33	1.67	60	2.83	1.28 (-)	4.11	69.37
25	228	90	6.67	1	60	2.86	3.17	6.03	67.53
26	147	70	5.33	1	53.33	2.05	2.76	4.82	61.30
27	145	70	5.33	1	40	2.31	3.06	5.37	47.97
28	146	70	5.33	1	46.67	2.04	2.67	4.71	54.64
29	52	30	8	1	60	1.02	2.18	3.20	70.32
30	169	70	6.67	1.67	40	1.60	1.09 (-)	2.69	48.61

Apendix Table B3 (Continued)

RunOrder	StdOrder	Input train				Output train			
		Injection speed (%)	Packing pressure (MPa)	Packing time (sec.)	Cooling time (sec.)	End point	Middle point	Warpage	Cycle time
31	226	90	6.67	1	46.67	2.63	2.92	5.55	54.20
32	57	30	8	1.67	40	5.49	2.31 (-)	7.79	50.99
33	108	50	6.67	1.67	60	2.76	1.22 (-)	3.97	69.33
34	254	90	8	2	46.67	3.63	1.80 (-)	5.43	55.18
35	183	70	8	1.33	53.33	1.22	2.26	3.47	61.58
36	55	30	8	1.33	53.33	2.48	1.17 (-)	3.65	63.98
37	223	90	5.33	2	53.33	3.29	1.60 (-)	4.89	61.89
38	229	90	6.67	1.33	40	1.61	2.39	4.00	47.86
39	148	70	5.33	1	60	2.04	2.85	4.89	67.97
40	74	50	4	1.67	46.67	2.62	1.29 (-)	3.91	56.10
41	89	50	5.33	1.67	40	1.80	1.07 (-)	2.88	49.37
42	129	70	4	1	40	2.16	2.94	5.10	48.02
43	130	70	4	1	46.67	2.14	2.76	4.90	54.69
44	35	30	6.67	1	53.33	1.09	2.21	3.30	63.68
45	184	70	8	1.33	60	1.34	2.31	3.65	68.25
46	4	30	4	1	60	1.90	2.24 (-)	4.14	70.46
47	29	30	5.33	2	40	8.41	3.66 (-)	12.07	51.38
48	9	30	4	1.67	40	5.92	2.37 (-)	8.29	51.13
49	200	90	4	1.33	60	1.48	2.44	3.92	67.94
50	70	50	4	1.33	46.67	1.13	2.59	3.72	55.76

Apendix Table B3 (Continued)

RunOrder	StdOrder	Input train				Output train			
		Injection speed (%)	Packing pressure (MPa)	Packing time (sec.)	Cooling time (sec.)	End point	Middle point	Warpage	Cycle time
51	97	50	6.67	1	40	2.31	3.29	5.60	48.66
52	231	90	6.67	1.33	53.33	1.40	2.24	3.64	61.19
53	249	90	8	1.67	40	1.33	0.98 (-)	2.31	48.18
54	170	70	6.67	1.67	46.67	1.39	0.81 (-)	2.20	55.28
55	116	50	8	1	60	1.90	2.93	4.83	68.64
56	72	50	4	1.33	60	1.31	2.69	4.00	69.09
57	182	70	8	1.33	46.67	1.19	2.11	3.30	54.92
58	255	90	8	2	53.33	3.95	1.92 (-)	5.87	61.84
59	59	30	8	1.67	53.33	6.29	2.67 (-)	8.96	64.32
60	211	90	5.33	1	53.33	2.54	3.07	5.61	60.89
61	150	70	5.33	1.33	46.67	1.44	2.43	3.87	54.97
62	201	90	4	1.67	40	1.59	1.30 (-)	2.89	48.28
63	102	50	6.67	1.33	46.67	1.24	2.60	3.83	55.66
64	15	30	4	2	53.33	9.00	4.03 (-)	13.03	64.79
65	122	50	8	1.67	46.67	1.82	0.95 (-)	2.77	55.98
66	47	30	6.67	2	53.33	8.97	4.05 (-)	13.01	64.68
67	20	30	5.33	1	60	0.95	2.27	3.22	70.38
68	37	30	6.67	1.33	40	1.98	1.04 (-)	3.02	50.68
69	137	70	4	1.67	40	1.87	1.58 (-)	3.45	48.69
70	30	30	5.33	2	46.67	8.55	3.79 (-)	12.34	58.05

Apendix Table B3 (Continued)

RunOrder	StdOrder	Input train				Output train			
		Injection speed (%)	Packing pressure (MPa)	Packing time (sec.)	Cooling time (sec.)	End point	Middle point	Warpage	Cycle time
71	10	30	4	1.67	46.67	6.45	2.63 (-)	9.08	57.80
72	243	90	8	1	53.33	3.09	3.26	6.35	60.84
73	192	70	8	2	60	4.13	1.95 (-)	6.08	68.92
74	73	50	4	1.67	40	1.82	1.15 (-)	2.96	49.43
75	141	70	4	2	40	2.65	1.19 (-)	3.84	49.02
76	121	50	8	1.67	40	1.80	0.96 (-)	2.75	48.69
77	65	50	4	1	40	1.97	3.17	5.13	48.76
78	27	30	5.33	1.67	53.33	6.47	2.75 (-)	9.22	64.38
79	142	70	4	2	46.67	3.39	1.54 (-)	4.93	55.69
80	41	30	6.67	1.67	40	5.56	2.27 (-)	7.83	51.02
81	14	30	4	2	46.67	8.53	3.73 (-)	12.26	58.13
82	158	70	5.33	2	46.67	3.59	1.69 (-)	5.29	55.64
83	98	50	6.67	1	46.67	2.19	3.19	5.38	55.33
84	113	50	8	1	40	2.08	3.12	5.21	48.64
85	190	70	8	2	46.67	4.01	1.89 (-)	5.90	55.59
86	11	30	4	1.67	53.33	6.74	2.75 (-)	9.48	64.46
87	209	90	5.33	1	40	2.28	2.79	5.07	47.56
88	163	70	6.67	1	53.33	2.00	2.65	4.64	61.27
89	90	50	5.33	1.67	46.67	2.59	1.20 (-)	3.79	56.04
90	242	90	8	1	46.67	3.14	3.41	6.55	54.18

Apendix Table B3 (Continued)

RunOrder	StdOrder	Input train				Output train			
		Injection speed (%)	Packing pressure (MPa)	Packing time (sec.)	Cooling time (sec.)	End point	Middle point	Warpage	Cycle time
91	240	90	6.67	2	60	3.81	1.84 (-)	5.66	68.53
92	25	30	5.33	1.67	40	5.58	2.25 (-)	7.84	51.05
93	103	50	6.67	1.33	53.33	1.06	2.39	3.45	62.32
94	79	50	4	2	53.33	4.81	2.23 (-)	7.04	63.09
95	123	50	8	1.67	53.33	2.46	1.11 (-)	3.57	62.64
96	217	90	5.33	1.67	40	1.52	1.33 (-)	2.85	48.23
97	104	50	6.67	1.33	60	1.01	2.48	3.49	68.99
98	152	70	5.33	1.33	60	1.16	2.23	3.39	68.30
99	67	50	4	1	53.33	2.00	3.16	5.16	62.09
100	16	30	4	2	60	9.10	4.09 (-)	13.19	71.46
101	225	90	6.67	1	40	2.91	3.10	6.01	47.53
102	206	90	4	2	46.67	3.12	1.47 (-)	4.60	55.28
103	135	70	4	1.33	53.33	1.24	2.45	3.68	61.68
104	64	30	8	2	60	8.82	4.06 (-)	12.87	71.32
105	138	70	4	1.67	46.67	1.60	0.95 (-)	2.55	55.36
106	33	30	6.67	1	40	1.37	2.55	3.92	50.35
107	180	70	8	1	60	2.35	3.10	5.45	67.92
108	100	50	6.67	1	60	2.14	3.12	5.26	68.66
109	45	30	6.67	2	40	8.36	3.73 (-)	12.09	51.35
110	112	50	6.67	2	60	4.91	2.28 (-)	7.19	69.66

Apendix Table B3 (Continued)

RunOrder	StdOrder	Input train				Output train			
		Injection speed (%)	Packing pressure (MPa)	Packing time (sec.)	Cooling time (sec.)	End point	Middle point	Warpage	Cycle time
111	178	70	8	1	46.67	2.38	3.11	5.49	54.59
112	114	50	8	1	46.67	2.12	3.10	5.22	55.31
113	48	30	6.67	2	60	8.86	4.07 (-)	12.93	71.35
114	7	30	4	1.33	53.33	2.81	1.31 (-)	4.12	64.12
115	81	50	5.33	1	40	2.17	3.17	5.33	48.70
116	93	50	5.33	2	40	4.02	1.83 (-)	5.85	49.70
117	164	70	6.67	1	60	2.01	2.79	4.80	67.94
118	126	50	8	2	46.67	4.20	1.92 (-)	6.12	56.31
119	17	30	5.33	1	40	1.18	2.37	3.55	50.38
120	199	90	4	1.33	53.33	1.56	2.51	4.06	61.27
121	205	90	4	2	40	2.88	1.32 (-)	4.20	48.61
122	69	50	4	1.33	40	1.12	2.62	3.74	49.09
123	212	90	5.33	1	60	2.37	2.97	5.34	67.56
124	105	50	6.67	1.67	40	1.53	0.93 (-)	2.47	49.33
125	34	30	6.67	1	46.67	1.31	2.54	3.85	57.02
126	219	90	5.33	1.67	53.33	1.19	0.88 (-)	2.07	61.56
127	177	70	8	1	40	2.55	3.36	5.90	47.92
128	26	30	5.33	1.67	46.67	6.02	2.49 (-)	8.51	57.72
129	101	50	6.67	1.33	40	1.50	2.80	4.30	48.99
130	124	50	8	1.67	60	2.70	1.21 (-)	3.91	69.31

Apendix Table B3 (Continued)

RunOrder	StdOrder	Input train				Output train			
		Injection speed (%)	Packing pressure (MPa)	Packing time (sec.)	Cooling time (sec.)	End point	Middle point	Warpage	Cycle time
131	50	30	8	1	46.67	1.28	2.52	3.80	56.99
132	139	70	4	1.67	53.33	2.02	1.02 (-)	3.04	62.02
133	51	30	8	1	53.33	1.13	2.23	3.36	63.65
134	221	90	5.33	2	40	2.70	1.35 (-)	4.05	48.56
135	176	70	6.67	2	60	4.44	2.10 (-)	6.54	68.94
136	220	90	5.33	1.67	60	1.34	0.80 (-)	2.14	68.23
137	75	50	4	1.67	53.33	3.25	1.39 (-)	4.64	62.76
138	77	50	4	2	40	4.03	1.81 (-)	5.84	49.76
139	128	50	8	2	60	4.76	2.17 (-)	6.93	69.64
140	194	90	4	1	46.67	2.51	3.01	5.52	54.28
141	22	30	5.33	1.33	46.67	2.08	1.10 (-)	3.17	57.38
142	244	90	8	1	60	3.07	3.21	6.28	67.51
143	155	70	5.33	1.67	53.33	1.55	0.93 (-)	2.47	61.97
144	84	50	5.33	1	60	2.10	3.20	5.30	68.70
145	144	70	4	2	60	3.67	1.70 (-)	5.37	69.02
146	32	30	5.33	2	60	8.87	4.02 (-)	12.90	71.38
147	49	30	8	1	40	1.38	2.46	3.84	50.32
148	106	50	6.67	1.67	46.67	2.16	1.09 (-)	3.25	56.00
149	256	90	8	2	60	3.67	1.81 (-)	5.48	68.51
150	86	50	5.33	1.33	46.67	1.23	2.62	3.85	55.70

Apendix Table B3 (Continued)

RunOrder	StdOrder	Input train				Output train			
		Injection speed (%)	Packing pressure (MPa)	Packing time (sec.)	Cooling time (sec.)	End point	Middle point	Warpage	Cycle time
151	117	50	8	1.33	40	1.22	2.61	3.83	48.97
152	66	50	4	1	46.67	1.94	3.08	5.03	55.43
153	3	30	4	1	53.33	0.96	2.29	3.25	63.79
154	232	90	6.67	1.33	60	1.40	2.34	3.74	67.86
155	186	70	8	1.67	46.67	1.45	0.81 (-)	2.26	55.26
156	202	90	4	1.67	46.67	1.22	0.86 (-)	2.08	54.95
157	159	70	5.33	2	53.33	3.44	1.62 (-)	5.06	62.30
158	87	50	5.33	1.33	53.33	1.37	2.79	4.16	62.36
159	208	90	4	2	60	3.22	1.54 (-)	4.76	68.61
160	54	30	8	1.33	46.67	2.46	1.16 (-)	3.62	57.32
161	247	90	8	1.33	53.33	1.49	2.38	3.87	61.17
162	241	90	8	1	40	3.71	3.69	7.39	47.51
163	76	50	4	1.67	60	2.89	1.30 (-)	4.19	69.43
164	143	70	4	2	53.33	3.57	1.64 (-)	5.21	62.35
165	216	90	5.33	1.33	60	1.43	2.40	3.83	67.89
166	167	70	6.67	1.33	53.33	1.23	2.27	3.50	61.60
167	56	30	8	1.33	60	2.77	1.21 (-)	3.98	70.65
168	71	50	4	1.33	53.33	2.24	2.36	4.60	62.42
169	31	30	5.33	2	53.33	8.53	3.89 (-)	12.42	64.71
170	125	50	8	2	40	4.12	1.87 (-)	5.98	49.64

Apendix Table B3 (Continued)

RunOrder	StdOrder	Input train				Output train			
		Injection speed (%)	Packing pressure (MPa)	Packing time (sec.)	Cooling time (sec.)	End point	Middle point	Warpage	Cycle time
171	132	70	4	1	60	1.93	2.67	4.60	68.02
172	239	90	6.67	2	53.33	3.57	1.79 (-)	5.36	61.86
173	224	90	5.33	2	60	3.42	1.67 (-)	5.09	68.56
174	91	50	5.33	1.67	53.33	2.88	1.30 (-)	4.18	62.70
175	227	90	6.67	1	53.33	2.68	2.99	5.66	60.86
176	134	70	4	1.33	46.67	1.29	2.38	3.67	55.02
177	196	90	4	1	60	2.09	2.77	4.87	67.61
178	131	70	4	1	53.33	2.04	2.81	4.85	61.35
179	18	30	5.33	1	46.67	1.16	2.43	3.59	57.05
180	107	50	6.67	1.67	53.33	2.69	1.20 (-)	3.88	62.66
181	39	30	6.67	1.33	53.33	2.69	1.19 (-)	3.87	64.01
182	5	30	4	1.33	40	2.37	1.20 (-)	3.58	50.79
183	78	50	4	2	46.67	4.13	1.86 (-)	6.00	56.43
184	175	70	6.67	2	53.33	4.22	1.97 (-)	6.19	62.27
185	140	70	4	1.67	60	2.58	1.11 (-)	3.69	68.69
186	173	70	6.67	2	40	3.46	1.68 (-)	5.13	48.94
187	252	90	8	1.67	60	1.45	0.84 (-)	2.29	68.18
188	96	50	5.33	2	60	4.60	2.14 (-)	6.74	69.70
189	174	70	6.67	2	46.67	4.30	2.08 (-)	6.37	55.61
190	58	30	8	1.67	46.67	5.75	2.44 (-)	8.19	57.66

Apendix Table B3 (Continued)

RunOrder	StdOrder	Input train				Output train			
		Injection speed (%)	Packing pressure (MPa)	Packing time (sec.)	Cooling time (sec.)	End point	Middle point	Warpage	Cycle time
191	250	90	8	1.67	46.67	1.32	0.81 (-)	2.12	54.85
192	118	50	8	1.33	46.67	1.09	2.45	3.54	55.64
193	43	30	6.67	1.67	53.33	6.25	2.67 (-)	8.91	64.35
194	193	90	4	1	40	2.46	3.00	5.46	47.61
195	151	70	5.33	1.33	53.33	1.31	2.43	3.75	61.63
196	156	70	5.33	1.67	60	2.21	1.00 (-)	3.20	68.64
197	218	90	5.33	1.67	46.67	1.23	0.84 (-)	2.07	54.90
198	203	90	4	1.67	53.33	1.27	0.87 (-)	2.15	61.61
199	99	50	6.67	1	53.33	2.10	3.14	5.24	61.99
200	166	70	6.67	1.33	46.67	1.23	2.14	3.37	54.94

Apendix Table B4 Data for test ANN model that warpage and process cycle time of the roof tile were outputs

RunOrder	StdOrder	Input train				Output train			
		Injection speed (%)	Packing pressure (MPa)	Packing time (sec.)	Cooling time (sec.)	End point	Middle point	Warpage	Cycle time
201	253	90	8	2	40	3.08	1.64 (-)	4.72	48.51
202	94	50	5.33	2	46.67	4.39	2.00 (-)	6.39	56.37
203	82	50	5.33	1	46.67	2.16	3.22	5.38	55.37

Apendix Table B4 (Continued)

RunOrder	StdOrder	Input train				Output train			
		Injection speed (%)	Packing pressure (MPa)	Packing time (sec.)	Cooling time (sec.)	End point	Middle point	Warpage	Cycle time
204	19	30	5.33	1	53.33	1.06	2.27	3.34	63.71
205	161	70	6.67	1	40	2.43	3.09	5.51	47.94
206	233	90	6.67	1.67	40	1.29	1.02 (-)	2.31	48.20
207	85	50	5.33	1.33	40	1.50	2.83	4.32	49.03
208	127	50	8	2	53.33	4.61	2.10 (-)	6.72	62.97
209	119	50	8	1.33	53.33	1.17	2.53	3.71	62.30
210	248	90	8	1.33	60	1.43	2.34	3.77	67.84
211	172	70	6.67	1.67	60	2.18	0.99 (-)	3.17	68.61
212	160	70	5.33	2	60	3.79	1.79 (-)	5.58	68.97
213	62	30	8	2	46.67	8.32	3.73 (-)	12.06	57.99
214	136	70	4	1.33	60	1.17	2.32	3.49	68.35
215	154	70	5.33	1.67	46.67	1.51	0.90 (-)	2.41	55.31
216	157	70	5.33	2	40	2.98	1.41 (-)	4.39	48.97
217	24	30	5.33	1.33	60	2.99	1.33 (-)	4.32	70.71
218	36	30	6.67	1	60	0.99	2.19	3.18	70.35
219	60	30	8	1.67	60	6.56	2.84 (-)	9.40	70.99
220	68	50	4	1	60	2.00	3.17	5.17	68.76
221	21	30	5.33	1.33	40	1.79	1.14 (-)	2.93	50.71
222	6	30	4	1.33	46.67	2.49	1.23 (-)	3.72	57.46
223	181	70	8	1.33	40	1.47	2.67	4.13	48.25

Apendix Table B4 (Continued)

RunOrder	StdOrder	Input train				Output train			
		Injection speed (%)	Packing pressure (MPa)	Packing time (sec.)	Cooling time (sec.)	End point	Middle point	Warpage	Cycle time
224	179	70	8	1	53.33	2.49	3.12	5.60	61.25
225	188	70	8	1.67	60	2.06	1.02 (-)	3.07	68.59
226	198	90	4	1.33	46.67	1.57	2.51	4.08	54.61
227	171	70	6.67	1.67	53.33	1.44	0.86 (-)	2.30	61.94
228	83	50	5.33	1	53.33	2.20	3.18	5.38	62.03
229	111	50	6.67	2	53.33	4.90	2.22 (-)	7.12	62.99
230	189	70	8	2	40	3.23	1.58 (-)	4.81	48.92
231	109	50	6.67	2	40	4.03	1.88 (-)	5.91	49.66
232	187	70	8	1.67	53.33	1.67	0.86 (-)	2.53	61.92
233	238	90	6.67	2	46.67	3.58	1.76 (-)	5.34	55.20
234	214	90	5.33	1.33	46.67	1.53	2.45	3.98	54.56
235	12	30	4	1.67	60	6.99	2.94 (-)	9.93	71.13
236	197	90	4	1.33	40	1.57	2.46	4.04	47.94
237	61	30	8	2	40	7.91	3.56 (-)	11.47	51.32
238	44	30	6.67	1.67	60	6.21	2.70 (-)	8.90	71.02
239	246	90	8	1.33	46.67	1.47	2.36	3.83	54.51
240	115	50	8	1	53.33	2.03	3.03	5.06	61.97
241	8	30	4	1.33	60	3.41	1.47 (-)	4.88	70.79
242	222	90	5.33	2	46.67	3.20	1.59 (-)	4.79	55.23
243	13	30	4	2	40	8.28	3.57 (-)	11.84	51.46

Apendix Table B4 (Continued)

RunOrder	StdOrder	Input train				Output train			
		Injection speed (%)	Packing pressure (MPa)	Packing time (sec.)	Cooling time (sec.)	End point	Middle point	Warpage	Cycle time
244	40	30	6.67	1.33	60	2.79	1.24 (-)	4.03	70.68
245	168	70	6.67	1.33	60	1.18	2.31	3.49	68.27
246	23	30	5.33	1.33	53.33	2.51	1.16 (-)	3.68	64.04
247	234	90	6.67	1.67	46.67	1.16	0.96 (-)	2.12	54.87
248	235	90	6.67	1.67	53.33	1.22	0.91 (-)	2.13	61.53
249	191	70	8	2	53.33	3.94	1.88 (-)	5.82	62.25
250	213	90	5.33	1.33	40	1.78	2.57	4.35	47.89
251	204	90	4	1.67	60	1.56	0.85	2.41	68.28
252	38	30	6.67	1.33	46.67	2.50	1.16	3.66	57.35
253	63	30	8	2	53.33	8.65	3.92	12.57	64.65
254	165	70	6.67	1.33	40	1.42	2.40	3.82	47.89
255	95	50	5.33	2	53.33	4.49	2.07	6.55	63.03
256	185	70	8	1.67	40	1.66	1.49	3.15	48.59

Appendix C

The ANN command line

Apendix Table C1 The ANN command line that residual stress and process cycle time of the rectangular lid were outputs

```
load traindata.txt;
load testdata.txt;
trd = traindata;
ted =testdata;
%training data arrangement
MeT = trd(:,1)/(2*max(trd(:,1)));
IS = trd(:,2)/(2*max(trd(:,2)));
PP = trd(:,3)/(2*max(trd(:,3)));
PT = trd(:,4)/(2*max(trd(:,4)));
CT = trd(:,5)/(2*max(trd(:,5)));
RS = trd(:,6);
CyT = trd(:,7);
%testing data arrangement
MeT2 = ted(:,1)/(2*max(ted(:,1)));
IS2 = ted(:,2)/(2*max(ted(:,2)));
PP2 = ted(:,3)/(2*max(ted(:,3)));
PT2 = ted(:,4)/(2*max(ted(:,4)));
CT2 = ted(:,5)/(2*max(ted(:,5)));
RS2 = ted(:,6);
CyT2 = ted(:,7);
%design input data and target data
%inp = input data & tst = test data &
  tar = target data
inp = [MT IS PP PT CT];
tst = [MT2 IS2 PP2 PT2 CT2];
tar = [RS CyT];
%input train data & test data into network
input = inp';
test = tst';
target = tar';
%network structure
%h1 is number of neuron in 1st hidden layer
h1 = 7;
%op is number of neuron in output layer
op = 2;
% network configuration
net = newff(minmax(input),[h1 op],
{'logsig' 'purelin'},'trainlm');
%training parameters setup
w = initial_weight(h1,minmax(input));
net.iw{1,1} = w;
w2 = layer_weight7(op,h1);
net.lw{2,1} = w2;
b1 = ones(h1,1);
net.b{1} = b1;
b2 = ones(op,1);
net.b{2} = b2;
net.trainParam.epochs =1000;
net.trainParam.show =1000;
net.trainParam.goal =1e-5;
net.trainParam.lr =.01;
%train network
net=train(net,input,target);
%test network
a=sim(net,test);
%final weight&bias
w; w_out = net.iw{1,1};
w2; w2_out = net.lw{2,1};
b1;b1_out=net.b{1};
b2;b2_out=net.b{2};
%performance network
error1=[RS2]-[a(1,:)'];
error2=[CyT2]-[a(2,:)'];
u1=abs(error1)./RS2*100;
u2=abs(error2)./CyT2*100;
v1=sum(u1);
v2=sum(u2);
err1=v1/43;
err2=v2/43;
accuracy1=100-err1;
accuracy2=100-err2;
%display
accuracy1
accuracy2
```

Apendix Table C2 The ANN command line that warpage and process cycle time of the roof tile were outputs

```
load traindata.txt;
load testdata.txt;
trd = traindata;
ted =testdata;
%training data arrangement
IS = trd(:,1)/(2*max(trd(:,1)));
PP = trd(:,2)/(2*max(trd(:,2)));
PT = trd(:,3)/(2*max(trd(:,3)));
CT = trd(:,4)/(2*max(trd(:,4)));
WP = trd(:,5);
CyT = trd(:,6);
%testing data arrangement
IS2 = ted(:,1)/(2*max(ted(:,1)));
PP2 = ted(:,2)/(2*max(ted(:,2)));
PT2 = ted(:,3)/(2*max(ted(:,3)));
CT2 = ted(:,4)/(2*max(ted(:,4)));
WP2 = ted(:,5);
CyT2 = ted(:,6);
%design input data and target data
%inp = input data & tst = test data &
  tar = target data
inp = [IS PP PT CT];
tst = [IS2 PP2 PT2 CT2];
tar = [WP CyT];
%input train data & test data into network
input = inp';
test = tst';
target = tar';
%network structure
%h1 is number of neuron in 1st hidden layer
h1 = 9;
%h2 is number of neuron in 2nd hidden layer
h2 = 16;
%op is number of neuron in output layer
op = 2;
% network configuration
net = newff(minmax(input),[h1 h2 op],
{'logsig' 'logsig' 'purelin'},'trainlm');
%training parameters setup
w = initial_weight(h1,minmax(input));
net.iw{1,1} = w;
w2 = layer_weight9_16(h2,h1);
net.lw{2,1} = w2;
w3 = layer_weight16_2(op,h2);
net.lw{3,2} = w3;
b1 = ones(h1,1);
net.b{1} = b1;
b2 = ones(h2,1);
net.b{2} = b2;
B3 = ones(op,1);
net.b{3} = b3;
net.trainParam.epochs =3000;
net.trainParam.show =1000;
net.trainParam.goal =1e-5;
net.trainParam.lr =.09;
%train network
net=train(net,input,target);
%test network
a=sim(net,test);
%final weight&bias
w; w_out = net.iw{1,1};
w2; w2_out = net.lw{2,1};
w3; w3_out = net.lw{3,2};
b1;b1_out=net.b{1};
b2;b2_out=net.b{2};
b3;b3_out=net.b{3};
%performance network
error1=[WP2]-[a(1,:)'];
error2=[CyT2]-[a(2,:)'];
u1=abs(error1)./WP2*100;
u2=abs(error2)./CyT2*100;
v1=sum(u1);
v2=sum(u2);
err1=v1/56;
err2=v2/56;
accuracy1=100-err1;
accuracy2=100-err2;
%display
accuracy1
accuracy2
```

Appendix D

The results of Experiment 3-12

Apendix Table D1 Results of Experiment 3

RunOrder	StdOrder	Characteristic of input	Transfer function	Accuracy (%) Residual Stress	Accuracy (%) Cycle Time	Average Accuracy (%)
1	16	Normalization	tansig	99.1842	99.7208	99.4525
2	4	Normalization	tansig	99.0907	99.75	99.42035
3	10	Normalization	logsig	99.163	99.7412	99.4521
4	17	Unnormalization	logsig	95.0028	98.4066	96.7047
5	13	Unnormalization	logsig	98.6443	99.5579	99.1011
6	7	Unnormalization	tansig	93.4836	97.7016	95.5926
7	15	Unnormalization	tansig	98.1942	99.5988	98.8965
8	2	Normalization	logsig	99.2945	99.7442	99.51935
9	12	Normalization	tansig	98.7015	99.1864	98.94395
10	11	Unnormalization	tansig	93.7817	99.2325	96.5071
11	8	Normalization	tansig	99.0592	99.7308	99.395
12	5	Unnormalization	logsig	95.1412	99.5682	97.3547
13	9	Unnormalization	logsig	96.5237	98.9529	97.7383
14	19	Unnormalization	tansig	98.4168	99.5615	98.98915
15	3	Unnormalization	tansig	98.1239	99.576	98.84995
16	14	Normalization	logsig	99.2526	99.7402	99.4964
17	1	Unnormalization	logsig	98.4754	98.7439	98.60965
18	20	Normalization	tansig	99.2642	99.6216	99.4429
19	6	Normalization	logsig	98.9684	99.6996	99.334
20	18	Normalization	logsig	99.119	99.5878	99.3534

Apendix Table D2 Results of Experiment 4

RunOrder	StdOrder	Learning Rate	Epoch	Accuracy (%) Residual Stress	Accuracy (%) Cycle Time	Average Accuracy (%)
1	32	0.05	3000	98.9799	99.5896	99.2848
2	26	0.09	3000	99.2302	99.7285	99.4794
3	10	0.01	1000	99.2909	99.5909	99.4409
4	18	0.09	5000	98.935	99.5477	99.2414
5	34	0.09	1000	99.3149	99.5939	99.4544
6	20	0.01	3000	98.9801	99.5858	99.2830
7	8	0.09	3000	99.0597	99.7362	99.3980
8	17	0.09	3000	99.1812	99.735	99.4581
9	14	0.05	3000	99.0363	97.1182	98.0773
10	29	0.01	3000	99.315	99.5932	99.4541
11	33	0.05	5000	99.1902	99.5983	99.3943
12	2	0.01	3000	99.2548	99.66	99.4574
13	1	0.01	1000	99.2231	99.7364	99.4798
14	5	0.05	3000	99.3365	99.6003	99.4684
15	22	0.05	1000	98.535	99.6473	99.0912
16	36	0.09	5000	98.937	99.5916	99.2643
17	15	0.05	5000	99.0737	99.3407	99.2072
18	31	0.05	1000	99.38	99.7503	99.5652
19	23	0.05	3000	99.1457	99.7231	99.4344
20	25	0.09	1000	99.0216	99.5866	99.3041
21	44	0.09	3000	98.6505	99.5954	99.1230
22	45	0.09	5000	99.3774	99.7353	99.5564
23	41	0.05	3000	99.1436	99.6044	99.3740

Apendix Table D2 (Continued)

RunOrder	StdOrder	Learning Rate	Epoch	Accuracy (%) Residual Stress	Accuracy (%) Cycle Time	Average Accuracy (%)
24	21	0.01	5000	99.1859	99.7281	99.4570
25	4	0.05	1000	99.0536	99.5222	99.2879
26	7	0.09	1000	98.9799	99.4908	99.2354
27	6	0.05	5000	99.134	99.7108	99.4224
28	39	0.01	5000	99.1092	99.7431	99.4262
29	43	0.09	1000	98.8915	99.589	99.2403
30	3	0.01	5000	99.2273	99.5977	99.4125
31	24	0.05	5000	99.3477	99.6419	99.4948
32	42	0.05	5000	98.9918	99.5964	99.2941
33	35	0.09	3000	99.1588	99.7201	99.4395
34	16	0.09	1000	98.8806	98.778	98.8293
35	12	0.01	5000	99.1783	99.6051	99.3917
36	9	0.09	5000	99.1515	99.735	99.4433
37	19	0.01	1000	98.9893	99.7416	99.3655
38	11	0.01	3000	98.5801	99.588	99.0841
39	27	0.09	5000	98.9531	99.5928	99.2730
40	28	0.01	1000	99.0658	99.6984	99.3821
41	40	0.05	1000	99.364	99.591	99.4775
42	13	0.05	1000	99.0858	99.6284	99.3571
43	30	0.01	5000	99.2071	99.5973	99.4022
44	37	0.01	1000	99.0854	99.6653	99.3754
45	38	0.01	3000	99.2831	99.7051	99.4941

Apendix Table D3 Results of Experiment 5

RunOrder	StdOrder	Bias	Accuracy (%) Residual Stress	Accuracy (%) Cycle Time	Average Accuracy (%)
1	13	bias = 1	99.119	99.6676	99.3933
2	10	bias = 0.5	99.119	99.5878	99.3534
3	14	bias = 1	99.1856	99.5951	99.3904
4	5	without bias	99.2668	99.628	99.4474
5	6	bias = 0.5	98.9728	98.5357	98.7543
6	8	bias = 0.5	99.1093	99.7047	99.4070
7	1	without bias	99.0261	99.7323	99.3792
8	7	bias = 0.5	99.2132	99.5702	99.3917
9	9	bias = 0.5	99.2909	99.5909	99.4409
10	12	bias = 1	99.2338	99.7132	99.4735
11	3	without bias	99.132	99.5844	99.3582
12	2	without bias	98.9667	99.5908	99.2788
13	15	bias = 1	99.0696	99.4961	99.2829
14	4	without bias	99.1695	99.5948	99.3822
15	11	bias = 1	99.0738	99.7574	99.4156

Apendix Table D4 Results of Experiment 6

RunOrder	StdOrder	Number of neuron in 1st hidden layer	Accuracy (%) Residual Stress	Accuracy (%) Cycle Time	Average Accuracy (%)
1	20	6	99.2443	99.7278	99.4861
2	35	9	99.2770	99.7030	99.4900

Apendix Table D4 (Continued)

RunOrder	StdOrder	Number of neuron in 1st hidden layer	Accuracy (%) Residual Stress	Accuracy (%) Cycle Time	Average Accuracy (%)
3	6	4	98.9530	99.5929	99.2730
4	16	6	99.2516	99.6015	99.4266
5	31	9	99.3346	99.7426	99.5386
6	24	7	99.4669	99.7360	99.6015
7	27	8	99.3365	99.7206	99.5286
8	28	8	99.3723	99.7690	99.5707
9	15	5	99.1387	99.5812	99.3600
10	38	10	99.0576	99.7635	99.4106
11	12	5	98.5944	99.0568	98.8256
12	17	6	98.9331	99.5877	99.2604
13	10	4	98.7979	99.5985	99.1982
14	13	5	99.0647	99.5957	99.3302
15	29	8	99.4360	99.7131	99.5746
16	30	8	99.4098	99.6653	99.5376
17	34	9	99.2669	99.5978	99.4324
18	23	7	99.3688	99.7363	99.5526
19	40	10	99.1130	99.7555	99.4343
20	36	10	99.2021	99.6980	99.4501
21	4	3	98.9586	99.5876	99.2731
22	11	5	98.8482	99.5835	99.2159
23	21	7	99.3901	99.7511	99.5706
24	45	11	99.2748	99.7147	99.4948
25	7	4	98.9375	99.5955	99.2665

Apendix Table D4 (Continued)

RunOrder	StdOrder	Number of neuron In 1st hidden layer	Accuracy (%) Residual Stress	Accuracy (%) Cycle Time	Average Accuracy (%)
26	5	3	98.0355	97.0020	97.5188
27	8	4	98.6430	99.5883	99.1157
28	41	11	99.2625	99.7375	99.5000
29	42	11	99.0658	99.6984	99.3821
30	9	4	99.0416	99.6932	99.3674
31	44	11	99.0854	99.6653	99.3754
32	19	6	99.0466	99.5905	99.3186
33	33	9	99.2095	99.5954	99.4025
34	43	11	99.2190	99.7042	99.4616
35	25	7	99.3221	99.7382	99.5302
36	32	9	99.0320	99.7151	99.3736
37	1	3	98.6430	99.5883	99.1157
38	26	8	99.2800	99.7335	99.5068
39	2	3	98.9531	99.5930	99.2731
40	22	7	99.4283	99.7306	99.5795
41	39	10	99.1572	99.6840	99.4206
42	14	5	98.8399	99.5686	99.2043
43	37	10	99.2544	99.7403	99.4974
44	18	6	99.2529	99.7050	99.4790
45	3	3	98.9620	99.5918	99.2769

Apendix Table D5 Results of Experiment 7

RunOrder	StdOrder	Number of neuron in 2nd hidden layer	Accuracy (%) Residual Stress	Accuracy (%) Cycle Time	Average Accuracy (%)
1	45	13	98.5211	99.6456	99.08335
2	26	10	99.3002	99.5852	99.4427
3	36	12	98.6275	99.6643	99.1459
4	21	9	99.2462	99.7073	99.47675
5	53	15	98.3969	99.7219	99.0594
6	10	6	99.4678	99.7247	99.59625
7	55	15	98.4672	98.8132	98.6402
8	33	11	99.0691	99.6038	99.33645
9	32	11	99.1848	99.6195	99.40215
10	37	12	99.0184	99.605	99.3117
11	46	14	99.0645	99.5229	99.2937
12	50	14	99.1589	99.6728	99.41585
13	1	5	99.1483	99.7131	99.4307
14	8	6	99.3447	99.7291	99.5369
15	23	9	98.9643	99.5553	99.2598
16	14	7	98.9235	99.6415	99.2825
17	11	7	98.5471	99.4417	98.9944
18	7	6	99.3128	99.7243	99.51855
19	40	12	98.3254	99.5638	98.9446
20	35	11	99.099	99.5468	99.3229
21	24	9	99.0915	99.7256	99.40855
22	6	6	99.3126	99.724	99.5183
23	44	13	98.0875	99.716	98.90175

Apendix Table D5 (Continued)

RunOrder	StdOrder	Number of neuron in 2nd hidden layer	Accuracy (%) Residual Stress	Accuracy (%) Cycle Time	Average Accuracy (%)
24	16	8	99.0058	99.6378	99.3218
25	49	14	98.9184	99.5895	99.25395
26	29	10	99.3188	99.5666	99.4427
27	5	5	99.0099	99.7116	99.36075
28	47	14	99.4304	99.5888	99.5096
29	15	7	98.6812	99.7058	99.1935
30	19	8	99.1116	99.7351	99.42335
31	52	15	98.1759	99.7322	98.95405
32	12	7	99.1818	99.583	99.3824
33	27	10	99.009	99.5874	99.2982
34	2	5	99.3079	99.5908	99.44935
35	4	5	98.8303	99.6859	99.2581
36	30	10	99.2497	99.6902	99.46995
37	39	12	99.1839	99.7223	99.4531
38	34	11	98.941	99.5817	99.26135
39	48	14	99.2505	99.7196	99.48505
40	42	13	98.7381	99.6248	99.18145
41	54	15	98.4779	99.6159	99.0469
42	51	15	98.1491	99.76	98.95455
43	13	7	99.0483	99.7343	99.3913
44	41	13	98.6631	99.7673	99.2152
45	43	13	98.5798	99.6943	99.13705
46	20	8	99.137	99.5128	99.3249

Apendix Table D5 (Continued)

RunOrder	StdOrder	Number of neuron in 2nd hidden layer	Accuracy (%) Residual Stress	Accuracy (%) Cycle Time	Average Accuracy (%)
47	38	12	99.2416	99.706	99.4738
48	25	9	98.9388	99.58	99.2594
49	18	8	98.9837	99.6930	99.33835
50	22	9	99.3216	99.7414	99.5315
51	28	10	99.2418	99.7477	99.49475
52	9	6	99.3833	99.7298	99.55655
53	3	5	99.2407	99.6025	99.4216
54	31	11	98.5142	99.7130	99.1136
55	17	8	99.2791	99.7551	99.5171

Apendix Table D6 Results of Experiment 8

RunOrder	StdOrder	Characteristic of input	Transfer function	Accuracy (%) Warpage	Accuracy (%) Cycle Time	Average Accuracy (%)
1	15	Normalization	logsig	90.8302	99.6223	95.22625
2	9	Unnormalization	logsig	59.1758	91.6636	75.4197
3	11	Normalization	logsig	90.8699	99.5839	95.2269
4	17	Unnormalization	logsig	58.0546	99.4315	78.74305
5	8	Normalization	tansig	91.7923	99.7072	95.74975
6	16	Normalization	tansig	89.7979	99.5400	94.66895
7	3	Normalization	logsig	86.9932	99.6114	93.3023

Apendix Table D6 (Continued)

RunOrder	StdOrder	Characteristic of input	Transfer function	Accuracy (%) Warpage	Accuracy (%) Cycle Time	Average Accuracy (%)
8	20	Normalization	tansig	85.0402	99.6178	92.329
9	2	Unnormalization	tansig	57.8534	87.7551	72.80425
10	14	Unnormalization	tansig	58.0546	99.4315	78.74305
11	18	Unnormalization	tansig	60.5149	91.6648	76.08985
12	19	Normalization	logsig	91.4061	99.8612	95.63365
13	1	Unnormalization	logsig	60.5148	91.6648	76.0898
14	6	Unnormalization	tansig	58.0546	99.4315	78.74305
15	13	Unnormalization	logsig	58.0546	99.4315	78.74305
16	4	Normalization	tansig	86.9835	99.6086	93.29605
17	7	Normalization	logsig	90.6271	99.5622	95.09465
18	5	Unnormalization	logsig	57.8534	87.7551	72.80425
19	12	Normalization	tansig	91.3746	99.9289	95.65175
20	10	Unnormalization	tansig	57.8534	87.7551	72.80425

Apendix Table D7 Results of Experiment 9

RunOrder	StdOrder	Learning Rate	Epoch	Accuracy (%) Warpage	Accuracy (%) Cycle Time	Average Accuracy (%)
1	22	0.05	1000	91.7866	99.7073	95.74695
2	37	0.01	1000	90.6271	99.5622	95.09465

Apendix Table D7 (Continued)

RunOrder	StdOrder	Learning Rate	Epoch	Accuracy (%) Warpage	Accuracy (%) Cycle Time	Average Accuracy (%)
3	7	0.09	1000	93.2692	99.9238	96.5965
4	44	0.09	3000	94.5072	99.9426	97.2249
5	32	0.05	3000	94.6014	99.9097	97.25555
6	24	0.05	5000	93.6986	99.9452	96.8219
7	26	0.09	3000	93.9712	99.7733	96.87225
8	17	0.09	3000	94.4394	99.9407	97.19005
9	43	0.09	1000	93.7082	99.9319	96.82005
10	30	0.01	5000	90.8545	99.5629	95.2087
11	14	0.05	3000	93.3717	99.9267	96.6492
12	33	0.05	5000	93.9051	99.9606	96.93285
13	2	0.01	3000	90.8545	99.5629	95.2087
14	45	0.09	5000	90.8545	99.5629	95.2087
15	16	0.09	1000	94.1685	99.8753	97.0219
16	8	0.09	3000	94.1505	99.9587	97.0546
17	41	0.05	3000	92.761	99.6014	96.1812
18	1	0.01	1000	82.5904	99.9345	91.26245
19	4	0.05	1000	91.786	99.7073	95.74665
20	25	0.09	1000	93.7023	99.9445	96.8234
21	11	0.01	3000	93.9644	99.8272	96.8958
22	42	0.05	5000	90.8545	99.5629	95.2087
23	38	0.01	3000	93.5089	99.9266	96.71775
24	19	0.01	1000	93.565	99.9472	96.7561
25	5	0.05	3000	93.0553	99.7879	96.4216

Apendix Table D7 (Continued)

RunOrder	StdOrder	Learning Rate	Epoch	Accuracy (%) Warpage	Accuracy (%) Cycle Time	Average Accuracy (%)
26	15	0.05	5000	94.5270	99.942	97.2345
27	34	0.09	1000	94.1691	99.8753	97.0222
28	29	0.01	3000	93.9895	99.8887	96.9391
29	27	0.09	5000	93.5941	99.9437	96.7689
30	13	0.05	1000	93.5969	99.9429	96.7699
31	36	0.09	5000	94.2596	99.8504	97.055
32	10	0.01	1000	93.8434	99.9294	96.8864
33	39	0.01	5000	93.5355	99.6872	96.61135
34	18	0.09	5000	94.6757	99.9407	97.3082
35	20	0.01	3000	93.9712	99.7733	96.87225
36	6	0.05	5000	93.7563	99.9502	96.85325
37	9	0.09	5000	93.153	99.9503	96.55165
38	40	0.05	1000	89.3524	99.8157	94.58405
39	12	0.01	5000	93.765	99.9618	96.8634
40	23	0.05	3000	94.545	99.9609	97.25295
41	31	0.05	1000	93.7017	99.9447	96.8232
42	21	0.01	5000	90.8545	99.5629	95.2087
43	28	0.01	1000	86.9948	99.6126	93.3037
44	35	0.09	3000	94.654	99.9379	97.29595
45	3	0.01	5000	93.6383	99.8765	96.7574

Apendix Table D8 Results of Experiment 10

RunOrder	StdOrder	Bias	Accuracy (%) Warpage	Accuracy (%) Cycle Time	Average Accuracy (%)
1	12	bias = 1	94.6257	99.9308	97.2783
2	5	without bias	94.2472	99.9541	97.1007
3	8	bias = 0.5	94.1124	99.9509	97.0317
4	10	bias = 0.5	93.5763	99.9417	96.7590
5	6	bias = 0.5	94.0200	99.9376	96.9788
6	4	without bias	94.1700	99.9305	97.0503
7	13	bias = 1	94.7344	99.944	97.3392
8	11	bias = 1	94.5323	99.9384	97.2354
9	1	without bias	94.2579	99.9495	97.1037
10	7	bias = 0.5	93.7794	99.9327	96.8561
11	15	bias = 1	94.8276	99.952	97.3898
12	9	bias = 0.5	94.2316	99.958	97.0948
13	2	without bias	94.2572	99.8562	97.0567
14	14	bias = 1	94.8536	99.9409	97.3973
15	3	without bias	94.6111	99.9484	97.2798

Apendix Table D9 Results of Experiment 11

RunOrder	StdOrder	Number of neuron in 1st hidden layer	Accuracy (%) Warpage	Accuracy (%) Cycle Time	Average Accuracy (%)
1	15	5	94.0986	99.9263	97.0125
2	32	9	94.4855	99.9410	97.2133

Apendix Table D9 (Continued)

RunOrder	StdOrder	Number of neuron in 1st hidden layer	Accuracy (%) Warpage	Accuracy (%) Cycle Time	Average Accuracy (%)
3	35	9	94.6824	99.9525	97.3175
4	4	3	76.9947	99.4876	88.2412
5	30	8	94.6092	99.9425	97.2759
6	6	4	86.9942	99.6112	93.3027
7	34	9	94.8304	99.9477	97.3891
8	33	9	95.0923	99.9592	97.5258
9	2	3	83.0811	99.5668	91.3240
10	27	8	94.9107	99.9513	97.4310
11	8	4	90.8545	99.5629	95.2087
12	9	4	86.9941	99.6112	93.3027
13	26	8	94.4723	99.9036	97.1880
14	1	3	81.0714	99.5067	90.2891
15	10	4	90.8545	99.5629	95.2087
16	20	6	93.2815	99.8778	96.5797
17	18	6	94.6810	99.9271	97.3041
18	25	7	95.0160	99.8652	97.4406
19	28	8	94.9613	99.9484	97.4549
20	14	5	90.8303	99.6223	95.2263
21	11	5	86.9942	99.6112	93.3027
22	12	5	94.2623	99.9638	97.1131
23	7	4	89.6688	99.6184	94.6436
24	5	3	81.0714	99.5067	90.2891
25	3	3	78.0233	99.8538	88.9386

Apendix Table D9 (Continued)

RunOrder	StdOrder	Number of neuron in 1st hidden layer	Accuracy (%) Warpage	Accuracy (%) Cycle Time	Average Accuracy (%)
26	17	6	93.8260	99.8692	96.8476
27	19	6	94.0917	99.8735	96.9826
28	31	9	94.6445	99.9389	97.2917
29	13	5	92.1454	99.5951	95.8703
30	16	6	94.1207	99.8824	97.0016
31	21	7	94.2132	99.9550	97.0841
32	23	7	93.7623	99.8829	96.8226
33	22	7	93.8549	99.9315	96.8932
34	24	7	93.9560	99.9414	96.9487
35	29	8	94.7380	99.9355	97.3368

Apendix Table D10 Results of Experiment 12

RunOrder	StdOrder	Number of neuron in 2nd hidden layer	Accuracy (%) Warpage	Accuracy (%) Cycle Time	Average Accuracy (%)
1	54	16	95.0677	99.9389	97.5033
2	46	15	89.4689	99.9402	94.70455
3	37	13	93.2147	99.9303	96.5725
4	35	12	94.5342	99.8883	97.21125
5	12	8	93.4191	99.9408	96.67995
6	41	14	86.1344	99.9486	93.0415
7	59	17	95.0375	99.8966	97.46705

Apendix Table D10 (Continued)

RunOrder	StdOrder	Number of neuron in 2nd hidden layer	Accuracy (%) Warpage	Accuracy (%) Cycle Time	Average Accuracy (%)
8	69	19	82.3247	99.9671	91.1459
9	38	13	91.6582	99.9465	95.80235
10	51	16	94.9156	99.9532	97.4344
11	50	15	93.7741	99.9352	96.85465
12	11	8	94.8821	99.9469	97.4145
13	9	7	94.0253	99.9515	96.9884
14	42	14	95.3201	99.9602	97.64015
15	39	13	76.0903	99.3873	87.7388
16	40	13	93.3564	99.9262	96.6413
17	49	15	90.0321	99.9441	94.9881
18	32	12	92.9531	99.9363	96.4447
19	8	7	91.3242	99.9492	95.6367
20	3	6	93.7037	99.9444	96.82405
21	31	12	92.1846	99.9461	96.06535
22	1	6	93.2253	99.9548	96.59005
23	27	11	89.042	99.8958	94.4689
24	45	14	92.2601	99.9575	96.1088
25	10	7	94.0207	99.943	96.98185
26	20	9	92.6224	99.9452	96.2838
27	7	7	94.2814	99.9596	97.1205
28	13	8	94.2664	99.9521	97.10925
29	19	9	90.4535	99.9407	95.1971
30	65	18	94.0409	99.9486	96.99475

Apendix Table D10 (Continued)

RunOrder	StdOrder	Number of neuron in 2nd hidden layer	Accuracy (%) Warpage	Accuracy (%) Cycle Time	Average Accuracy (%)
31	47	15	89.4034	99.9678	94.6856
32	60	17	94.7087	99.9446	97.32665
33	61	18	94.3947	99.8542	97.12445
34	28	11	89.7279	99.9499	94.8389
35	56	17	92.6134	99.9147	96.26405
36	16	9	78.3087	99.5666	88.93765
37	44	14	89.2609	99.9587	94.6098
38	24	10	94.0277	99.9492	96.98845
39	52	16	94.8849	99.9539	97.4194
40	63	18	91.6701	99.9592	95.81465
41	26	11	87.3413	99.9545	93.6479
42	17	9	90.8614	99.9131	95.38725
43	18	9	93.52	99.9536	96.7368
44	57	17	94.5065	99.954	97.23025
45	25	10	93.9659	99.8849	96.9254
46	55	16	95.249	99.9152	97.5821
47	48	15	92.0083	99.9543	95.9813
48	64	18	92.374	99.9557	96.16485
49	23	10	86.6439	99.9296	93.28675
50	15	8	94.0330	99.9503	96.99165
51	70	19	92.2082	99.9412	96.0747
52	68	19	86.7278	99.9417	93.33475
53	53	16	95.0747	99.9506	97.51265

Apendix Table D10 (Continued)

RunOrder	StdOrder	Number of neuron in 2nd hidden layer	Accuracy (%) Warpage	Accuracy (%) Cycle Time	Average Accuracy (%)
54	6	7	93.7674	99.9407	96.85405
55	2	6	94.0400	99.9498	96.9949
56	43	14	91.5068	99.9503	95.72855
57	58	17	93.9969	99.9472	96.97205
58	14	8	95.2647	99.9421	97.6034
59	36	13	87.0945	99.9458	93.52015
60	4	6	95.2058	99.945	97.5754
61	29	11	93.8257	99.9521	96.8889
62	66	19	88.7067	99.9275	94.3171
63	62	18	94.3444	99.9415	97.14295
64	30	11	77.8176	99.9644	88.891
65	34	12	93.4505	99.9578	96.70415
66	33	12	91.8688	99.9596	95.9142
67	67	19	84.1847	99.9768	92.08075
68	21	10	86.6439	99.9296	93.28675
69	22	10	92.0881	99.915	96.00155
70	5	6	92.65	99.8982	96.2741

Appendix E

The GA command with ‘gatool’ in MATLAB

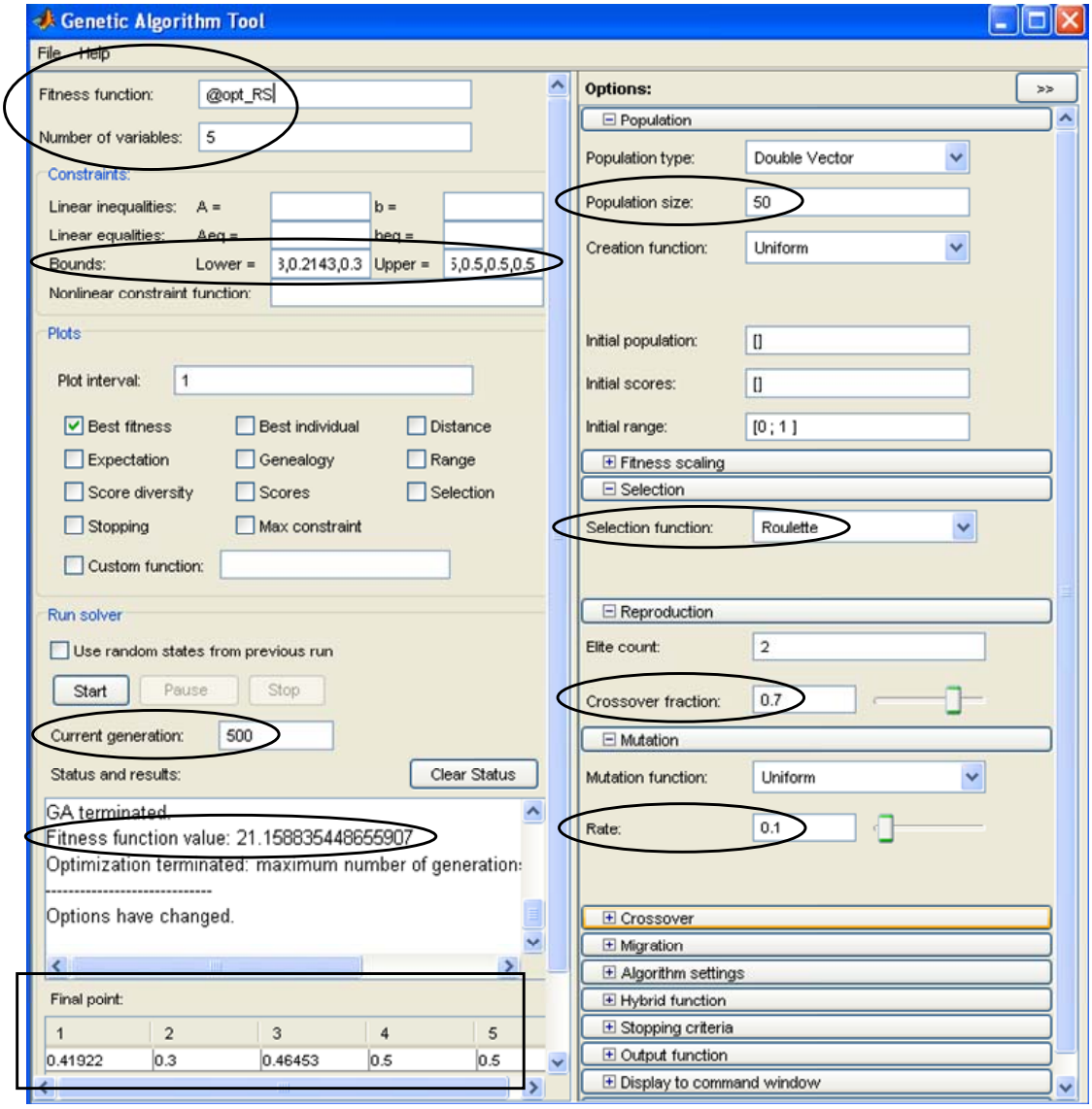

Appendix Figure E1 The GA command with 'gatool' in MATLAB

Appendix F

The results of appropriate GA parameters

Apendix Table F1 A result of appropriate population size of GA for the rectangular lid

RunOrder	StdOrder	Population size	Crossover rate	Mutation rate	Solution (Residual stress, MPa)
1	7	50	0.3	0.1	21.3755
2	8	50	0.3	0.1	21.1597
3	3	10	0.3	0.1	21.3761
4	4	30	0.3	0.1	21.3755
5	6	30	0.3	0.1	21.1607
6	9	50	0.3	0.1	21.1588
7	5	30	0.3	0.1	21.3754
8	1	10	0.3	0.1	21.4674
9	2	10	0.3	0.1	21.3790

Apendix Table F2 A result of appropriate crossover rate of GA for the rectangular lid

RunOrder	StdOrder	Population size	Crossover rate	Mutation rate	Solution (Residual stress, MPa)
1	6	50	0.5	0.1	21.1588
2	2	50	0.3	0.1	21.3754
3	9	50	0.7	0.1	21.1589
4	1	50	0.3	0.1	21.3755
5	8	50	0.7	0.1	21.1588
6	7	50	0.7	0.1	21.1588
7	5	50	0.5	0.1	21.1588
8	4	50	0.5	0.1	21.4670
9	3	50	0.3	0.1	21.1588

Apendix Table F3 A result of appropriate mutation rate of GA for the rectangular lid

RunOrder	StdOrder	Population size	Crossover rate	Mutation rate	Solution (Residual stress, MPa)
1	8	50	0.5	0.3	21.1588
2	2	50	0.5	0.1	21.1588
3	3	50	0.5	0.1	21.1588
4	5	50	0.5	0.2	21.1588
5	7	50	0.5	0.3	21.1588

Apendix Table F3 (Continued)

RunOrder	StdOrder	Population size	Crossover rate	Mutation rate	Solution (Residual stress, MPa)
6	4	50	0.5	0.2	21.1588
7	9	50	0.5	0.3	21.1588
8	1	50	0.5	0.1	21.1588
9	6	50	0.5	0.2	21.1588

Apendix Table F4 A result of appropriate population size of GA for the roof tile

RunOrder	StdOrder	Population size	Crossover rate	Mutation rate	Solution (Warpage, mm)
1	7	50	0.3	0.1	2.0303
2	8	50	0.3	0.1	2.0303
3	3	10	0.3	0.1	2.2837
4	4	30	0.3	0.1	2.0303
5	6	30	0.3	0.1	2.2837
6	9	50	0.3	0.1	1.9903
7	5	30	0.3	0.1	2.0303
8	1	10	0.3	0.1	2.0303
9	2	10	0.3	0.1	2.2837

Apendix Table F5 A result of appropriate crossover rate of GA for the roof tile

RunOrder	StdOrder	Population size	Crossover rate	Mutation rate	Solution (Warpage, mm)
1	6	50	0.5	0.1	1.9903
2	2	50	0.3	0.1	2.0303
3	9	50	0.7	0.1	2.0303
4	1	50	0.3	0.1	2.0303
5	8	50	0.7	0.1	1.9903
6	7	50	0.7	0.1	1.9903
7	5	50	0.5	0.1	2.0303
8	4	50	0.5	0.1	1.9903
9	3	50	0.3	0.1	2.0303

Apendix Table F6 A result of appropriate mutation rate of GA for the roof tile

RunOrder	StdOrder	Population size	Crossover rate	Mutation rate	Solution (Warpage, mm)
1	8	50	0.5	0.3	1.9903
2	2	50	0.5	0.1	1.9903
3	3	50	0.5	0.1	1.9903
4	5	50	0.5	0.2	1.9903
5	7	50	0.5	0.3	1.9903
6	4	50	0.5	0.2	1.9903
7	9	50	0.5	0.3	1.9903
8	1	50	0.5	0.1	1.9903
9	6	50	0.5	0.2	1.9903

CIRRICULUM VITAE

NAME : Mr. Pitchakorn Chavanatnusorn

BIRTH DATE : July 14, 1983

BIRTH PLACE : Songkhla, Thailand

EDUCATION :	**YEAR**	**INSTITUTE**	**DEGREE/DIPLOMA**
	2004	Prince of Songkla Univ.	B.Sc. (Agro-Industry Technology Management)

SCHOLARSHIP/AWARDS : International Graduate Program Scholarship 2006-2007